



U.S. Department
of Transportation
**National Highway
Traffic Safety
Administration**



DOT HS 811 633

April 2013

Test Track Lateral Stability Performance of Motorcoaches Equipped With Electronic Stability Control Systems

DISCLAIMER

This publication is distributed by the U.S. Department of Transportation, National Highway Traffic Safety Administration, in the interest of information exchange. The opinions, findings, and conclusions expressed in this publication are those of the authors and not necessarily those of the Department of Transportation or the National Highway Traffic Safety Administration. The United States Government assumes no liability for its contents or use thereof. If trade names, manufacturers' names, or specific products are mentioned, it is because they are considered essential to the object of the publication and should not be construed as an endorsement. The United States Government does not endorse products or manufacturers.

NOTE
REGARDING COMPLIANCE WITH
AMERICANS WITH DISABILITIES ACT SECTION 508

For the convenience of visually impaired readers of this report using text-to-speech software, additional descriptive text has been provided within the body of the report for graphical images to satisfy Section 508 of the Americans with Disabilities Act (ADA).

Technical Report Documentation Page

1. Report No. DOT HS 811 633	2. Government Accession No.	3. Recipient's Catalog No.	
4. Title and Subtitle Test Track Lateral Stability Performance of Motorcoaches Equipped With Electronic Stability Control Systems		5. Report Date April 2013	
		6. Performing Organization Code NHTSA/NVS-312	
7. Author(s) Devin Elsasser and Frank S. Barickman, National Highway Traffic Safety Administration Heath Albrecht, Jason Church, Guogang Xu and Mark Heitz; Transportation Research Center		8. Performing Organization Report No.	
		10. Work Unit No. (TRAIS)	
9. Performing Organization Name and Address National Highway Traffic Safety Administration Vehicle Research and Test Center P.O. Box 37 East Liberty, OH 43319		11. Contract or Grant No.	
		13. Type of Report and Period Covered Final Report	
12. Sponsoring Agency Name and Address National Highway Traffic Safety Administration 1200 New Jersey Avenue, SE Washington, D.C. 20590		14. Sponsoring Agency Code	
		15. Supplementary Notes The authors would like to acknowledge the technical support of Mike Thompson, Don Meddles, Chris Boday, Lyle Heberling, Dr. Kamel Salaani, Jim Preston, Larry Smith, Timothy Vanbuskirk, and Dr. Tom Ranney of the Transportation Research Center Inc.	
16. Abstract The research detailed in this report supports The Motorcoach Safety Action Plan released by the Department of Transportation (DOT) on November 16, 2009 and ongoing safety research by DOT's National Highway Traffic Safety Administration (NHTSA). Electronic stability control (ESC), a crash avoidance technology was identified in the plan as a potential motorcoach safety enhancement designed to improve stability in rollover and loss-of-control scenarios. The research described in this report was performed by the NHTSA's Vehicle Research and Test Center (VRTC) from 2008-2010. The goals of this testing were to evaluate motorcoach lateral stability and understand how motorcoach ESC systems modify the handling and stability characteristics on the test track. Measures of performance from preceding commercial vehicle research with truck tractors were evaluated to determine their potential use in assessing lateral stability and responsiveness of motorcoaches equipped with stability control systems. Performance maneuvers evaluated were the sine with dwell, half-sine with dwell, ramp with dwell, ramp steer maneuver, slowly increasing steer maneuver, and the constant radius maneuver. These test track maneuvers are representative of lane changes, obstacle avoidance, or negotiating-a-curve crash scenarios. Using these maneuvers, three commercial Class 8 (air braked) motorcoaches were equipped with safety outriggers and tested with and without ESC enabled. The motorcoaches and ESC systems were evaluated lightly loaded and at a loaded weight with simulated passengers. Maneuvers were performed on high friction dry asphalt and reduced friction Jennite test surfaces. Using data from this test track research, several measures of performance were analyzed that have merit for use in evaluating the lateral stability performance of commercial vehicles.			
17. Key Words Heavy Vehicle, Motorcoach, Electronic Stability Control, Roll Stability Control, Rollover, Roll Propensity, Yaw Propensity, Yaw Control, Directional Control, Loss of Control, Ramp Steer Maneuver, Slowly Increasing Steer, Sine with Dwell, Half-Sine with Dwell, Constant Radius, Ramp with Dwell, Jennite, Lateral Acceleration Ratio, Yaw Rate Ratio, ESC, YSC, RSC, Outrigger, Responsiveness, Bus, Test Track		18. Distribution Statement Document is available to the public from the National Technical Information Service www.ntis.gov	
19. Security Classif. (of this report) Unclassified	20. Security Classif. (of this page) Unclassified	21. No. of Pages 175	22. Price

Form DOT F 1700.7 (8-72)

Reproduction of completed page authorized

TABLE OF CONTENTS

LIST OF FIGURES	iv
LIST OF TABLES	ix
EXECUTIVE SUMMARY	xi
1 INTRODUCTION.....	1
1.1 Background.....	1
1.2 Study Objectives	2
2 TEST METHOD	3
2.1 Test Vehicles	3
2.2 Instrumentation	3
2.3 Steering Controller	4
2.4 Load Conditions.....	5
2.5 Testing Surface and Ambient Conditions.....	5
2.6 Test Maneuvers	6
2.6.1 Constant Radius Maneuver (CR)	7
2.6.2 Slowly Increasing Steer Maneuver (SIS).....	7
2.6.3 Ramp Steer Maneuver (RSM).....	9
2.6.4 Sine with Dwell Maneuver (SWD)	10
2.6.5 Half-Sine With Dwell Maneuver (HSWD)	11
2.6.6 Ramp With Dwell (RWD) Maneuver.....	13
3 PERFORMANCE MANEUVER RESEARCH.....	14
3.1 150 foot Constant Radius Test Results.....	14
3.2 SIS Test Results	22
3.2.1 Vehicle Dynamics Changes from ESC Intervention	22
3.2.2 SIS – High Surface Friction – LLVW Load Condition	23
3.2.3 SIS – High Surface Friction – GPOW Load Condition.....	31
3.2.4 Determining Maneuver Amplitude from SIS Test Results	39
3.3 RSM Test Results	40
3.3.1 RSM – High Surface Friction – LLVW Load Condition	40
3.3.2 RSM – High Surface Friction – GPOW Load Condition.....	48
3.3.3 RSM – Reduced Surface Friction – GPOW Load Condition.....	57
3.4 RWD Maneuver Test Results	70
3.5 SWD Maneuver Test Results.....	80
3.5.1 SWD – High Surface Friction - LLVW Load Condition.....	80
3.5.2 SWD – High Surface Friction – GPOW Load Condition	84
3.5.3 SWD – Low Surface Friction – GPOW Load Condition	90
3.6 HSWD Test Results	92
3.6.1 HSWD – High Surface Friction - LLVW Load Condition	92
3.6.2 HSWD – High Surface Friction – GPOW Load Condition.....	95
3.7 Maneuver Discussion and Summary	97

3.7.1	Testing Surface	97
3.7.2	Loading Conditions.....	101
3.7.3	Maneuvers	101
3.7.4	Broken Roll Stabilizer Link	103
4	MEASURES OF PERFORMANCE.....	105
4.1	Engine Torque Reduction in SIS maneuvers	105
4.2	LAR from RSMs.....	106
4.3	LAR and YRR from SWD maneuvers	110
4.4	Motorcoach Responsiveness.....	116
5	CONCLUSIONS.....	120
5.1	Motorcoach Test Track Performance.....	120
5.2	Measures of Performance.....	121
	APPENDIX A	127
A.	Testing Procedures.....	127
	APPENDIX B	131
B.	Motorcoach Parameters	131
	APPENDIX C	132
C.	Instrumentation and Safety Equipment	132
	APPENDIX D	135
D.	Load Condition Information	135
	APPENDIX E	137
E.	Safety Outrigger Information and Drawings.....	137

LIST OF FIGURES

Figure 2.1. TRC VDA dry and Jennite wet peak and slide coefficients of friction for the testing period.	6
Figure 2.2. Example of the steering wheel profile used for SIS tests.....	8
Figure 2.3. Steering wheel profile used for RSM tests.	10
Figure 2.4. Sine with Dwell profile	11
Figure 2.6. Example of steering wheel profile used for RWD tests.	13
Figure 3.1. Graphs show test data from the MCI #1 CR maneuver counter-clockwise in the GPOW load condition with ESC enabled only.	17
Figure 3.2. Graphs show torque and brake pressure test data from the MCI #1 CR maneuver in the GPOW load condition with ESC enabled only. At ESC activation, the driver requested 100 percent throttle.	18
Figure 3.3. Graphs show test data from the Prevost CR maneuver in the GPOW load condition with ESC enabled and disabled. The ESC disabled test is shown in red and the ESC enabled test is shown in blue.....	19
Figure 3.4. Graphs show torque and brake pressure test data from the Prevost CR maneuver in the GPOW load condition with ESC enabled only. At ESC activation the driver requested 100 percent throttle.	20
Figure 3.5. Graphs show test data from the MCI #2 CR maneuver in the GPOW load condition with ESC enabled and disabled. The ESC disabled test is shown in red and the ESC enabled test is shown in blue.....	21
Figure 3.6. Graphs show torque and brake pressure test data from the MCI #2 CR maneuver in the GPOW load condition with ESC enabled only. At ESC activation the driver requested 100 percent throttle.	22
Figure 3.7. Graph shows an example of test data from the MCI #1 SIS maneuver one (one left and one right) in the LLVW load condition with ESC enabled and disabled.	24
Figure 3.8. Graphs show brake pressures at each wheel and torque outputs for the MCI #1 during a SIS maneuver to the right, with ESC enabled in the LLVW load condition.	25
Figure 3.9. Graphs show an example of test data from the Prevost SIS maneuver one (one left and one right) in the LLVW load condition, with ESC enabled and disabled.	26
Figure 3.10. Graphs show brake pressures at each wheel and torque outputs for the Prevost during a SIS maneuver to the right, with ESC enabled, in the LLVW load condition.	27
Figure 3.11. Graphs show an example of test data from the MCI #2 SIS maneuver one (one left and one right) in the LLVW load condition, with ESC enabled and disabled.	28
Figure 3.12. Graph shows brake pressures at each wheel and torque outputs for the MCI #2 during a SIS maneuver to the right, with ESC enabled in the LLVW load condition.	29
Figure 3.13. Graphs show an example of test data from the MCI #1 SIS maneuver one (one left and one right) in the GPOW load condition, with ESC enabled only.....	32
Figure 3.14. Graphs show brake pressures at each wheel and torque outputs for the MCI #1 during a SIS maneuver to the right, with ESC enabled in the GPOW load condition.	33
Figure 3.15. Graph shows an example of test data from the Prevost SIS maneuver one (one left and one right) in the GPOW load condition, with ESC enabled and disabled.....	34

Figure 3.16. Graphs show brake pressures at each wheel and torque outputs for the Prevost during a SIS maneuver to the right, with ESC enabled in the GPOW load condition. 35

Figure 3.17. Graphs show an example of test data from the MCI #2 SIS maneuver one (one left and one right) in the GPOW load condition, with ESC enabled and disabled..... 36

Figure 3.18. Graphs show brake pressures at each wheel and torque outputs for the MCI #2 during a SIS maneuver to the right, with ESC enabled in the GPOW load condition. 37

Figure 3.19. Graphs show RSM test data from the MCI #1 in the LLVW load condition with ESC enabled and disabled. Tests shown in this figure were performed at an approximate MES of 38 to 50 mph for ESC enabled and a MES of 38 mph ESC disabled. For the ESC disabled test shown in red, wheel lift of two inches was observed in the data. 42

Figure 3.20. Graph shows brake pressures observed for RSM test data from the MCI #1 in the LLVW load condition ESC enabled and disabled. Tests shown in this figure were performed at an approximate MES of 40 to 50 mph ESC enabled. 43

Figure 3.21. Graphs show RSM test data from the Prevost in the LLVW load condition with ESC enabled and disabled. Tests shown in this figure were performed at an approximate MES of 40 to 50 mph with ESC enabled, and at a MES of 50 mph with ESC disabled. The ESC disabled test is shown in red. No wheel lift was observed for the ESC off test at 50 mph. 44

Figure 3.22. Graphs show brake pressures observed for the RSM test data from the Prevost in the LLVW load condition with ESC enabled. Tests shown in this figure were performed at an approximate MES of 40 to 50 mph. 45

Figure 3.23. Graphs show RSM test data from the MCI #2 in the LLVW load condition with ESC enabled and disabled. Tests shown in this figure were performed at an approximate MES of 40 to 50 mph with ESC enabled, and a MES of 40 mph with ESC disabled. For the ESC disabled test shown in red, wheel lift of two inches was observed in the data. 47

Figure 3.24. Graphs show brake pressures observed for RSM test data from the MCI #2 in the LLVW load condition with ESC enabled and disabled. Tests shown in this figure were performed at an approximate MES of 40 to 50 mph ESC enabled. 48

Figure 3.25. Graphs show RSM test data from the MCI #1 in the GPOW load condition with ESC enabled and disabled. Tests shown in this figure were performed at MESs of 38 to 50 mph with ESC enabled and at 37 mph with ESC disabled. For the ESC disabled test shown in red, wheel lift of two inches was observed for the ESC disabled test. 50

Figure 3.26. Graphs show brake pressures observed for RSM test data from the MCI #1 in the GPOW load condition ESC enabled. Tests shown in this figure were performed at MESs of 38 to 50 mph. 51

Figure 3.27. Graphs show RSM test data from the Prevost in the GPOW load condition with ESC enabled and disabled. Tests shown in this figure were performed at MESs of 40 to 48 mph with ESC enabled and at 39 mph with ESC disabled. The disabled test is shown in red. Wheel lift of two inches was observed for the ESC enabled tests at 48 mph and for the ESC disabled test at 39 mph. 53

Figure 3.28. Graphs show brake pressures observed for RSM test data from the Prevost in the GPOW load condition ESC enabled. Tests shown in this figure were performed at MESs of 40 to 50. 54

Figure 3.29. Graphs show RSM test data from the MCI #2 in the GPOW load condition ESC enabled and disabled. Tests shown in this figure were performed at MESs of 36 to 50 mph with ESC enabled and at 36 mph with ESC disabled. For the ESC disabled test is shown in red, wheel lift of over two inches was observed. 56

Figure 3.30. Graphs show brake pressures observed for RSM test data from the MCI #2 in the GPOW load condition with ESC enabled. Tests shown in this figure were performed at MESs of 36 to 50 mph.	57
Figure 3.31. Jennite survey example of space needed to conduct RSM.	58
Figure 3.32. MCI #1 RSM time history data from series performed on the Jennite with the GPOW load condition.	60
Figure 3.33. MCI #1 brake pressure data from RSM tests conducted on the Jennite (same tests as shown in Figure 3.32)	61
Figure 3.34. MCI #1 path data from RSM test performed on the Jennite.	62
Figure 3.35. Prevost RSM time history data from tests conducted on the Jennite surface.	64
Figure 3.36. Prevost brake pressure data from RSM test performed on the wet Jennite (same enabled tests as shown in Figure 3.35).	65
Figure 3.37. Prevost path data from RSMs performed on the Jennite.	66
Figure 3.38. MCI #2 RSM time history data from the test series conducted on the wet Jennite.	68
Figure 3.39. MCI #2 brake pressure data form RSMs performed on the Jennite with ESC enabled (same enabled tests as shown in Figure 3.38).	69
Figure 3.40. MCI #2 path data from RSMs performed on the Jennite test surface.	70
Figure 3.41. Survey of TRC's Jennite surface and the 500 foot radius.	72
Figure 3.42. Prevost time history data from the RWD maneuver and GPOW load condition. Example shows the RWD test with the lowest steering angle input that resulted in ESC activation.	74
Figure 3.43. Prevost brake pressure data form RWD tests conducted on the Jennite test surface with the GPOW load condition (same enabled tests as shown in Figure 3.42).	75
Figure 3.44. Prevost path data from the RWD and the GPOW load condition.	76
Figure 3.45. MCI #2 time history data from the RWD maneuver and GPOW load condition. Example shows the RWD test with the lowest steering angle input that resulted in ESC activation.	78
Figure 3.46. MCI #2 brake pressure data from RWD maneuvers with the GPOW load condition and ESC enabled.	79
Figure 3.47. MCI #2 path data from RWD maneuvers conducted on the Jennite and the GPOW load condition.	80
Figure 3.48. Prevost LLVW time history data from SWDs conducted with the 0.5 Hz frequency, 1.0 second dwell time, and 70% steering scalar at 50mph.	82
Figure 3.49. MCI #2 time history data from LLVW SWD test series conducted at the 0.5 Hz frequency, with the 1.0 second dwell time, and 100% steering scalar at 50 mph.	83
Figure 3.50. MCI #2 time history data from Gross Occupancy SWD test series conducted on dry high friction asphalt with the 0.5 Hz frequency, 1.0 second dwell time and 80% steering scalar at 45 mph.	87
Figure 3.51. MCI #2 time history data from Gross Occupancy SWD test series conducted on dry high friction asphalt at the 0.3 Hz frequency, 1.0 second dwell time, and 80% steering scalar at 45 mph.	88
Figure 3.52. MCI #2 time history data from the GPOW SWD test series conducted on wet Jennite surface with the 0.4 Hz frequency, 1.0 second dwell time, and 130% steering scalar at 30 mph.	92

Figure 3.53. Position data of the motorcoaches performing the RSM on the reduced friction surface. Lines approximate the path of the center of the front axle.	99
Figure 3.54. Time history data from the RSM test shown above in Figure 3.53.	100
Figure 3.55. Time history data of brake pressures from test shown in Figure 3.53.	101
Figure 3.56. Graph shows test data from the Prevost RSM in the GPOW load condition with ESC enabled for two tests with a MES of 42 mph but conducted on different days.	104
Figure 4.1. Average engine torque reduction for each motorcoach tested in the GPOW load condition. Also included was the average difference (percent change) for all tractors equipped with stability control tested in combination with four different trailers.	106
Figure 4.2. Time history data of steering wheel angle, lateral acceleration and the calculated LAR measure. This figure, key points of interest: BOS and ERI.	107
Figure 4.3. LAR versus time after ERI for MCI #1 RSM tests (GPOW load condition) conducted with a MES of 30–37 mph with ESC disabled and 30–50 mph with ESC enabled.	109
Figure 4.4. LAR versus time after ERI for Prevost RSM tests (GPOW load condition) conducted with a MES of 30–39 mph with ESC disabled and 30–48 mph with ESC enabled.	109
Figure 4.5. LAR versus time after ERI for MCI #2 RSM tests (GPOW load condition) conducted with a MES of 30–35 mph with ESC disabled and 30–50 mph with ESC enabled.	110
Figure 4.6. Key events in the SWD maneuver’s steering input and measured lateral acceleration and yaw rate signals that were used calculate the LAR and YRR measures.	112
Figure 4.7. SWD LAR and YRR observations produced by the MCI #1 motorcoach with the GPOW load condition. Steering Scalars from 80–100 percent are shown for ESC enabled and disabled test series.	114
Figure 4.8. SWD LAR and YRR observations produced by the Prevost motorcoach with the GPOW load condition at steering scalars between 70 – 100 percent for ESC enabled and disabled.	115
Figure 4.9. LAR and YRR observations produced by the MCI #2 motorcoach with the GPOW load condition. Steering Scalars between 80 – 100 percent are shown for ESC enabled and disabled tests.	116
Figure 4.10. Time history data from the SWD denotes BOS, responsiveness measure, COS and the maneuver avoidance and recovery regions.	118
Figure 4.11. Lateral Displacement versus Steering Scalar 1.5 sec. after BOS for SWD test at 0.5 Hz with 1.0 sec. dwell.	119
Figure 5.1. RSM LAR after ERI event for all three motorcoaches with ESC enabled at 40 mph (solid lines) and disabled (dotted lines) at 35 – 39 mph with the GPOW load condition.	122
Figure 5.2. SWD LAR and YRR after COS event for all three motorcoaches with ESC enabled with the 90 percent steering scalar (solid lines denoted with “9”) and disabled tests with 80 – 90 percent steering scalars (dotted lines denoted with “8” or “9”) with the GPOW load condition.	123
Figure 5.3. 0.5Hz SWD (1.0 second dwell) lateral displacement of truck-tractors and motorcoaches with and without stability control.	124
AP Figure 1. Outriggers.	134
AP Figure 2. Driver restraint system.	134
AP Figure 3. 175 lb. water Dummies were used to ballast the motorcoaches to the GPOW load condition.	136
AP Figure 4. Outboard Outrigger Beam Assembly Drawing – Exploded View.	138

AP Figure 5. Dimensional Outrigger Assembly Drawing - Side-view.....	139
AP Figure 6. Completed outrigger assembly installed on a motorcoach.	139
AP Figure 7. Photographs of adjustment plate and mounting plate in the MCI installation (left photo) and in the Prevost installation (right photo).	140
AP Figure 8. Dimensional drawing of the outrigger mounting plate.	141
AP Figure 9. Photograph of the outrigger mounting plate during fabrication.	141
AP Figure 10. Dimensioned drawing for the Prevost adjustment plate.	142
AP Figure 11. Photograph of the under-slung (lower) mounting frame installed on the MCI motorcoach.	143
AP Figure 12. Photograph of the attachment of the adjustment plate to the lower frame.	143
AP Figure 13. Photograph of the tube center joiner.....	144
AP Figure 14. Sketch of the outrigger beam-upper mounting framework-plan.....	145
AP Figure 15. Side view drawing of the complete MCI mounting framework shown with the outboard outrigger beam assembly.	145
AP Figure 16. Photograph of MCI upper mounting framework.	146
AP Figure 17. Dimensioned engineering drawing of the Prevost lower 6 x 3 inch steel tube.....	147
AP Figure 18. Engineering drawing of the Prevost 6 x 4 inch aluminum rectangular tube.	148
AP Figure 19. Photograph of Prevost lower 6 inch x 3 inch steel tube and the 6 inch x 4 inch aluminum rectangular tube.	148
AP Figure 20. Engineering drawing of the Prevost lower steel support.	149
AP Figure 21. Engineering drawing of the Prevost connecting link.	150
AP Figure 22. Labeled photograph of the steel lower supports and Prevost connecting link.	150
AP Figure 23. Dimensioned drawing of the Prevost upper mounting plate, left side.	151
AP Figure 24. Photographs of the fabrication of the Prevost upper mounting plates. Left: Driver-side upper mounting plate bolted in place with clamping plates and the upper support Tube before the tabs were installed. Right: This photo is of the same mounting plate shows the clamping plate on the inside of the stainless steel tubing of the motorcoach and the aluminum upper support tube (center background).....	152
AP Figure 25. Dimensioned drawing of the Prevost lower mounting plate for the left side.	152
AP Figure 26. Photographs of the fabrication of the Prevost lower mounting plates. Left: Driver-side lower mounting plate is bolted to the Prevost lower 6 x 3 inch steel tube and with clamping plates. Right: This photo is of the same mounting plate showing the clamping plate on the inside of the stainless steel tubing of the motorcoach and the Prevost steel lower support tube.	153
AP Figure 27. Engineering drawing of the Prevost upper support tube for the right side.	154
AP Figure 28. Photograph of the right side Prevost upper support tube installed.	154
AP Figure 29. Prevost mounting frame assembly drawing view from the left rear of the motorcoach.	155
AP Figure 30. Photographs of the motorcoach outrigger and mount static load testing. Left: MCI motorcoach. Right: Prevost motorcoach.....	156

LIST OF TABLES

Table 2.1. Motorcoaches tested.	3
Table 2.2. Motorcoach sensor information.	4
Table 2.3. J1939 vehicle bus information.	4
Table 3.1. Maneuvers and parameters used on dry asphalt (0.96 peak friction co-efficient) test surface.	14
Table 3.2. Maneuvers and parameters used on wet Jennite (0.3 peak friction co-efficient) test surface.	14
Table 3.3. Maximum speed obtained during the constant radius increasing velocity tests.	15
Table 3.4. Maximum lateral acceleration observed during the constant radius increasing velocity tests.	15
Table 3.5. SIS maneuver average speed in one second intervals from ESC activation for each motorcoach tested in the LLVW load condition.	30
Table 3.6. SIS maneuver average lateral acceleration in one second intervals from ESC activation for each motorcoach tested in the LLVW load condition.	30
Table 3.7. Average speed reduction for each motorcoach tested in the GPOW load condition.	38
Table 3.8. Average lateral acceleration for each motorcoach tested in the GPOW load condition.	38
Table 3.9. SIS tests results for the three Motorcoaches in the LLVW and GPOW load conditions.	39
Table 3.10. Example of scalars used for SWD and HSWD maneuvers.	40
Table 3.11. Presents the lowest target MES that resulted in 2.0 inches or more of wheel lift during the RSM test series with a LLVW load.	41
Table 3.12. MCI #1 lateral acceleration, yaw rate, and roll angle values and changes observed at the instant in time (shown in Figure 3.19) that maximum wheel lift was observed with ESC disabled. The MES was 38 mph for ESC enabled and disabled tests.	41
Table 3.13. MCI #2 lateral acceleration, yaw rate, and roll angle values and changes observed at the instant in time (shown in Figure 3.23) that maximum wheel lift was observed with ESC disabled. The MES was 40 mph for both ESC enabled and disabled tests.	46
Table 3.14. Presents the lowest target MES that resulted in 2.0 inches or more of wheel lift during the RSM test series with a GPOW load.	49
Table 3.15. MCI #1 lateral acceleration, yaw rate, and roll angle values and changes observed at the instant in time (shown in Figure 3.25) that maximum wheel lift was observed with ESC disabled. The MES was 37 mph with ESC disabled compared to a MES of 38 mph with ESC enabled.	49
Table 3.16. Prevost lateral acceleration, yaw rate, and roll angle values and changes observed at the instant in time (shown in Figure 3.27) that maximum wheel lift was observed with ESC disabled. The MES was 39 mph with ESC disabled compared to a MES of 40 mph with ESC enabled.	52
Table 3.17. MCI #2 lateral acceleration, yaw rate, and roll angle values and changes observed at the instant in time (shown in Figure 3.29) that maximum wheel lift was observed with ESC disabled. The MES was 35 mph with ESC disabled, compared to a MES of 36 mph with ESC enabled.	55
Table 3.18. RWD test series lowest steering angle that resulted in ESC activation	72
Table 3.19. RWD tests series lowest steering angle that resulted in instability	72

Table 3.20. LLVW condition SWD stability results.	81
Table 3.21. Motorcoach yaw angle maxima results from SWD test series with the LLVW.	84
Table 3.22. Motorcoach roll angle maxima results from SWD test series with the LLVW.	84
Table 3.23. SWD results with ESC disabled and the GPOW condition.	85
Table 3.24. SWD results with ESC enabled and the GPOW condition.	85
Table 3.25. Motorcoach yaw angle maxima results from SWD test series with the GPOW load.	89
Table 3.26. Motorcoach roll angle maxima results from SWD test series with the GPOW load.	89
Table 3.27. Yaw angle maxima from SWD test series conducted on the low friction wet Jennite.	90
Table 3.28. Roll angle maxima from SWD test series conducted on the low friction wet Jennite.	91
Table 3.30. LLVW condition HSWD stability results with ESC enabled.	93
Table 3.31. Yaw angle maxima from LLVW HSWD test series conducted on the high friction dry asphalt.	94
Table 3.32. Roll angle maxima from LLVW HSWD test series conducted on the high friction dry asphalt.	94
Table 3.33. GPOW condition HSWD stability results with ESC disabled.	95
Table 3.34. GPOW condition HSWD stability results with ESC enabled.	95
Table 3.35. Yaw angle maxima from GPOW HSWD test series conducted on the dry asphalt.	96
Table 3.36. Roll angle maxima from GPOW HSWD test series conducted on the dry asphalt.	97
Table 5.1. Lateral Acceleration at ESC activation in the SIS test maneuver.	120
AP Table 1. General Information	131
AP Table 2. Tire Specifications	131
AP Table 3. GAWRs and GVWRs	131
AP Table 4. Dimensions	131
AP Table 5. CG Positions (LLVW Load Condition)	131
AP Table 6. LLVW Load Condition Weights	135
AP Table 7. GPOW Load Condition Weights	135
AP Table 8. NHTSA Outrigger Specifications	137
AP Table 9. Outrigger Outboard Beam Assembly Parts	137

EXECUTIVE SUMMARY

Researchers at the Vehicle Research and Test Center (VRTC) performed test track research with three class 8 motorcoaches equipped with electronic stability control (ESC). Motorcoaches that were tested included a 2007 MCI D4500 (herein referred to as MCI #1), a 2009 Prevost H3 (herein referred to as Prevost), and a second 2007 MCI D4500 (herein referred to as MCI #2). The MCI coaches were equipped with Meritor WABCO ESC and the Prevost was equipped with a Bendix ESC system. All of the motorcoaches were equipped with air disc brakes.

Each motorcoach was tested using two primary ballast conditions. The first condition was a lightly loaded vehicle weight (LLVW) that included the weight of the test instrumentation, outriggers, and driver. The second load condition, gross person occupancy weight (GPOW), included the LLVW weight plus the addition of 175 lb. water dummies in each available passenger seat, without exceeding the gross vehicle weight rating (GVWR) of the vehicle. This condition was used to represent a reasonably high center-of-gravity load that an in-service coach may experience.

Maneuvers from the previous tractor semitrailer stability control research [[1],[2],[3]] were used to evaluate the test track performance of motorcoach stability control. Test maneuvers that were conducted included the 150 ft. constant radius (CR) increasing velocity test, the slowly increasing steer (SIS) test, the ramp steer maneuver (RSM), the half sine with dwell (HSWD), sine with dwell (SWD) and the ramp with dwell (RWD). The severity for each test maneuver was incremented either by increasing speed or increasing steering wheel angle. The SIS, CR, RSM, SWD, and HSWD maneuvers were performed on dry asphalt. Discussion regarding the HSWD was not included in this executive summary. The SIS, RSM, SWD, and RWD maneuvers were performed on the reduced friction wet Jennite. These maneuvers were used to evaluate the roll and yaw stability performance of motorcoaches on the test track. These maneuvers are representative of negotiating-a-curve, lane change, or obstacle avoidance scenarios. These maneuvers can challenge a vehicle's lateral stability leading to rollover, to a spinout (severe oversteer), or plowout (severe understeer). Discussion regarding the SIS, RSM, and SWD conducted on the wet Jennite were not included in this executive a summary.

Motorcoach 150 ft. Constant Radius Testing

Tests were conducted in both the LLVW and GPOW loading conditions, in both the left and right direction, and with ESC enabled and disabled. For all conditions tested, no instabilities were observed. With ESC disabled, the motorcoaches would reach a certain velocity and begin to lose forward traction on the inside drive wheels as the weight transferred away from the center of the radius, this was observed to limit the maximum speed achievable, no wheel lift was observed.

Constant radius tests conducted with stability control enabled showed similar results when comparing the three motorcoaches. Each of the motorcoaches' systems were

observed to reduce or limit engine torque even though the drivers were commanding more torque (pressing fuel pedal to floor) in attempts to increase speed. Review of vehicle network data revealed that ESC was not commanding the engine torque reduction. Since the motorcoaches were losing forward traction with the controller disabled it is believed that the traction control system commanded the engine torque reduction to limit wheel slip. But, this could not be confirmed since the traction control system information was not collected from the vehicles communication network. ESC was not observed to command any braking in constant radius tests conducted with MCI #1. Small amounts of braking commanded by the ESC systems were observed in constant radius tests conducted with the Prevost, and MCI #2.

Motorcoach Slowly Increasing Steer Testing

SIS maneuvers (large decreasing radius curve) were conducted to characterize the steering to lateral acceleration response for each motorcoach at 30 mph. Maneuvers were conducted under both loading conditions, with ESC enabled and disabled, and to the left and right directions.

SIS tests were conducted to evaluate the ability of the ESC systems to reduce speed by limiting engine torque as the steering wheel angle was slowly increased to a large magnitude traveling at 30 mph. Following ESC activation, the systems were observed to command reductions in engine output torque and reduce speed in all three motorcoaches.

Motorcoach Ramp Steer Maneuver Testing

RSM (similar to a J-turn) testing on the dry asphalt was completed for each motorcoach to evaluate its roll propensity while loaded in the LLVW and GPOW conditions. Tests were conducted following the RSM protocol developed for tractor semitrailers [1]. RSMs were conducted with both ESC enabled and disabled.

For RSM tests with ESC disabled and the motorcoaches loaded in the LLVW condition, wheel lift was observed for MCI #1 at a maneuver entrance speeds (MES) of 38 mph and for MCI #2 at 40 mph, while no wheel lift was observed for tests with the Prevost for the speeds tested. Testing in the GPOW condition, wheel lift was observed for the MCI #1 at 37 mph, the Prevost at 39 mph, and for the MCI #2 at 35 mph.

For RSM tests with stability control enabled and the motorcoaches loaded in the LLVW condition, no instances of wheel lift were observed over the range of speeds tested (up to 50 mph). During tests in the GPOW load condition wheel lift was not observed in either MCI over the range of speeds tested, but wheel lift was observed for the Prevost at 48 mph.

Testing on the low friction surface produced no wheel lift, but as the target MES was increased each of the motorcoaches began to plow. Data analysis revealed that the

ESC was improving each motorcoaches' position (sharper turning radius) by reducing plow.

Motorcoach Ramp with Dwell Testing

RWD (decreasing radius curve) maneuvers conducted on the wet Jennite test surface were performed in the GPOW load condition. This maneuver was added to the test matrix after the MCI #1 lease had expired. Therefore, this maneuver was performed with the Prevost and MCI #2 motorcoaches.

RWD test data indicated that both motorcoach ESC systems were commanding brake pressures in a way to limit plow out (brake pressure was biased towards the wheels closest to the inside of the curve). ESC activation occurred at the second steering increment for the Prevost and the third increment for MCI #2. The Prevost and MCI #2 experienced no instability for the ESC enabled or disabled test conditions.

RWD and RSM results from the wet Jennite surface showed that ESC was able to detect and mitigate events on reduced friction surfaces. However the observed changes between enabled and disabled tests with the same given inputs were not always discernable when comparing performance data from both motorcoaches. These types of observations showed that improvements in performance were limited to comparing an individual coach's performance with and without ESC. Pursuing a RWD or alternate performance test on reduced friction surfaces would require further maneuver design and development testing.

Motorcoach Sine with Dwell

LLVW SWD tests were performed at 50 mph and GPOW tests were performed at 45 mph on the dry asphalt. All tests were conducted with ESC enabled and disabled. The SWD tests were run using frequencies of 0.3, 0.4, 0.5, and 0.6 Hz for the sinusoid and 0.5, or 1.0 second for the dwell time. Test severity was incremented by multiplying the extrapolated steering angle at 0.5G (determined from the SIS maneuver) by a scalar from 30 to 130 percent in 10 percent increments. A test series was terminated if the motorcoach experienced wheel lift in excess of 2.0 inches (roll instability), yaw angle change greater than 90 degrees (spinout, yaw instability) was observed, or the terminating steering input scalar of 130 percent was reached.

Some test series in both the SWD and HSWD maneuvers were terminated at steering scalars less than 130 percent due to ESC malfunctions. In these series, the larger steering scalars were observed to overwhelm the motorcoach's power steering system and produced malfunctions that disabled the motorcoaches ESC system.

Neither wheel lift nor yaw instability were observed from any of the SWD tests in the LLVW load condition whether ESC was enabled or disabled. All three motorcoaches with ESC enabled were able to reduce yaw and roll angles during SWD testing. With the GPOW loading condition several instances of wheel lift were observed. While not

every series was completed with ESC enabled; ESC was able to extend the vehicle's stability to higher steering scalars before wheel lift was observed.

Each ESC system intervened with foundation braking for a majority of the maneuvers evaluated with the GPOW load condition. All three motorcoaches with ESC were able to reduce yaw angles and roll angles during SWD testing. Results from SWD testing demonstrated that the motorcoaches were fairly stable in the yaw plane and no instances of spinout were observed. Even though the motorcoaches were yaw stable, the test results demonstrated that the test was challenging the motorcoaches' roll propensity. Tests under certain conditions produced wheel lift and caused all the wheels on one side of the bus to exceed 2 inches of liftoff from the test surface.

SWD maneuvers performed with a longer dwell time were observed to produce larger dynamic responses with less steering amplitude. For the GPOW series, tests were observed to have larger maximum yaw angle responses with the 0.5 Hz frequency versus SWD series at 0.4 Hz and 0.6 Hz. Based on these observations, the 0.5 Hz SWD (1.0 second dwell) was selected as the candidate SWD maneuver used to assess transient measures of performance for ESC equipped motorcoaches.

Test track results from both the SWD conducted on dry asphalt show that the maneuvers were capable of exciting dynamic responses from vehicles of this size and weight. There were clear differences in test data between ESC enabled and disabled test series. This shows that both maneuvers are viable objective performance tests. The SWD maneuver was favored over the HSWD because it could be conducted in a smaller area, was representative of crash avoidance or lane change type maneuvers, and its previous use in Federal Motor Vehicle Safety Standard No. 126 accelerated the measure of performance research.

Measures of Performance

The SIS, RSM, and SWD test track data from the motorcoaches in the GPOW load condition were used to assess potential measures of performance. The same measures of performance developed for evaluating truck-tractors were assessed against motorcoach data. These measures indicated that ESC systems were capable of exerting control over the engine/power unit and of foundation braking control to increase stability, while maintaining the same level of maneuverability or responsiveness.

From the SIS test data, the engine torque output measures available on the vehicles' communication bus were concluded to be potential measures for indicating engine torque was reduced. In all cases, the "engine torque output" was much less than the "driver requested torque" when ESC activated and speed was reduced.

From RSM test data, the lateral acceleration ratio measure was determined to be capable of assessing the roll stability of an ESC equipped motorcoach. The metric was observed to show clear differences between ESC enabled and disabled states.

Reductions to observed lateral acceleration ratio show that the ESC systems were able to mitigate roll instabilities.

From the SWD test data, lateral acceleration ratio and yaw rate ratio were confirmed to be good measures of assessing roll and yaw responses. They were observed to show clear differences between ESC enabled and disabled states. Although the lateral stability measures showed similar results to the tractors, the lateral responsiveness measure (obstacle avoidance capability) showed that the motorcoaches produced less lateral displacement for similar speed and steering inputs. This was observed with the system enabled and disabled, indicating that the motorcoaches were naturally less responsive due to their physical characteristics and not a result of ESC interventions.

Overall, this research indicated that ESC equipped motorcoaches could possibly use similar objective performance maneuvers to those that were developed for tractors. This research demonstrated that similar performance measures could be used to assess lateral stability, while responsiveness criteria would need to be lower for motorcoaches than for tractors. While some of these measures could be used, the results did show that there were some characteristic differences between tractors and motorcoaches.

1 INTRODUCTION

The research detailed in this report supports The Motorcoach Safety Action Plan [4] released by the Department of Transportation (DOT) on November 16, 2009 and ongoing safety research by DOT's National Highway Traffic Safety Administration (NHTSA). The plan released by DOT acknowledges that motorcoach travel is a safe mode of transportation in the United States. However, motorcoach crashes result, on average, in 19 motorcoach occupant fatalities per year with additional fatalities among the pedestrians, drivers, and passengers of other vehicles involved in these crashes. The plan identifies several motorcoach safety issues and planned actions to address outstanding safety problems.

From an analysis of motorcoach crashes, several causes and contributing factors were identified as opportunities to enhance motorcoach safety. These included: driver errors resulting from fatigue, distraction, medical conditions, and inexperience; vehicle maintenance and safety; and passenger motor carrier regulatory compliance. Improvements in motorcoach safety by the addition of crash avoidance technologies, and measures to protect occupants in the event of a crash such as seat belts, roof strength, fire safety, and emergency egress, are also included for consideration in the plan. This document covers NHTSA's Vehicle Research and Test Center's (VRTC) test track research on motorcoaches equipped with Electronic Stability Control (ESC) systems. This crash avoidance technology was identified in the plan as a potential motorcoach safety enhancement designed to improve stability in rollover and loss-of-control scenarios.

Heavy vehicle stability control systems have been developed to help reduce crashes involving rollover and loss-of-control of truck tractors, motorcoaches and other heavy vehicles. ESC is a crash avoidance technology that can mitigate roll and/or yaw instabilities. To mitigate on-road, un-tripped rollovers the ESC systems automatically decelerate the vehicle by reducing engine torque and applying the foundation brakes. To mitigate plow out (severe understeer) or spinout (severe oversteer) conditions associated with vehicle loss of yaw control, ESC systems automatically reduce engine torque and apply selective brakes to generate a restoring yaw moment that helps the driver maintain directional control of the vehicle. To test the performance capabilities of these systems, test track maneuvers developed for truck-tractors were used to evaluate motorcoach stability. The test data from this research were then used to determine if the previously developed maneuvers and measures of performance could be used to objectively assess motorcoach stability.

1.1 **Background**

Researchers at the agency's Vehicle VRTC in East Liberty, Ohio, initiated a test program in 2006 to evaluate the performance of heavy vehicle stability control systems under controlled conditions on a test track. An outcome of that work was to develop objective test procedures and measures of performance that could form the basis of a new federal motor vehicle safety standard. At that time ESC was only available on a limited number of commercial truck tractors. The test vehicles included three tractors

equipped with stability control. By 2008 more types of commercial vehicles were available with ESC including motorcoaches. In this study three motorcoaches equipped with ESC were leased and evaluated on the test track.

The previous research conducted with commercial truck-tractors is documented in two Department of Transportation (DOT) reports. Phase I and II research results are documented in the report titled “Tractor Semitrailer Stability Objective Performance Test Research – Roll Stability” (DOT HS 811 467) [1]. Results from Phase I are also summarized in the paper “NHTSA’s Class 8 Truck-Tractor Stability Control Test Track Effectiveness” (ESV 2009. Paper No. 09-0552) [2]. Phase III of that research is documented in the report titled “Tractor Semitrailer Stability Objective Performance Test Research – Yaw Stability” [3]

1.2 Study Objectives

For this research, NHTSA performed objective testing of commercially available motorcoaches equipped with ESC systems. The goals of this testing were to evaluate the lateral stability performance and:

1. Understand how motorcoach ESC systems modify the handling characteristics as compared to the base vehicle without ESC.
2. Understand how adding passengers can modify and influence ESC performance.
3. Determine if the maneuvers used for truck-tractor ESC research are feasible for testing motorcoaches.
4. Determine if the maneuvers can discriminate between motorcoaches with and without ESC technology.
5. Determine if the truck-tractor measures of performance are capable of assessing the lateral stability of motorcoaches.

2 TEST METHOD

2.1 Test Vehicles

Three motorcoaches were used for the research described in this report: two 2007 MCI D4500 motorcoaches and a 2009 Prevost H3. The following sections provide descriptions of each motorcoach, test instrumentation, and the safety equipment used in performing this research. For complete detailed information on each motorcoach, please refer to Appendix B

Testing with the first MCI motorcoach was limited due anti-rollover safety outriggers prematurely engaging the test surface before wheel lift (indication that motorcoach is near its rollover threshold) was observed (all the wheels remained in contact with the test surface). As a result, a second MCI motorcoach was leased and different outriggers were utilized to allow greater roll angles and outrigger to surface clearance.

The MCI motorcoaches were equipped with Meritor WABCO ESC system and the Prevost was equipped with a Bendix ESC system. Only ESC was offered on motorcoaches, thus a motorcoach equipped with a roll stability control (RSC, available on truck-tractors) system was not evaluated. Each motorcoach was equipped with air disc brakes. Both of the MCIs tested had a GVWR of 48,000 lb and a wheel base of 317 in. The Prevost tested (herein referred to as Prevost) had a GVWR of 53,000 lb and a wheel base of 317 in. Table 2.1 presents the year, make, model, type, wheelbase, and ESC supplier for the motorcoaches used in this study.

Table 2.1. Motorcoaches tested.

Year	Make	Model	Type	Wheel base (inches)	ESC Supplier
2007	MCI	D4500	Tour/Charter	317	Meritor WABCO ESC
2009	Prevost	H3	Tour/Charter	317	Bendix ESC
2007	MCI	D4500	Tour/Charter	317	Meritor WABCO ESC

2.2 Instrumentation

The three motorcoaches evaluated were instrumented with sensors, data acquisition systems, and a programmable steering machine. This section briefly describes the test equipment and instrumentation used. For detailed information, please refer to Appendix C. Table 2.2 describes the sensors used by NHTSA to measure vehicle responses. Sensors are listed with the data channel measured in the first column of the table. Additional columns list the sensor type, sensor range, sensor manufacturer, and sensor model number.

CAN data from the SAE J1939 [13] and/or SAE J1708 [14] bus were recorded when available.

Table 2.3 describes the Suspect Parameter Numbers (SPNs) that were recorded when available. Signals are listed with the data channel measured in the first column of the

table. Additional columns list the Suspect Parameter Number (SPN), data length, resolution, data range, and type of measure.

Table 2.2. Motorcoach sensor information.

Data Measured	Type	Range	Manufacturer	Model Number
Steering Wheel Angle	Angle Encoder	±720 degrees	Automotive Testing, Inc.	Integral with ATI Steering Machine
Brake Treadle Application	Switch (normally open)	On/Off	NA	NA
Throttle Position	Direct tap OEM sensor	0-4.5 volts	NA	NA
Longitudinal, Lateral, Vertical Acceleration Roll, Yaw, Pitch Rate	Multi-Axis Inertial Sensing System	Accelerometers: ±2 g, Angular Rate Sensors: ±100°/s	BEI Technologies, Inc., Systron Donner Inertial Division	MotionPak Multi-Axis Inertial Sensing System MP-1
Frame Rail Height(L/R) (to determine roll)	Non-contact infrared beam	12-51 inches	Wenglor	HT77MGV80
Rear Axle Height(L/R) (to determine lift)	Non-contact infrared beam	14-35 inches	Wenglor	HT66MGV80
Vehicle Speed	GPS Non-contact 100 Hz speed and distance	0.1-1000 mph	RaceLogic	VBOX III SPS 100HZ Gps Speed Sensor
Glad Hand valve pressure	Volt Output pressure transducer	0-200 psi	Transducers Direct.	TDG-AD2F2002GAA0022

Table 2.3. J1939 vehicle bus information.

Data Recorded	Suspect Parameter Number	Data length	Resolution	Data Range	Type
Accelerator pedal Position 1	SPN 91	1 byte	0.4%/bit, 0 offset	0 to 100 %	Measured
VDC Fully Operational	SPN 1814	2 bits	4 states/ 2 bit, 0 offset	0 to 3	Status
VDC Brake Light Request	SPN 1815	2 bits	4 states/ 2 bit, 0 offset	0 to 3	Status
VDC ROP Engine Control Active	SPN 1816	2 bits	4 states/ 2 bit, 0 offset	0 to 3	Status
YC Engine Control Active	SPN 1817	2 bits	4 states/ 2 bit, 0 offset	0 to 3	Status
ROP Brake Control Active	SPN 1818	2 bits	4 states/ 2 bit, 0 offset	0 to 3	Status
YC Brake Control Active	SPN 1819	2 bits	4 states/ 2 bit, 0 offset	0 to 3	Status
Actual Engine – Percent Torque	SPN 513	1 byte	1%/bit, -125 % offset	-125 to 125 %	Measured
Drivers Demanded Engine – Percent Torque	SPN 512	1 byte	1%/bit, -125 % offset	-125 to 125 %	Measured

2.3 Steering Controller

A programmable steering machine produced by Automotive Testing, Inc. (ATI) was used to provide steering inputs for all motorcoach test maneuvers. Descriptions of the

steering machine, including features and technical specifications, have been previously documented [15] [16].

2.4 Load Conditions

Each motorcoach was tested using two primary ballast conditions. The first condition was a lightly loaded vehicle weight (LLVW) that included the weight of the test instrumentation, outriggers, three-quarters full tank of fuel, and driver. The second load condition, gross person occupancy weight (GPOW), included the LLVW weight plus the addition of 175 lb. water dummies in each available passenger seat without exceeding the gross vehicle weight rating (GVWR) of the vehicle. This condition was used to represent a reasonably high CG load that an in-service coach may experience. For information about the loading conditions, see Appendix D.

2.5 Testing Surface and Ambient Conditions

All tests were performed on the Transportation Research Center, Inc. (TRC) Vehicle Dynamics Area (VDA) located in East Liberty, Ohio. The VDA is an 1800 by 1200 foot flat paved surface with a one percent longitudinal grade for drainage. Turn-around loops are provided on each end to facilitate high speed entry onto the VDA. The surface was paved with an asphalt mix representative of that used on many Ohio highways. Located on the VDA at the south end is a 301 by 555 foot reduced friction surface (Jennite pad). The Jennite pad consists of wet sealed asphalt with a peak coefficient of friction of 0.3-0.5.

The tests discussed in this study were performed between November 2008 and November 2009. All tests were performed while the VDA high-friction test surface was dry and all tests performed on the Jennite low-friction test surface were wet. Figure 2.1 summarizes the VDA's dry and Jennite's wet peak and slide coefficients of friction for the dates relevant to the 2008-09 test seasons. The peak and sliding coefficients of friction were generally monitored twice per month, weather-permitting, using American Society for Testing and Materials (ASTM) procedures. The peak coefficient was determined with ASTM procedure E1337 and an E1136 tire [18] [19]. Sliding coefficients were determined with ASTM procedure E274 and an E50 [20] [21].

The ambient temperatures and wind speeds were recorded at the beginning of each test session. The ambient air temperature ranged from 27 to 82 degrees Fahrenheit. The wind speeds ranged from 0 to 30 mph.

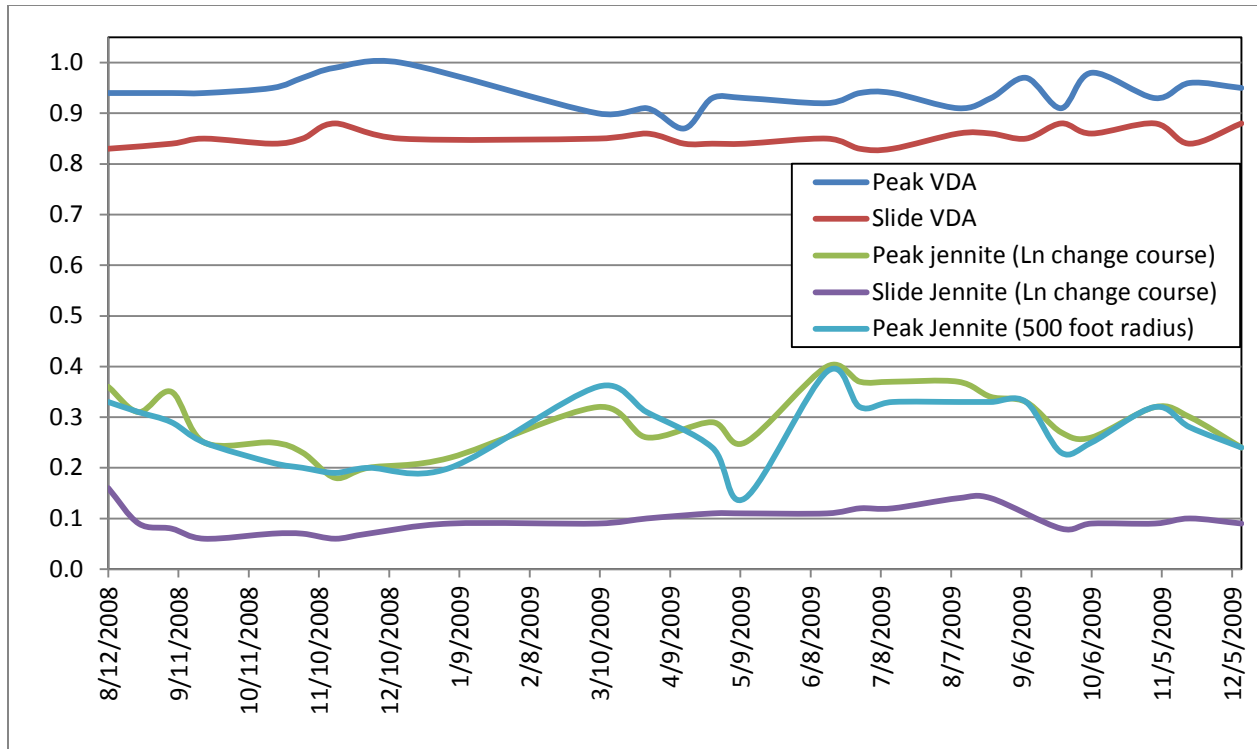


Figure 2.1. TRC VDA dry and Jennite wet peak and slide coefficients of friction for the testing period.

2.6 Test Maneuvers

A collection of maneuvers from Phases I – III for the tractor semitrailers were used to evaluate the test track performance of motorcoaches equipped with stability control. Test maneuvers conducted included the 150 ft. Constant Radius (CR) increasing velocity test, the Slowly Increasing Steer (SIS) maneuver, the Ramp Steer Maneuver (RSM), the Ramp with Dwell (RWD), the Sine with Dwell (SWD), and Half-Sine with Dwell (HSWD) maneuvers. These tests were used to evaluate the following:

- CR - evaluates the vehicle's reaction to "slower" dynamics and to evaluate the ESC's ability to mitigate roll instability in constant radius curves or circle maneuvers.
- SIS – allows evaluation of the vehicle's reaction to "slower" dynamics and to evaluate ESC's ability to mitigate instability in slowly decreasing radius curves maneuvers. Test data from SIS maneuvers were also used to determine the unique dynamic characteristic relationships (such as steering wheel angle to lateral acceleration gain) for each test vehicle. This characterization data were then used to normalize the steering inputs across different maneuvers and test conditions.
- RSM - evaluates the responsiveness to "faster" dynamics and simulates negotiating an exit ramp (no banking/super elevation) or decreasing radius curve.

- RWD - evaluates a vehicle's ESC system's yaw control and stability on a low friction surface in a prescribed curve with a decreasing radius.
- SWD – allows evaluation of the vehicle's reaction to “faster, transient input” dynamics and simulates an obstacle avoidance or lane change maneuver.
- HSWD – allows evaluation of the vehicle's reaction to “faster” dynamics and simulates negotiating a curve.

These tests were conducted using a steering robot, except for the constant radius maneuvers. Severity for each test maneuver was incremented either by increasing speed or increasing steering wheel angle. The following subsections provide brief descriptions for these maneuvers. For detailed maneuver test procedures see Appendix A.

2.6.1 Constant Radius Maneuver (CR)

Constant radius circles with increasing velocity tests were conducted on the 150-foot radius circles located on the center of the VDA. For this maneuver, the test driver followed the radius with either the passenger side steer tire (clockwise) or the driver side steer tire (counter-clockwise) while slowly increasing the vehicle's speed. As speed increased, the driver steered the vehicle to maintain the radius as the vehicle tended to understeer. The test was complete when:

- the driver was no longer able to follow the radius (vehicle plows out)
- could no longer increase velocity (drive axles loses traction)
- ESC activates and limits the velocity through a reduction to engine torque output and/or applies the brakes
- the wheels lifted more than 2 inches off the ground (outriggers making contact with the test surface).

2.6.2 Slowly Increasing Steer Maneuver (SIS)

The SIS test maneuver, developed in Phase II, was adapted from Society of Automotive Engineers (SAE) Surface Vehicle Recommended Practice J266. It is also described as the Constant Speed Tests – Variable Radius or Variable Steer Angle maneuver [23]. The maneuver is specifically recommended to characterize steady-state directional control properties for light passenger vehicles and has been adapted to normalize steering inputs for maneuvers¹ used by the Agency to evaluate dynamic stability. Like light passenger vehicles, various motorcoach configurations have different lateral acceleration to steering wheel gains that can be characterized using the SIS maneuver. SIS test results were extrapolated to determine the magnitude of steering input for the RSM, SWD, and HSWD maneuvers.

¹ Similar steering wheel input normalization methodology was developed for the NCAP Fishhook Test [24] [25] and for the 0.5 Hz Sine with Dwell Maneuver documented in [26].

SIS tests were conducted at a constant speed of 30 MPH. Using the steering controller, the test increased the steering wheel angle at 13.5 degrees/second until a magnitude of 400² degrees or greater was achieved. Using the maneuver a total of six tests were performed per test series. First, three were conducted with a left steering input followed by three with a right steering input. Tests were concluded when the maximum hand wheel angle was achieved, ESC intervened, or the vehicle experienced wheel lift. Figure 2.2 shows an example of the steering wheel profile used to perform the SIS maneuver.

Upon completing the test series, the average steering wheel angle needed to produce 0.5 g of lateral acceleration was extrapolated from the linear regression of the steering wheel angle and lateral acceleration measurements. That steering wheel angle was then used as the steering input magnitude for the RSM. This same angle was also scaled from 30 percent to 130 percent for use with the SWD, and HSWD maneuvers.

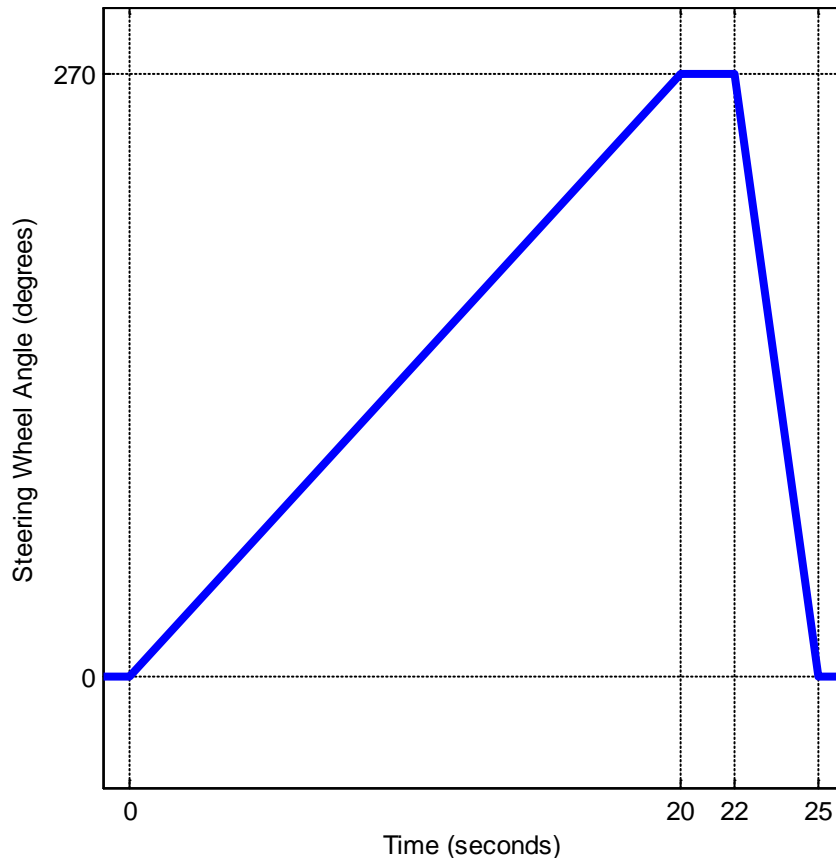


Figure 2.2. Example of the steering wheel profile used for SIS tests.

² To make comparisons between ESC enabled and disabled SIS tests, larger steering amplitudes were used for some test series to obtain stability control activation levels.

2.6.3 Ramp Steer Maneuver (RSM)

The RSM is similar to a path-following J-Turn maneuver. The RSM is based on a steering wheel input at a constant rate until a target steering magnitude is achieved. Automated steering robots were used to achieve precise steering wheel magnitudes and rates. The RSM can be manipulated by either changing the rate or the magnitude of the steering controlled maneuver. The RSMs documented in this report utilized fixed steering wheel magnitude (from the SIS data, see 2.6.2) and a fixed rate (175 deg/sec). Test severity was controlled by incrementally increasing the maneuver entrance speed (MES) from 20 mph by 2 mph increments. In a limited number of tests the entrance speed was incremented in 1 mph increments when the test vehicles began to exhibit signs of instability. The definition of the RSM is shown graphically in Figure 2.3 which shows the steering wheel profile and specific timing marks of interest. Time zero marks the initiation of the maneuver, the magnitude is equal to δ^{Test} , and "t" is equal to $\delta^{Test}/175$ deg/sec. If any of the following were observed the test series was terminated:

1. Vehicle observed to be stable at 50 mph entrance speed
2. Wheel lift greater than 2 inches at the motorcoach's drive axle
3. Wheel lift greater than 2 inches at the motorcoach's steer axle

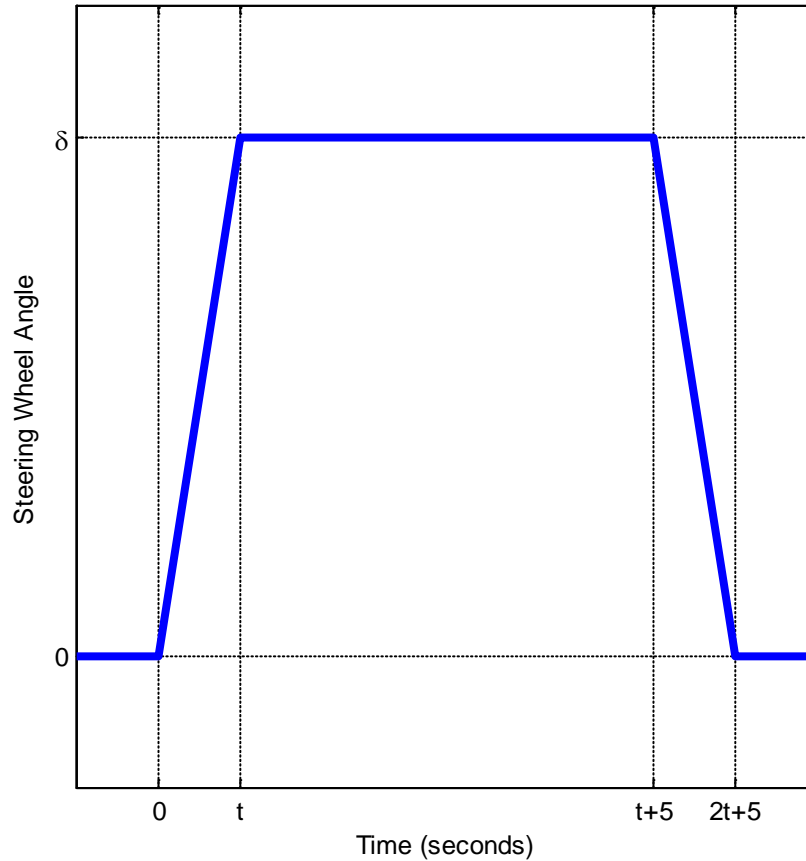


Figure 2.3. Steering wheel profile used for RSM tests.

2.6.4 Sine with Dwell Maneuver (SWD)

The SWD maneuver was based on a single cycle of sinusoidal steering input with a given frequency. Although the peak magnitudes of the first and second half cycles were identical, the SWD maneuver included a 0.5 or 1.0 second pause or “dwell” after completion of the third quarter-cycle of the sinusoid. A generic steering wheel angle profile is shown in Figure 2.4. For discussion on steering frequency, amplitude and controlling maneuver severity see the following section 2.6.5.

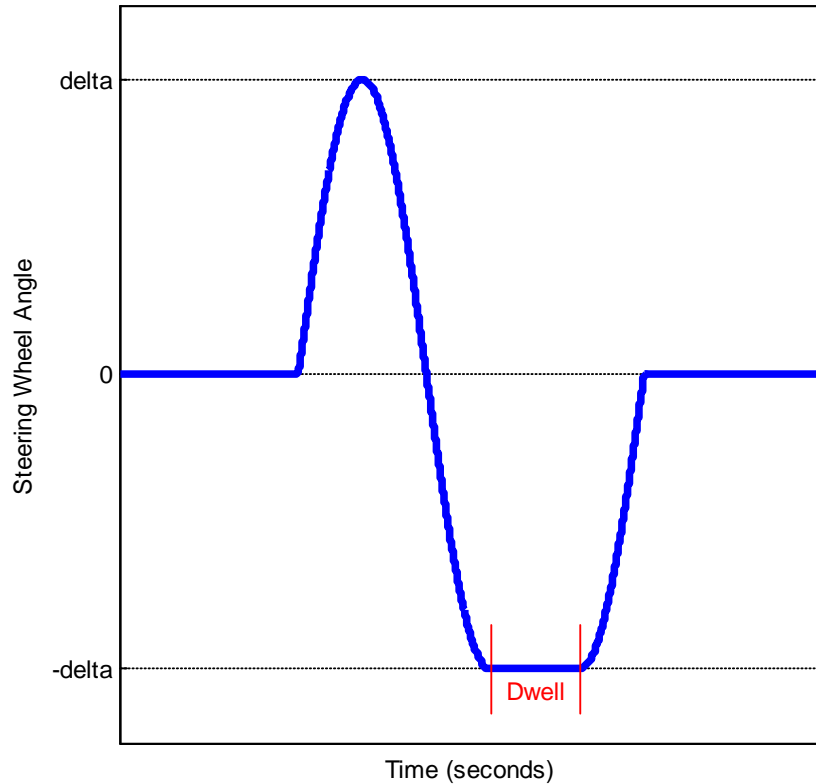


Figure 2.4. Sine with Dwell profile

2.6.5 Half-Sine With Dwell Maneuver (HSWD)

The HSWD maneuver was based on half of a single cycle of sinusoidal steering input. The HSWD maneuver included a 0.5 or 1.0 second dwell after completion of the first quarter-cycle of the sinusoid. A generic steering wheel angle profile is shown in Figure 2.5.

SWD and HSWD Steering Input Frequency

For the SWD and HSWD maneuvers, the duration or period over which the maneuvers were conducted was changed by incrementing the steering input frequency. A range of frequencies between 0.3 and 0.6 Hz were evaluated since there was no prior testing experience with motorcoaches to suggest that a narrow range of input frequencies could be utilized. These frequencies were found to cover the intermediate to upper end of frequency response spectrum for these vehicles.

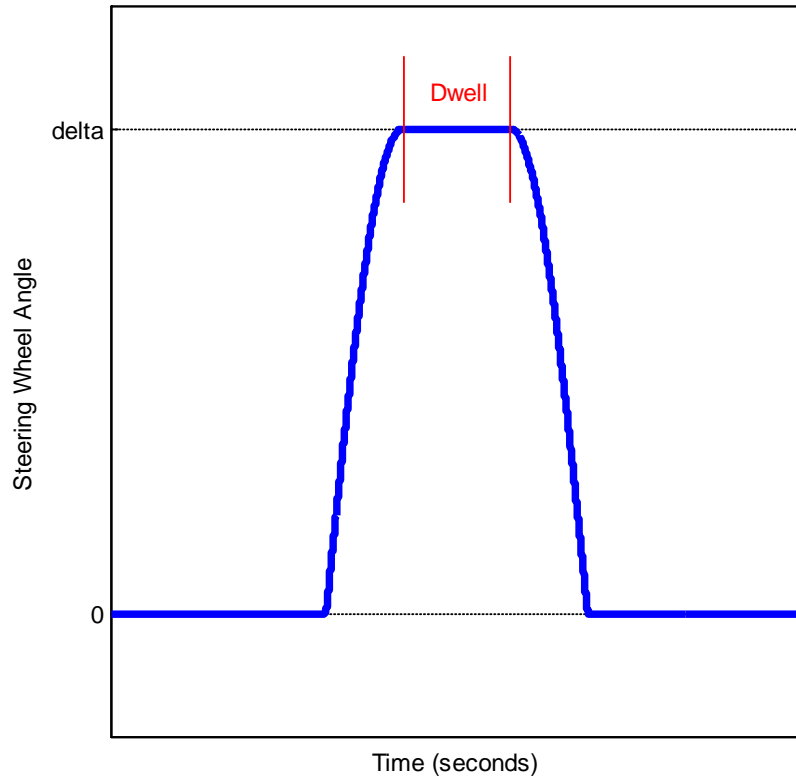


Figure 2.5. Half-cycle Sine with Dwell profile

SWD and HSWD Steering Input Amplitude

For both the Sine with Dwell (SWD) and the Half Sine with Dwell (HSWD) maneuvers the entrance speed was fixed and the steering amplitude was incremented through a series of steering scalars in subsequent maneuver runs. Test series were performed at 45 and 50 mph. To control maneuver severity for a given speed, the steering amplitude increments started at 30 percent of SWA at 0.5g (from SIS data, see 2.6.2) and were increased in 10 percent increments to 130 percent of the SWA at 0.5g for a given input speed. Steering amplitudes and frequencies were controlled by an automated steering robot. If the vehicle achieved the maximum amplitude without an excessive yaw angle or wheel lift the series was terminated. If any of the following were observed the test series was terminated:

1. Yaw Angle in excess of 90 degrees from original path
2. Wheel lift greater than 2 inches of the motorcoach drive axle
3. Wheel lift greater than 2 inches of the motorcoach steer axle

2.6.6 Ramp With Dwell (RWD) Maneuver

The Ramp with Dwell maneuver developed by the commercial vehicle industry was considered for evaluating motorcoaches equipped with ESC systems. The maneuver was designed to use the wet Jennite surface used for Federal Motor Vehicle Safety Standard (FMVSS) No. 121 [17] antilock brake system testing. The tests primary focus was on isolating yaw control on a low friction surface. The RWD steering profile is based on a steering wheel input at a constant rate until a magnitude is achieved similar to the RSM in example Figure 2.3. The RWD is different from the RSM because the steering angle is not at zero degrees when the maneuver is initially executed. In Figure 2.6 δ_{dt} is the drive through angle needed to negotiate a 500 ft. radius curve on the Jennite surface at the maximum drive through speed. From the initial drive through angle, the steering input is ramped in 1.0 second to the desired magnitude, and then held at that magnitude for 3.0 seconds. Then, in 1.0 second the steering angle is returned to zero degrees and the maneuver is complete. The maneuver amplitudes were determined by multiplying a constant (K) integer with a value from 2 to 6 times the characterization drive through angle rounded to the nearest 90 degrees. For each test K is increased by 1 until ESC activation occurs. These maneuvers were performed with an automated steering robot.

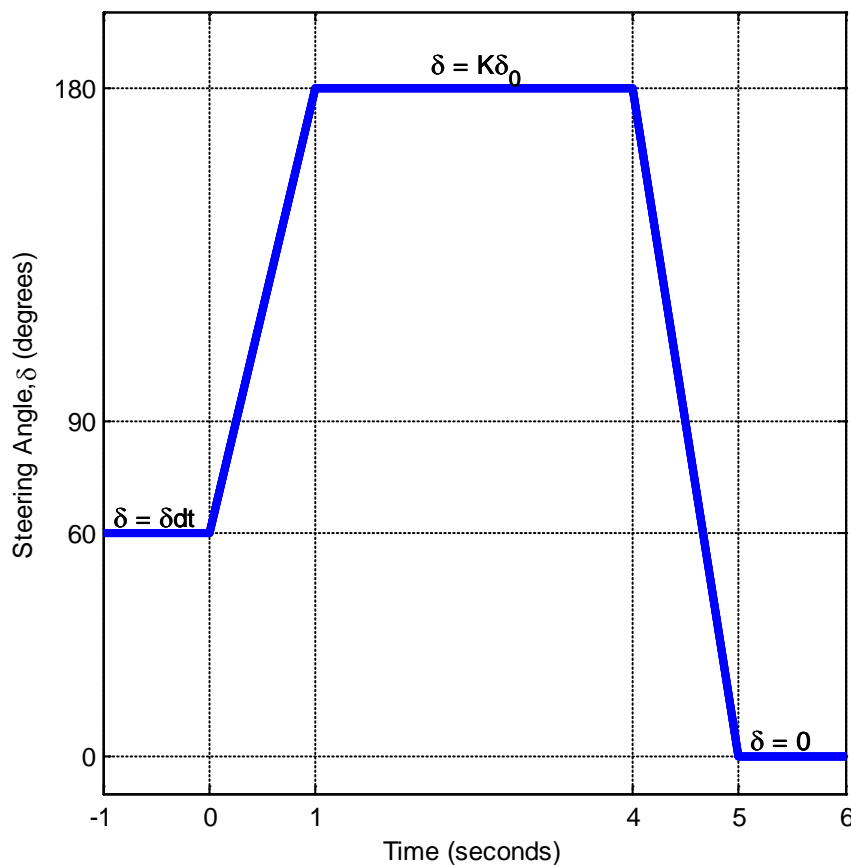


Figure 2.6. Example of steering wheel profile used for RWD tests.

3 PERFORMANCE MANEUVER RESEARCH

The input parameters used to define the test maneuvers were manipulated to evaluate motorcoach lateral stability. Table 3.1 and Table 3.2 shows the test matrices used to explore parameters such as frequency, amplitude, speed, load, and dwell time. Maneuvers shown in Table 3.1 were conducted on dry high friction asphalt. Maneuvers shown in Table 3.2 were conducted on the reduced friction wet Jennite test surface.

Table 3.1. Maneuvers and parameters used on dry asphalt (0.96 peak friction co-efficient) test surface.

Maneuver	Frequencies/Rates	Dwell Time (sec)	Load Conditions	Entrance Speed (mph)
CR	Driver	Driver	GPOW	0-Maximum
SIS	13.5 deg/sec	2.0	LLVW, GPOW	30
RSM	175 deg/sec	5.0	LLVW, GPOW	20-50
SWD	0.3,0.4,0.5,0.6 Hz	0.5,1.0	LLVW, GPOW	50,45
HSWD	0.3,0.4,0.5,0.6 Hz	0.5,1.0	LLVW, GPOW	50,45

Table 3.2. Maneuvers and parameters used on wet Jennite (0.3 peak friction co-efficient) test surface.

Maneuver	Frequencies/Rates	Dwell Time (sec)	Load Conditions	Entrance Speed (mph)
SIS	27 deg/sec	2.0	LLVW, GPOW	30
SWD	0.2,0.3,0.4,0.5	0.5,1.0	LLVW, GPOW	30
RSM	175 deg/sec	5.0	LLVW, GPOW	20-40
RWD	t=1 sec. to SWA 500ft.	3.0	GPOW	20 – Max. Drive-Through

The maneuvers shown in the test matrices were performed with each motorcoach and ESC system. The matrices were completed with the ESC systems disabled and enabled.

3.1 150 foot Constant Radius Test Results

Tests were conducted following a 150-foot constant radius (CR) circle by slowly increasing vehicle speed to evaluate the ability of ESC to improve roll stability in a steady state maneuver with a high C.G. load. Tests were conducted with and without ESC enabled, with the GPOW load condition on the high friction dry asphalt. In each test with ESC disabled, the motorcoach would begin to lose forward traction at the drive wheels (closest to the center of the radius) as the velocity increased, limiting the maximum speed achievable. This is an indication that the normal forces being applied on the inside wheels of the drive axle are very light due to weight transfer as the body rolls. The motorcoaches were observed to be both yaw and roll stable for the GPOW load condition with ESC enabled and disabled.

Table 3.3 and Table 3.4 summarize the results in terms of maximum speed and lateral acceleration achieved during the maneuver for the GPOW load condition. The speeds and lateral accelerations were representative of all runs in a series including both clockwise and counter-clockwise maneuvers.

Comparing the maximums obtained for each vehicle during the maneuver, the MCI #1 was able to achieve a maximum speed of 34 mph and a lateral acceleration of 0.53 g with stability control enabled; no tests were conducted with stability control disabled.

The Prevost in the GPOW load condition with ESC disabled achieved a maximum speed of 33 mph and a lateral acceleration of 0.49 g. With ESC enabled the maximum speed achieved was 26 mph that produced a lateral acceleration of 0.30 g. No instabilities were observed. For the ESC disabled test series no instabilities were observed, but the drive wheels started to lose traction.

For the MCI #2 in the GPOW load condition a maximum speed of 30 mph and a lateral acceleration of 0.42 g were attained with ESC disabled. With the ESC system enabled the maximum speed achieved was 28 mph with a lateral acceleration of 0.35 g and no instabilities were observed. For the ESC disabled test series no instabilities were observed, but the drive wheels started to lose traction.

Table 3.3. Maximum speed obtained during the constant radius increasing velocity tests.

Tractor	CR Test Results (mph)		
	Load Condition	ESC Condition	
		Enabled	Disabled
MCI #1	GPOW	34*	NT
Prevost	GPOW	26	33**
MCI #2	GPOW	28	30**

* Test series consisted of 1 maneuver.

** Drive wheels lost traction.

Table 3.4. Maximum lateral acceleration observed during the constant radius increasing velocity tests.

Tractor	CR Test Results (g)		
	Load Condition	ESC Condition	
		Enabled	Disabled
MCI #1	GPOW	0.53*	NT
Prevost	GPOW	0.30	0.49**
MCI #2	GPOW	0.35	0.42**

* Test series consisted of 1 maneuver.

** Drive wheels lost traction.

Figure 3.1, Figure 3.3, and Figure 3.5 present time history data of the CR maneuver in the GPOW load condition for each motorcoach. Each figure shows the steering wheel angle, speed, lateral acceleration, longitudinal acceleration, yaw rate, roll angle, wheel height, and throttle position. Each figure shows one counter-clockwise maneuver with ESC enabled and disabled (except for MCI #1). Blue pentagrams denote ESC activation. Following the figures described above are Figure 3.2, Figure 3.4, and Figure 3.6, respectively. These figures show engine torque, driver torque, retarder torque, and the brake pressure observed at each wheel for the ESC enabled maneuver.

In Figure 3.1 for the MCI #1, only ESC enabled time history data are shown. At the time of this testing, no maneuvers were conducted with ESC disabled so no comparisons can be made. Looking at the lateral acceleration trace and the ESC activation marker, it can be observed that lateral acceleration still continues to build for a short period of time before leveling off. Shown in Figure 3.2 are the torque and brake pressure time history data that show only engine torque reduction is occurring at ESC activation. Engine torque reduction can be observed by the separation between driver demanded and the engine torque signals at the ESC activation marker. Driver demanded torque gradually increased to 100 percent and engine torque gradually decreases to zero percent. As the dynamics change following ESC activation, engine torque was allowed to increase. All brake pressures were at zero psi for the duration of the maneuver.

In Figure 3.3 for the Prevost ESC, enabled and disabled time history data are shown. Comparing the enabled to disabled tests, ESC was able to limit lateral acceleration and speed while reducing the roll angle. In the ESC disabled test using the ESC activation marker as a reference speed, lateral acceleration and roll angle both continue to build until the drive wheels lose traction. Shown in Figure 3.4 for the ESC enabled test, both torque reduction and a small amount of braking can be observed.

In Figure 3.5 for the MCI #2 both ESC enabled and disabled, time history data are shown. Comparing the ESC enabled to the ESC disabled tests, ESC was able to limit lateral acceleration and speed while reducing the roll angle. In the ESC disabled test using the ESC activation marker as a reference speed, lateral acceleration and roll angle both continue to build until the drive wheels loose traction. Once the drive wheels lost traction, speed, lateral acceleration, and roll angle resembled the ESC enabled test. Shown in Figure 3.6 for the ESC enabled test both torque reduction and a small amount of braking can be observed.

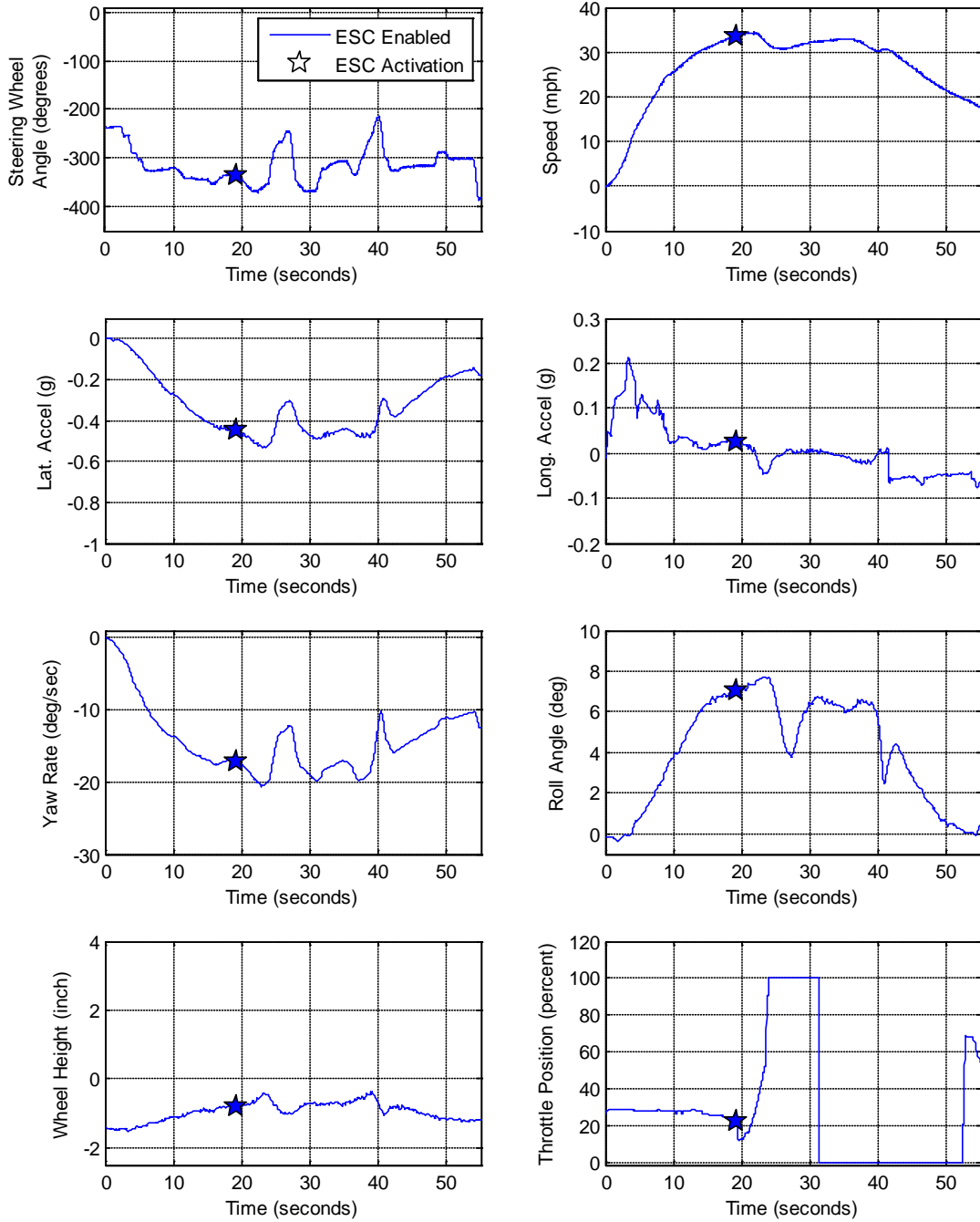


Figure 3.1. Graphs show test data from the MCI #1 CR maneuver counter-clockwise in the GPOW load condition with ESC enabled only.

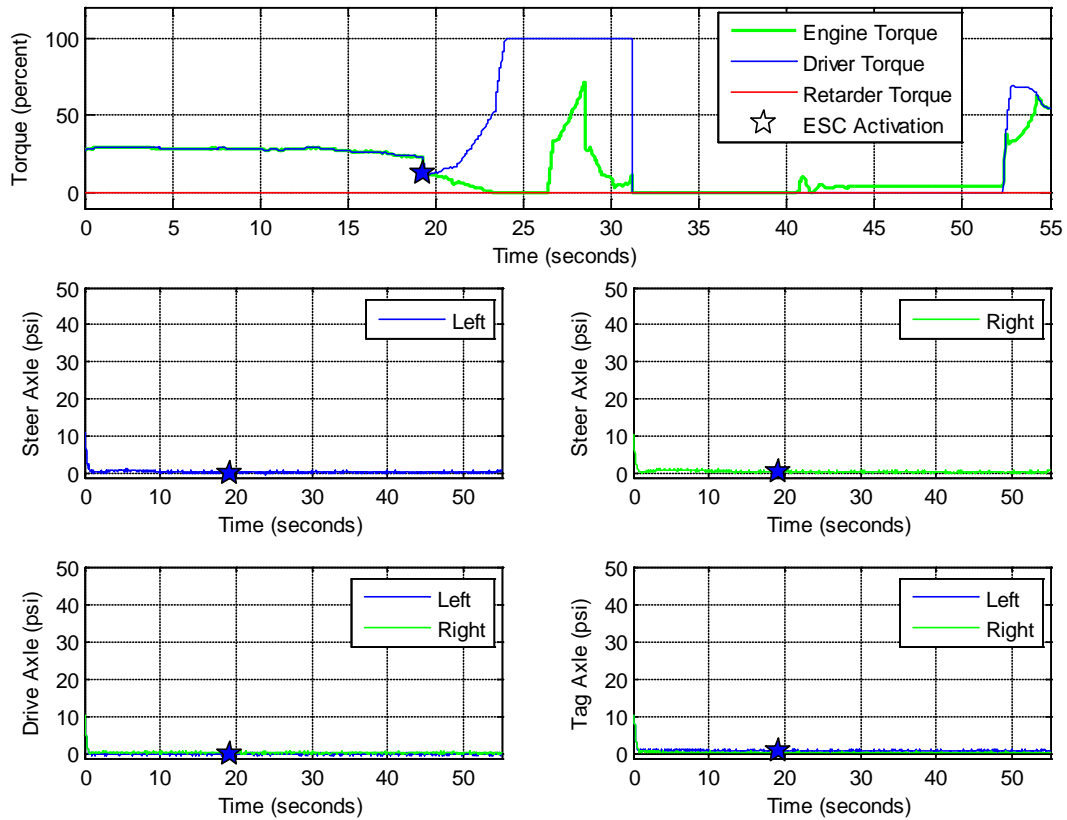


Figure 3.2. Graphs show torque and brake pressure test data from the MCI #1 CR maneuver in the GPOW load condition with ESC enabled only. At ESC activation, the driver requested 100 percent throttle.

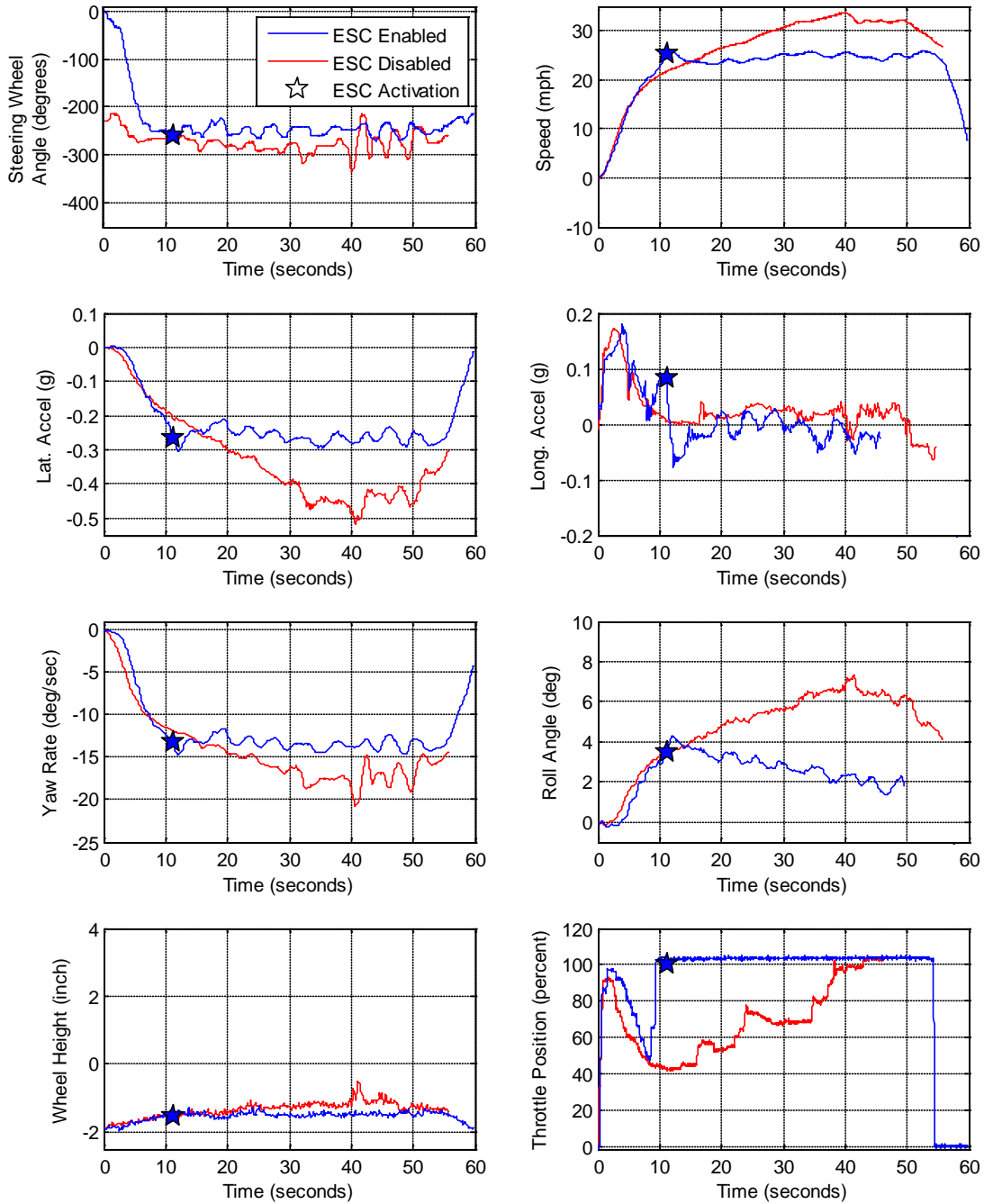


Figure 3.3. Graphs show test data from the Prevoist CR maneuver in the GPOW load condition with ESC enabled and disabled. The ESC disabled test is shown in red and the ESC enabled test is shown in blue.

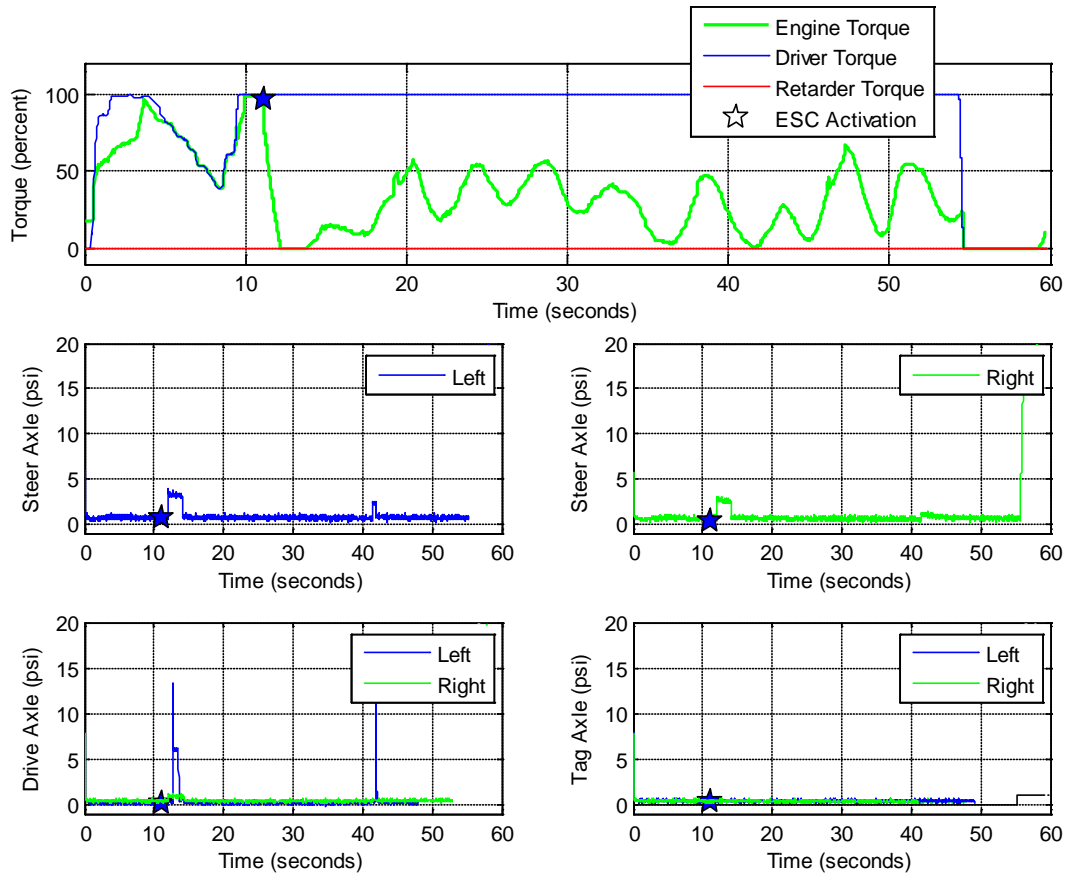


Figure 3.4. Graphs show torque and brake pressure test data from the Prevost CR maneuver in the GPOW load condition with ESC enabled only. At ESC activation the driver requested 100 percent throttle.

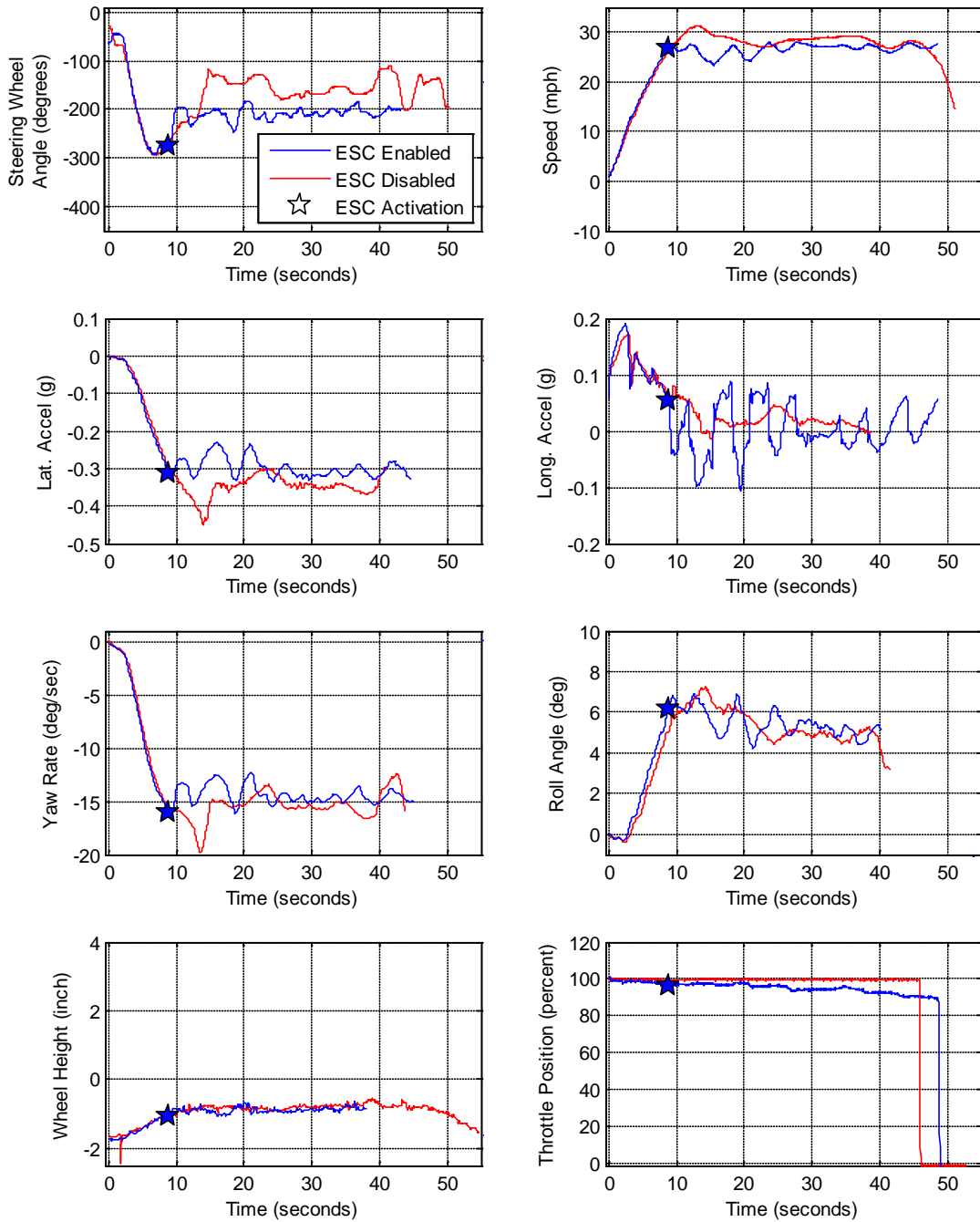


Figure 3.5. Graphs show test data from the MCI #2 CR maneuver in the GPOW load condition with ESC enabled and disabled. The ESC disabled test is shown in red and the ESC enabled test is shown in blue.

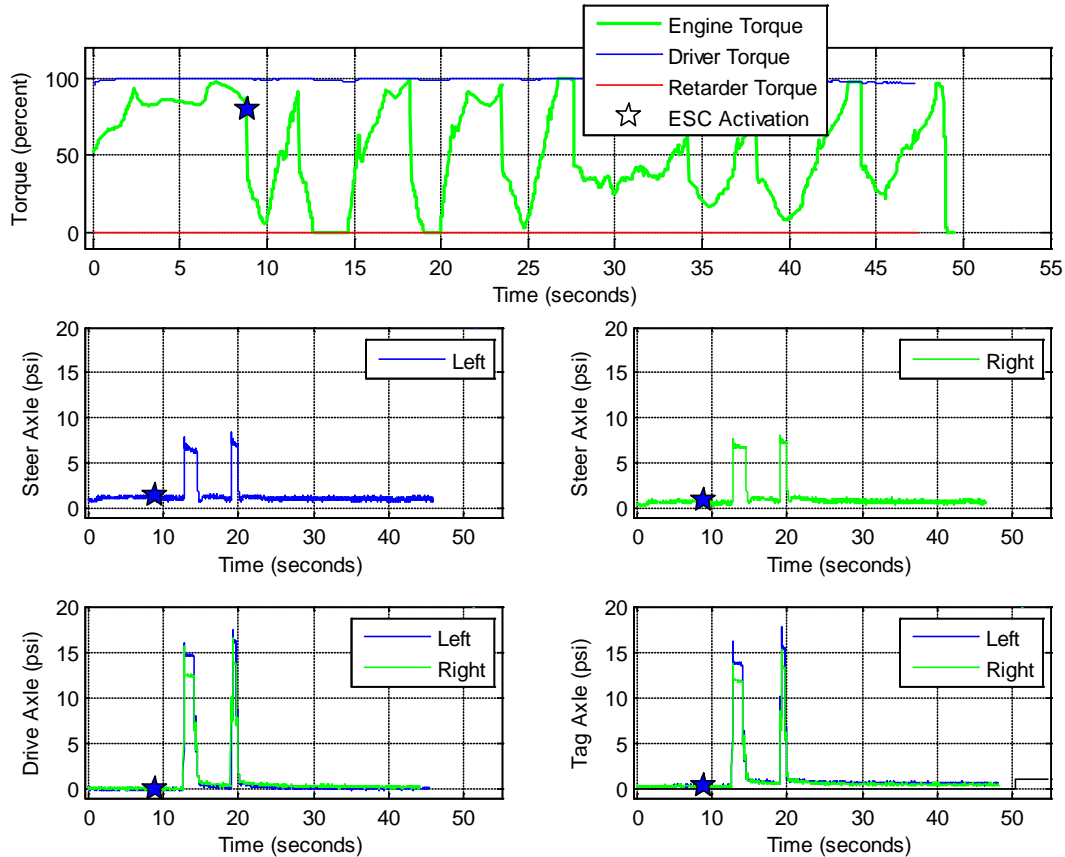


Figure 3.6. Graphs show torque and brake pressure test data from the MCI #2 CR maneuver in the GPOW load condition with ESC enabled only. At ESC activation the driver requested 100 percent throttle.

3.2 SIS Test Results

This section presents the SIS test results conducted with each of the motorcoaches. These test series were conducted in the LLVW and GPOW load condition with ESC enabled and disabled. The following subsections present results for each motorcoach with ESC enabled and disabled, and show changes to vehicle behavior from ESC intervention. The remaining sections are devoted to the characterization and linear regression analysis performed with SIS test results.

3.2.1 Vehicle Dynamics Changes from ESC Intervention

The ESC systems all responded similarly in the SIS test maneuver, regardless of vehicle, ESC system, or load condition. As the steering input was increased in a slow linear manner, the system eventually activated by applying the brakes and reducing engine torque output which in turn reduced the vehicle speed so that lateral acceleration was limited as the radius of the vehicle path continued to decrease. With ESC enabled, none of the SIS tests resulted in terminal understeer (plow), oversteer (spin), or roll instability. To demonstrate what was observed in the SIS maneuver, time history data

for each vehicle, in the LLVW and GPOW load conditions, and for ESC enabled and disabled are shown in the next two sections.

For this section, the common event point was ESC activation. Since this event did not occur when ESC was disabled, an equivalent event point (time) was determined from the enabled series to allow the comparisons for each vehicle. In the tables following the figures, the speed and lateral acceleration average values were reported in 1 second increments up to 6 seconds after ESC activation.

3.2.2 SIS – High Surface Friction – LLVW Load Condition

Figure 3.7, Figure 3.9, and Figure 3.11 present time history data for each motorcoach. Each figure shows the steering wheel angle, speed, lateral acceleration, longitudinal acceleration, yaw rate, roll angle, wheel height, and throttle position. Each figure shows one left and one right SIS maneuver with ESC enabled and disabled. Each coach is in the LLVW load condition. Blue pentagrams denote ESC activation. Similar to the figures described above are Figure 3.8, Figure 3.10, and Figure 3.12. These figures show engine torque, driver torque, retarder torque, and the brake pressure observed at each wheel for one SIS maneuver conducted to the right with ESC enabled.

In Figure 3.7 for MCI #1, when ESC activation occurs, the driver increases throttle gradually to try to maintain the 30 mph MES. Eventually, the driver requests 100 percent throttle during the maneuver. Following ESC activation, the lateral acceleration still continues to build for a short period of time before leveling off or decreasing slightly. Shown in Figure 3.8 at ESC activation engine torque reduction is occurring by observing the separation in the driver demanded torque and engine torque, but it's not until brake pressure is observed at each wheel that the lateral acceleration starts to decrease slightly. The ESC system was able to reduce speed and limit the lateral acceleration to just under 0.4 g for the maneuver.

In Figure 3.9 for Prevost, when ESC activation occurs, the driver increases the throttle gradually to try to maintain the 30 mph MES. Eventually, the driver requests 100 percent throttle during the maneuver. Directly following ESC activation the lateral acceleration levels off and over time decrease slightly. Shown in Figure 3.10 at ESC activation both engine torque reduction and brake pressure at each wheel is observed. For the maneuver, the ESC system was able to reduce speed and limited the lateral acceleration to approximately 0.3 g.

In Figure 3.11 for MCI #2, when ESC activation occurs, the driver increases the throttle gradually to try to maintain the 30 mph MES. Eventually, the driver requests 100 percent throttle during the maneuver. Similar to MCI #1, following ESC activation, the lateral acceleration still continues to build for a short period of time before leveling off or decreasing slightly. Shown in Figure 3.12, engine torque reduction is occurring, but it is not until brake pressure is observed at each wheel that the lateral acceleration levels off and then decreases slightly. The ESC system was able to reduce speed and limit the lateral acceleration to just under 0.4 g for the maneuver.

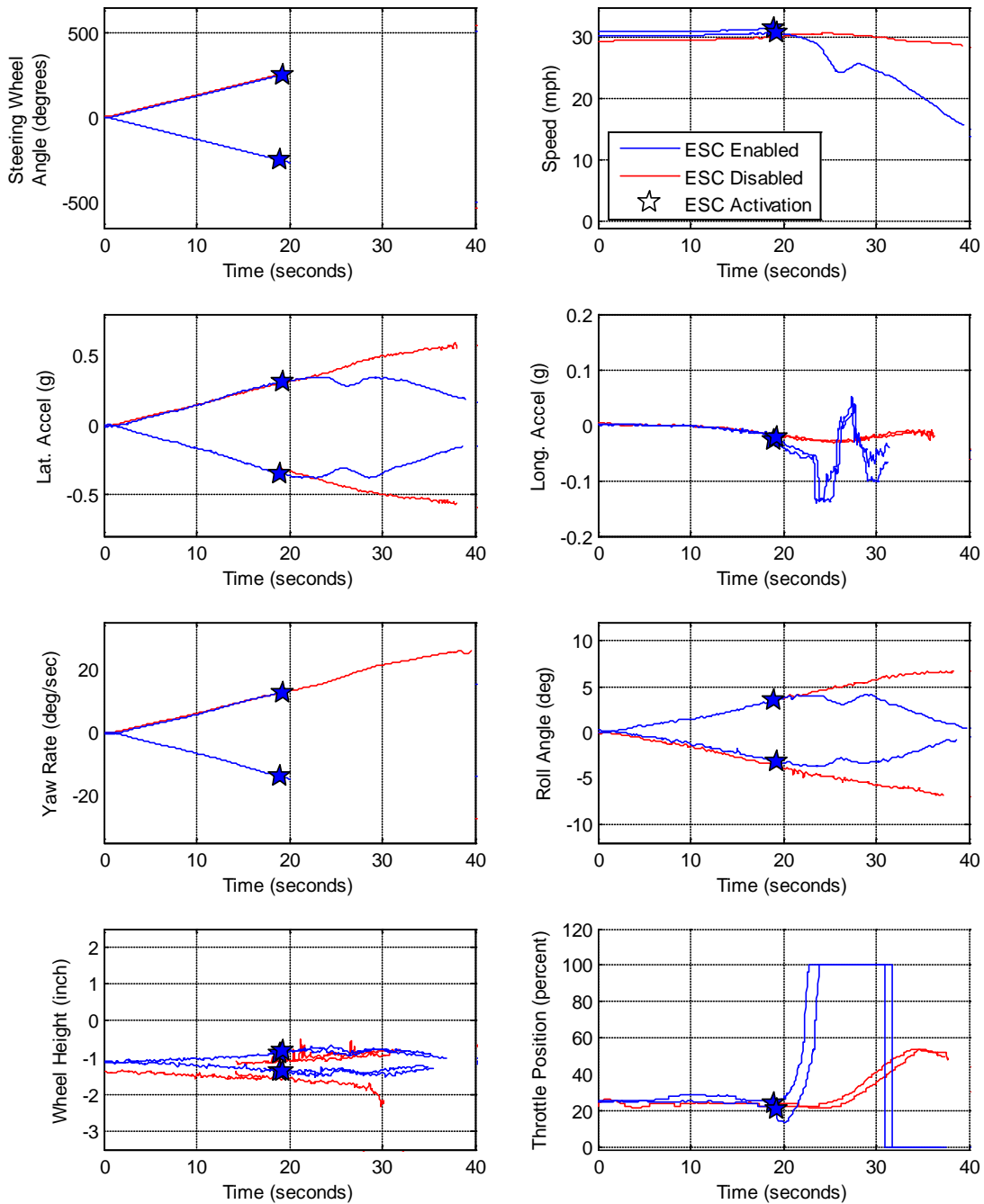


Figure 3.7. Graph shows an example of test data from the MCI #1 SIS maneuver one (one left and one right) in the LLVW load condition with ESC enabled and disabled.

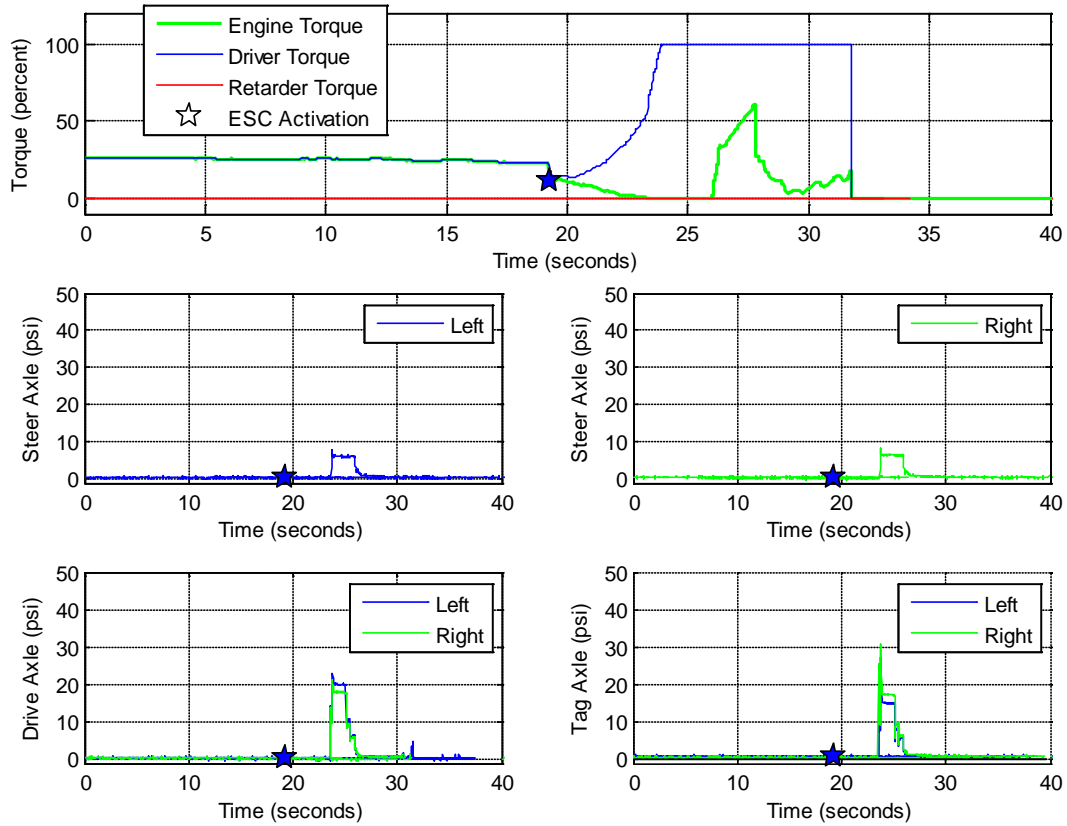


Figure 3.8. Graphs show brake pressures at each wheel and torque outputs for the MCI #1 during a SIS maneuver to the right, with ESC enabled in the LLVW load condition.

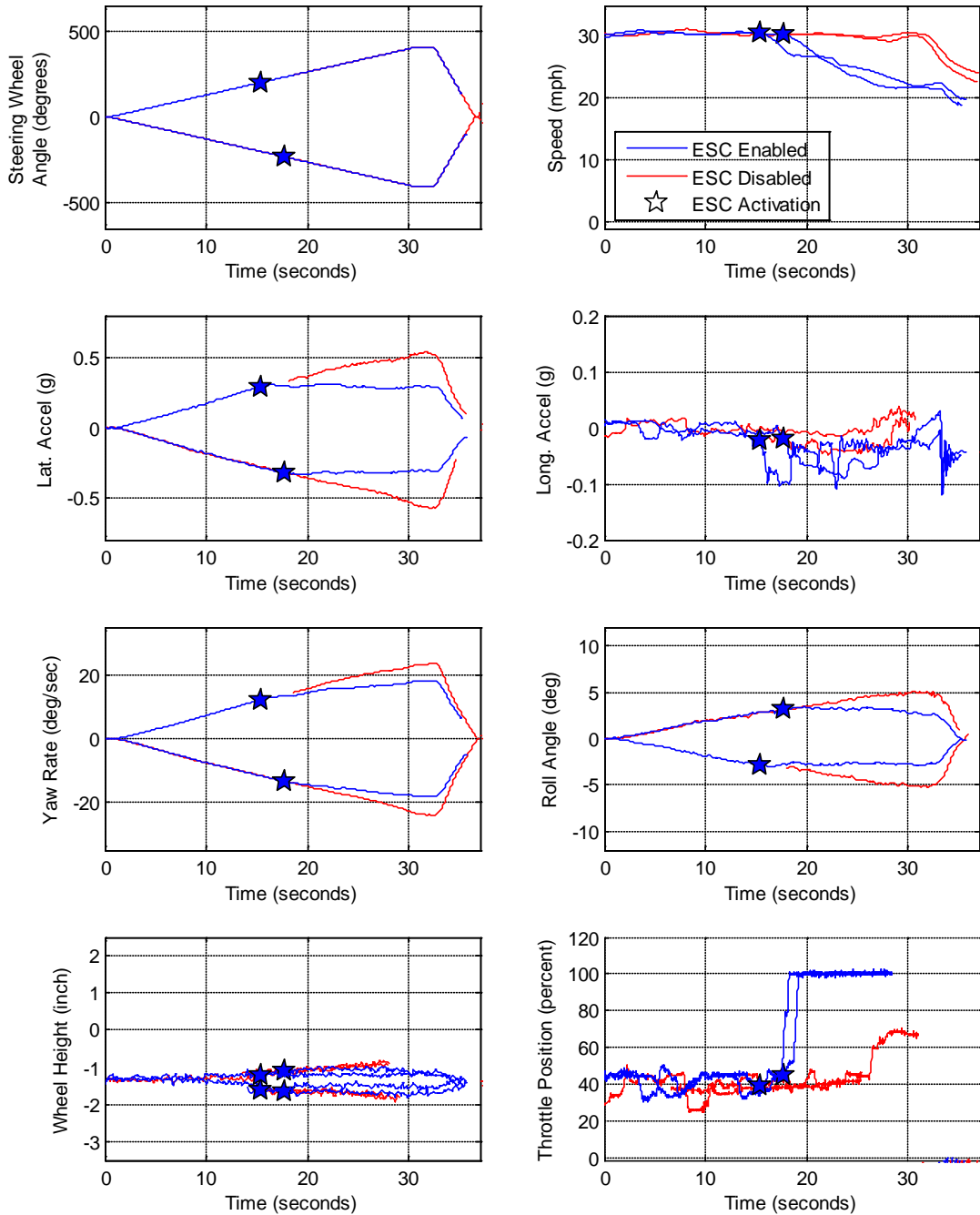


Figure 3.9. Graphs show an example of test data from the Prevest SIS maneuver one (one left and one right) in the LLVW load condition, with ESC enabled and disabled.

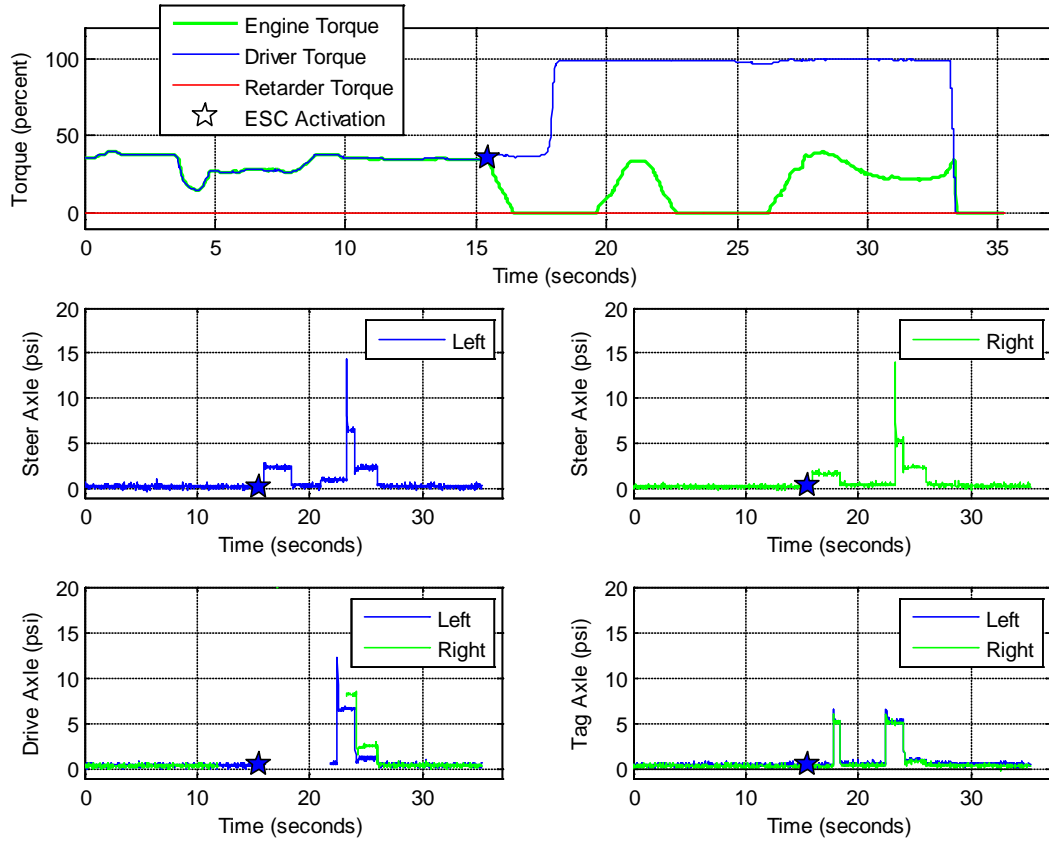


Figure 3.10. Graphs show brake pressures at each wheel and torque outputs for the Prevost during a SIS maneuver to the right, with ESC enabled, in the LLVW load condition.

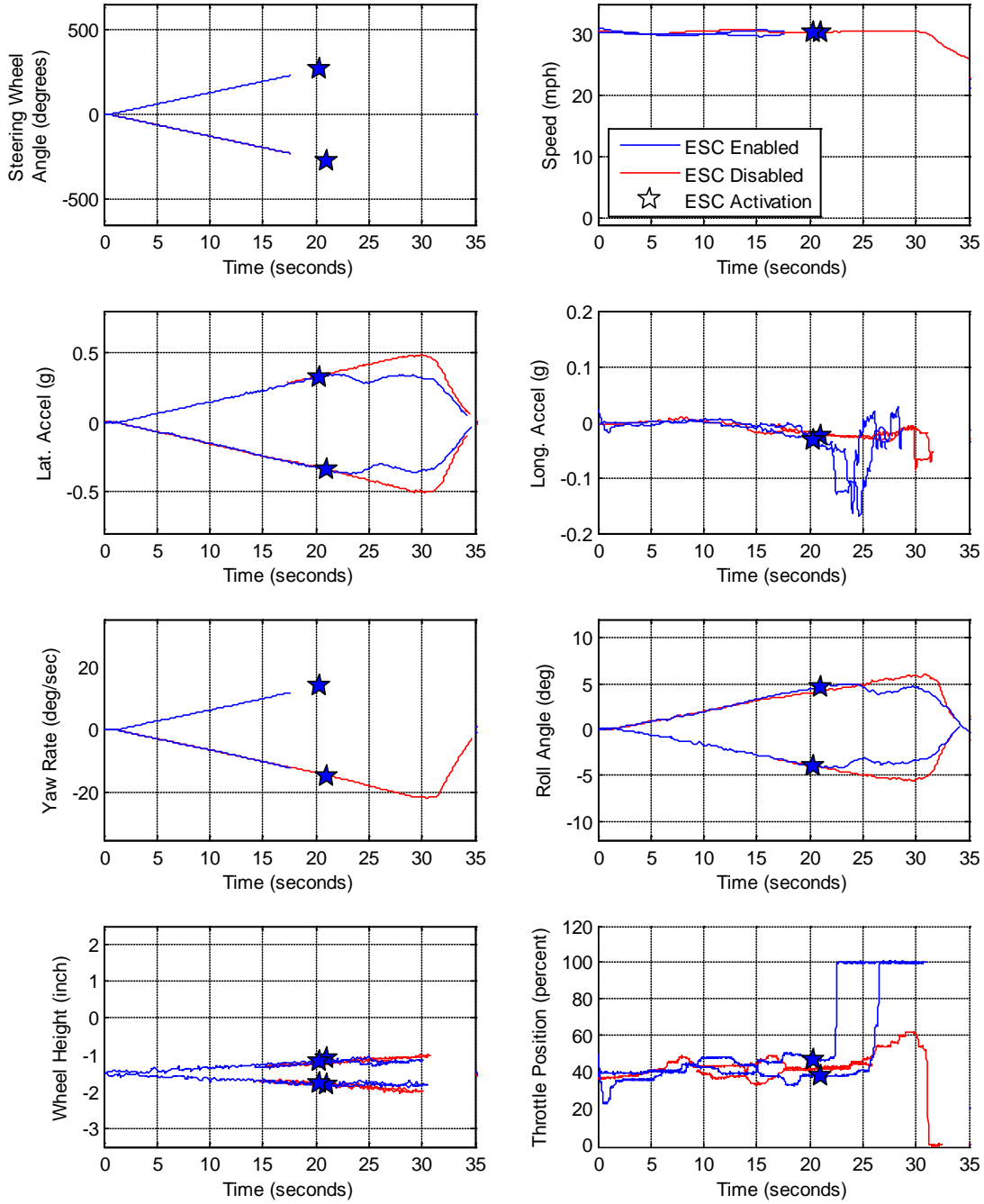


Figure 3.11. Graphs show an example of test data from the MCI #2 SIS maneuver one (one left and one right) in the LLVW load condition, with ESC enabled and disabled.

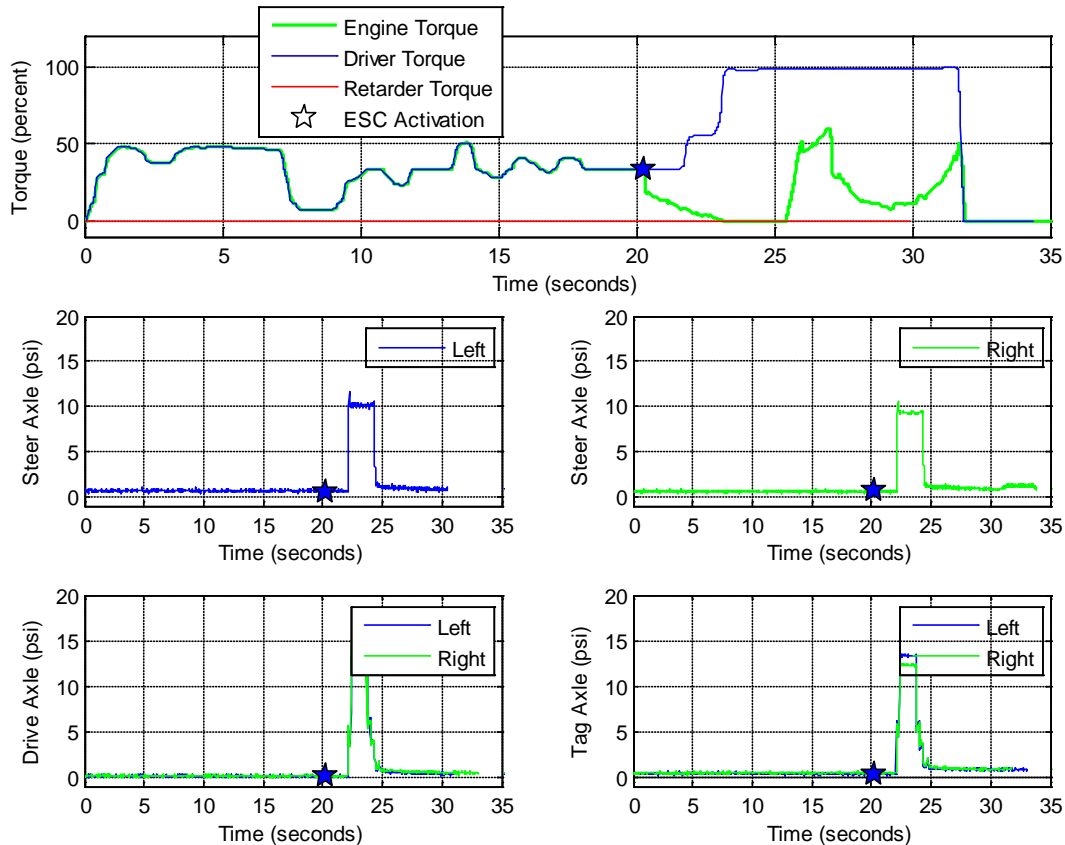


Figure 3.12. Graph shows brake pressures at each wheel and torque outputs for the MCI #2 during a SIS maneuver to the right, with ESC enabled in the LLVW load condition.

The figures above for each of the motorcoaches show that once ESC activated, the forward velocity began to decrease and remained below the speeds observed in the disabled tests for the duration of the maneuver. These speed reductions were observed even with the test driver's effort to maintain a speed of 30 mph. This observation is quantified in Table 3.5. At ESC activation the average speed (the average from 3 left and 3 right direction SIS maneuvers for each motorcoach) ranged between 30.0 and 31.2 mph. At six seconds following ESC activation, the average speed for the MCI #1 was 25.7 mph, 26.2 mph for the Prevost, and 25.3 mph for the MCI #2. For the ESC disabled test series, speed was held constant at approximately 30 mph. The change associated with the six second time increment shows that the average speed reduction ranged from 13.9 percent to 17.5 percent for the enabled series while disabled series tests had limited reductions that ranged from 0.4 percent to 3.2 percent.

Different from speed, the average lateral acceleration for the SIS test series began to decrease at activation or within a few seconds following and remained below the disabled tests series for the duration of the maneuver. This observation is quantified in Table 3.6. At time zero, the range of the average lateral acceleration at ESC activation for ESC enabled tests series was observed to be between 0.31 g and 0.34 g. The table shows that six seconds after the ESC systems activated the average lateral acceleration was around 0.32 g while the disabled test series ranged from 0.40 g to 0.43 g. The change associated with the six second time increment shows that ESC

enabled series average lateral acceleration ranged between -4.6 percent and 6.1 percent while disabled series tests were observed to increase by 27.4 percent to 36.8 percent.

Table 3.5. SIS maneuver average speed in one second intervals from ESC activation for each motorcoach tested in the LLVW load condition.

Vehicle	ESC Condition	Series Average Speed (mph) At Given Time Increments (Event Point = 0.0 s)						
		0.0	1.0	2.0	3.0	4.0	5.0	6.0
MCI #1	Enabled	31.2	30.9	30.6	30.0	29.3	27.9	25.7
	Disabled	30.4	30.4	30.5	30.6	30.6	30.6	30.6
Prevost	Enabled	30.4	29.6	28.9	28.1	27.4	26.8	26.2
	Disabled	30.2	30.2	30.3	30.4	30.3	30.3	30.4
MCI #2	Enabled	30.0	29.8	29.5	28.5	26.7	25.6	25.3
	Disabled	30.4	30.3	30.3	30.2	29.7	29.4	29.4
Vehicle	ESC Condition	Series Average Speed Change (percent) At Given Time Increments (Event Point = 0.0 s)						
		0.0	1.0	2.0	3.0	4.0	5.0	6.0
MCI #1	Enabled	0.0	-0.7	-2.0	-3.7	-5.8	-10.3	-17.5
	Disabled	0.0	0.0	0.3	0.4	0.4	0.4	0.4
Prevost	Enabled	0.0	-2.6	-5.1	-7.5	-9.9	-11.8	-13.9
	Disabled	0.0	0.1	0.4	0.5	0.4	0.4	0.4
MCI #2	Enabled	0.0	-0.7	-1.8	-5.0	-11.1	-14.9	-15.8
	Disabled	0.0	-0.1	-0.2	-0.6	-2.2	-3.1	-3.2

Table 3.6. SIS maneuver average lateral acceleration in one second intervals from ESC activation for each motorcoach tested in the LLVW load condition.

Vehicle	ESC Condition	Series Average Lat. Acceleration (g) At Given Time Increments (Event Point = 0.0 s)						
		0.0	1.0	2.0	3.0	4.0	5.0	6.0
MCI #1	Enabled	0.34	0.35	0.36	0.37	0.37	0.36	0.32
	Disabled	0.31	0.34	0.35	0.37	0.39	0.40	0.42
Prevost	Enabled	0.31	0.31	0.31	0.31	0.31	0.31	0.32
	Disabled	0.27	0.32	0.33	0.35	0.37	0.38	0.40
MCI #2	Enabled	0.33	0.34	0.35	0.35	0.33	0.31	0.32
	Disabled	0.33	0.35	0.37	0.38	0.39	0.40	0.43
Vehicle	ESC Condition	Average Lat. Acceleration Change (percent) At Given Time Increments (Event Point = 0.0 s)						
		0.0	1.0	2.0	3.0	4.0	5.0	6.0
MCI #1	Enabled	0.0	4.1	6.8	8.2	8.6	5.9	-4.6
	Disabled	0.0	7.2	11.8	18.0	23.5	29.2	35.6
Prevost	Enabled	0.0	4.2	3.4	3.8	4.6	4.4	6.1
	Disabled	0.0	6.9	11.4	19.8	25.1	29.8	36.8
MCI #2	Enabled	0.0	4.4	7.2	8.3	1.9	-3.6	-2.7
	Disabled	0.0	7.0	11.3	16.0	19.8	22.1	27.4

3.2.3 SIS – High Surface Friction – GPOW Load Condition

Figure 3.13, Figure 3.15, and Figure 3.17 present time history data for each motorcoach. Each figure shows the steering wheel angle, speed, lateral acceleration, longitudinal acceleration, yaw rate, roll angle, wheel height, and throttle position. Each figure shows one left and one right SIS maneuver, with ESC enabled and disabled (except for MCI #1), and in the GPOW load condition. Blue pentagrams denote ESC activation. Following each figure described above are Figure 3.14, Figure 3.16, and Figure 3.18 that show engine torque, driver torque, retarder torque, and the brake pressure observed at each wheel for one SIS maneuver conducted to the right with ESC enabled.

Looking at Figure 3.13 for MCI #1, when ESC activation occurs, the driver increases throttle gradually to try to maintain 30 mph. Eventually, the driver requests 100 percent throttle during the maneuver. Following ESC activation, the lateral acceleration still continues to build for a short period of time before leveling off, then decreases slightly. Shown in Figure 3.14, at ESC activation, engine torque reduction can be seen to occur by observing the separation in the driver demanded torque and engine torque, but it is not until brake pressure is observed at each wheel that the lateral acceleration starts to decrease slightly. The ESC system was able to reduce speed and limit the lateral acceleration to approximately 0.35 g for the maneuver. Maneuvers were not conducted with ESC disabled for this vehicle.

In Figure 3.15 for the Prevost, when ESC activation occurs, the driver increases the throttle gradually to try to maintain 30 mph. Eventually, the driver requests 100 percent throttle during the maneuver. Directly following ESC activation the lateral acceleration levels off and over time decreases slightly. Shown in Figure 3.16, both engine torque reduction and brake pressure at each wheel are observed. For the maneuver, the ESC system was able to reduce speed and limited the lateral acceleration to approximately 0.3 g.

Looking at Figure 3.17 for MCI #2, when ESC activation occurs, the driver increases the throttle gradually to try to maintain 30 mph. Eventually, the driver requests 100 percent throttle during the maneuver. Similar to MCI #1, the lateral acceleration still continues to build for a short period of time before leveling off and decreasing slightly. Shown in Figure 3.18, ESC was commanding engine torque reduction, but it's not until brake pressure is observed at each wheel that the lateral acceleration starts to level off and then decreases slightly. The ESC system was able to reduce speed and limit the lateral acceleration to approximately 0.35 g for the maneuver.

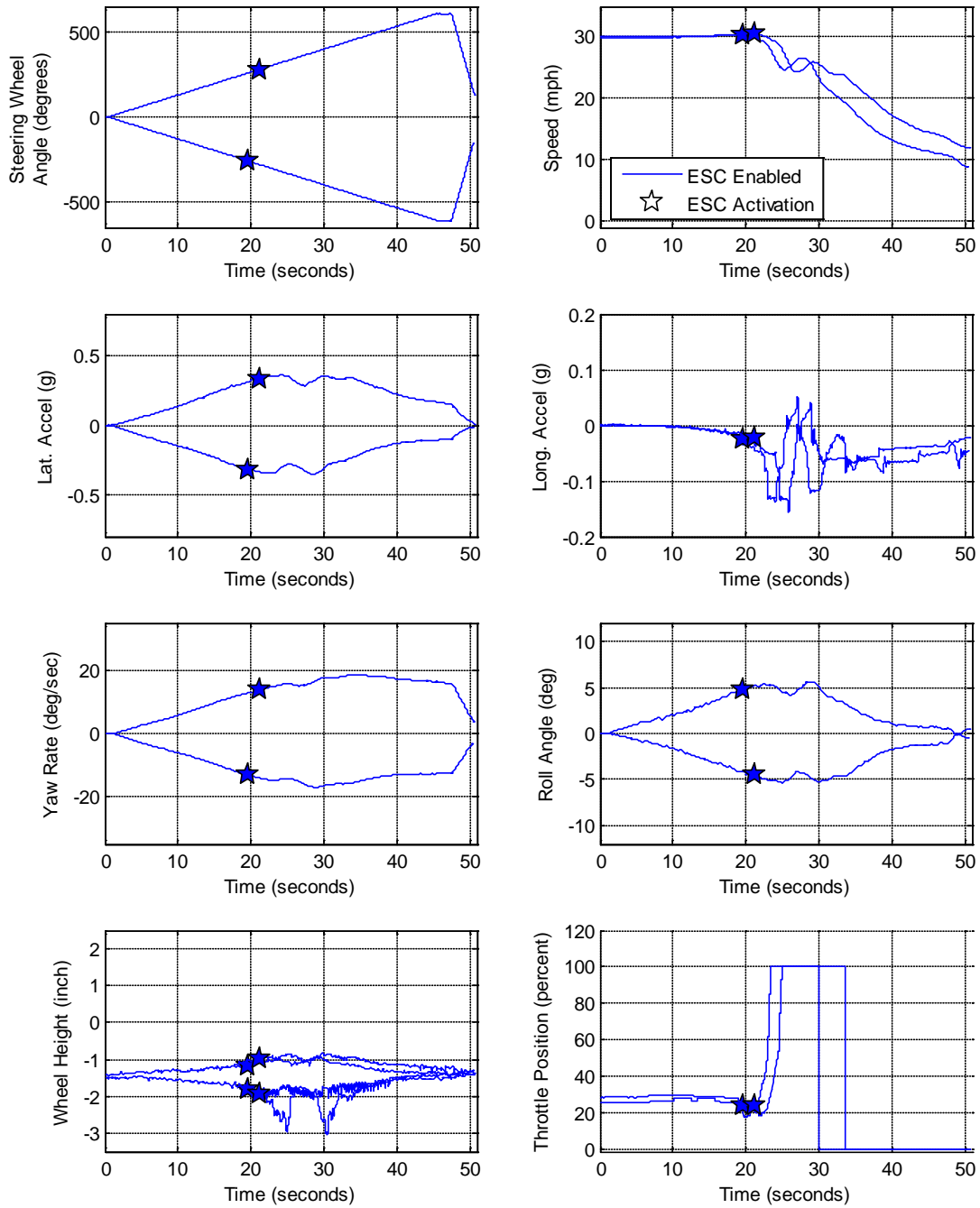


Figure 3.13. Graphs show an example of test data from the MCI #1 SIS maneuver one (one left and one right) in the GPOW load condition, with ESC enabled only.

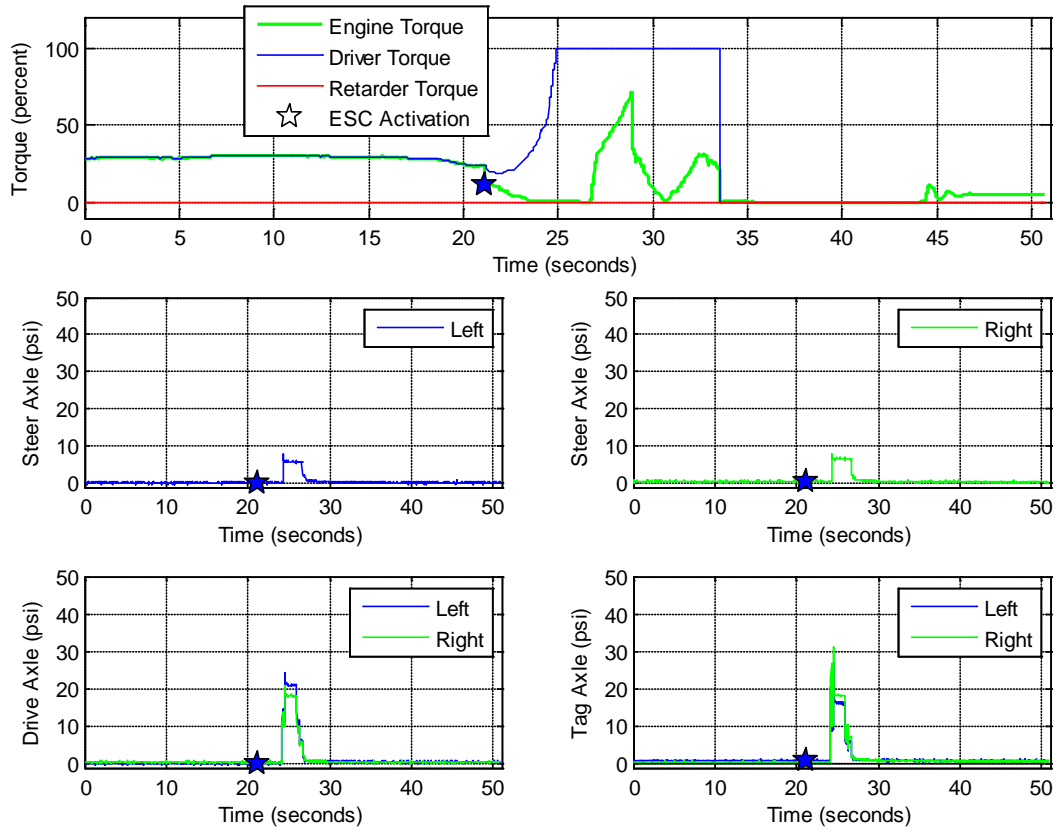


Figure 3.14. Graphs show brake pressures at each wheel and torque outputs for the MCI #1 during a SIS maneuver to the right, with ESC enabled in the GPOW load condition.

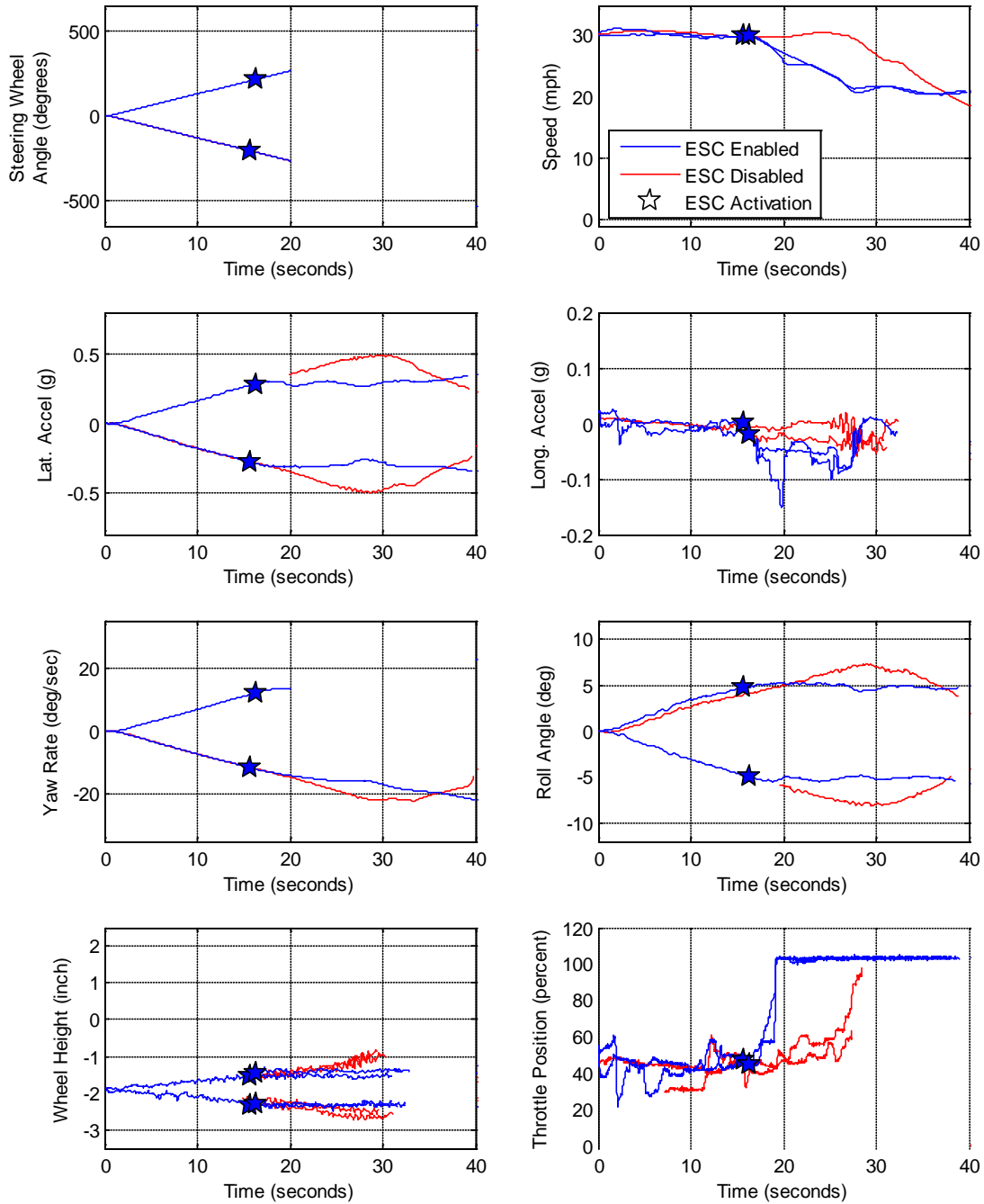


Figure 3.15. Graph shows an example of test data from the PrevoSt SIS maneuver one (one left and one right) in the GPOW load condition, with ESC enabled and disabled.

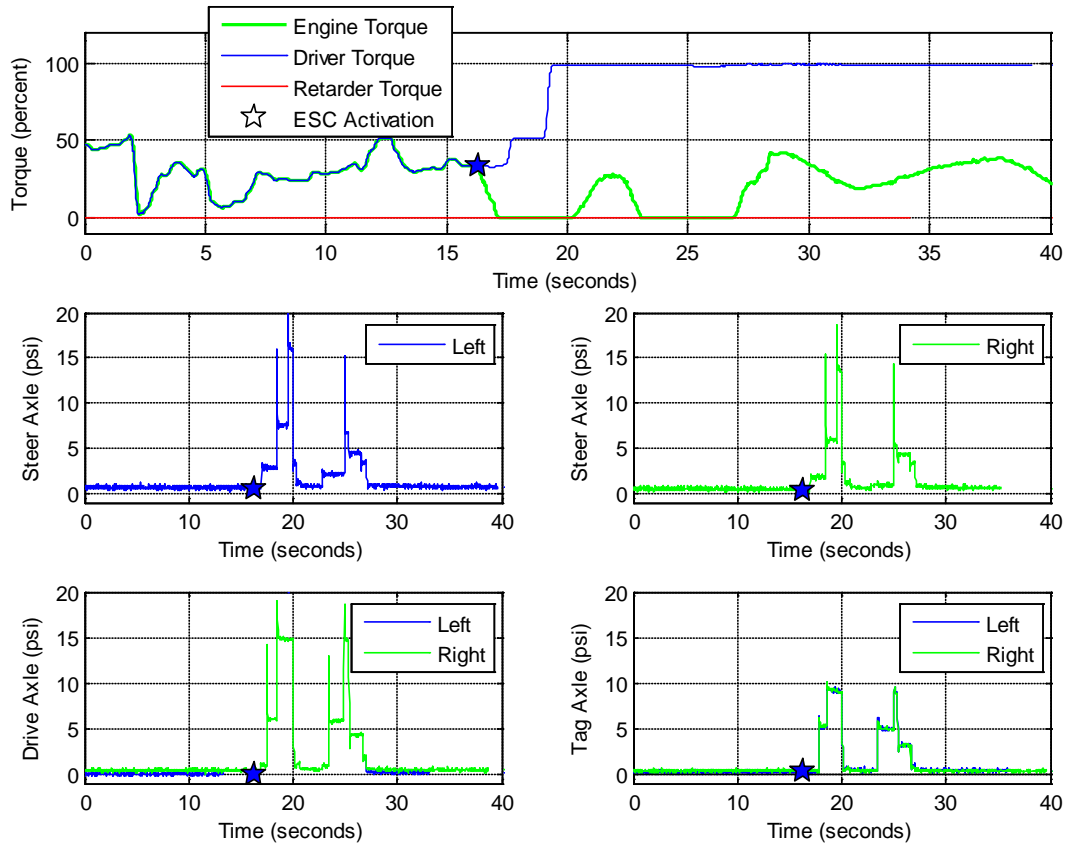


Figure 3.16. Graphs show brake pressures at each wheel and torque outputs for the Prevost during a SIS maneuver to the right, with ESC enabled in the GPOW load condition.

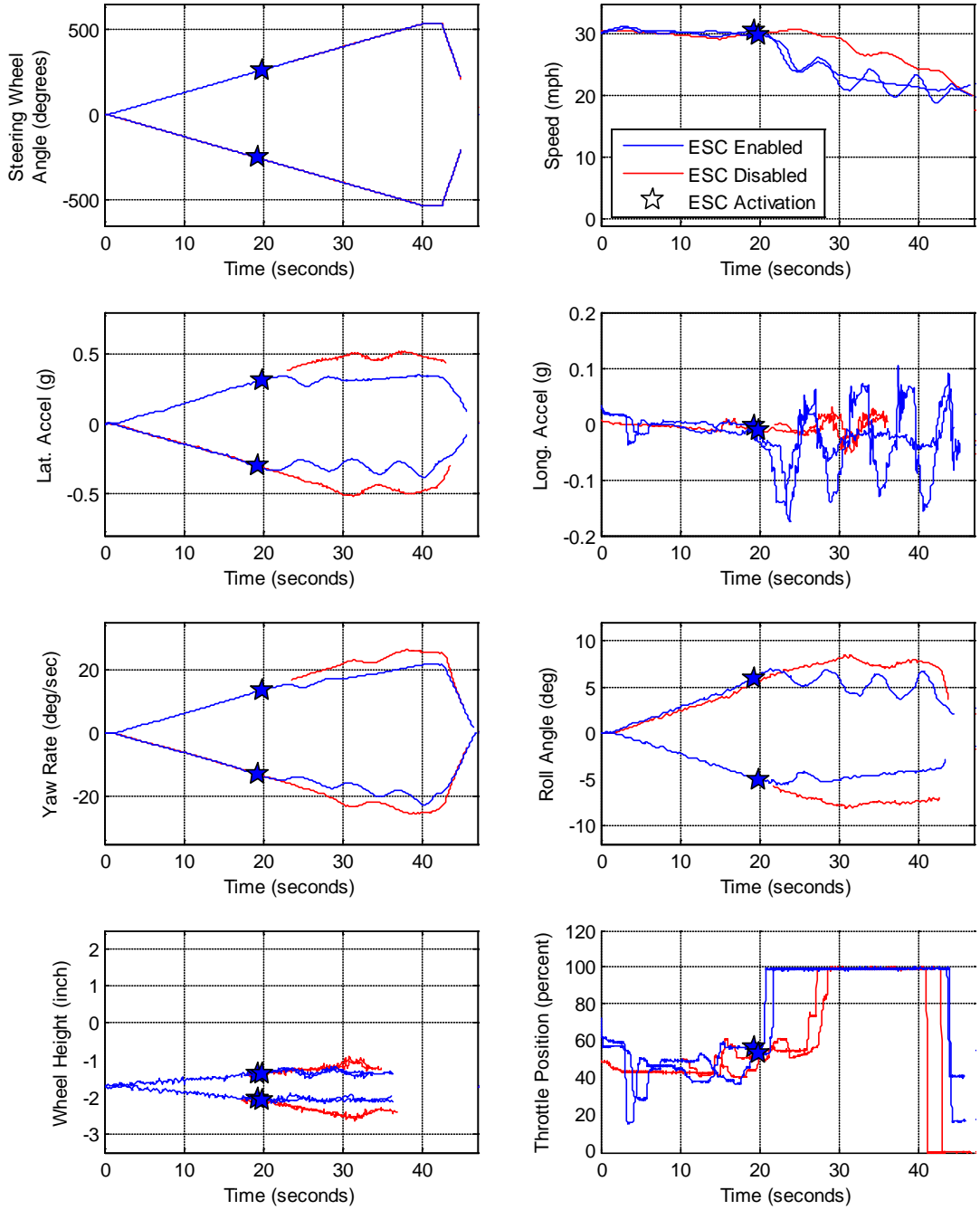


Figure 3.17. Graphs show an example of test data from the MCI #2 SIS maneuver one (one left and one right) in the GPOW load condition, with ESC enabled and disabled.

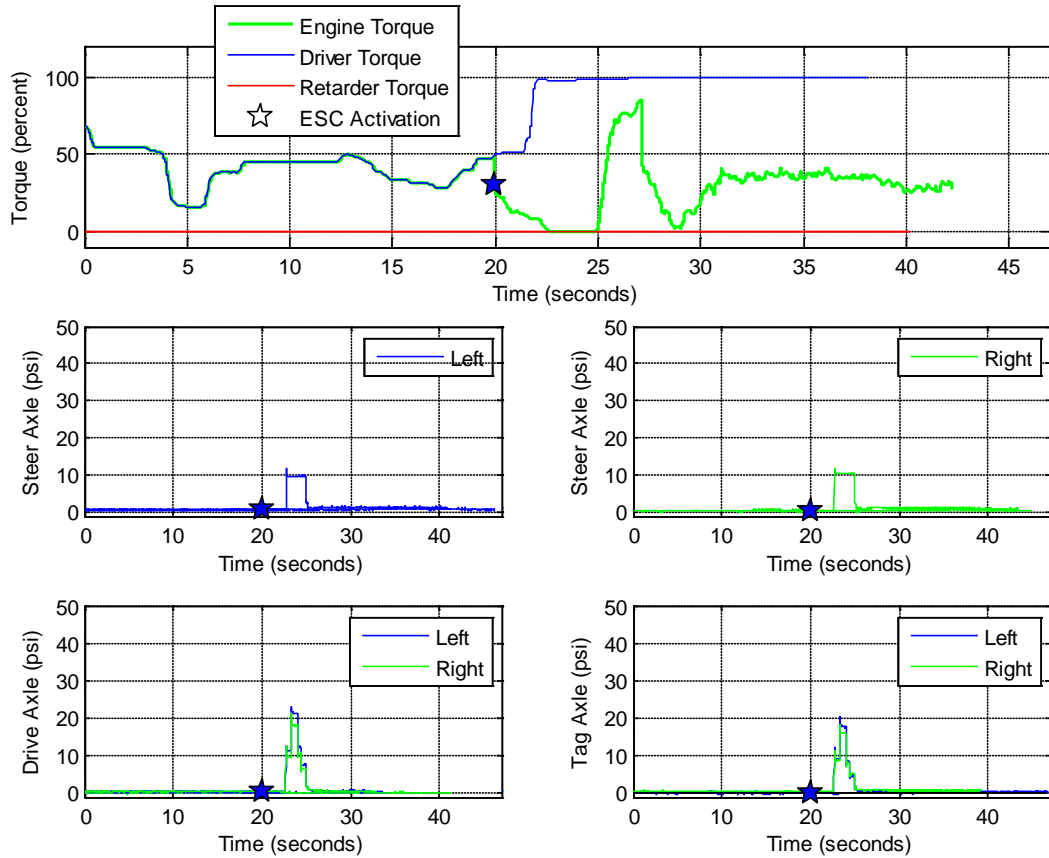


Figure 3.18. Graphs show brake pressures at each wheel and torque outputs for the MCI #2 during a SIS maneuver to the right, with ESC enabled in the GPOW load condition.

The figures above for each of the motorcoaches show that, once the ESC activated, the forward velocity for the SIS test began to decrease and remained below the speeds observed in the disabled tests for the duration of the maneuver. This observation is quantified in Table 3.7. At ESC activation the average speed ranged between 29.9 and 30.6 mph. At six seconds following ESC activation, the average speed for the MCI #1 was 24.6 mph, 25.7 mph for the Prevost, and 23.7 mph for the MCI #2. For the ESC disabled test series, the speed was held constant at approximately 30 mph. The change associated with the six second time increment shows that the average speed reduction ranged from 14.2 to 20.6 percent for the enabled series while disabled series tests speed remained within 0.5 percent of 30 mph.

The average lateral acceleration for the SIS test series began to level off at activation or within a few seconds following and remained below the disabled tests series for the duration of the maneuver. This observation is quantified in Table 3.8. At time zero, the range of the average lateral acceleration at ESC activation for the SIS enabled test series was observed to be between 0.28 g and 0.33 g. The table shows that six seconds after the ESC systems activated the average lateral acceleration ranged from 0.28 g to 0.30 g while for the disabled test series the values ranged from 0.38 g to 0.42 g. The change associated with the six second time increment shows that for the ESC

enabled series lateral acceleration ranged between -12.0 to 7.4 percent while for the disabled series the values were observed to increase by 33.7 to 37.9 percent.

Table 3.7. Average speed reduction for each motorcoach tested in the GPOW load condition.

Vehicle	ESC Condition	Series Average Speed (mph) At Given Time Increments (Event Point = 0.0 s)						
		0.0	1.0	2.0	3.0	4.0	5.0	6.0
MCI #1	Enabled	30.6	30.4	30.0	29.4	27.9	25.7	24.6
	Disabled	Data not available for this test condition						
Prevost	Enabled	30.0	29.8	29.0	27.9	26.6	26.1	25.7
	Disabled	30.1	30.1	30.0	30.1	30.1	30.2	30.2
MCI #2	Enabled	29.9	29.5	29.0	28.2	26.6	24.5	23.7
	Disabled	30.1	30.2	30.3	30.3	30.3	30.3	30.2
Vehicle	ESC Condition	Average Speed Change (percent) At Given Time Increments (Event Point = 0.0 s)						
		0.0	1.0	2.0	3.0	4.0	5.0	6.0
MCI #1	Enabled	0.0	-0.8	-2.1	-3.9	-8.8	-15.9	-19.6
	Disabled	Data not available for this test condition						
Prevost	Enabled	0.0	-0.8	-3.3	-7.1	-11.6	-13.1	-14.2
	Disabled	0.0	-0.1	-0.2	-0.1	0.1	0.2	0.3
MCI #2	Enabled	0.0	-1.1	-2.8	-5.4	-10.8	-17.8	-20.6
	Disabled	0.0	0.3	0.7	0.8	0.9	0.8	0.4

Table 3.8. Average lateral acceleration for each motorcoach tested in the GPOW load condition.

Vehicle	Condition	Series Average Lat. Acceleration (g) At Given Time Increments (Event Point = 0.0 s)						
		0.0	1.0	2.0	3.0	4.0	5.0	6.0
MCI #1	Enabled	0.33	0.34	0.35	0.35	0.349	0.32	0.29
	Disabled	Data not available for this test condition						
Prevost	Enabled	0.28	0.30	0.30	0.30	0.29	0.29	0.30
	Disabled	0.28	0.29	0.31	0.33	0.35	0.37	0.38
MCI #2	Enabled	0.31	0.33	0.33	0.34	0.33	0.30	0.28
	Disabled	0.31	0.33	0.35	0.37	0.38	0.40	0.42
Vehicle	Condition	Average Lat. Acceleration Change (percent) At Given Time Increments (Event Point = 0.0 s)						
		0.0	1.0	2.0	3.0	4.0	5.0	6.0
MCI #1	Enabled	0.0	3.6	6.6	8.0	6.6	-3.8	-12.0
	Disabled	Data not available for this test condition						
Prevost	Enabled	0.0	6.3	8.3	8.9	4.7	4.9	7.4
	Disabled	0.0	6.4	12.3	18.7	25.2	32.5	37.9
MCI #2	Enabled	0.0	4.9	6.8	7.4	4.0	-5.1	-11.7
	Disabled	0.0	5.5	11.3	17.0	22.6	27.9	33.7

3.2.4 Determining Maneuver Amplitude from SIS Test Results

Table 3.9. shows the average extrapolated steering angles (the average from 3 left and 3 right direction SIS maneuvers for each motorcoach) at 0.5 g calculated for the LLVW and GPOW load conditions with ESC. The table shows, from left to right, the vehicle, the load condition, the test series range of input speeds, average steering angle extrapolated at 0.5 g, and the R² statistic For the LLVW load condition the SWA to achieve 0.5 g was calculated to be 405 deg for the MCI #1, 352 deg for the Prevost, and 407 deg for the MCI #2. In the GPOW loading condition, SWA's were found to be 405 deg for the MCI #1, 383 for the Prevost, and 461 for the MCI #2.

Table 3.9. SIS tests results for the three Motorcoaches in the LLVW and GPOW load conditions. .

Vehicle Tested	Load conditions	Input Speed Range (mph)	Average of Angles (L/R) At 0.5 g	R ² Range (From Linear Regression)
MCI #1 (6 Tests)	LLVW	29.6 – 30.9	405	0.992 – 0.997
Prevost (6 Tests)	LLVW	30.1 – 30.5	352	0.996 – 0.998
MCI #2 (6 Tests)	LLVW	29.9 – 30.6	407	0.995 – 0.998
MCI #1 (6 Tests)	GPOW	29.5 – 30.3	405	0.992 – 0.998
Prevost (6 Tests)	GPOW	30.0 30.1	383	0.996 – 0.998
MCI #2 (6 Tests)	GPOW	29.9 – 30.8	461	0.988 – 0.998

Since each motorcoach has a different steering wheel angle to lateral acceleration gain, the SIS test data were used to normalize the steering inputs for the RSM, SWD, and HSWD maneuvers. From SIS test data collected with each motorcoach and load condition, the SWA at 0.5 g was determined. This SWA at 0.5g was then used as an input to the RSM, SWD, and HSWD maneuvers.

The resulting RSM steering magnitudes³ used for each of the vehicles in the LLVW load condition were 400 degrees for the MCI #1, 373 degrees for the Prevost, and 404 degrees for the MCI #2. The SWAs at 0.5 g for GPOW RSMs were 400 degrees for the MCI #1, 373 degrees for the Prevost, and 462 degrees for the MCI #2. For these maneuvers the steering input magnitudes remained constant for each vehicle but the speed was increased from test to test to control maneuver severity.

The SWAs at 0.5 g³ for LLVW SWD and HSWD maneuvers were 400 degrees for the MCI #1, 379 degrees for the Prevost, and 404 for the MCI #2. The SWAs at 0.5 g³ for GPOW maneuvers were 400 degrees for the MCI #1, 379 degrees for the Prevost, and 462 for the MCI #2. For these maneuvers, the steering inputs are were incrementally increased from one test to the next to control test severity. Multiple steering amplitudes were calculated based on a percentage (scaled between 30 - 130 percent) of the SWA at 0.5 g. Table 3.10 is provided to relate the 30 through 130 percent steering scalars to

³ These magnitudes were extrapolated from each vehicles steering wheel angle to lateral acceleration gain. The lateral acceleration data that were utilized were corrected for roll angle motion and sensor offset from the vehicles center-of-gravity. The values shown in Table 3.9 were additionally corrected for yaw motion and surface inclination angle.

the target steering wheel amplitude used with each of the motorcoaches and load conditions for both SWD and HSWD maneuvers.

Table 3.10. Example of scalars used for SWD and HSWD maneuvers.

Steering Scalar (percent)	Average Steering Wheel Angle Increments (degrees)					
	MCI #1		Prevost		MCI #2	
	LLVW	GPOW	LLVW	GPOW	LLVW	GPOW
30% (1 st test)	120	120	114	114	121	139
40% (2 nd test)	160	160	152	152	162	185
50% (3 rd test)	200	200	190	190	202	231
60% (4 th test)	240	240	227	227	242	277
70% (5 th test)	280	280	265	265	283	323
80% (6 th test)	320	320	303	303	323	370
90% (7 th test)	360	360	341	341	364	416
100% (8 th test)	400*	400*	379*	379*	404*	462*
110% (9 th test)	440	440	417	417	444	508
120% (10 th test)	480	480	455	455	485	554
130% (11 th test)	520	520	493	493	525	601

* Normalized steering wheel angle determined from SIS maneuver data. Value represents angle extrapolated to generate 0.5 g of lateral acceleration at 30mph for each vehicle.

3.3 RSM Test Results

RSM testing was completed for each motorcoach to evaluate dynamic roll propensity while loaded in the LLVW and GPOW conditions. Tests were conducted following the RSM protocol developed for tractor semitrailers. Using the robotic steering controller, programmed with the SWA at 0.5G calculated from the SIS maneuver, tests were conducted with both ESC enabled and disabled. The initial MES was 20 mph and it was incrementally increased in subsequent runs until two inches of wheel lift occurred at any of the motorcoach wheels, the vehicle lost yaw stability (spinout), or the MES reached 50 mph without a roll or yaw instability condition.

3.3.1 RSM – High Surface Friction – LLVW Load Condition

Table 3.11 presents the speed at which the maneuvers were terminated for the LLVW load condition for ESC enabled and disabled. With ESC enabled, all of the motorcoaches completed testing up to a MES of 50 mph with no instabilities. For ESC disabled, the MCI #1 had wheel lift on the drive axle at 38 mph, the Prevost completed testing to a MES of 50 mph with no instabilities, and the MCI #2 had wheel lift on the drive axle at 40 mph.

Table 3.11. Presents the lowest target MES that resulted in 2.0 inches or more of wheel lift during the RSM test series with a LLVW load.

Vehicle	LLVW Load Condition	
	ESC	
	Enabled	Disabled
MCI #1	TC	38 D
Prevost	TC	TC
MCI #2	TC	40 D

D = Wheel lift observed at drive axle wheels
 TC = Test Complete up to a MES of 50 mph

Figure 3.19 for MCI #1 presents the steering wheel angle, speed, lateral acceleration, longitudinal acceleration, yaw rate, roll angle, and drive axle wheel ride height for the RSM at MESs of 38 to 50 mph. Shown in each figure are ESC enabled tests for the range of MESs, and for ESC disabled tests for the first MES that produced two inches of wheel lift.

In Figure 3.19 for MCI #1, to understand how ESC changed the dynamics of the vehicle, kinematic data were compared using the point in time at which maximum wheel lift was observed for the ESC disabled condition. The maximum wheel lift height was observed to be ~4.74 seconds for this example as indicated by the red and blue triangles. The values at 4.74 seconds for speed, lateral acceleration, yaw rate, and roll angle for the two ESC test conditions are shown in Table 3.12.

As shown in Table 3.12, the MCI #1 with ESC enabled was able to increase roll stability by reducing the vehicle's speed by 44.8 percent, which in turn reduced lateral acceleration by 68.1 percent, the yaw rate by 41.9 percent, and its roll angle by 76.2 percent. These changes can be linked to the amount of braking commanded by the ESC system shown in Figure 3.20.

Table 3.12. MCI #1 lateral acceleration, yaw rate, and roll angle values and changes observed at the instant in time (shown in Figure 3.19) that maximum wheel lift was observed with ESC disabled. The MES was 38 mph for ESC enabled and disabled tests.

ESC Condition	Speed (mph) [Change (%)]	Lateral Acceleration (g) [Change (%)]	Yaw Rate (deg/sec) [Change (%)]	Roll Angle (deg) [Change (%)]
ESC Disabled	31.9	-0.57	-22.9	10.6
ESC Enabled	17.6 [-44.8%]	-0.19 [-68.1%]	-13.3 [-41.9%]	2.50 [-76.2%]

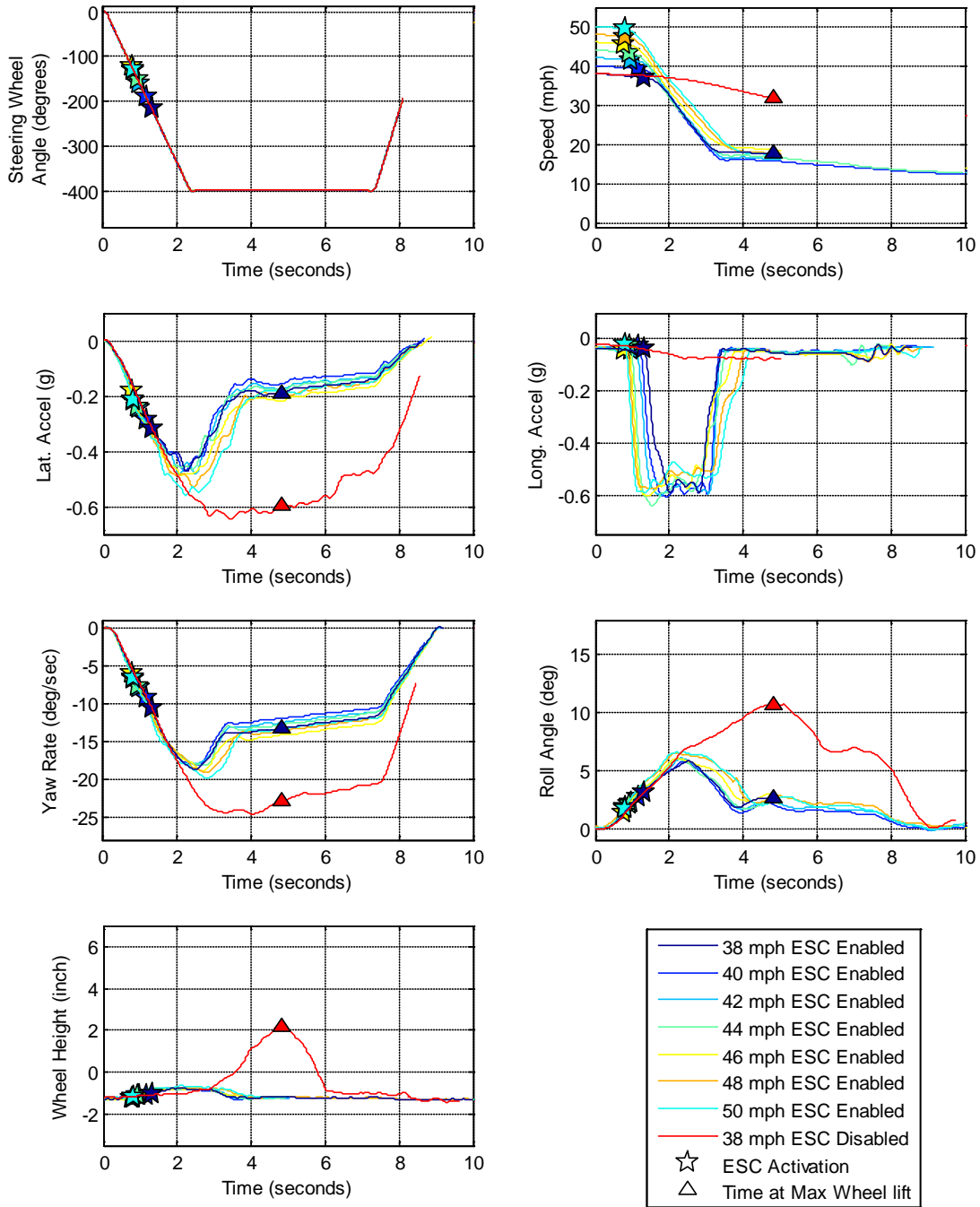


Figure 3.19. Graphs show RSM test data from the MCI #1 in the LLVW load condition with ESC enabled and disabled. Tests shown in this figure were performed at an approximate MES of 38 to 50 mph for ESC enabled and a MES of 38 mph ESC disabled. For the ESC disabled test shown in red, wheel lift of two inches was observed in the data.

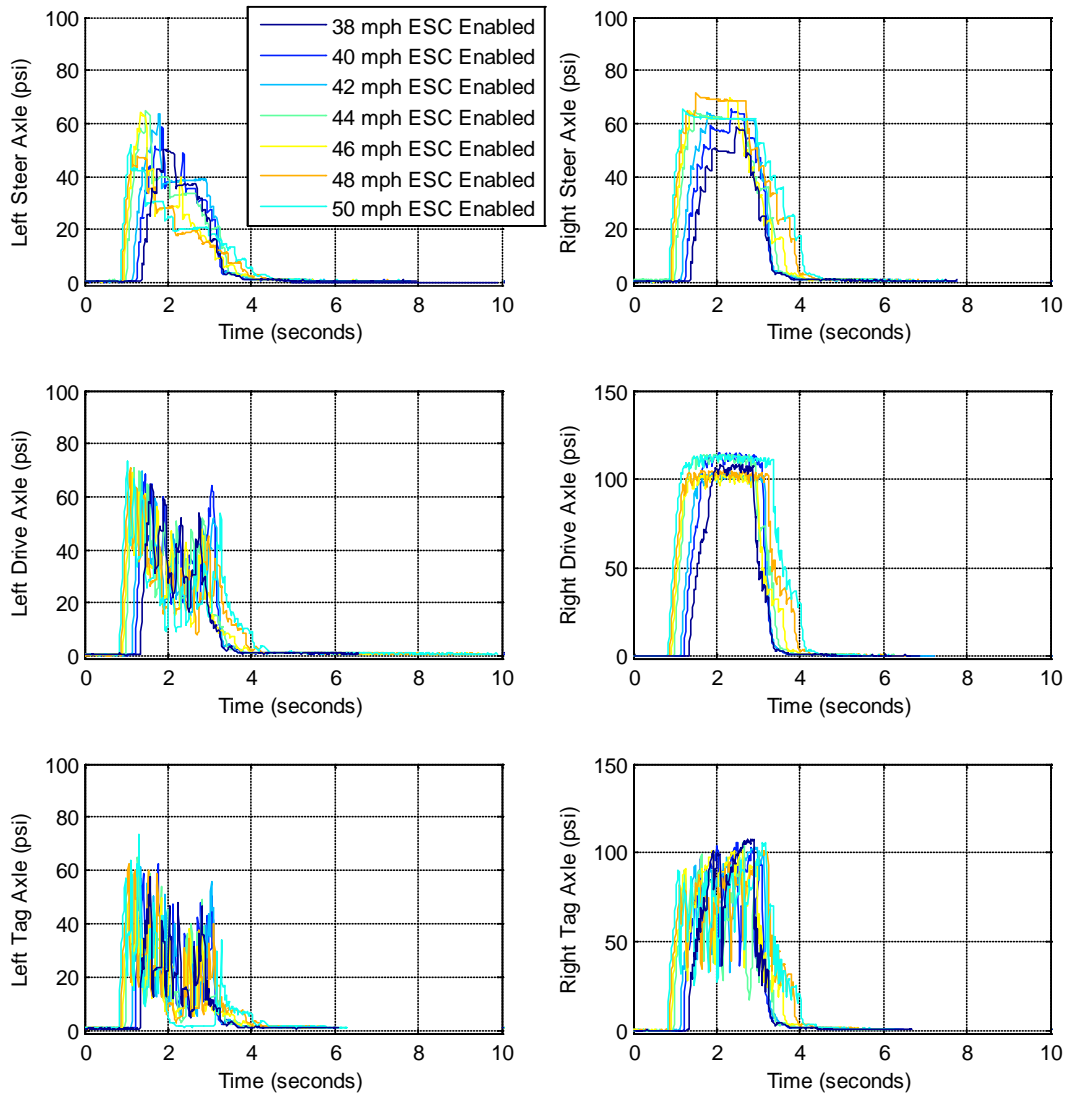


Figure 3.20. Graph shows brake pressures observed for RSM test data from the MCI #1 in the LLVW load condition ESC enabled and disabled. Tests shown in this figure were performed at an approximate MES of 40 to 50 mph ESC enabled.

Figure 3.21 presents for the Prevost, the steering wheel angle, speed, lateral acceleration, longitudinal acceleration, yaw rate, roll angle, and drive axle wheel ride height for RSMs with MESs of 40 through 50 mph. Shown in each figure are ESC enabled tests for the range of MESs and for ESC disabled test for the MES of 50 mph. No wheel lift was observed for the ESC disabled test at 50 mph.

Figure 3.22 shows the Prevost brake pressures at each wheel for the range of MESs with ESC enabled in the RSM tests.

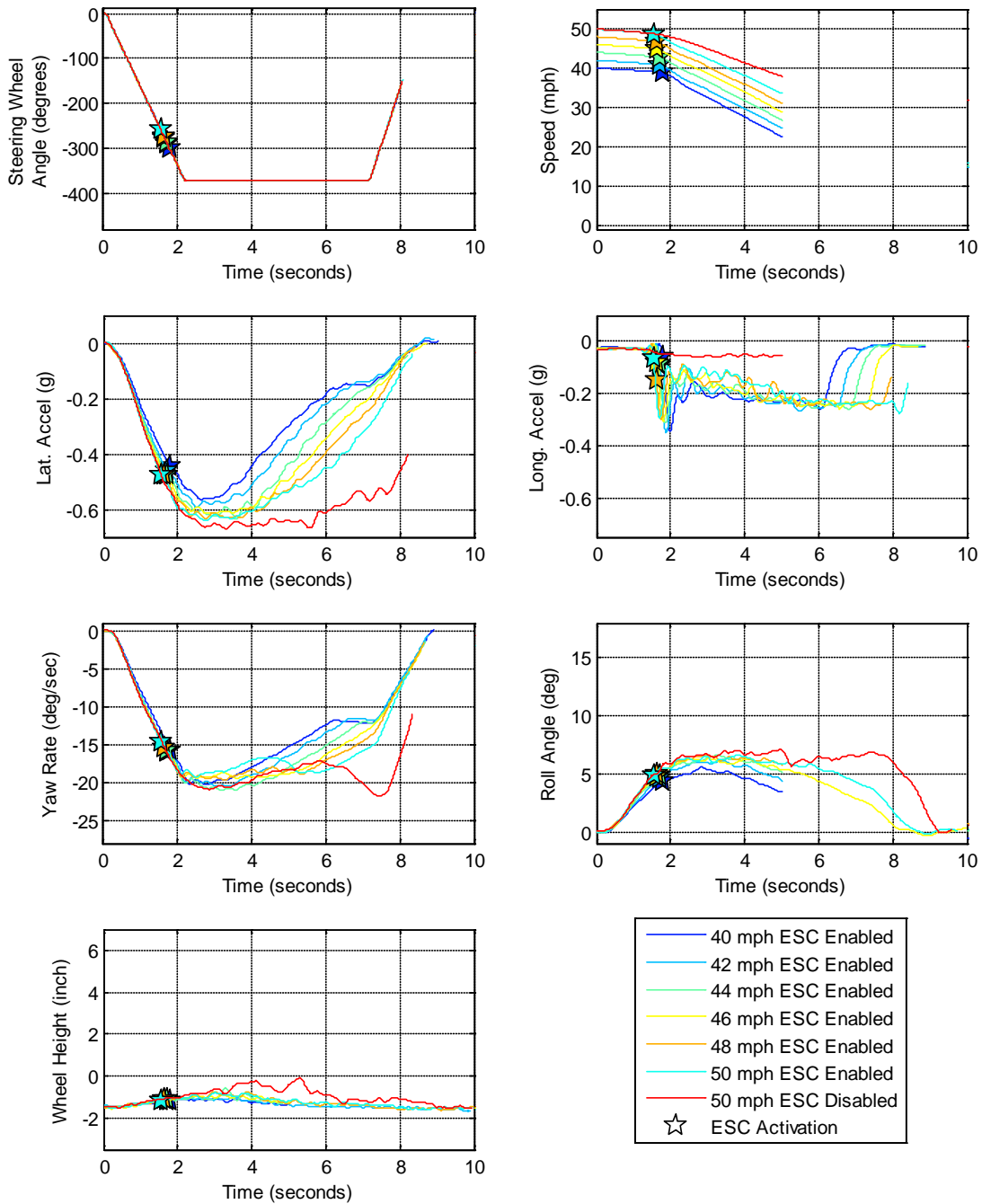


Figure 3.21. Graphs show RSM test data from the Prevost in the LLVW load condition with ESC enabled and disabled. Tests shown in this figure were performed at an approximate MES of 40 to 50 mph with ESC enabled, and at a MES of 50 mph with ESC disabled. The ESC disabled test is shown in red. No wheel lift was observed for the ESC off test at 50 mph.

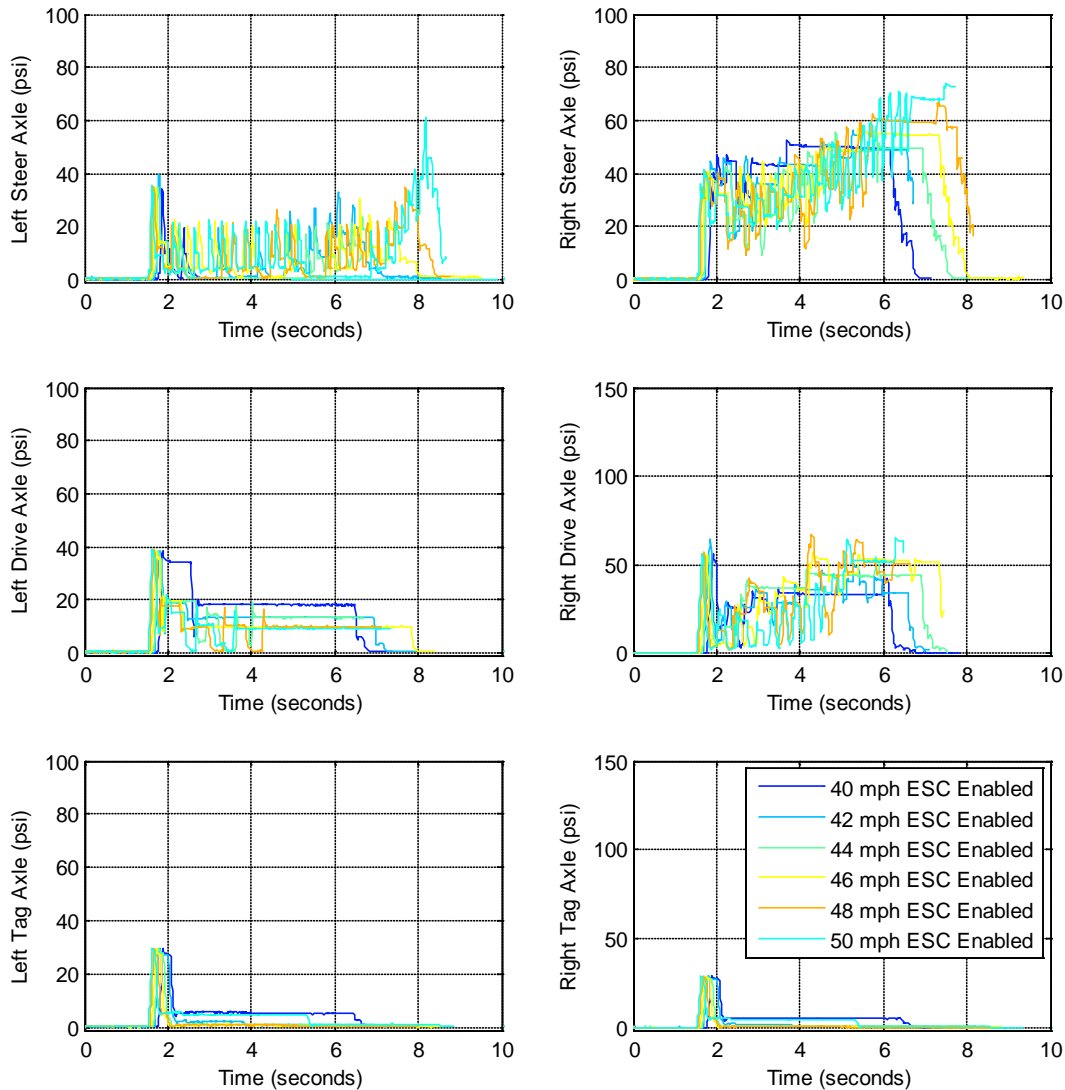


Figure 3.22. Graphs show brake pressures observed for the RSM test data from the Prevost in the LLVW load condition with ESC enabled. Tests shown in this figure were performed at an approximate MES of 40 to 50 mph.

Figure 3.23 presents data for MCI #2. This figure shows the steering wheel angle, speed, lateral acceleration, longitudinal acceleration, yaw rate, roll angle, and drive axle wheel ride height for RSMs with MESs of 40 to 50 mph. This figure shows ESC enabled tests for the range of MESs. For comparison, it also shows the first MES (40MPH) test with ESC disabled that produced two inches of wheel lift.

Figure 3.23 shows how ESC changed the dynamics of the MCI #2. To compare ESC enabled versus ESC disabled tests, the time at maximum wheel lift when ESC was disabled (red trace) was used. For these tests the time used for comparison was ~4.48 seconds. The values at 4.48 seconds for speed, lateral acceleration, yaw rate, and roll angle for the two ESC test conditions are shown in Table 3.13.

With ESC enabled, the MCI #2 was able to increase roll stability by reducing the vehicle's speed by 46.1 percent, which in turn reduced lateral acceleration by 68.2 percent, the yaw rate by 41.3 percent, and its roll angle by 70.3 percent. The changes can be linked to the amount of braking commanded by the ESC system shown in Figure 3.24.

Table 3.13. MCI #2 lateral acceleration, yaw rate, and roll angle values and changes observed at the instant in time (shown in Figure 3.23) that maximum wheel lift was observed with ESC disabled. The MES was 40 mph for both ESC enabled and disabled tests.

ESC Condition	Speed (mph) [Change (%)]	Lateral Acceleration (g) [Change (%)]	Yaw Rate (deg/sec) [Change (%)]	Roll Angle (deg) [Change (%)]
ESC Disabled	33.5	-0.64	-24.1	11.29
ESC Enabled	18.1 [-46.1%]	-0.20 [-68.2%]	-14.1 [-41.3%]	3.35 [-70.3%]

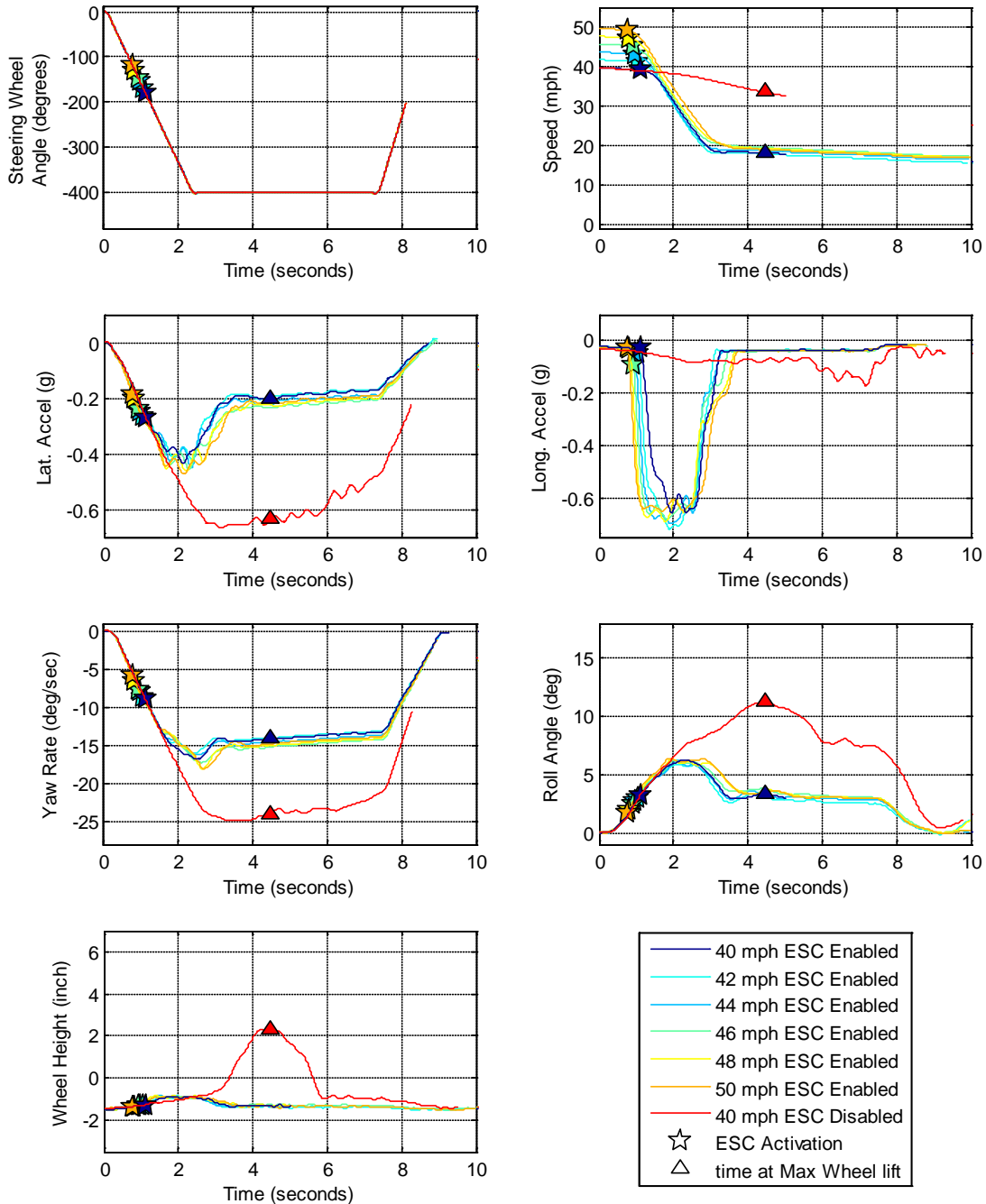


Figure 3.23. Graphs show RSM test data from the MCI #2 in the LLVW load condition with ESC enabled and disabled. Tests shown in this figure were performed at an approximate MES of 40 to 50 mph with ESC enabled, and a MES of 40 mph with ESC disabled. For the ESC disabled test shown in red, wheel lift of two inches was observed in the data.

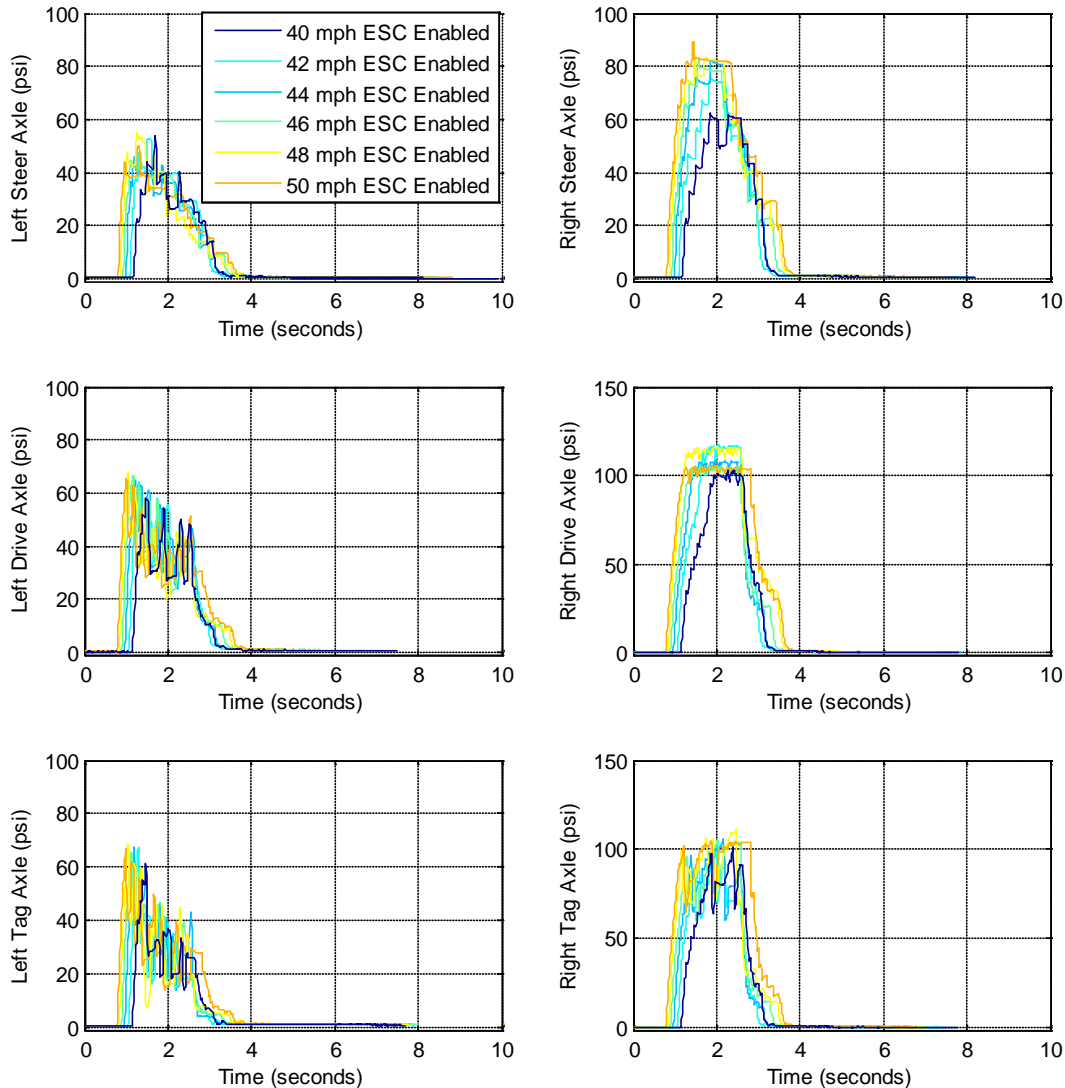


Figure 3.24. Graphs show brake pressures observed for RSM test data from the MCI #2 in the LLVW load condition with ESC enabled and disabled. Tests shown in this figure were performed at an approximate MES of 40 to 50 mph ESC enabled.

3.3.2 RSM – High Surface Friction – GPOW Load Condition

Table 3.14 presents the speed at which RSMs were terminated for the GPOW load condition with ESC enabled and disabled. In the table “TC” indicates that the motorcoach was able to complete the RSM test series up to the maximum MES of 50 mph without observing instability. “D” indicates tests in which drive axle wheel lift was observed.

In Table 3.14 for ESC enabled the MCI #1 completed testing up to a MES of 50 mph with no roll or yaw instabilities. With ESC disabled wheel lift was observed at a MES of 37 mph. The Prevost with ESC enabled completed RSM tests up to a MES of 48 mph before where wheel lift was observed. When disabling ESC, wheel lift was observed at 39 mph with the Prevost. MCI #2 with ESC enabled completed RSM testing up to 50

mph with no roll or yaw instabilities. With ESC disabled, wheel lift was observed at 35 mph.

Table 3.14. Presents the lowest target MES that resulted in 2.0 inches or more of wheel lift during the RSM test series with a GPOW load.

Vehicle	GPOW Load Condition	
	ESC	
	Enabled	Disabled
MCI #1	TC	37 D
Prevost	48 D	39 D
MCI #2	TC	35 D

D = Wheel lift observed at drive axle wheels
 TC = Test Complete up to a MES of 50 mph

Figure 3.25 presents the steering wheel angle, speed, lateral acceleration, longitudinal acceleration, yaw rate, roll angle, and drive axle wheel ride height for RSMs conducted with MCI #1. Shown in each figure are ESC enabled tests for the range of MES. For comparison, it also shows the 37 mph test with ESC disabled that produced two inches of wheel lift. This shows how ESC reduced the dynamics of the MCI #1's response to the speed and steering inputs. To compare ESC enabled versus ESC disabled tests, the time at maximum wheel lift when ESC was disabled (red trace) was used. For these tests the time used for comparison was ~4.71 seconds. The values at 4.71 seconds for speed, lateral acceleration, yaw rate, and roll angle for the two ESC test conditions are shown in Table 3.15.

From Table 3.15, with ESC enabled the MCI #1 was able to increase roll stability by reducing the vehicle's speed by 44.4 percent, which in turn reduced lateral acceleration by 68.7 percent, the yaw rate by 46.5 percent, and its roll angle by 71.9 percent. These changes can be linked to the amount of braking commanded by the ESC system shown in Figure 3.26.

Table 3.15. MCI #1 lateral acceleration, yaw rate, and roll angle values and changes observed at the instant in time (shown in Figure 3.25) that maximum wheel lift was observed with ESC disabled. The MES was 37 mph with ESC disabled compared to a MES of 38 mph with ESC enabled.

ESC Condition	Speed (mph) [Change (%)]	Lateral Acceleration (g) [Change (%)]	Yaw Rate (deg/sec) [Change (%)]	Roll Angle (deg) [Change (%)]
ESC Disabled	29.9	-0.57	-23.6	9.98
ESC Enabled	16.6 [-44.4%]	-0.18 [-68.7%]	-12.6 [-46.5%]	2.81 [-71.9%]

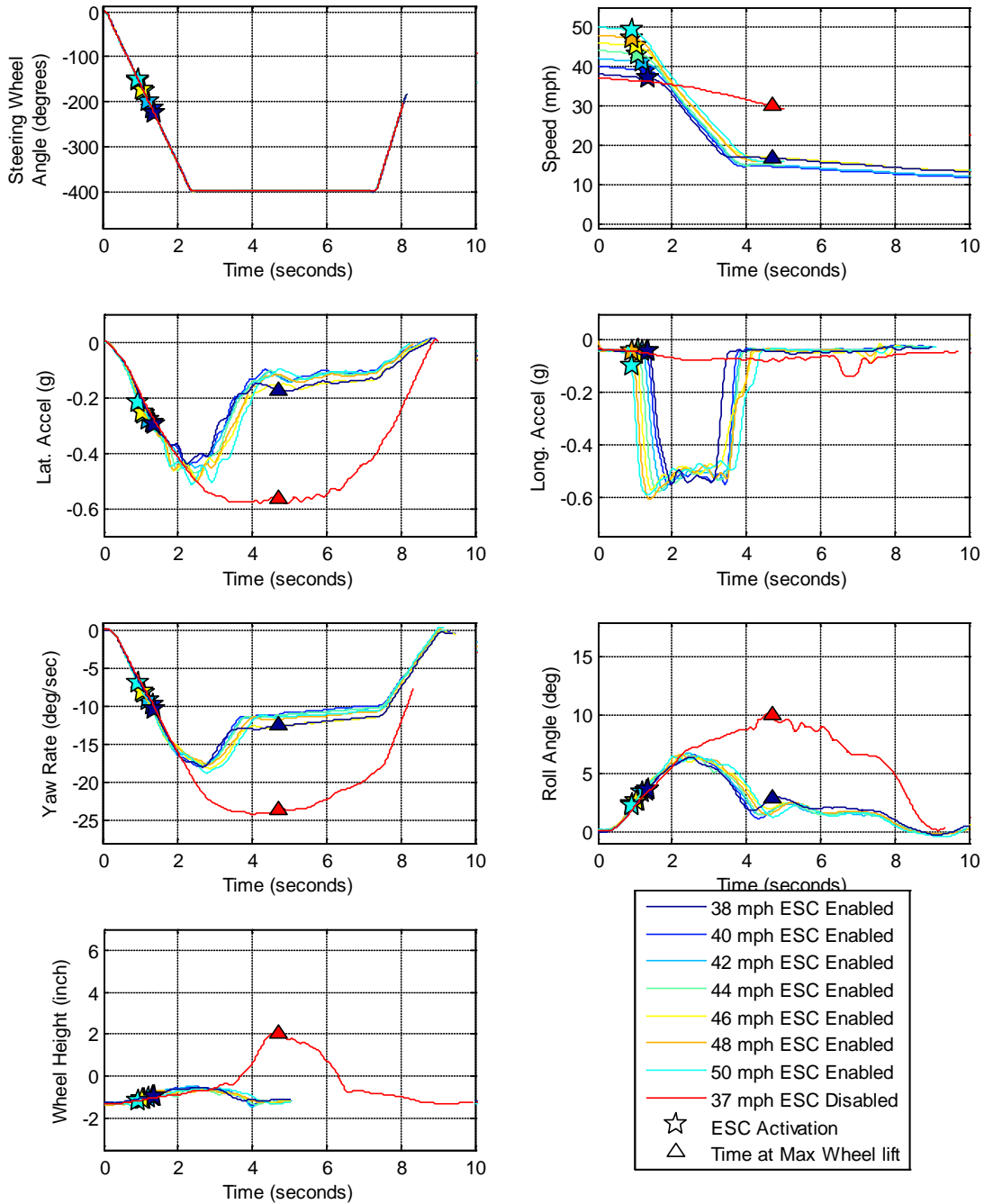


Figure 3.25. Graphs show RSM test data from the MCI #1 in the GPOW load condition with ESC enabled and disabled. Tests shown in this figure were performed at MESs of 38 to 50 mph with ESC enabled and at 37 mph with ESC disabled. For the ESC disabled test shown in red, wheel lift of two inches was observed for the ESC disabled test.

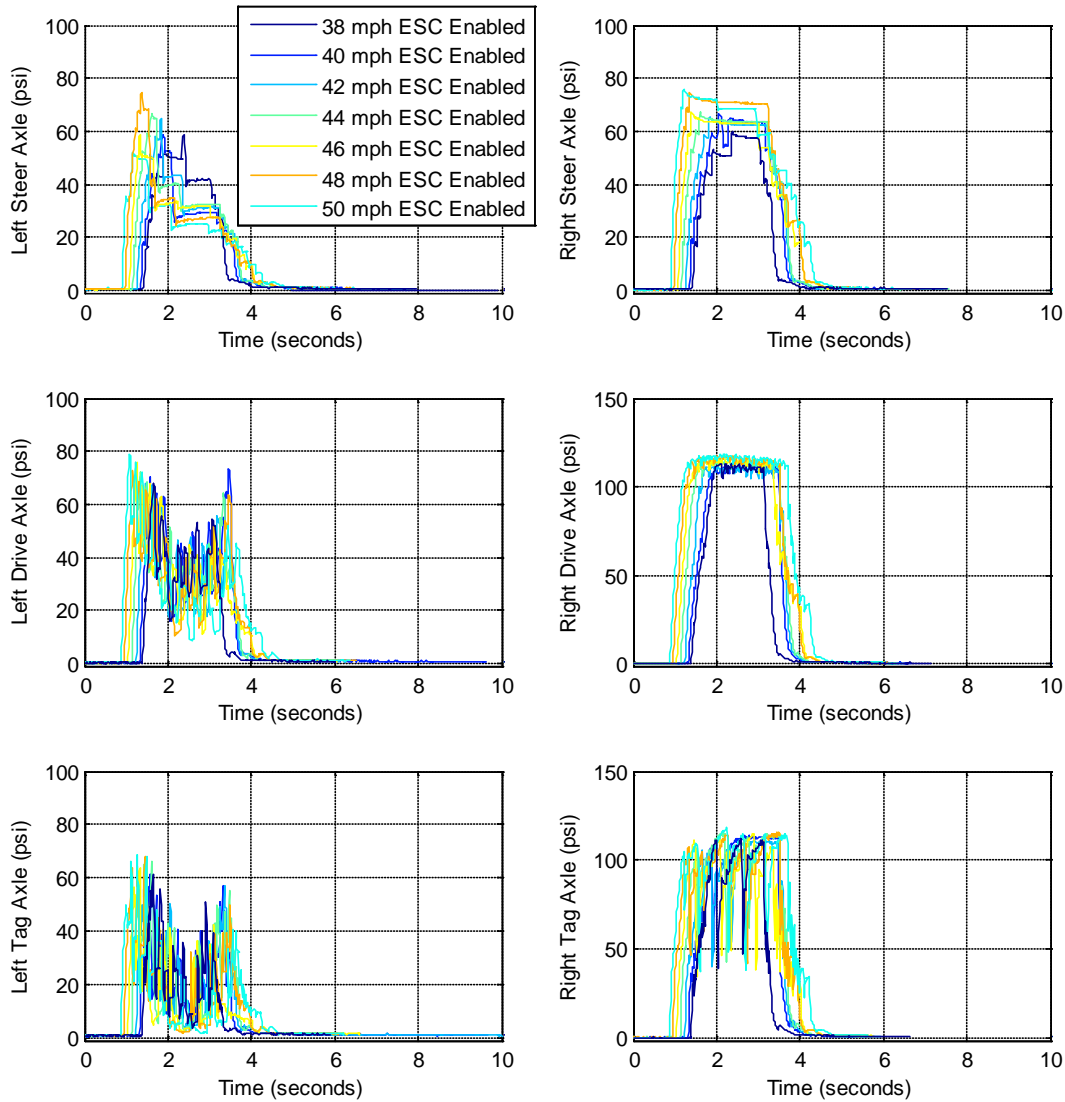


Figure 3.26. Graphs show brake pressures observed for RSM test data from the MCI #1 in the GPOW load condition ESC enabled. Tests shown in this figure were performed at MESs of 38 to 50 mph.

Figure 3.27 for the Prevost presents the steering wheel angle, speed, lateral acceleration, longitudinal acceleration, yaw rate, roll angle, and drive axle wheel ride height for RSMs for MES of 40 to 48 mph with ESC enabled. For comparison time history data from the disabled test conducted at 39 mph that produced two inches of wheel lift is also shown.

Figure 3.27 shows how ESC changed the dynamics of the Prevost. Comparing ESC enabled versus ESC disabled tests, the time at maximum wheel lift when ESC was disabled (red trace) was used. For these tests the time used for comparison was ~4.16 seconds. The values at 4.16 seconds for speed, lateral acceleration, yaw rate, and roll angle for the two ESC test conditions are shown in Table 3.16.

In Table 3.16, with ESC enabled the Prevost was able to increase roll stability by reducing the vehicle's speed by 13.3 percent, which in turn reduced lateral acceleration by 10.9 percent, the yaw rate by 19.7 percent, and its roll angle by 33 percent. Figure 3.28 shows the brake pressures observed at each wheel for the ESC enabled tests.

Table 3.16. Prevost lateral acceleration, yaw rate, and roll angle values and changes observed at the instant in time (shown in Figure 3.27) that maximum wheel lift was observed with ESC disabled. The MES was 39 mph with ESC disabled compared to a MES of 40 mph with ESC enabled.

ESC Condition	Speed (mph) [Change (%)]	Lateral Acceleration (g) [Change (%)]	Yaw Rate (deg/sec) [Change (%)]	Roll Angle (deg) [Change (%)]
ESC Disabled	32.4	-0.54	-21.7	10.7
ESC Enabled	28.1 [-13.3%]	-0.48 [-10.9%]	-17.4 [-19.7%]	7.2 [-33%]

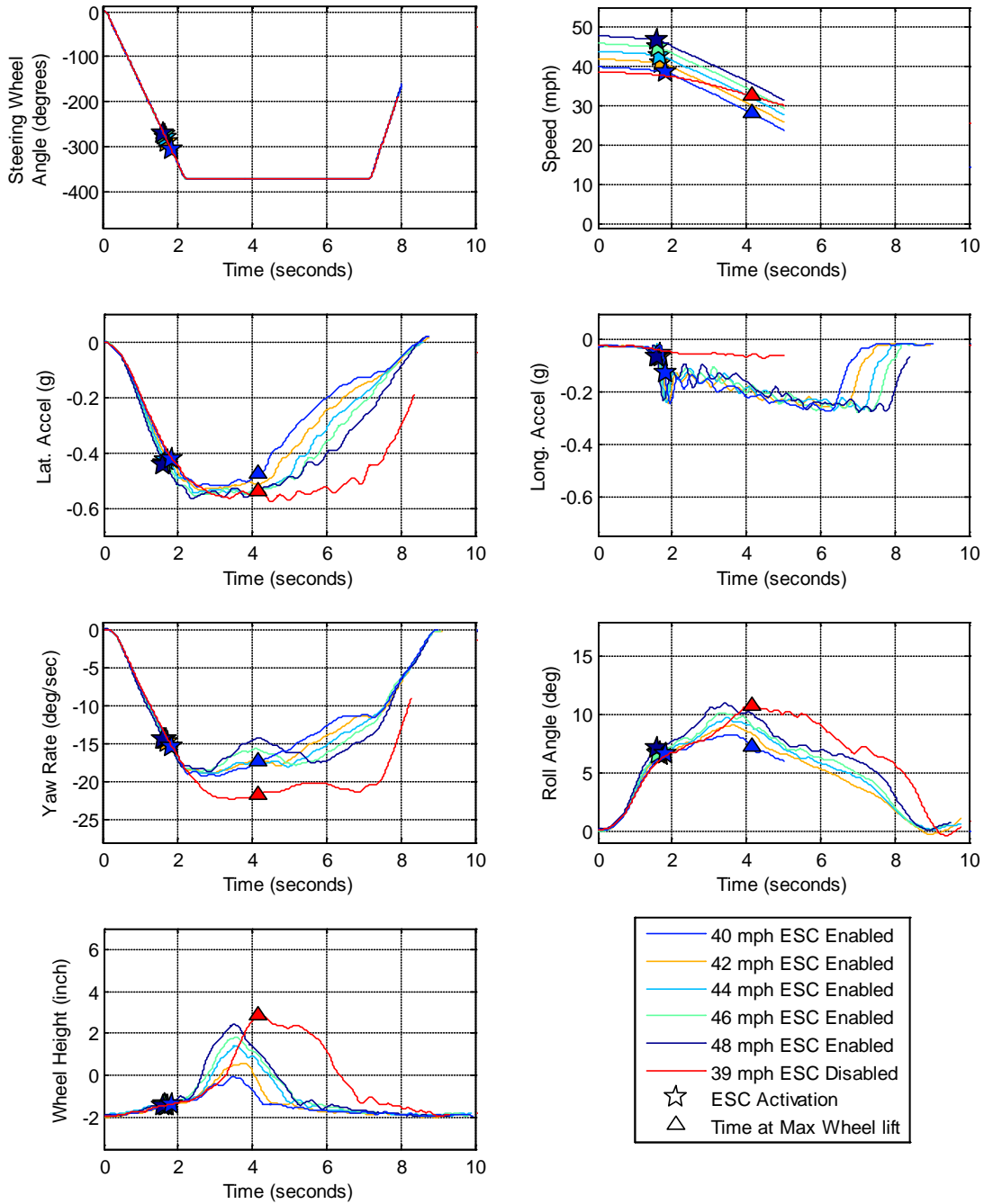


Figure 3.27. Graphs show RSM test data from the Prevost in the GPOW load condition with ESC enabled and disabled. Tests shown in this figure were performed at MESs of 40 to 48 mph with ESC enabled and at 39 mph with ESC disabled. The disabled test is shown in red. Wheel lift of two inches was observed for the ESC enabled tests at 48 mph and for the ESC disabled test at 39 mph.

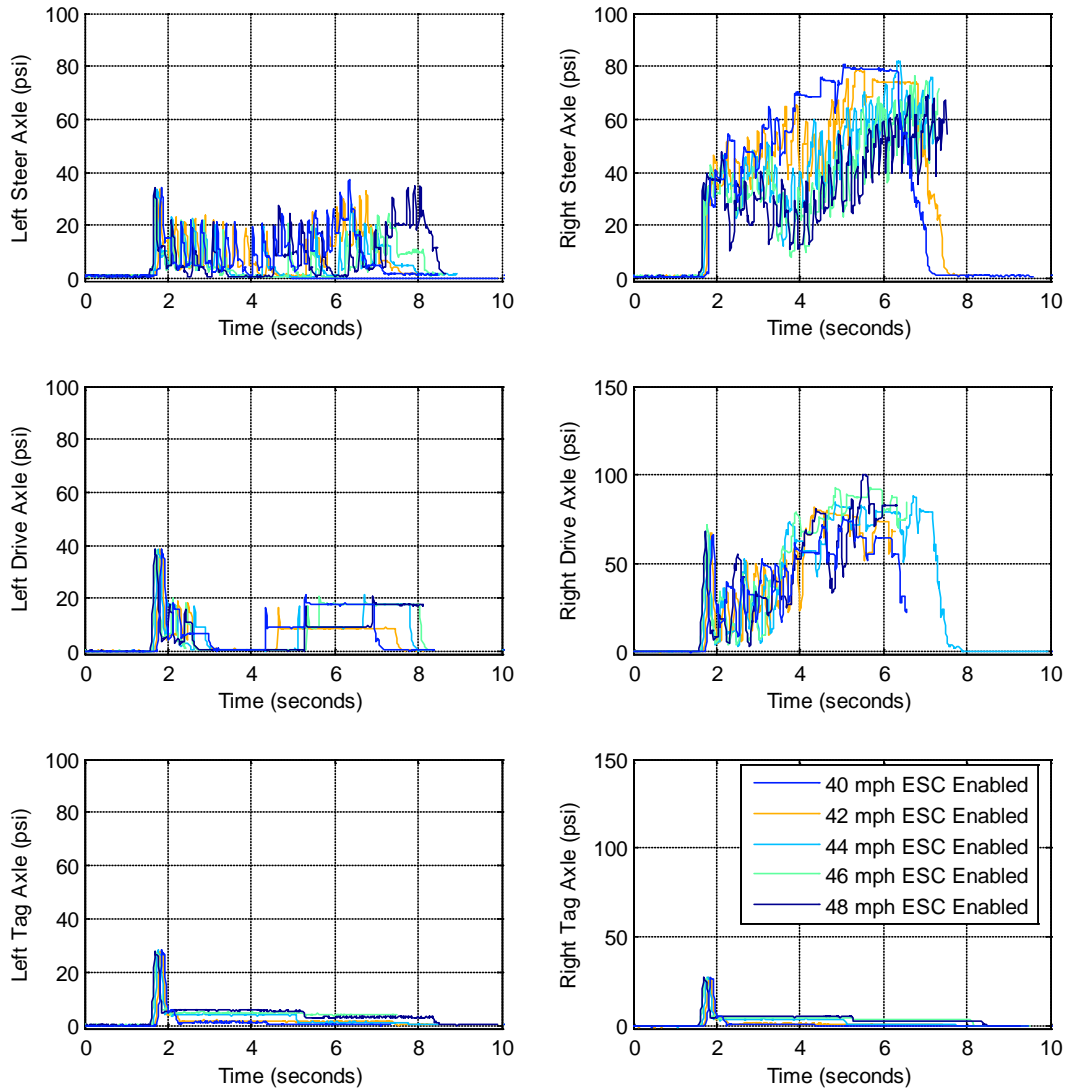


Figure 3.28. Graphs show brake pressures observed for RSM test data from the Prevost in the GPOW load condition ESC enabled. Tests shown in this figure were performed at MESs of 40 to 50.

Figure 3.29 for MCI #2 presents the steering wheel angle, speed, lateral acceleration, longitudinal acceleration, yaw rate, roll angle, and drive axle wheel ride height for RSMs. Shown in each figure are ESC enabled tests for MESs of 36 to 50 mph. For comparison time history data from the ESC disabled at 35 mph that produced two inches of wheel lift is also shown.

Figure 3.29 shows how ESC changed the dynamics of the MCI #2. To compare ESC enabled versus ESC disabled tests, the time at maximum wheel lift when ESC was disabled (red trace) was used. For these tests the time used for comparison was ~4.98 seconds. The values at 4.98 seconds for speed, lateral acceleration, yaw rate, and roll angle for the two ESC test conditions are shown in Table 3.17.

As shown in the table, the MCI #2 ESC system when enabled was able to increase roll stability by reducing the vehicle's speed by 39.6 percent, which in turn reduced lateral acceleration by 65.8 percent, the yaw rate by 41.0 percent, and its roll angle by 66 percent. Figure 3.30 shows brake pressures observed at each wheel for the ESC enabled tests.

Table 3.17. MCI #2 lateral acceleration, yaw rate, and roll angle values and changes observed at the instant in time (shown in Figure 3.29) that maximum wheel lift was observed with ESC disabled. The MES was 35 mph with ESC disabled, compared to a MES of 36 mph with ESC enabled.

ESC Condition	Speed (mph) [Change (%)]	Lateral Acceleration (g) [Change (%)]	Yaw Rate (deg/sec) [Change (%)]	Roll Angle (deg) [Change (%)]
ESC Disabled	27.2	-0.55	-24.5	12.4
ESC Enabled	16.4 [-39.6%]	-0.19 [-65.8%]	-14.5 [-41.0%]	4.2 [-66%]

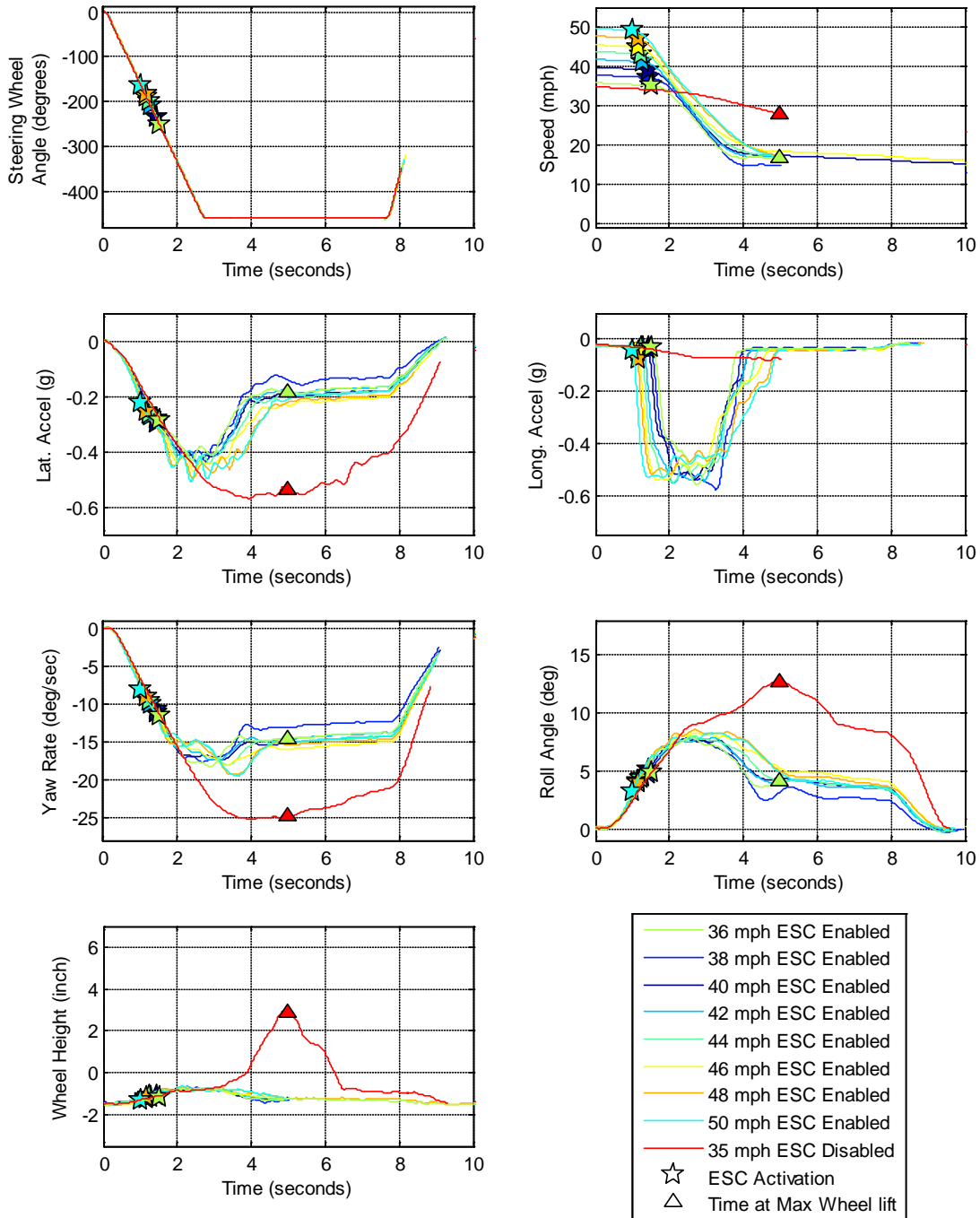


Figure 3.29. Graphs show RSM test data from the MCI #2 in the GPOW load condition ESC enabled and disabled. Tests shown in this figure were performed at MESs of 36 to 50 mph with ESC enabled and at 36 mph with ESC disabled. For the ESC disabled test is shown in red, wheel lift of over two inches was observed.

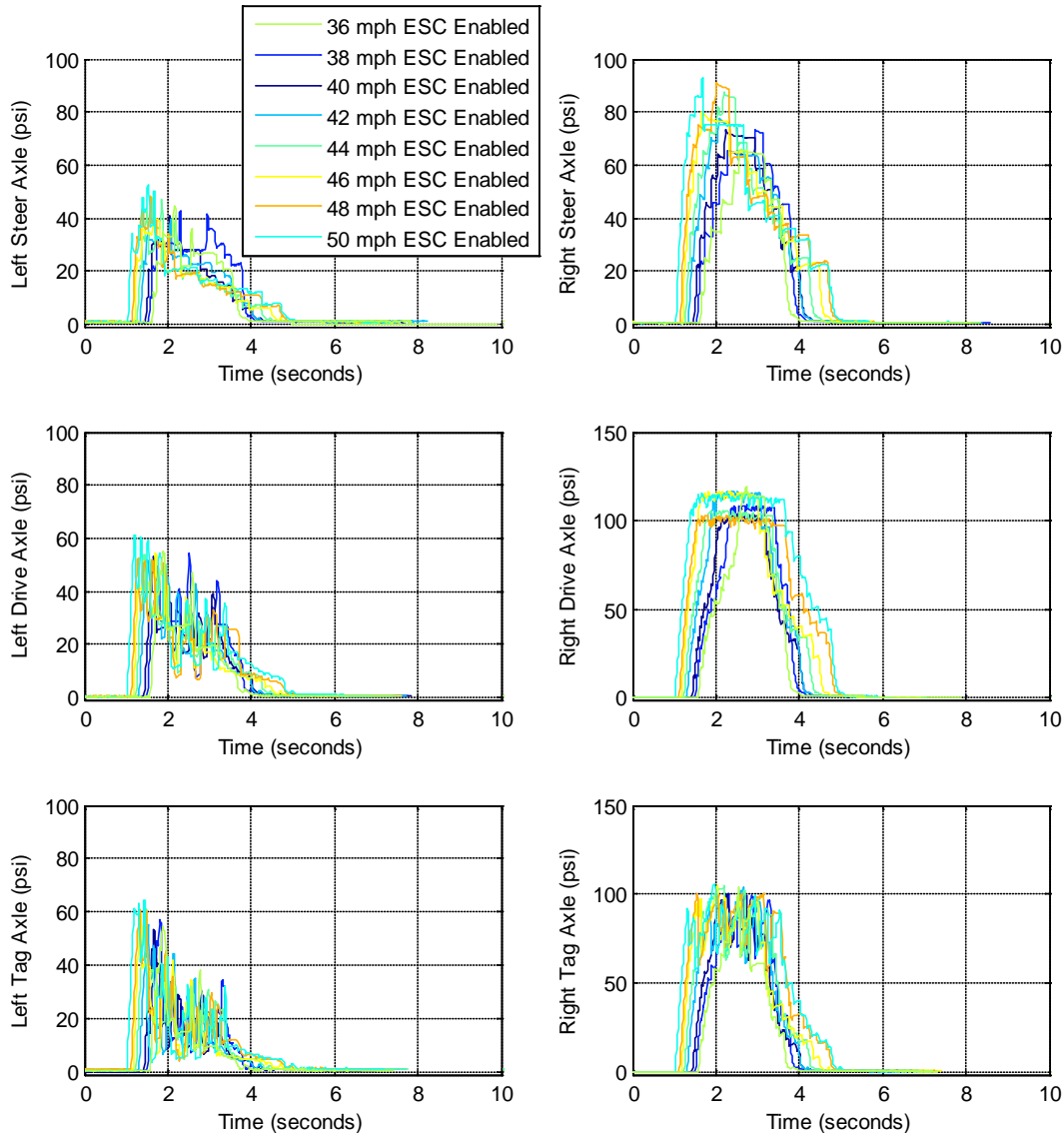


Figure 3.30. Graphs show brake pressures observed for RSM test data from the MCI #2 in the GPOW load condition with ESC enabled. Tests shown in this figure were performed at MESs of 36 to 50 mph.

3.3.3 RSM – Reduced Surface Friction – GPOW Load Condition

This section presents motorcoach test results from RSM tests performed on the reduced friction wet Jennite surface with the GPOW load condition. The initial MES was 20 mph, and it was incrementally increased in subsequent runs until two inches of wheel lift were observed, the vehicle went into a limit understeer condition (plow out), or the MES reached 40 mph without a roll or yaw instability. Testing on the low friction surface produced no wheel lift, but as the target MES was increased each of the motorcoaches began to understeer. Testing was terminated at MES of 40 mph because of plow out conditions and a lack of available test area to perform the maneuver at higher speeds.

One of the challenges in performing this maneuver was accelerating to the target MES. To conduct the RSM on the low friction surface, the vehicle must travel from north to south and make a 90 degree turn to line up for the approach. At higher MESs, during the 90 degree turn some ESC system activations occurred, slowing the vehicles down. At lower speeds, typically the vehicle made the transition to the low friction surface, the target MES was reached, and the driver could execute the maneuver. At higher speeds when ESC activated on the approach, speed was decreased, and the driver could not subsequently reach the target MES. In Figure 3.31 this can be observed comparing the solid orange trace (enabled) and the red dotted trace (disabled) for two runs both with a MES of 36 mph. The ESC enabled test took more time to reach the target MES. Comparing the beginning of steer (BOS) markers for the ESC enabled test to the ESC disabled test, it took about 100 feet more before the target MES was reached with ESC enabled.

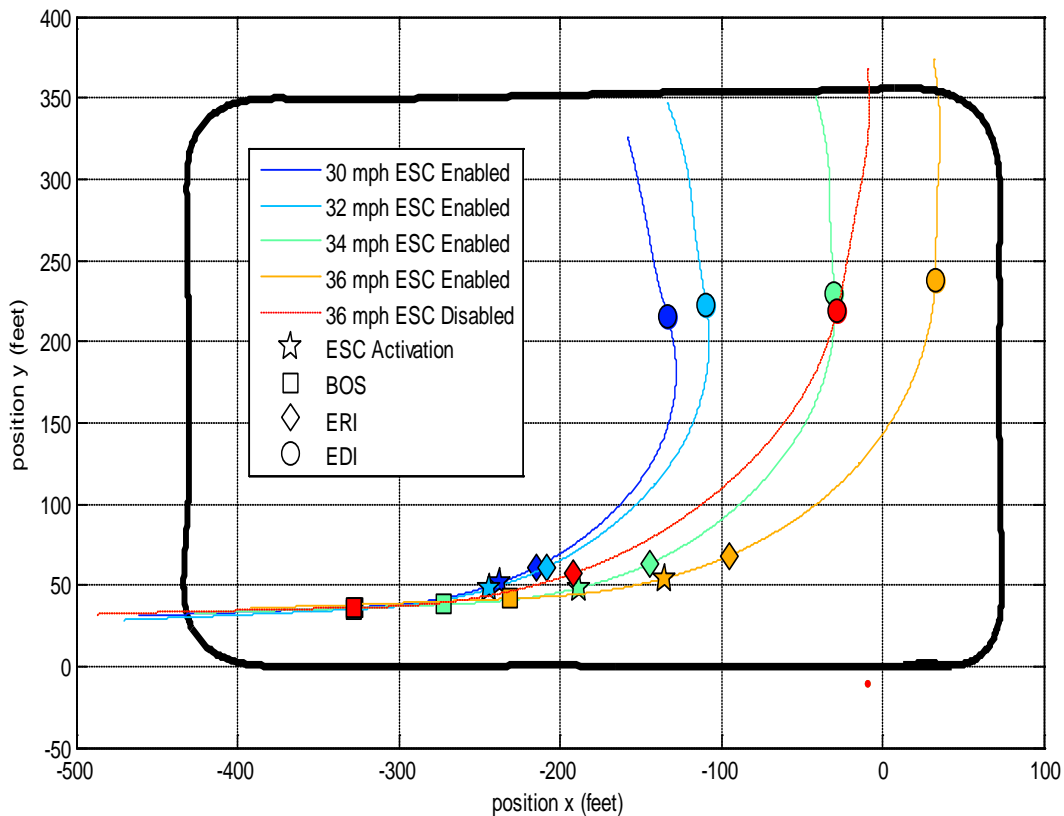


Figure 3.31. Jennite survey example of space needed to conduct RSM.

Figure 3.32 presents the steering wheel angle, speed, lateral acceleration, longitudinal acceleration, yaw rate, and throttle position for the MCI #1 conducting the RSM for a range of MESs. The yaw rate response up to the MES at which ESC activation occurred was similar for the ESC enabled and ESC disabled tests, but following activation a difference in yaw rate can be observed. For the ESC disabled test at 34 mph, yaw rate does not continue to build for the given steering input and indicates the vehicle is less responsive or plowing through the curve. For the ESC enabled test, following activation, yaw rate continues to build indicating that the ESC system is

addressing the severe understeer/plowout condition. The ESC system was observed to selectively apply brake torques making the vehicle more responsive to the steering input.

Figure 3.33 shows the brake pressures recorded at each wheel for the ESC enabled tests. By looking at the brake pressures it can be observed that braking was applied to the left wheels on both the drive and tag axles only for the range of MES shown. Brake pressures applied to these wheels shows that ESC is trying to mitigate the plow out event, which for the ESC enabled condition could cause the yaw rate to increase as shown in Figure 3.32.

Figure 3.34 is a GPS plot of vehicle path for the ESC enabled and disabled tests. The enabled tests are shown with solid lines and the disabled tests with dashed lines. For each MES shown, the ESC enabled and ESC disabled test are the same color traces. To compare the ESC enabled to the ESC disabled tests the position data were zeroed and oriented so that the vertical axis was approximately parallel to the direction of motion of the vehicle at BOS. Included in the figure is a subplot of the steering input with markers to indicate the BOS, end of (initial) ramp input (ERI), and end of dwell input (EDI). Those same markers are overlaid onto the position plots for a time reference. Comparing ESC enabled to disabled, a small deviation in path can be observed. For each MES shown, the path of the motorcoach with ESC enabled had a smaller radius than the path with ESC disabled.

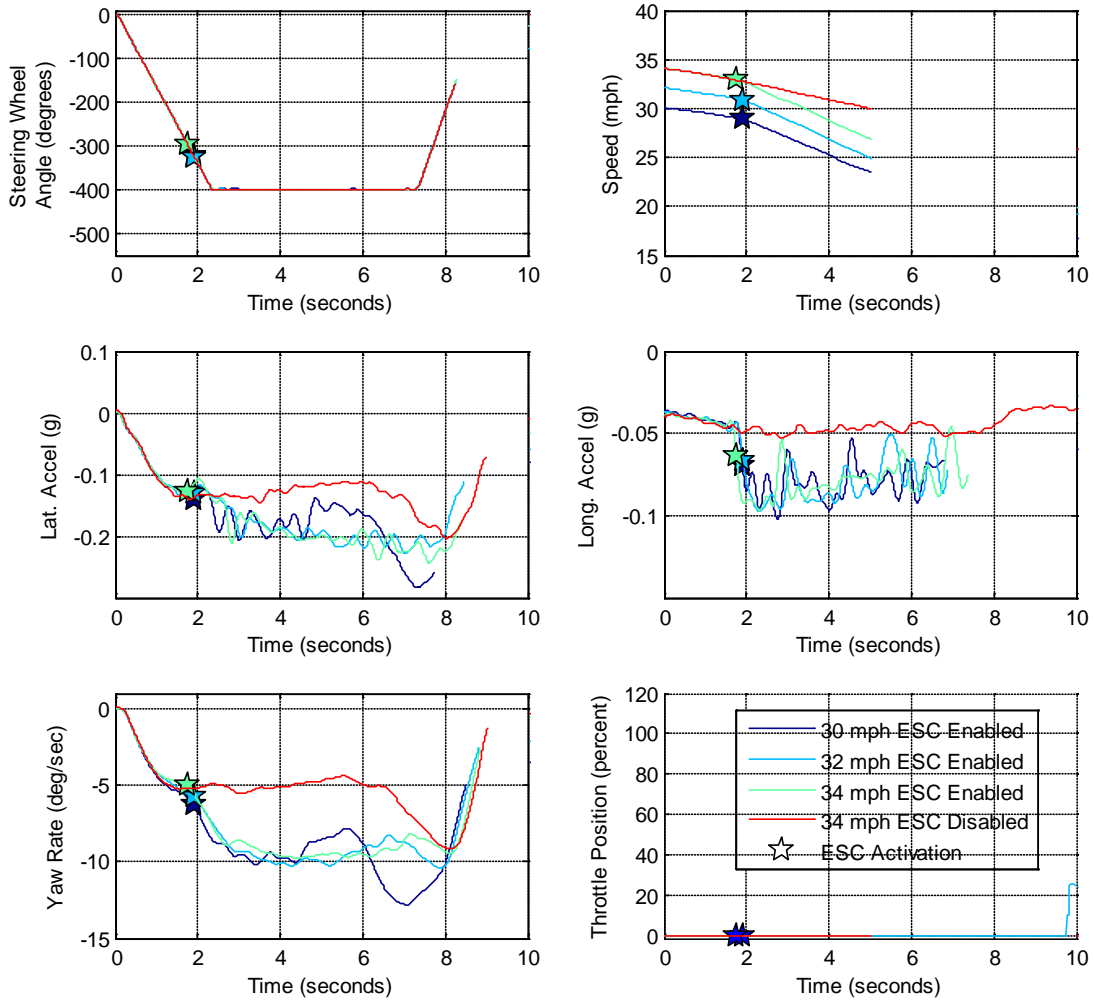


Figure 3.32. MCI #1 RSM time history data from series performed on the Jennite with the GPOW load condition.

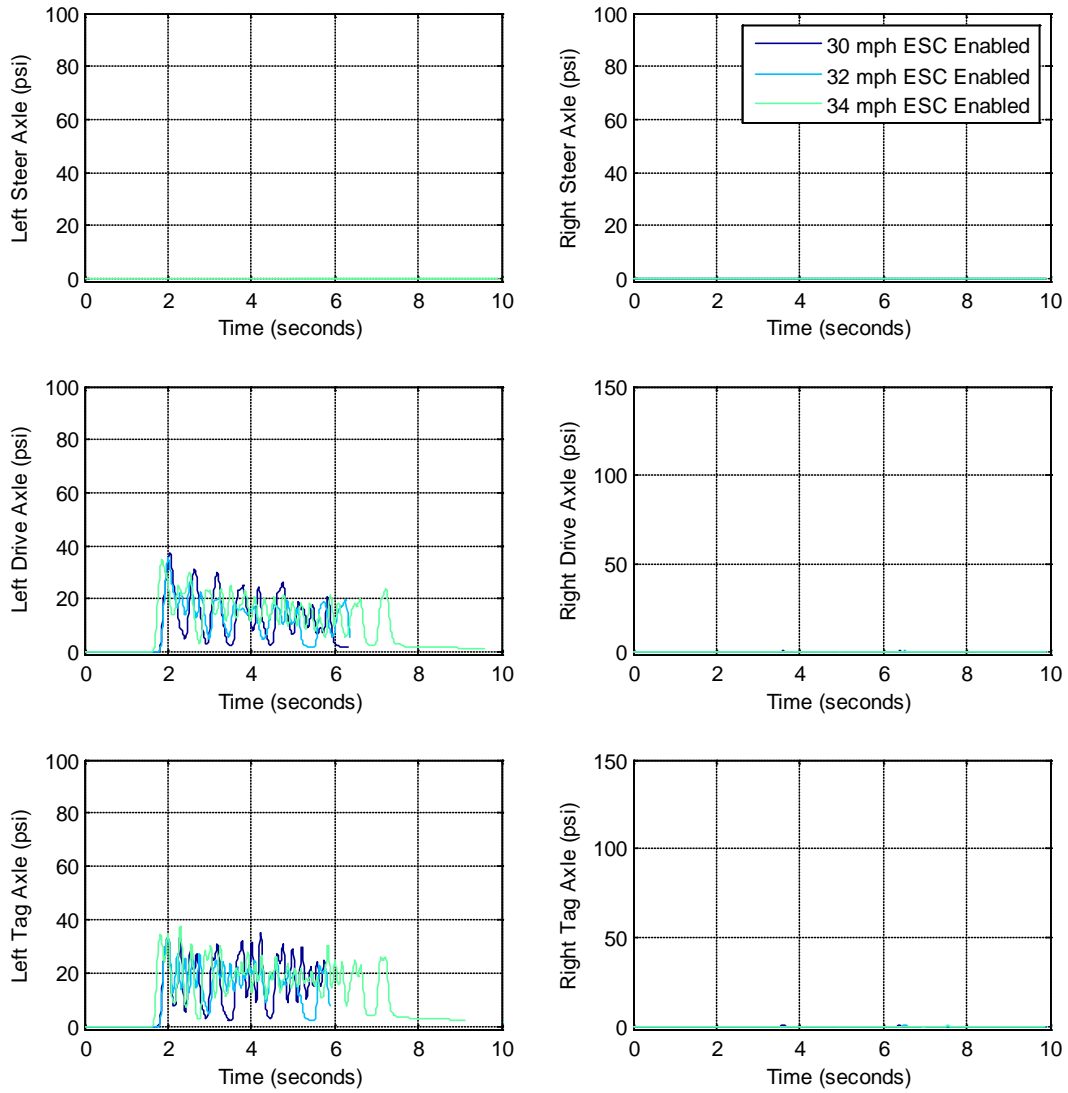


Figure 3.33. MCI #1 brake pressure data from RSM tests conducted on the Jennite (same tests as shown in Figure 3.32)

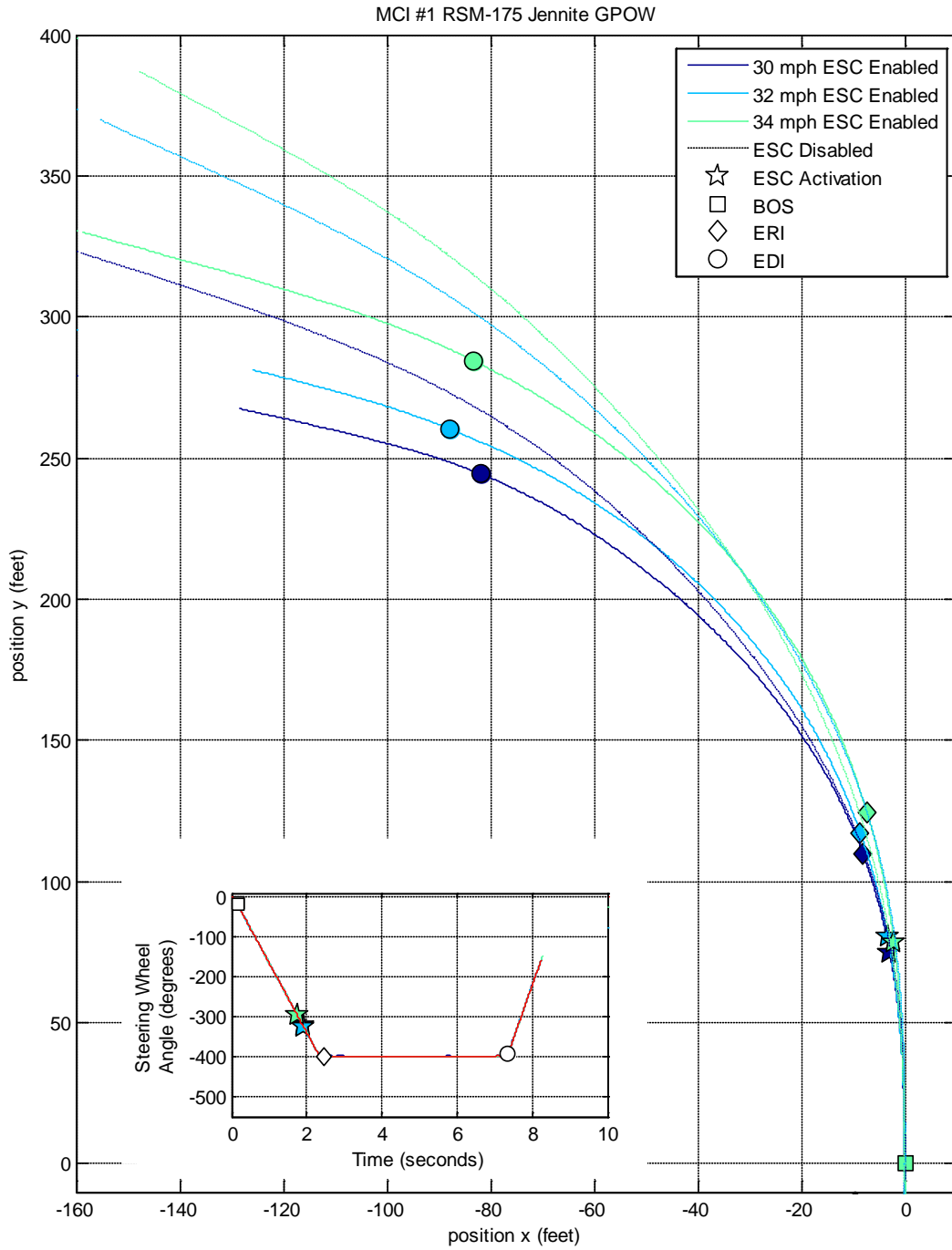


Figure 3.34. MCI #1 path data from RSM test performed on the Jennite.

Figure 3.35 presents RSM time history data for the Prevost for a range of MESs. The yaw rate response up to ESC activation was similar for the enabled and disabled tests, but following activation a difference in yaw rate was observed. For the ESC disabled test at 34 mph, yaw rate does not continue to build for the given steering input and indicates the vehicle is less responsive or plowing through the curve. For the ESC enabled test, following activation, yaw rate continues to build indicating that the ESC system is addressing the severe understeer/plowout condition. The ESC system was observed to selectively apply brake torques making the vehicle more responsive to the steering input.

Figure 3.36 shows the brake pressures recorded at each wheel for the ESC enabled tests. These brake pressure data shows that the Prevost's ESC system was commanding brakes to be applied during the maneuver.

Figure 3.37 is a GPS plot of the Prevost paths for the ESC enabled and disabled tests. Position data are only shown for a range of MES up to 36 mph. Tests at MESs of 38 and 40 mph did not have valid GPS test data so these were excluded. The enabled tests are shown with solid lines and the disabled tests with dashed lines. For each MES shown, the enabled and disabled tests are the same color traces. Comparing ESC enabled to disabled tests, a small deviation in path was observed. For each MES shown, the path of the motorcoach with ESC enabled had a smaller radius than the path with ESC disabled.

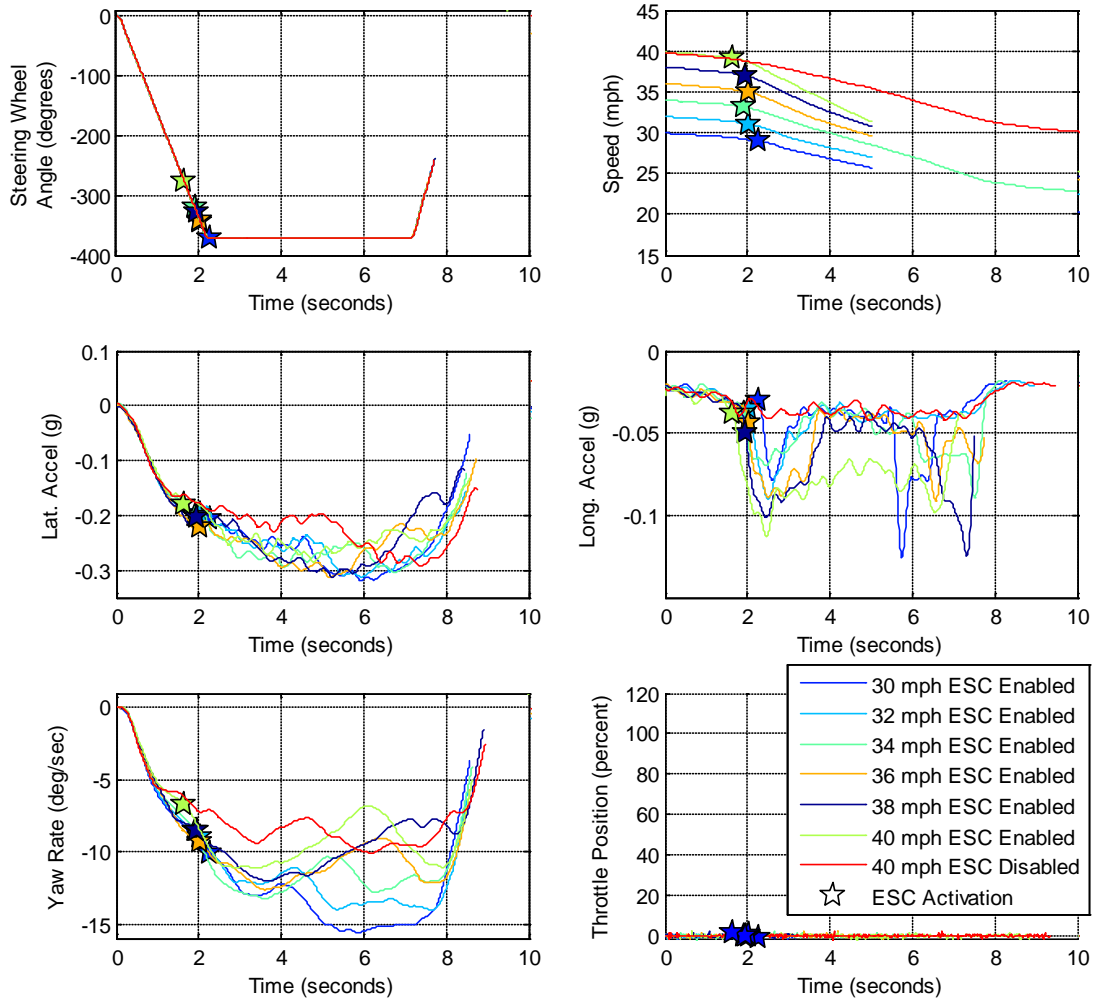


Figure 3.35. Prevost RSM time history data from tests conducted on the Jennite surface.

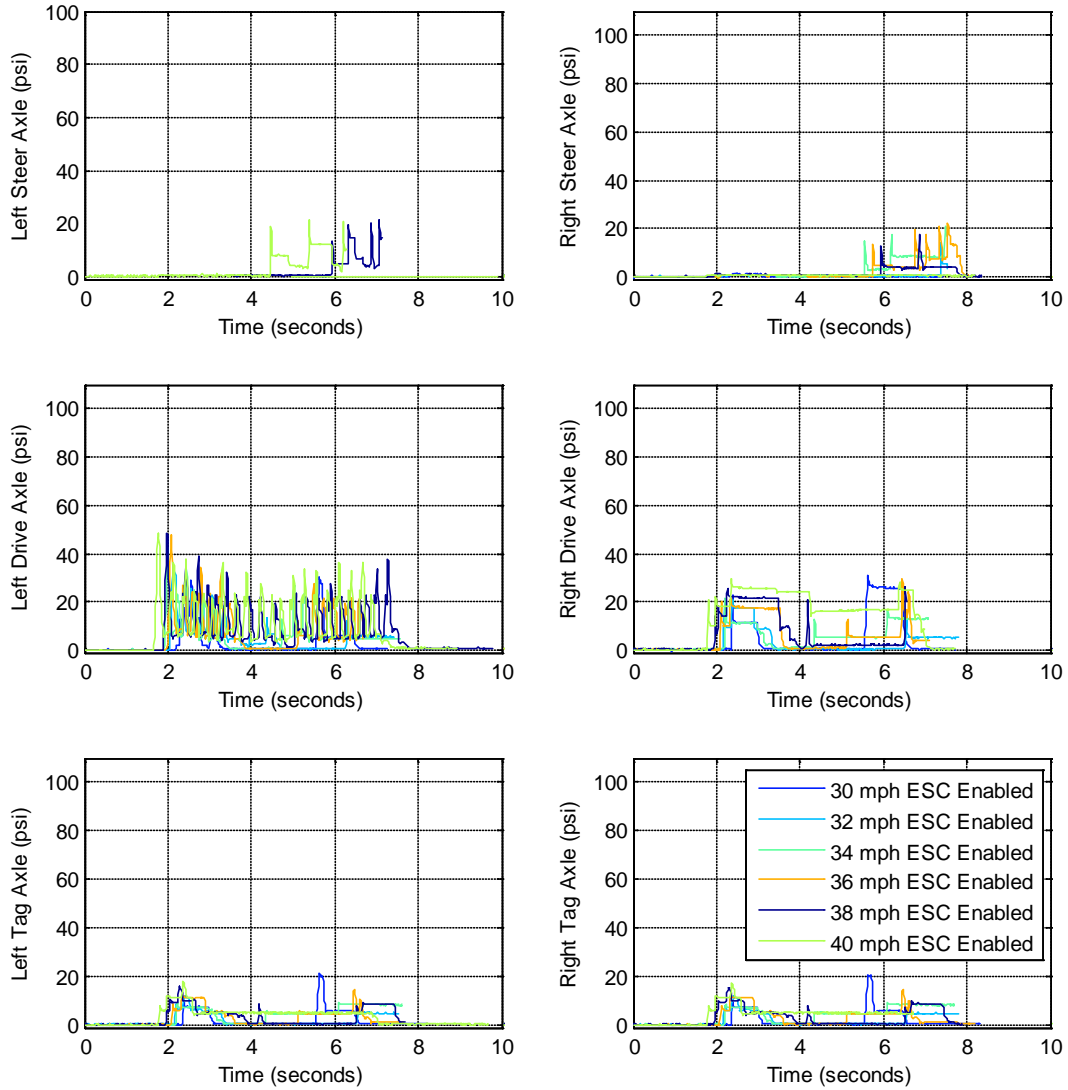


Figure 3.36. Prevost brake pressure data from RSM test performed on the wet Jennite (same enabled tests as shown in Figure 3.35).

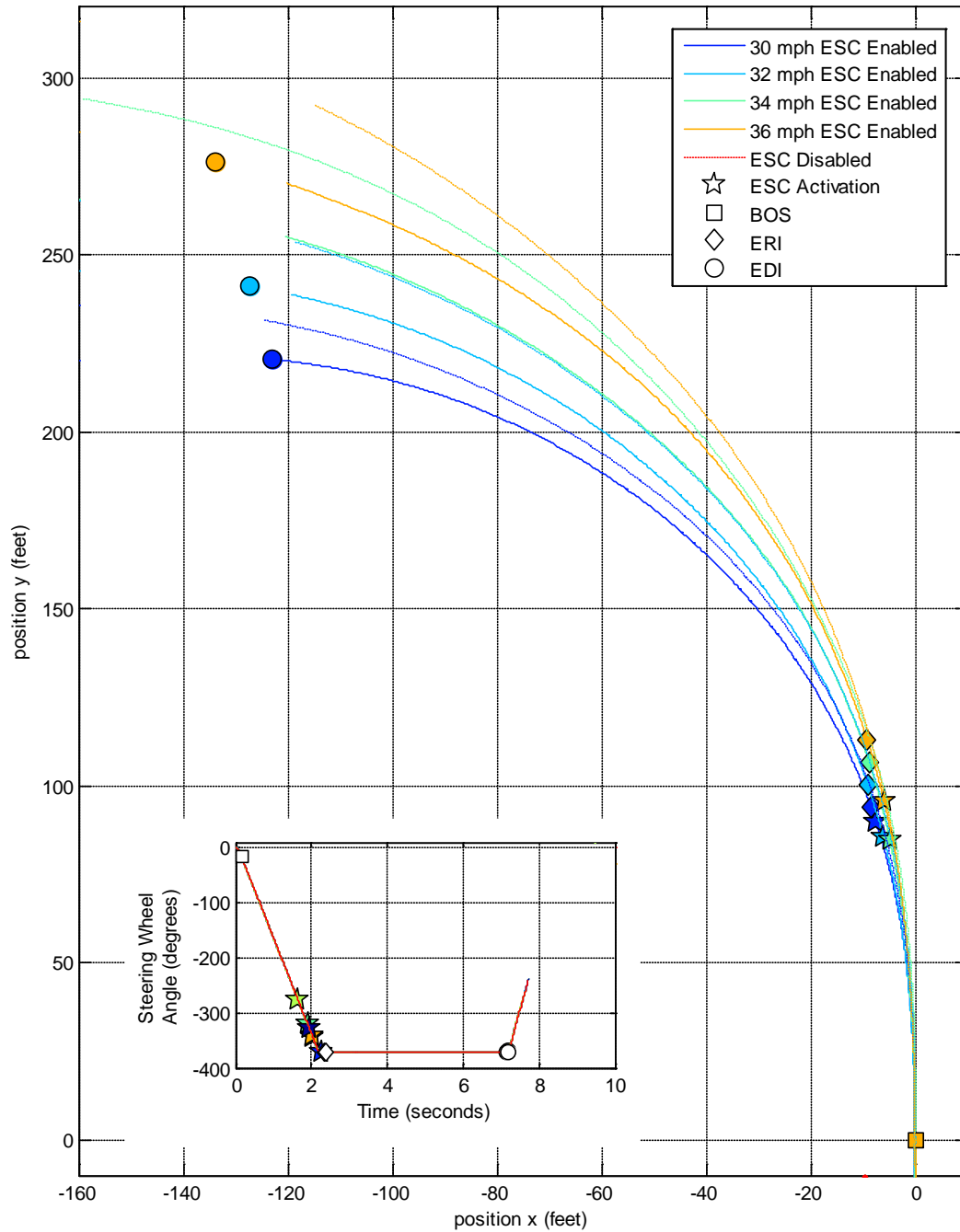


Figure 3.37. Prevost path data from RSMs performed on the Jennite.

Figure 3.38 presents RSM time history data for the MCI #2 for a range of MESs. The yaw rate response up to ESC activation is similar for the enabled and disabled tests, but following activation a difference in yaw rate was observed. For the ESC disabled test at a 34 mph yaw rate does not continue to build for the given steering input and indicates the vehicle is less responsive or plowing through the curve. For the ESC enabled test, following activation, yaw rate continues to build indicating that the ESC system is addressing the severe understeer/plowout condition. The ESC system was observed to selectively apply brake torques making the vehicle more responsive to the steering input. Figure 3.39 shows the brake pressures applied to improve MCI #2's response to the speed and steering inputs for the ESC enabled tests.

Figure 3.40 is a GPS plot of vehicle path for ESC enabled and disabled tests. The enabled tests are shown with solid lines and the disabled tests with dashed lines. For each MES shown, the enabled and disabled test are the same color traces. Comparing ESC enabled to disabled tests, a small deviation in path was observed. For each MES shown the path of the motorcoach with ESC enabled had a smaller radius than the path with ESC disabled.

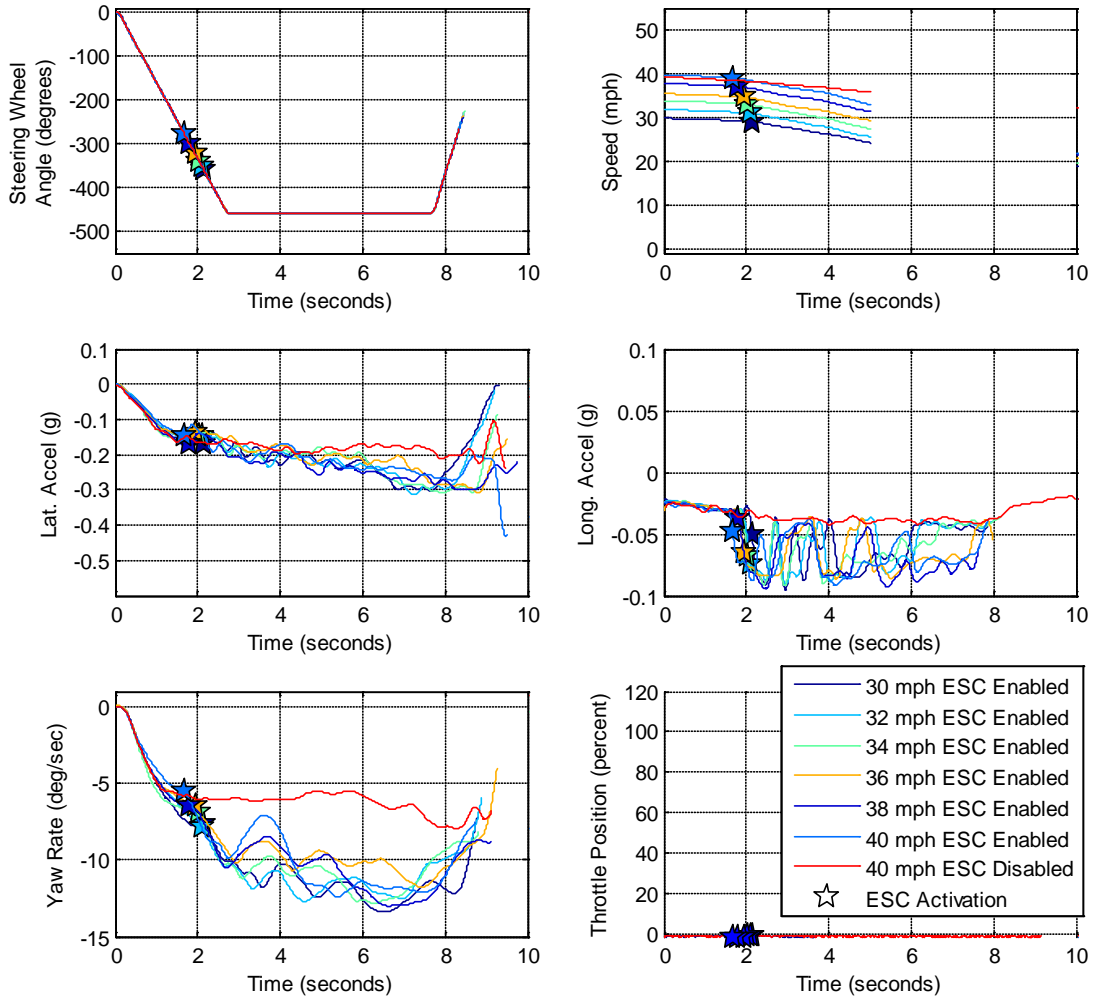


Figure 3.38. MCI #2 RSM time history data from the test series conducted on the wet Jennite.

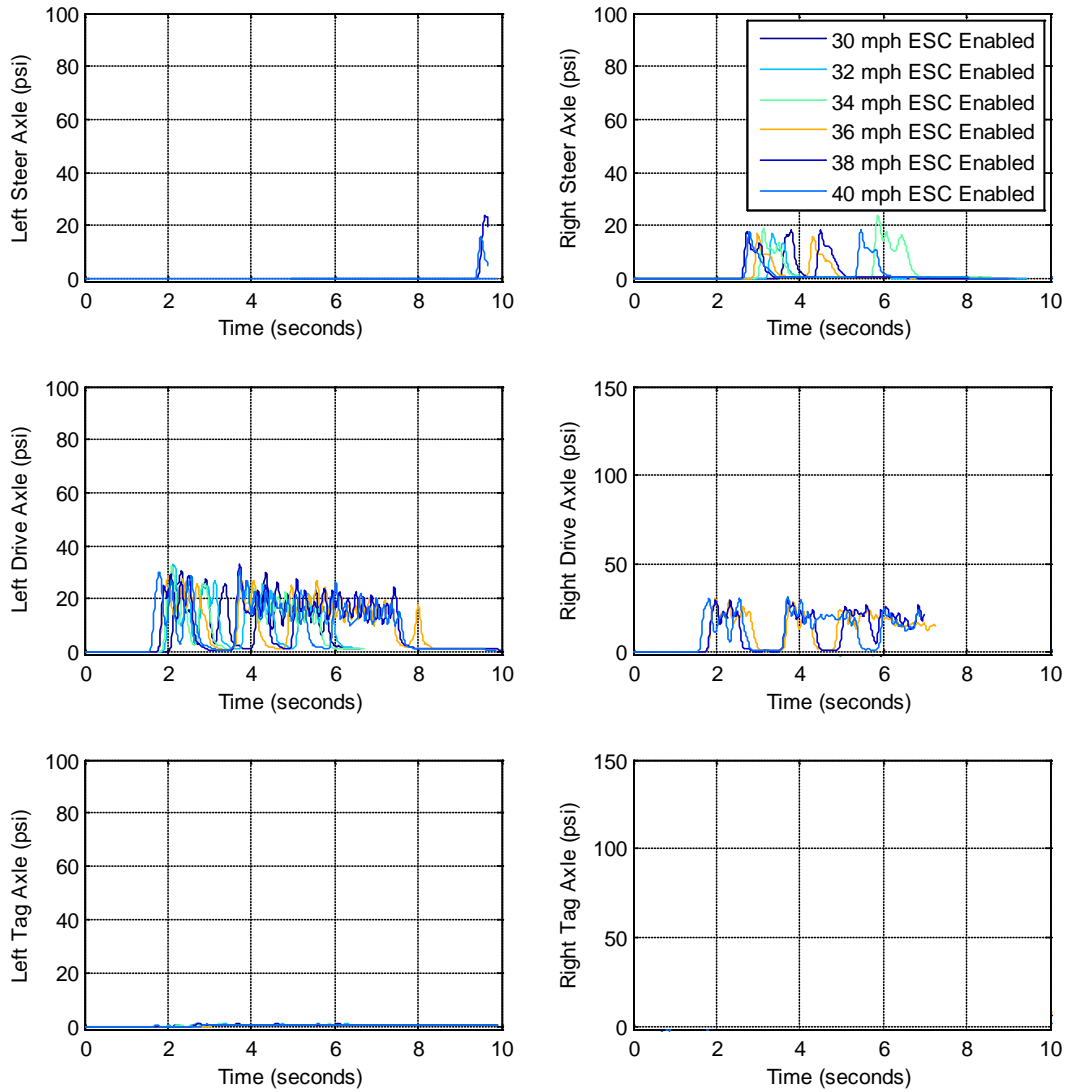


Figure 3.39. MCI #2 brake pressure data form RSMs performed on the Jennite with ESC enabled (same enabled tests as shown in Figure 3.38).

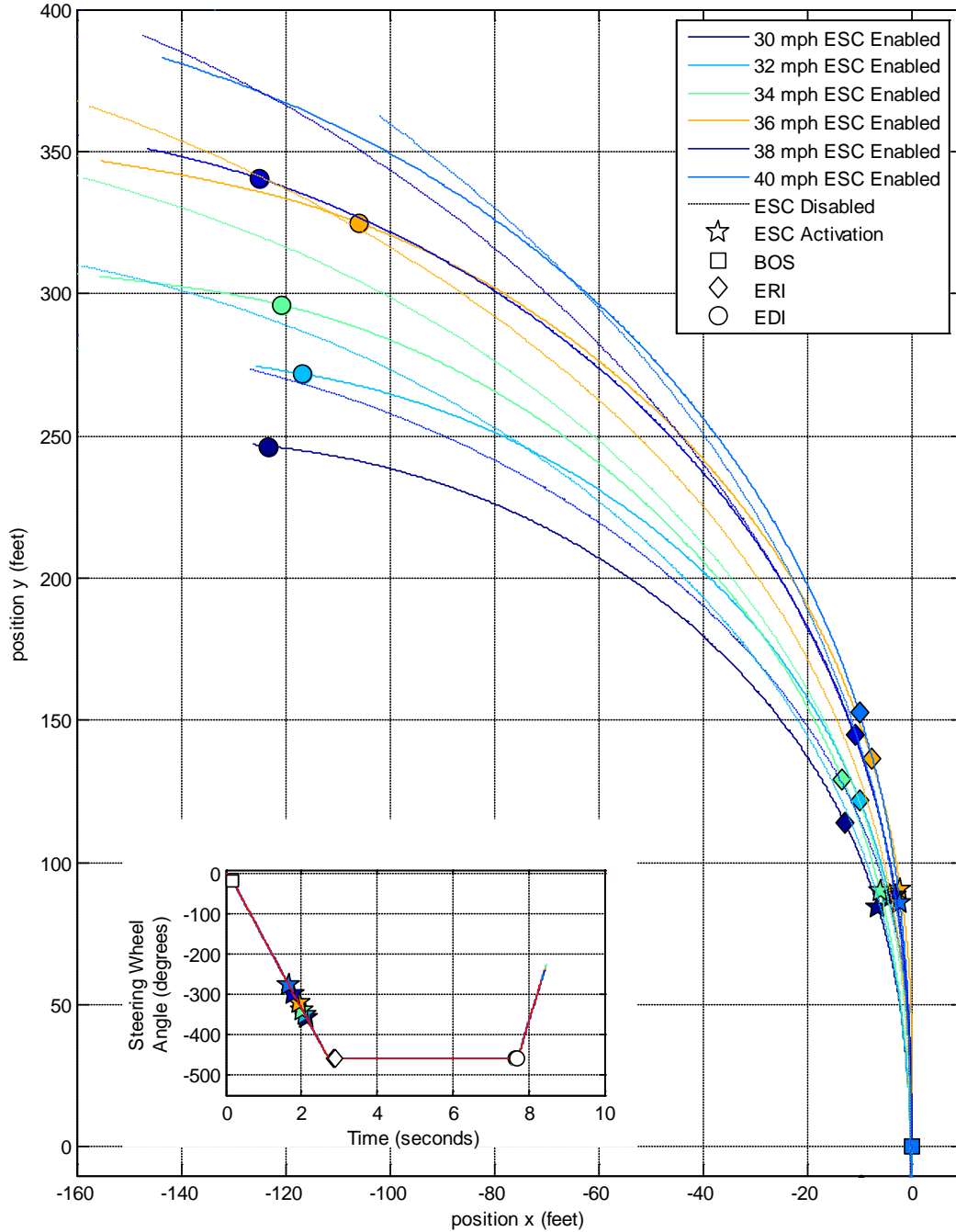


Figure 3.40. MCI #2 path data from RSMs performed on the Jennite test surface.

3.4 RWD Maneuver Test Results

This section presents the GPOW load condition RWD test results conducted on the reduced friction wet Jennite test surface. The RWD maneuver (similar to the RSM or a decreasing radius curve maneuver) was developed to create deviation between the driver's intended path and the actual vehicle path. This deviation in path activated the yaw control algorithms in the ESC systems installed in the motorcoaches. By design,

this maneuver then allowed yaw performance comparisons to be made between the motorcoaches with and without aid from the ESC system. This maneuver was added to the test matrix after the MCI #1 lease had expired. Therefore, this maneuver was only performed with the Prevost and MCI #2 motorcoaches.

For this maneuver, a drive-through speed and steering angle were determined for each motorcoach by finding the maximum speed not to exceed 35 mph that the driver could maintain control within the 12 foot lane marking the 500 foot radius curve. Figure 3.41 is a survey of TRC's Jennite surface and the 500 foot radius curve that was used to find the drive-through angle and conduct the RWD maneuvers.

None of the vehicles tested reached 35 mph during the drive-through tests without exiting the lane. The Prevost drive-through speed was 32 mph and the MCI #2 was 26 mph. The actual speed used to conduct the RWD maneuver is 90 percent of the drive-through speed. The speed at which RWD maneuver was conducted for the Prevost was 29 mph and for the MCI #2 it was 23 mph.

The drive-through steering angle at 32 mph for the Prevost was 80 degrees and for the MCI #2 it was 100 degrees. Steering profiles were created and programmed into the steering controller so that from the initial drive-through angle the steering input could be ramped up in 90 degree increments and held for some period of time. The RWD maneuver was conducted by navigating the vehicle through the 500' radius at 90 percent of the drive-through speed. At the appropriate time the driver initiated the first steering increment to the left. The maneuver amplitudes were determined by multiplying a constant (K) integer value from 2 through 6 to the drive-through angle rounded to the nearest 90 degrees. The terminating condition for this maneuver was the steering increment that caused the ESC system to activate⁴. If no ESC activation was observed then additional tests were performed with increased K values. This methodology resulted in steering magnitudes of 180, 270, and 360 degrees for K equal to 2-4 for each motorcoach.

⁴ Activation in this research was determined from the vehicles J1939 CAN network control signals for the manufacturers brake and engine controllers and measured brake pressure data.

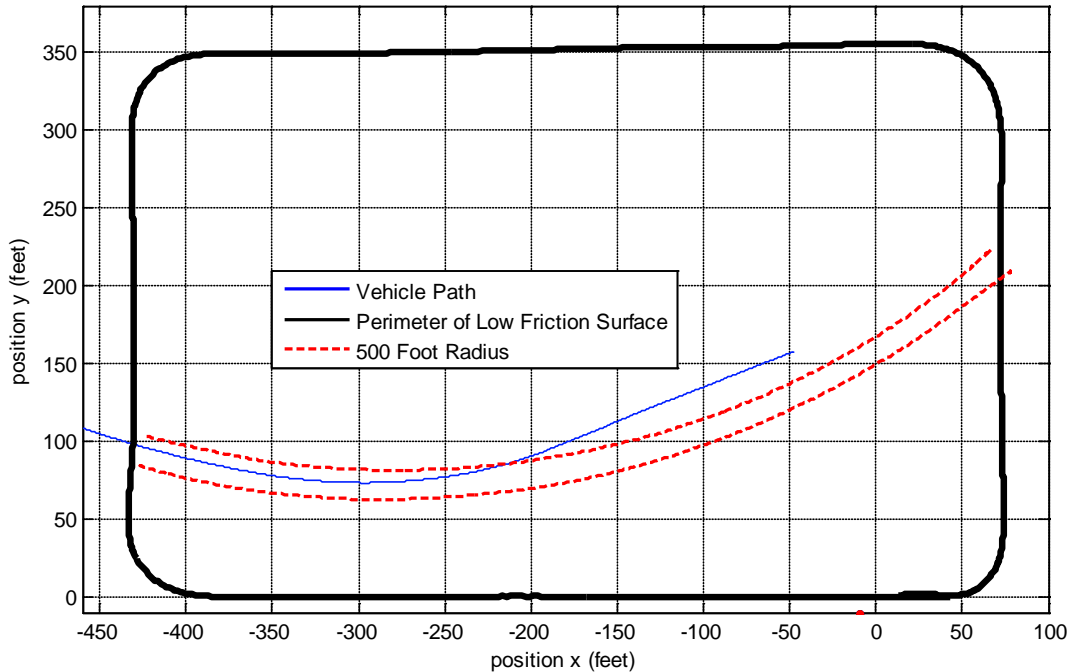


Figure 3.41. Survey of TRC's Jennite surface and the 500 foot radius.

In Table 3.18 ESC activation occurred at the second steering increment for the Prevost and the third increment for MCI #2 from the initial drive-through angle. The resultant angle for the Prevost was 270 degrees and for the MCI #2 it was 360 degrees.

The Prevost and MCI #2 was observed to be stable for 180, 270, and 360 degree steering inputs with ESC enabled and disabled test conditions (Table 3.19). Both motorcoaches were observed to understeer.

Table 3.18. RWD test series lowest steering angle that resulted in ESC activation

Motorcoach	Lowest Steering Angle That Resulted In ESC Activation (degrees)
Prevost	270
MCI #2	360

Table 3.19. RWD tests series lowest steering angle that resulted in instability

Motorcoach	Lowest Steering Angle That Resulted In Instability (degrees)	
	Enabled	Disabled
Prevost	TC	TC
MCI #2	TC	TC

TC = Test Completed for Inputs of 180, 270, and 360 degrees

Figure 3.42 shows time history data from the Prevost with ESC enabled and disabled for the lowest steering angle that resulted in ESC activation. The steering wheel input was 180 degrees from the initial drive-through angle resulting in a maximum angle of 270 degrees. The speed at which the maneuver was conducted was 29 mph and was held constant by the driver. From top to bottom, and left to right, the figure shows steering wheel angle, speed, lateral acceleration, longitudinal acceleration, yaw rate, and throttle position. The blue pentagram indicates where ESC activation first occurs during the maneuver. For the ESC enabled tests there is a reduction in speed following activation as compared to the ESC disabled test where speed is fairly constant for the duration of the maneuver. By reducing speed and activating the brake system, the ESC system was able to increase the vehicle's lateral acceleration and yaw rate, thereby reducing the possibility of plowing through the intended path.

Figure 3.43 shows torque and brake pressure time history data from the Prevost for the ESC enabled test only. The top plot contains driver torque, engine torque, and retarder torque. Following from top to bottom, and left to right, are individual brake pressures at each wheel. At ESC activation, engine torque reduction can be observed by the separation between driver-demanded and engine torque signals. Driver-demanded torque gradually increases to 100 percent and engine torque gradually decreases to zero. As the dynamics change following ESC activation, engine torque is allowed to increase. Only brake pressure on the drive and tag axles (biased towards the wheels closest to the inside of the curve) can be observed following ESC activation.

Figure 3.44 is a GPS plot of the Prevost path for ESC enabled and disabled tests. To compare the ESC enabled to the ESC disabled tests, the position data was zeroed and oriented so that the vertical axis was approximately parallel to the direction of motion of the vehicle at beginning of steering input (BOS). Included in the figure is a subplot of the steering input with markers to indicate the BOS, end of the ramp input (ERI), and the end of dwell input (EDI). Those same markers are overlaid onto the position plot for a time reference. Comparing ESC enabled to ESC disabled results, a small deviation in path was observed.

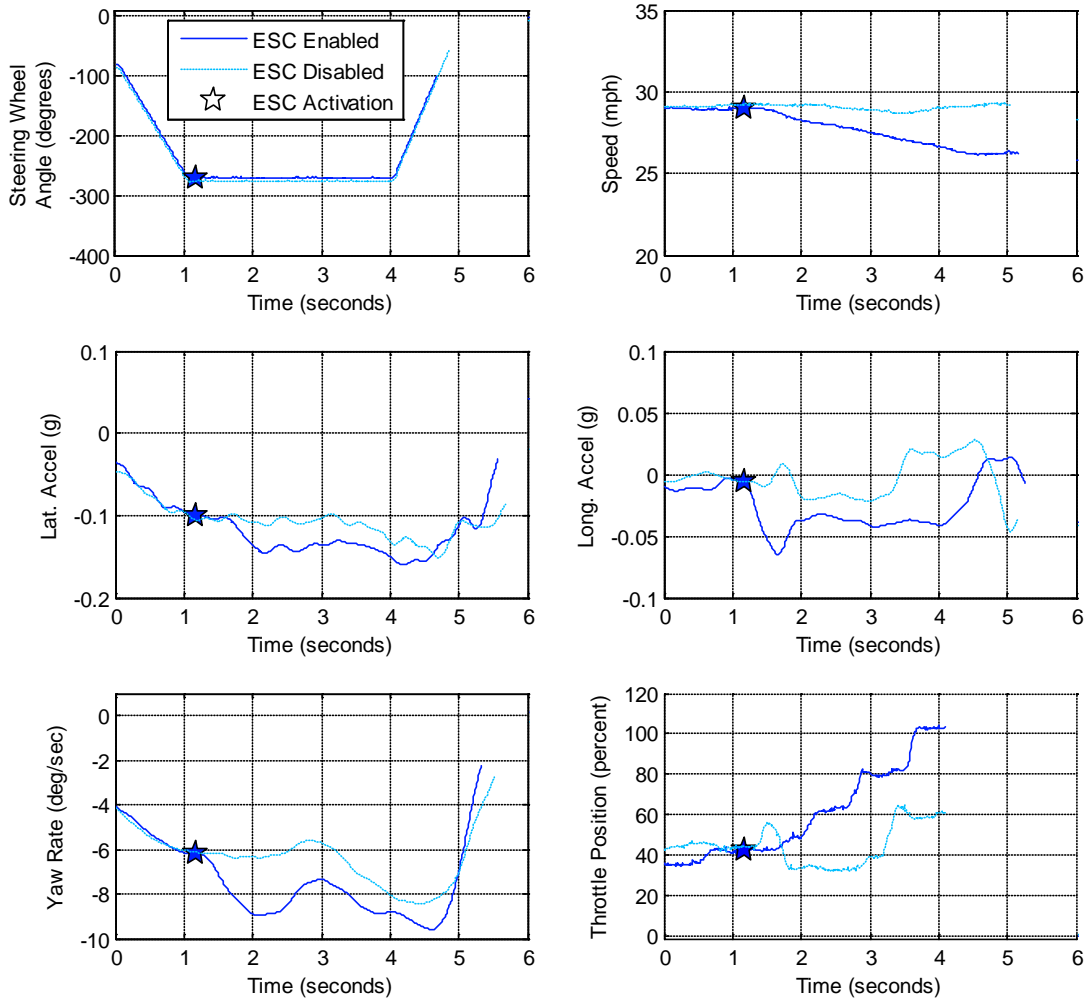


Figure 3.42. Prevost time history data from the RWD maneuver and GPOW load condition. Example shows the RWD test with the lowest steering angle input that resulted in ESC activation.

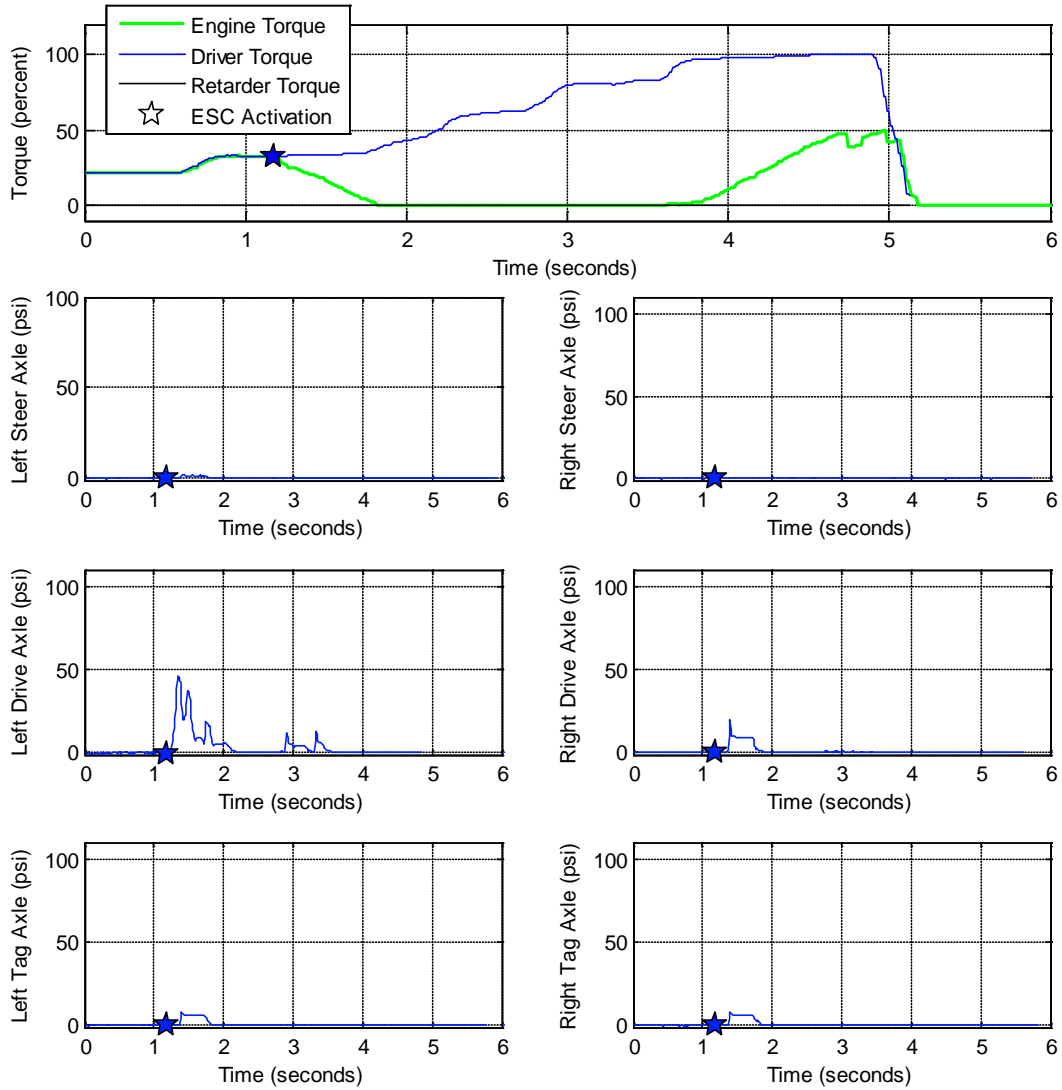


Figure 3.43. Prevost brake pressure data form RWD tests conducted on the Jennite test surface with the GPOW load condition (same enabled tests as shown in Figure 3.42).

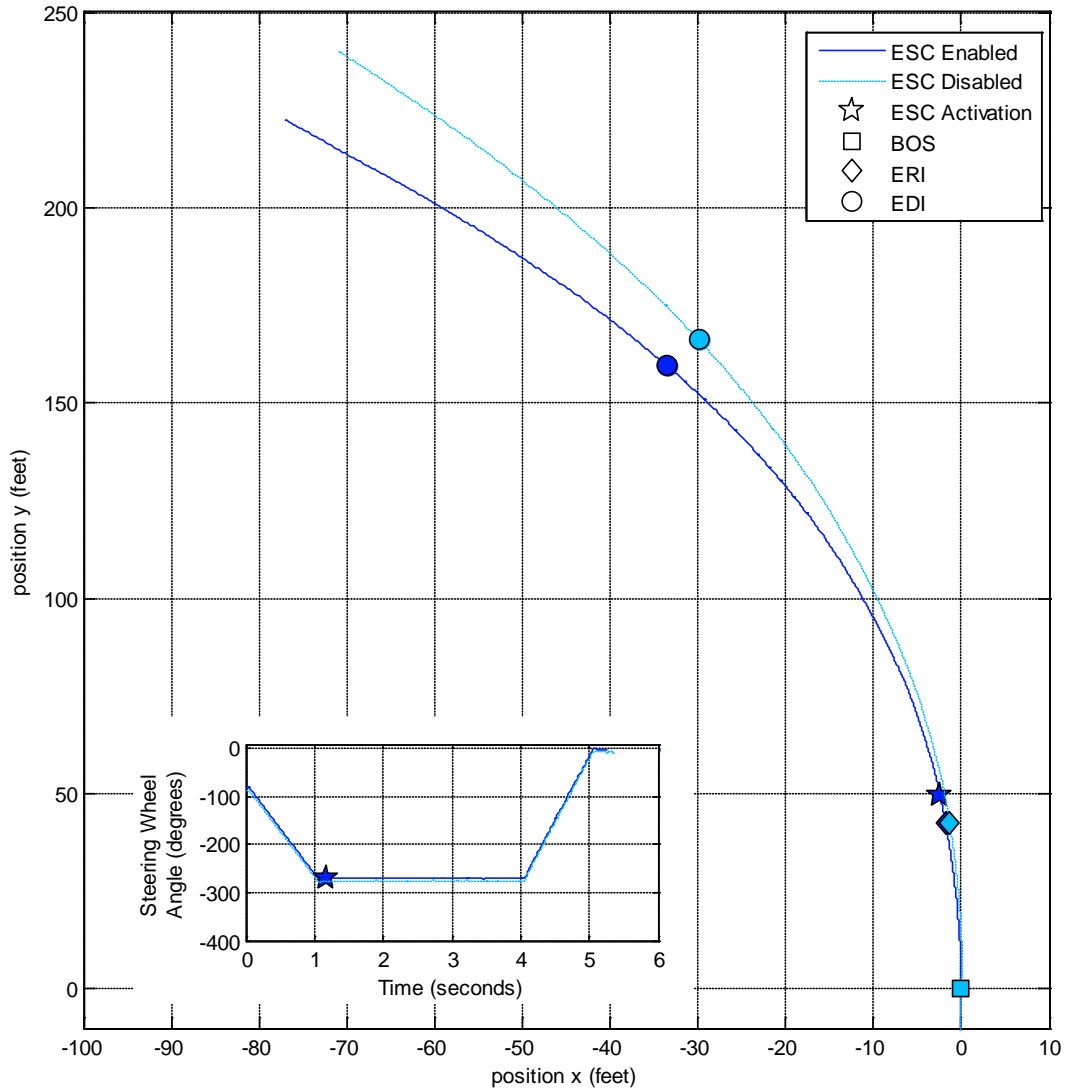


Figure 3.44. Prevost path data from the RWD and the GPOW load condition.

Figure 3.45 shows time history data from the MCI #2 with ESC enabled and disabled from the test with the lowest steering angle that resulted in ESC activation. The steering wheel increment was 270 degrees from the initial drive-through angle resulting in a maximum steering wheel angle of 360 degrees. The speed at which the maneuver was conducted was 23 mph and was held constant by the driver. Following ESC activation, there was very little reduction in speed. Just prior to activation and following activation, the data from the test with ESC enabled shows that the motorcoach was producing less lateral acceleration and yaw rate. Even though these measures were reduced, the magnitudes in yaw rate and lateral acceleration were similar to those observed with the Prevost with ESC enabled.

Figure 3.46 shows torque and brake pressure time history data from the MCI #2 for the ESC enabled test. At ESC activation engine torque reduction can be observed by the separation between driver demanded and engine torque signals. Driver demanded torque gradually increases and engine torque gradually decreases. As the dynamics change following ESC activation, engine torque is allowed to increase. Only brake pressure on the drive axle left wheel can be observed following ESC activation.

Figure 3.47 is a plot of the MCI #2 paths for ESC enabled and disabled tests. Comparing ESC enabled to ESC disabled, a small deviation in path can be observed.

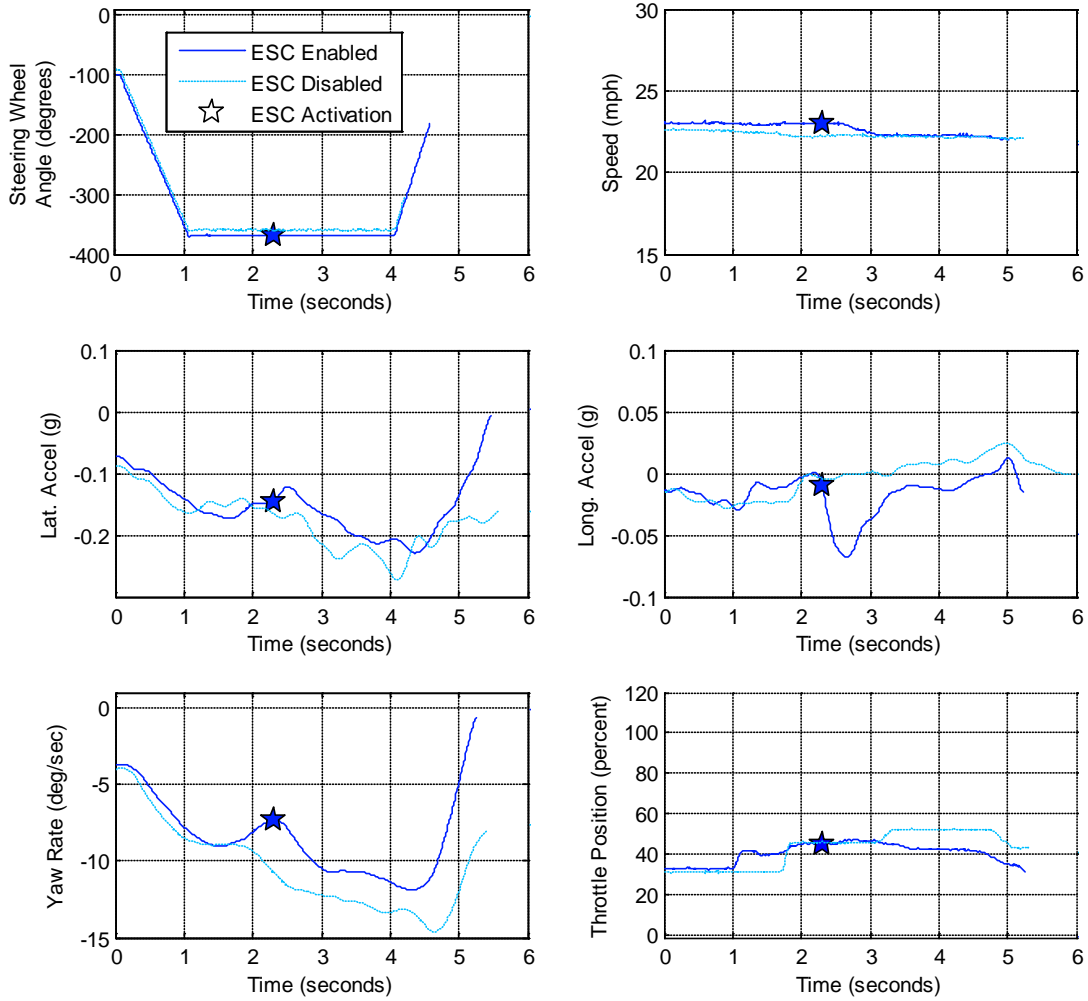


Figure 3.45. MCI #2 time history data from the RWD maneuver and GPOW load condition. Example shows the RWD test with the lowest steering angle input that resulted in ESC activation.

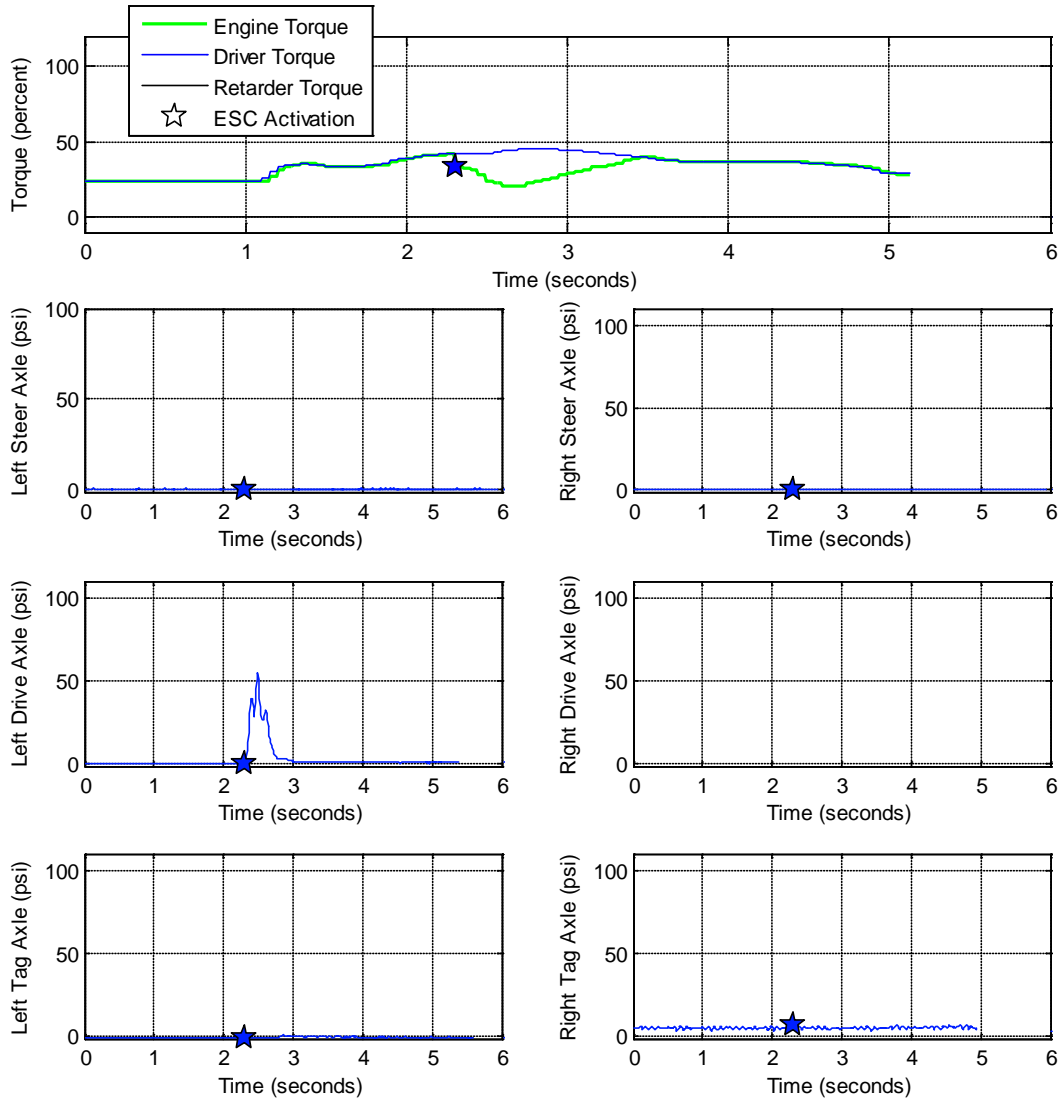


Figure 3.46. MCI #2 brake pressure data from RWD maneuvers with the GPOW load condition and ESC enabled.

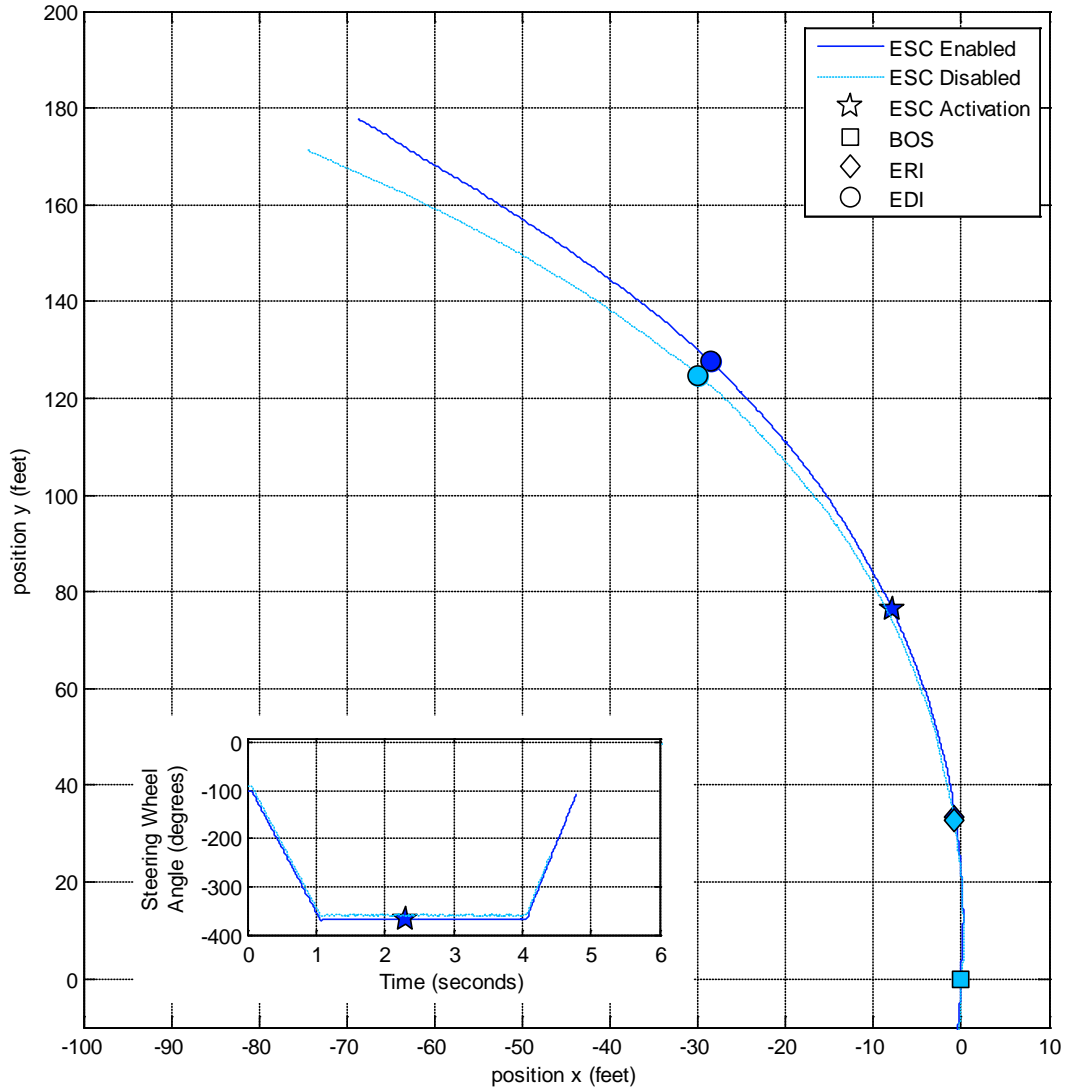


Figure 3.47. MCI #2 path data from RWD maneuvers conducted on the Jennite and the GPOW load condition.

3.5 SWD Maneuver Test Results

3.5.1 SWD – High Surface Friction - LLVW Load Condition

SWD test series results for the LLVW load condition on the dry high friction asphalt are presented in Table 3.20. The table presents the lowest steering scalar for each series of SWD maneuvers that resulted in the loss of stability at 50 mph.

If there was no loss of stability then the series were considered test complete and were denoted as “TC” (130 percent steering scalar) in the table. Test series denoted as partially complete (PC) in the table were terminated early due to ESC system

malfunction. In these series, the larger steering scalars⁵ were observed to overwhelm the motorcoach’s power steering system and produced malfunctions that disabled the motorcoaches ESC system. Series marked “NT” were not tested because the test condition was not included in the test matrix at that point in time.

The table shows that none of the three motorcoaches had wheel lift or yaw instabilities when conducting the SWD (up to the maximum scalar tested) with the LLVW load condition whether ESC was enabled or disabled.

Table 3.20. LLVW condition SWD stability results.

Motorcoach	Lowest Steering Scalar that Resulted in Instability [ESC Disabled, and Enabled]								
	Freq. (Hz)	0.3		0.4		0.5		0.6	
	Dwell (sec)	0.5	1.0	0.5	1.0	0.5	1.0	0.5	1.0
MCI #1	Scalar (%)	PC ^{A#}	PC ^{A#}	NT	PC ^{A#}	PC ^{B#}	PC ^{C#}	NT	NT
MCI #2	Scalar (%)	TC	TC	TC	TC	PC ^{D#}	PC ^{D#}	PC ^{B#}	PC ^{B#}
Prevost	Scalar (%)	TC	TC	TC	TC	TC	TC	PC ^{A#}	PC ^{A#}

A - Steering Scalar is 110%, B - Steering Scalar is 90%, C - Steering Scalar is 80%, D - Steering Scalar is 120%
 #- Maximum scalar tested due to ESC system malfunction

For this load condition and maneuver, each ESC system was observed to intervene with foundation braking for a majority of the steering scalars. Due to ESC commanded foundation braking, differences in time history data were observed between the ESC enabled and ESC disabled test conditions.

Figure 3.48 shows a graphical example of the Prevost bus performing a 0.5Hz, 1.0 second dwell SWD maneuver at the 70 percent steering scalar. From top to bottom, and left to right, the figure shows steering wheel angle, speed, lateral acceleration, longitudinal acceleration, yaw rate, wheel height, yaw angle, and roll angle. This figure shows how the Prevost’s ESC system reduced the vehicle’s speed during the maneuver, thus reducing lateral acceleration, roll angle, yaw rate, and yaw angle, which increases the vehicle’s roll and yaw stability.

⁵ The ESC malfunctions were believed to be caused by a combination of the steering wheel input amplitude and the large steering rates needed to complete the larger steering scalars for the SWD and HSWD maneuvers. This resulted in malfunctions occurring at smaller scalars as the steering frequency was increased.

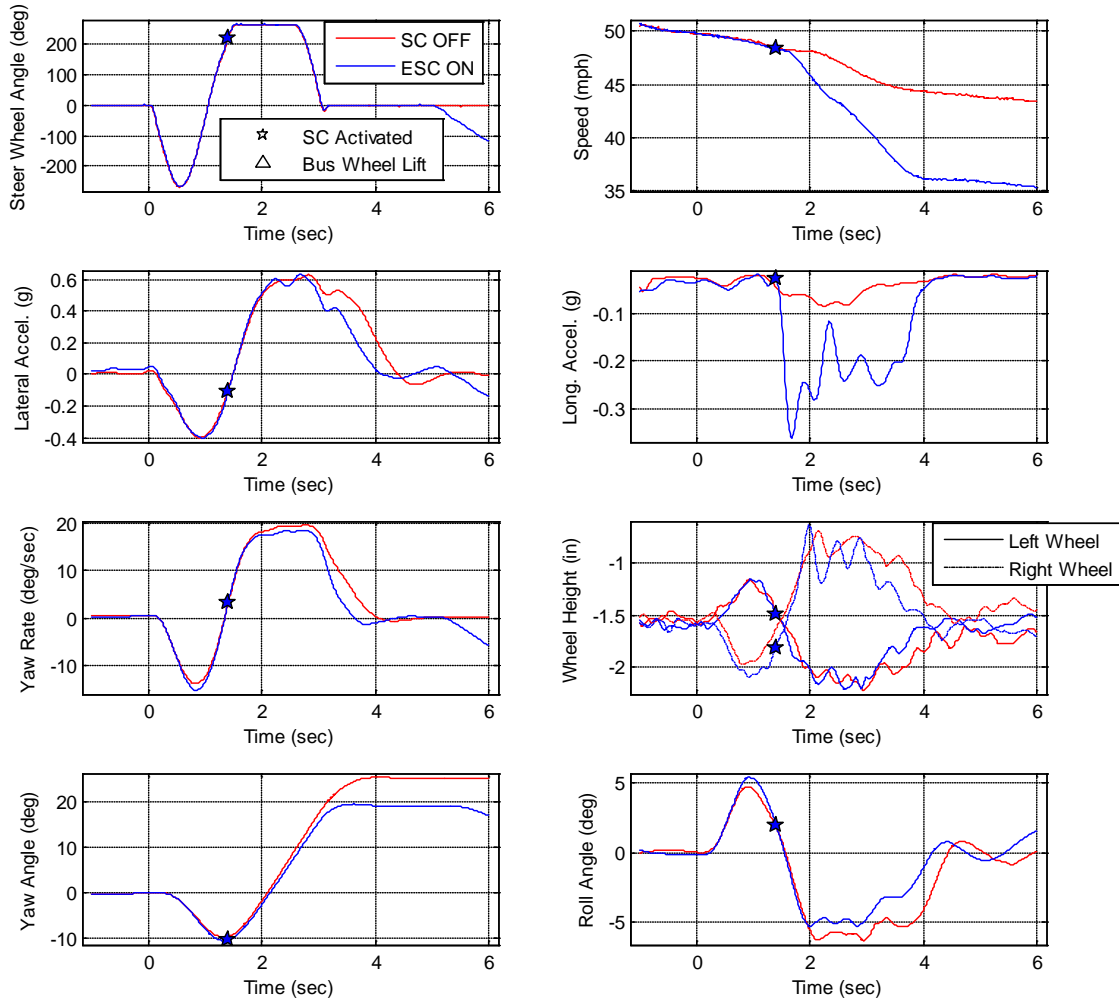


Figure 3.48 Prevost LLVW time history data from SWDs conducted with the 0.5 Hz frequency, 1.0 second dwell time, and 70% steering scalar at 50mph.

Figure 3.49 shows a graphical example of MCI #2 performing a 0.5Hz, 1.0 second dwell SWD maneuver at the 100 percent steering scalar. This figure shows how MCI #2's ESC reduced the vehicle's speed during the maneuver, thus reducing lateral acceleration, yaw rate, and yaw angle, which increased the vehicle's lateral stability. The steering angle trace shows a jog in the signal for both tests just after 1.0 second into the maneuver. This jog has been correlated to power steering pump performance and indicates that the torque feedback through the steering system is at or near the torque limit of the automated steering controller.

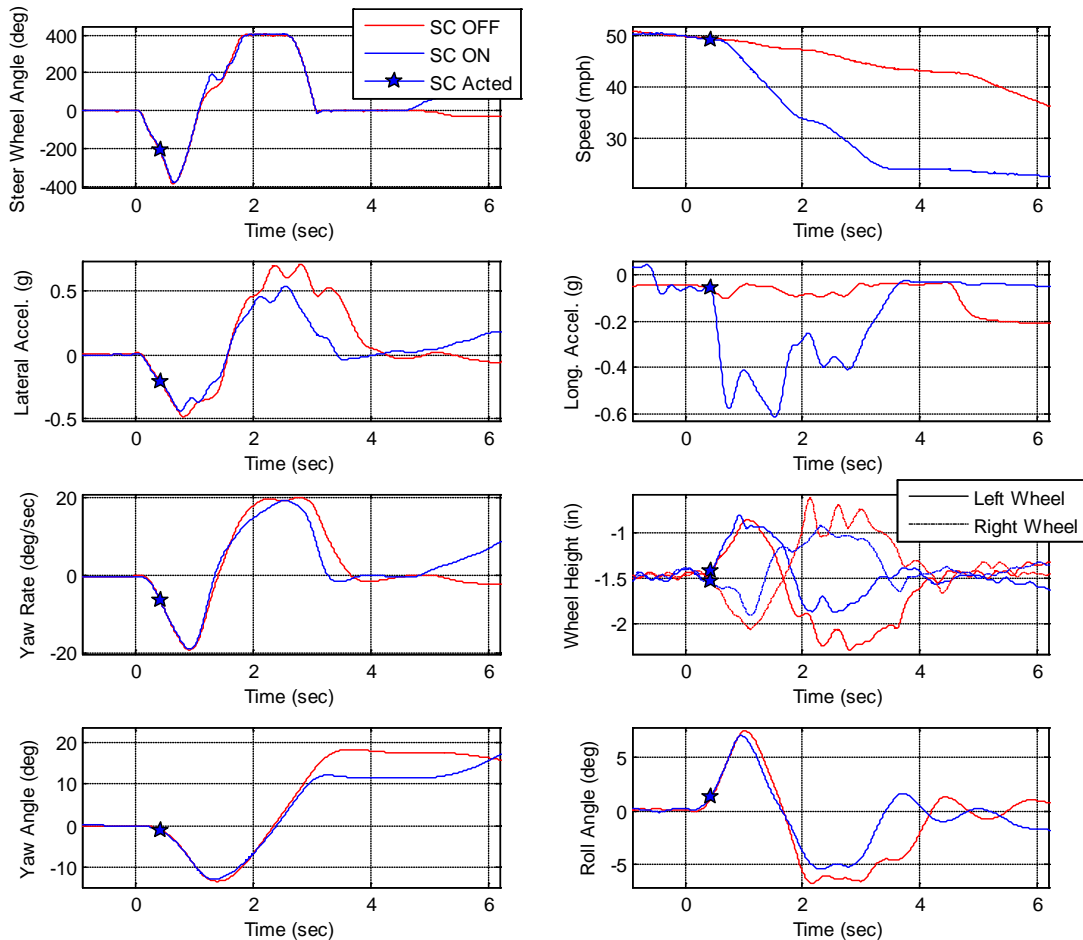


Figure 3.49. MCI #2 time history data from LLVW SWD test series conducted at the 0.5 Hz frequency, with the 1.0 second dwell time, and 100% steering scalar at 50 mph.

Maximum yaw angle and roll angle were used to show the changes ESC was making to the lateral performance of the motorcoaches that was observed in the time history data. Table 3.21 and Table 3.22 show the dynamic roll and yaw angle maximums observed for each SWD test condition evaluated for the LLVW load condition. The tables present the following:

1. Maximum yaw angle for each series of SWD maneuvers following the secondary steering input.
2. Maximum roll angle for each series of SWD maneuvers following the secondary steering input.

Angles are from tests at 130 percent steering scalar (Test Complete) unless power steering pump restriction limited maximum steering scalar input. In these cases, angles from the maximum tested steering scalar will be presented for both the ESC enabled and ESC disabled pair for that vehicle and SWD condition to show potential ESC effectiveness under the same SWD conditions.

Table 3.21. Motorcoach yaw angle maxima results from SWD test series with the LLVW.

Motorcoach	Maximum Yaw Angle (degrees)								
	Freq. (Hz)	0.3		0.4		0.5		0.6	
	Dwell (sec)	0.5	1.0	0.5	1.0	0.5	1.0	0.5	1.0
MCI #1	Enabled	3 ^{A#}	15 ^{A#}	13 ^{A#}	15 ^{A#}	6 ^{B#}	15 ^{C#}	NT	NT
	Disabled	16 ^A	24 ^A	NT	25 ^A	11 ^B	20 ^C	NT	NT
MCI #2	Enabled	0	11	5	10	4 ^{D#}	13 ^{D#}	8 ^{B#}	22 ^{B#}
	Disabled	5	14	6	12	7 ^D	17 ^D	11 ^B	27 ^B
Prevost	Enabled	7	17	12	19	8	21	6 ^A	6 ^A
	Disabled	21	26	18	27	17	28	6 ^A	10 ^A

A - Steering Scalar is 110%, B - Steering Scalar is 90%, C - Steering Scalar is 80%, D - Steering Scalar is 120%
 #- Maximum scalar tested due to ESC system malfunction

Table 3.22. Motorcoach roll angle maxima results from SWD test series with the LLVW.

Motorcoach	Maximum Roll Angle (degrees)								
	Freq. (Hz)	0.3		0.4		0.5		0.6	
	Dwell (sec)	0.5	1.0	0.5	1.0	0.5	1.0	0.5	1.0
MCI #1	Enabled	4.8 ^{A#}	4.7 ^{A#}	6.8 ^{A#}	5.8 ^{A#}	6.0 ^{B#}	5.9 ^{C#}	NT	NT
	Disabled	8.2 ^A	8.2 ^A	NT	7.1 ^A	7.1 ^B	6.5 ^C	NT	NT
MCI #2	Enabled	5.2	5.4	5.7	5.0	5.2 ^{D#}	6.2 ^{D#}	5.3 ^{B#}	5.8 ^{B#}
	Disabled	7.7	7.0	7.2	7.2	6.9 ^D	6.5 ^D	7.0 ^B	6.8 ^B
Prevost	Enabled	6.1	6.3	6.1	6.1	5.8	5.7	2.1 ^{A#}	2.3 ^{A#}
	Disabled	8.3	8.3	7.7	7.8	7.1	7.1	2.2 ^A	2.1 ^A

A - Steering Scalar is 110%, B - Steering Scalar is 90%, C - Steering Scalar is 80%
 #- Maximum scalar tested due to ESC system malfunction

These tables show that all three motorcoach ESC systems were able to reduce yaw angles and roll angles during SWD testing. On average, ESC reduced yaw angles by 46 percent and roll angles by 25 percent for MCI #1. For MCI #2, yaw angles were reduced by 33 percent and roll angles by 22 percent. For the Prevost, yaw angles were reduced by an average of 35 percent, and roll angles by 16 percent.

3.5.2 SWD – High Surface Friction – GPOW Load Condition

Like SWD results from the LLVW load condition, none of the motorcoaches were observed to lose yaw stability with ESC enabled or disabled when evaluated with the GPOW load condition at 45 mph. However, several instances of wheel lift were observed when the systems were disabled. Table 3.23 and Table 3.24 present these results for each ESC condition, frequency and dwell time evaluated with the GPOW

load condition. The tables present the lowest steering scalar for each series of SWD maneuvers that resulted in the loss of roll stability⁶ (two or more inches or wheel lift observed at any axle location). If the vehicle remained stable for the entire series then the series were considered test complete and were denoted as “TC” in the table. Test series denoted as partially complete (PC) in the table were terminated early due to ESC system malfunction or outrigger frame contact. Series marked “NT” were not tested because the test condition was not included in the test matrix at that point in time.

Series marked “NTO” were not tested due to outrigger frame contact. During testing of the MCI #1 bus, especially at higher MESs and steering scalars, it was found that the lower support portion of the outrigger frames would make contact with the test surface, potentially damaging the outrigger frame and/or the test surface, and influencing the dynamics of the vehicle. Experimenters decided not to test the MCI #1 bus in some conditions in order to reduce instances of contact. These tests conducted with MCI #1 at 0.3, 0.4, and 0.5 hz were limited due outrigger contact and ESC faults and were considered inconclusive.

Table 3.23. SWD results with ESC disabled and the GPOW condition.

Motorcoach	Lowest Steering Scalar that Resulted in Roll Instability								
	Freq. (Hz)	0.3		0.4		0.5		0.6	
	Dwell (sec)	0.5	1.0	0.5	1.0	0.5	1.0	0.5	1.0
MCI #1		NTO	NTO	NTO	PC ^{B^}	NTO	PC ^A	NT	NT
MCI #2		85%	80%	TC	TC	TC	TC	TC	TC
Prevost		75%	70%	70%	60%	80%	75%	80%	90%

A - Steering Scalar is 90%, B - Steering Scalar is 70%

^ - Maximum scalar tested due to outrigger frame contact with ground

Table 3.24. SWD results with ESC enabled and the GPOW condition.

Motorcoach	Lowest Steering Scalar that Resulted in Roll Instability								
	Freq. (Hz)	0.3		0.4		0.5		0.6	
	Dwell (sec)	0.5	1.0	0.5	1.0	0.5	1.0	0.5	1.0
MCI #1		NTO	NTO	NTO	PC ^{B^}	NTO	PC ^{A#}	NT	NT
MCI #2		TC	TC	PC ^{C#}	PC ^{C#}	PC ^{A#}	PC ^{A#}	TC	TC
Prevost		105%	110%	80%	65%	100%	100%	TC	90%

A - Steering Scalar is 90%, B - Steering Scalar is 70%, C - Steering Scalar is 120%,

#- Maximum scalar tested due to ESC system malfunction

^ - Maximum scalar tested due to outrigger frame contact with ground

For the ESC enabled test condition, seven out of the 19 series conducted were terminated due to wheel lift. When ESC was disabled, the number of series terminated due to wheel lift increased to 10 out of 18. While not every series was completed with ESC enabled, the tables show that with ESC enabled the vehicles’ performance was extended to higher steering scalars before wheel lift was observed.

⁶ SWD, HSWD, and RWD maneuver test series with the Prevost in the GPOW load condition were conducted with an unknown broken roll stabilizer bar link that likely increased roll propensity for this motorcoach. For more information see Section 3.7.4.

Table 3.23 and Table 3.24 show that the MCI #2 in the disabled condition experienced roll instability in only two out of 10 test conditions, and had no roll instabilities with ESC enabled. All ESC enabled roll instabilities occurred with the Prevost bus. Seven out of eight combinations of frequency and dwell time test series were terminated due to wheel lift. Test series were terminated at steering scalars between 65 and 110 percent. With ESC disabled the Prevost experienced roll instability in all eight combinations of frequency and dwell times evaluated. The wheel lift events were observed at steering scalars between 60 and 90 percent.

These tables show that ESC is capable of mitigating roll instabilities. Each ESC system intervened with foundation braking for a majority of the steering scalars greater than 50 percent (higher severity maneuvers) evaluated for each SWD test series with this load condition. Due to ESC commanded foundation braking, large differences in time history data were observed between the ESC enabled and disabled test conditions. Figure 3.50 and Figure 3.51, show graphical examples of these differences that were observed. From top to bottom, and left to right, the figures show: steering wheel angle, speed, lateral acceleration, longitudinal acceleration, yaw rate, wheel height, yaw angle, and roll angle.

Figure 3.50 shows a graphical example of MCI #2 performing a 0.5Hz, 1.0 second dwell SWD maneuver at the 80 percent steering scalar. This figure shows how the vehicle's ESC system reduced the vehicle's speed beginning early in the maneuver, thus reducing lateral acceleration, roll angle, yaw rate, and yaw angle, which increased the vehicle's roll stability.

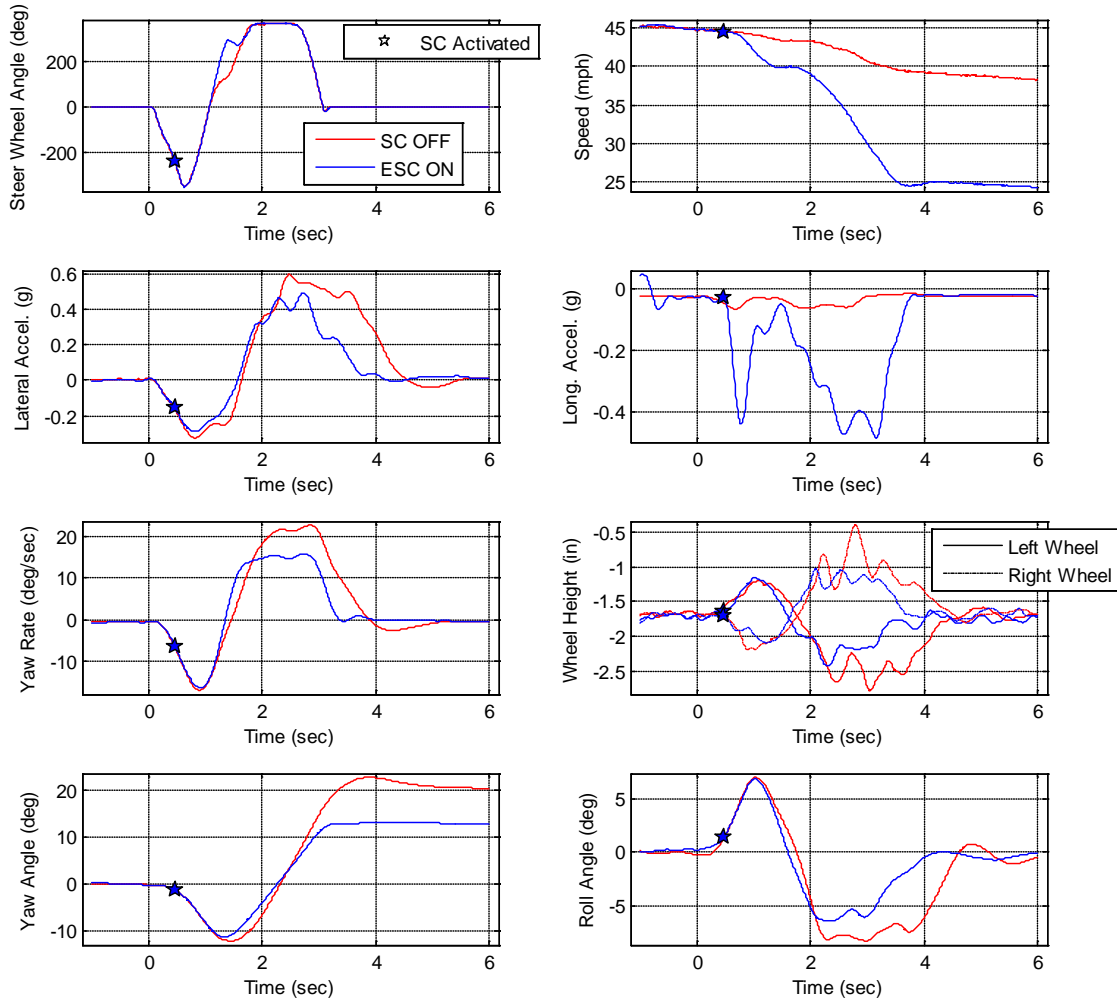


Figure 3.50. MCI #2 time history data from Gross Occupancy SWD test series conducted on dry high friction asphalt with the 0.5 Hz frequency, 1.0 second dwell time and 80% steering scalar at 45 mph.

Figure 3.51 shows a graphical example of MCI #2 performing a 0.3Hz, 1.0 second dwell SWD maneuver at the 80 percent steering scalar. This figure shows how the vehicle's ESC system activated very early into the maneuver, reducing the vehicle's speed, thus reducing lateral acceleration and roll angle which increases the vehicle's roll stability. Without ESC, the same inputs resulted in higher levels of lateral acceleration, roll angle, and wheel lift.

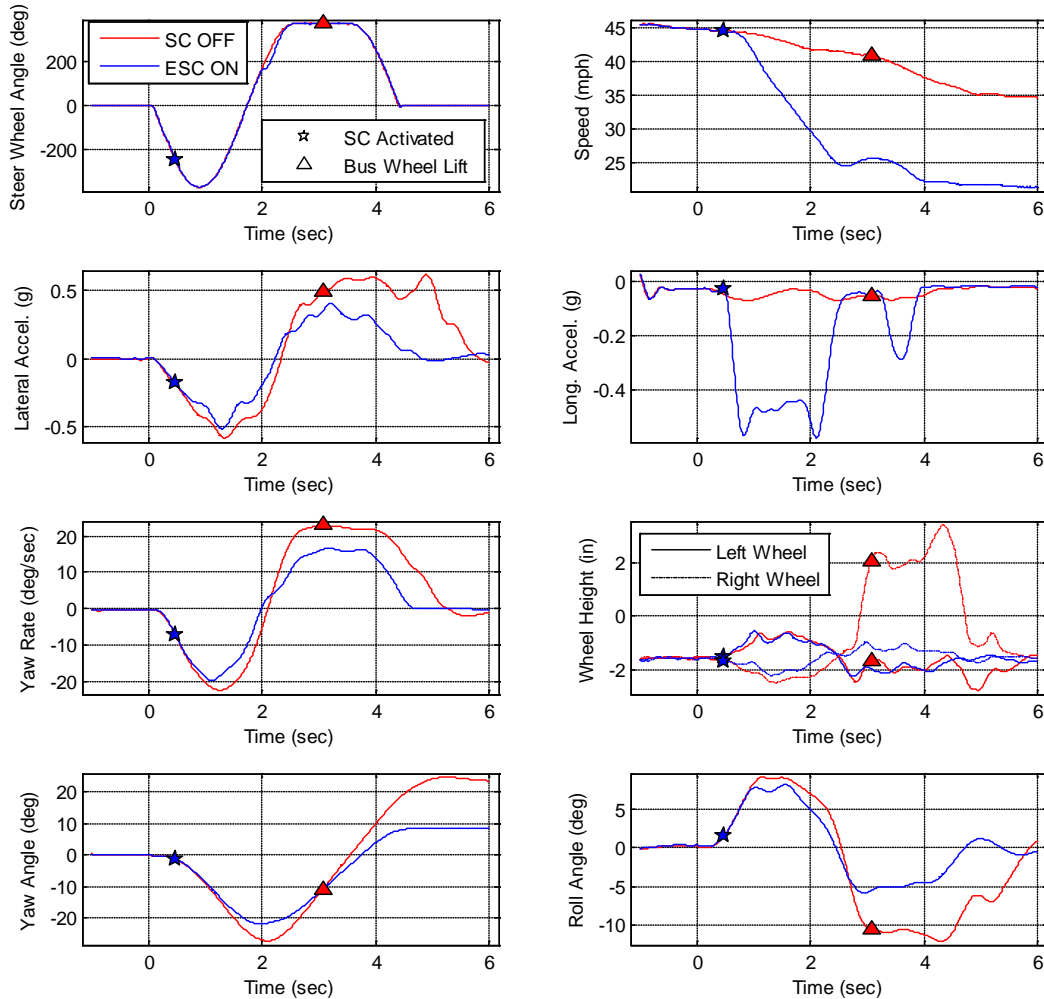


Figure 3.51. MCI #2 time history data from Gross Occupancy SWD test series conducted on dry high friction asphalt at the 0.3 Hz frequency, 1.0 second dwell time, and 80% steering scalar at 45 mph.

Maximum yaw angle and roll angle were used to show the changes that ESC was making to the lateral performance of the motorcoaches as observed in the time history data. The SWD test results for the GPOW load condition on the dry high friction asphalt are presented in Table 3.25 and Table 3.26. As in the previous section, the tables present the following:

1. Maximum yaw angle for each series of SWD maneuvers following the secondary steering input.
2. Maximum roll angle for each series of SWD maneuvers following the secondary steering input.

In these cases, as before, angles from the maximum tested steering scalar will be presented for both the ESC enabled and ESC disabled pair for that vehicle and SWD condition to show potential ESC effectiveness under the same SWD conditions.

Series marked “NTO” were not tested due to outrigger frame contact.

Table 3.25. Motorcoach yaw angle maxima results from SWD test series with the GPOW load.

Motorcoach	Maximum Yaw Angle (degrees)								
	Freq. (Hz)	0.3		0.4		0.5		0.6	
	Dwell (sec)	0.5	1.0	0.5	1.0	0.5	1.0	0.5	1.0
MCI #1	Enabled	NTO	NTO	NTO	10 ^E	NTO	17 ^{C#}	NT	NT
	Disabled	NTO	NTO	NTO	17 ^{E^}	NTO	23 ^C	NT	NT
MCI #2	Enabled	1 ^D	8 ^D	6 ^{A#}	15 ^{A#}	8 ^{C#}	17 ^{C#}	6 ^{D#}	15 ^{D#}
	Disabled	13 ^D WL	25 ^D WL	12 ^A	35 ^A	10 ^C	30 ^C	9 ^D	25 ^D
Prevost	Enabled	4 ^D	13 ^E	9 ^E	16 ^F	13 ^D	19 ^D	13 ^D	26 ^C
	Disabled	17 ^D WL	26 ^E WL	15 ^E WL	25 ^F WL	17 ^D WL	32 ^D WL	15 ^D WL	30 ^C WL

A - Steering Scalar is 120%, B - Steering Scalar is 100%, C - Steering Scalar is 90%, D - Steering Scalar is 80%, E - Steering Scalar is 70%, F - Steering Scalar is 60%

#- Maximum scalar tested due to ESC system malfunction

^ Maximum scalar tested due to outrigger frame contact with ground

WL- Vehicle experienced wheel lift

Table 3.26. Motorcoach roll angle maxima results from SWD test series with the GPOW load.

Motorcoach	Maximum Roll Angle (degrees)								
	Freq. (Hz)	0.3		0.4		0.5		0.6	
	Dwell (sec)	0.5	1.0	0.5	1.0	0.5	1.0	0.5	1.0
MCI #1	Enabled	NTO	NTO	NTO	5.1 ^E	NTO	6.8 ^{C#}	NT	NT
	Disabled	NTO	NTO	NTO	6.9 ^{E^}	NTO	9.1 ^C	NT	NT
MCI #2	Enabled	6.5 ^D	6.2 ^D	5.9 ^{A#}	6.2 ^{A#}	6.4 ^{C#}	7.0 ^{C#}	6.7 ^{D#}	6.4 ^{D#}
	Disabled	9.6 ^D WL	11.0 ^D WL	9.1 ^A	9.5 ^A	7.6 ^C	8.5 ^C	7.7 ^D	7.2 ^D
Prevost	Enabled	8.1 ^D	7.4 ^E	7.5 ^E	9.1 ^F	8.3 ^D	7.7 ^D	7.7 ^D	8.8 ^C
	Disabled	10.0 ^D WL	9.3 ^E WL	9.6 ^E WL	9.9 ^F WL	9.5 ^D WL	9.9 ^D WL	9.3 ^D WL	9.4 ^C WL

A - Steering Scalar is 120%, B - Steering Scalar is 100%, C - Steering Scalar is 90%, D - Steering Scalar is 80%, E - Steering Scalar is 70%, F - Steering Scalar is 60%

#- Maximum scalar tested due to ESC system malfunction

^ Maximum scalar tested due to outrigger frame contact with ground

WL- Vehicle experienced wheel lift

MCI #2 and the Prevost motorcoaches without ESC, in their base conditions, experienced roll instability (wheel lift) at steering scalars between 60 and 90percent. MCI #2 had wheel lift at a SWD frequency of 0.3Hz (both dwell times), and the Prevost at all SWD frequencies and dwell times. In these cases, when ESC was enabled, ESC reduced both yaw and roll angles sufficiently to prevent instability at the same steering scalar which produced wheel lift. Yaw angles were reduced an average of 45 percent, and roll angles were reduced an average of 20 percent.

All three motorcoaches' ESC systems were able to reduce yaw angles and roll angles during the SWD testing. For SWD conditions not resulting in instability, on average, the MCI #1 maximum yaw angles were reduced by 34 percent, and roll angles by 26 percent. For MCI #2, yaw angles were reduced by an average of 41 percent, and roll angles by 21 percent. For the Prevost, yaw angles were reduced by an average of 37 percent, and roll angles by 16 percent.

3.5.3 SWD – Low Surface Friction – GPOW Load Condition

SWD test series maxima results for the GPOW load condition on the wet Jennite are presented in Table 3.27 and Table 3.28. The MES for these tests was 30 mph. As in the previous section, the tables present the following:

1. Maximum yaw angle for each series of SWD maneuvers following the secondary steering input.
2. Maximum roll angle for each series of SWD maneuvers following the secondary steering input.

Angles are from tests at 130 percent steering scalar (Test Complete) unless a ESC malfunction limited the maximum steering scalar input. In these cases, as before, angles from the maximum tested steering scalar are presented for both the ESC enabled and ESC disabled pair for that motorcoach and SWD condition to show potential ESC effectiveness under the same SWD conditions.

Table 3.27. Yaw angle maxima from SWD test series conducted on the low friction wet Jennite.

Motorcoach	Maximum Yaw Angle (degrees)								
	Freq. (Hz)	0.2		0.3		0.4		0.5	
	Dwell (sec)	0.5	1.0	0.5	1.0	0.5	1.0	0.5	1.0
MCI #2	Enabled	15	25	13	19	10	19	6 ^{A#}	11 ^{A#}
	Disabled	15	22	13	15	8	13	5 ^A	10 ^A
Prevost	Enabled	NT	NT	4	11	9	17	9	14
	Disabled	NT	NT	4	12	9	17	8	16

A - Steering Scalar is 100%

#- Maximum scalar tested due to ESC system malfunction

Table 3.28. Roll angle maxima from SWD test series conducted on the low friction wet Jennite.

Motorcoach	Maximum Roll Angle (degrees)								
	Freq. (Hz)	0.2		0.3		0.4		0.5	
	Dwell (sec)	0.5	1.0	0.5	1.0	0.5	1.0	0.5	1.0
MCI #2	Enabled	4.8	5.2	3.9	4.4	3.1	3.6	3.9 ^{A#}	3.7 ^{A#}
	Disabled	4.5	4.4	3.8	4.2	3.1	3.2	3.8 ^A	4.0 ^A
Prevost	Enabled	NT	NT	5.4	4.8	5.1	4.8	5.0	4.8
	Disabled	NT	NT	5.3	4.9	4.9	5.0	5.4	5.4

A - Steering Scalar is 100%

#- Maximum scalar tested due to ESC system malfunction

Due to time constraints, SWD test series on a low friction surface were not performed with MCI #1. The Prevost was not tested at the 0.2Hz frequency for similar reasons.

The buses experienced neither yaw nor roll instabilities regardless of ESC condition, maneuver frequency or dwell time. The Prevost did not see a reduction in yaw or roll angles when ESC was enabled, but it should be noted that the bus did not experience any instabilities in the disabled condition.

MCI #2, with ESC enabled, showed slight increases in roll angles in six out of eight conditions, and also slight increases in yaw angles in six out of eight conditions. This shows MCI #2's ESC system's was mitigating plow out. Figure 3.52 shows a graphical example of MCI #2 performing a 0.4 Hz, 1.0 second dwell SWD maneuver at the 130 percent steering scalar. This figure shows how the vehicle's ESC system reduced the vehicle's speed beginning early in the maneuver, thus reducing plow, increasing yaw rate and yaw angle, which increases the vehicle's responsiveness.

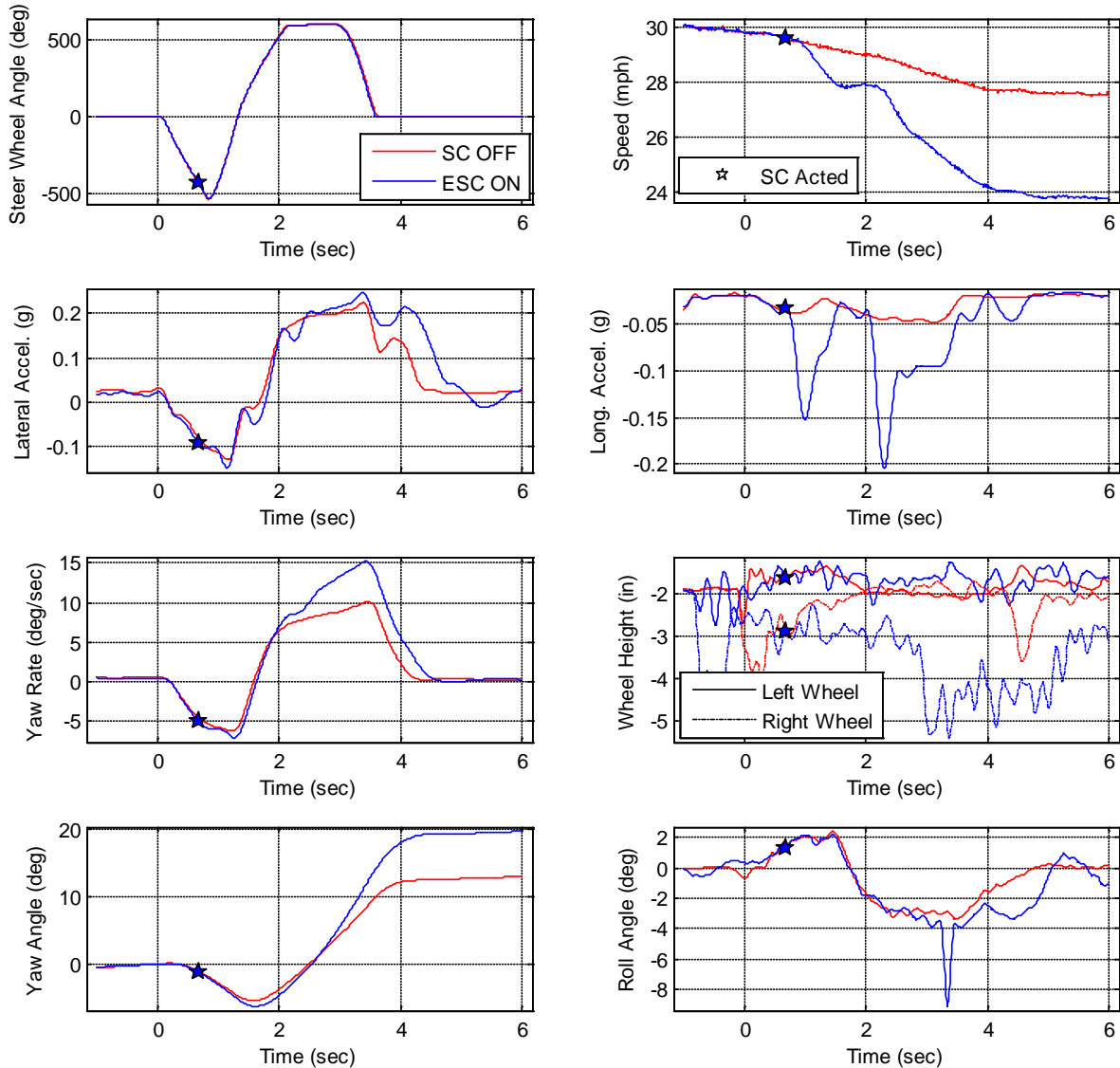


Figure 3.52. MCI #2 time history data from the GPOW SWD test series conducted on wet Jennite surface with the 0.4 Hz frequency, 1.0 second dwell time, and 130% steering scalar at 30 mph.

3.6 HSWD Test Results

3.6.1 HSWD – High Surface Friction - LLVW Load Condition

HSWD test series results for the LLVW load condition on the dry high friction asphalt are presented in Table 3.29 and Table 3.30. The tables presents the lowest steering scalar for each series of HSWD maneuvers that resulted in the loss of stability.

If there was no loss of stability then the series was considered test complete and was denoted as “TC” (130 percent steering scalar). Test series denoted as partially complete (PC) in the table were terminated early due to ESC system malfunction or

outrigger frame contact. Series marked “NT” were not tested because the test condition was not included in the test matrix at that point in time.

Table 3.29. LLVW condition HSWD stability results with ESC disabled.

Motorcoach	Lowest Steering Scalar that Resulted in Instability [ESC Disabled]								
	Freq. (Hz)	0.3		0.4		0.5		0.6	
	Dwell (sec)	0.5	1.0	0.5	1.0	0.5	1.0	0.5	1.0
MCI #1		80%	70%	90%	70%	PC ^B	70%	NT	NT
MCI #2		TC	60%	TC	65%	TC	TC	TC	TC
Prevost		TC	TC	TC	TC	TC	TC	TC	TC

B - Steering Scalar is 110%

Table 3.30. LLVW condition HSWD stability results with ESC enabled.

Motorcoach	Lowest Steering Scalar that Resulted in Instability [ESC Enabled]								
	Freq. (Hz)	0.3		0.4		0.5		0.6	
	Dwell (sec)	0.5	1.0	0.5	1.0	0.5	1.0	0.5	1.0
MCI #1		PC ^{BS}	NT	NT					
MCI #2		TC	TC	PC ^{A#}	PC ^{A#}	PC ^{B#}	PC ^{B#}	PC ^{C#}	PC ^{C#}
Prevost		TC							

A - Steering Scalar is 120%, B - Steering Scalar is 110%, C - Steering Scalar is 90%

S- Test performed at 45mph, not 50mph per LLVW load condition

#- Maximum scalar tested due to ESC system malfunction

MCI #1 was not tested at the 0.6 Hz frequency. Also, in the LLVW condition, MCI #1 was tested only at the reduced speed of 45 mph in the ESC enabled condition.

As with the SWD results from the LLVW load condition, none of the motorcoaches were observed to generate a yaw instability with or without ESC when evaluated with the HSWD maneuver. However, several instances of wheel lift were observed.

In their disabled conditions, the two MCI buses generated wheel lift in seven out of 14 conditions (4 frequencies and 2 dwell times) at steering scalars between 70 and 90 percent. MCI #1, with ESC disabled, had wheel lift at all tested HSWD frequencies and dwell times except at 0.5 Hz, 0.5 second dwell. MCI #2, with ESC disabled, had wheel lift at the 1.0 second dwell times for both the 0.3 Hz and 0.4 Hz frequencies.

Maximum yaw angle and roll angle show the changes ESC made to the lateral performance of the motorcoaches, as observed in the time history data. HSWD test series results for the LLVW load condition on the dry high friction asphalt are presented in Table 3.31 and Table 3.32. The tables show the maximum yaw angle and maximum roll angle for each series of HSWD maneuvers.

In these cases, as before, angles from the maximum tested steering scalar are presented for both the ESC enabled and ESC disabled tests for each motorcoach and HSWD test condition to show potential ESC effectiveness under the same HSWD conditions.

Table 3.31. Yaw angle maxima from LLVW HSWD test series conducted on the high friction dry asphalt.

Motorcoach	Maximum Yaw Angle (degrees)								
	Freq. (Hz)	0.3		0.4		0.5		0.6	
	Dwell (sec)	0.5	1.0	0.5	1.0	0.5	1.0	0.5	1.0
MCI #1	Enabled	31 ^{BS}	39 ^{BS}	25 ^{BS}	37 ^{BS}	20 ^{BS}	29 ^{BS}	NT	NT
	Disabled	39 ^E _{WL}	50 ^F _{WL}	32 ^D _{WL}	39 ^F _{WL}	25 ^B	34 ^F _{WL}	NT	NT
MCI #2	Enabled	32	35 ^F	25 ^{A#}	28 ^F	22 ^{B#}	30 ^{B#}	21 ^{D#}	28 ^{D#}
	Disabled	33	48 ^F _{WL}	26 ^A	38 ^F _{WL}	24 ^B	32 ^B	21 ^D	30 ^D
Prevost	Enabled	34	41	27	36	24	32	21	30
	Disabled	35	42	27	35	23	31	21	31

A - Steering Scalar is 120%, B - Steering Scalar is 110%, C - Steering Scalar is 100%, D - Steering Scalar is 90%, E - Steering Scalar is 80%, F - Steering Scalar is 70%
 S- Test performed at 45mph, not 50mph per LLVW load condition
 #- Maximum scalar tested due to ESC system malfunction
 ^- Maximum scalar tested due to outrigger frame contact with ground
 WL- Vehicle experienced Wheel Lift

Table 3.32. Roll angle maxima from LLVW HSWD test series conducted on the high friction dry asphalt.

Motorcoach	Maximum Roll Angle (degrees)								
	Freq. (Hz)	0.3		0.4		0.5		0.6	
	Dwell (sec)	0.5	1.0	0.5	1.0	0.5	1.0	0.5	1.0
MCI #1	Enabled	5.2 ^{BS}	5.7 ^{BS}	5.6 ^{BS}	5.7 ^{BS}	5.7 ^{BS}	5.7 ^{BS}	NT	NT
	Disabled	9.5 ^E _{WL}	10.8 ^F _{WL}	9.9 ^D _{WL}	11.1 ^F _{WL}	8.9 ^B	10.9 ^F _{WL}	NT	NT
MCI #2	Enabled	5.8	7.3 ^F	7.9 ^{A#}	7.3 ^F	7.7 ^{B#}	8.0 ^{B#}	5.7 ^{D#}	6.1 ^{D#}
	Disabled	7.3	9.6 ^F _{WL}	7.9 ^{A#}	12.1 ^F _{WL}	8.7 ^B	7.3 ^B	6.4 ^D	6.0 ^D
Prevost	Enabled	7.2	6.6	6.7	7.4	6.7	6.7	7.0	7.0
	Disabled	6.4	6.5	6.4	6.1	6.3	6.0	6.3	6.4

A - Steering Scalar is 120%, B - Steering Scalar is 110%, C - Steering Scalar is 100%, D - Steering Scalar is 90%, E - Steering Scalar is 80%, F - Steering Scalar is 70%
 S- Test performed at 45 mph, not 50 mph per LLVW load condition
 #- Maximum scalar tested due to ESC system malfunction
 ^- Maximum scalar tested due to outrigger frame contact with ground
 WL- Vehicle experienced Wheel Lift

In the ESC disabled conditions, the MCI motorcoaches generated wheel lift in seven out of 14 HSWD test series performed. When ESC was enabled, ESC reduced both yaw and roll angles sufficiently to prevent wheel lift events from being observed at the steering scalars evaluated. For both MCI motorcoaches, the ESC systems were able to reduce yaw angles and roll angles during HSWD testing. For HSWD conditions not resulting in instability, on average, the MCI #1 reduced yaw angles by 20 percent, and roll angles by 36 percent. The MCI #2 reduced yaw angles by an average of 11

percent, and roll angles by 12 percent. The Prevost was not observed to reduce yaw or roll angle maxima, but it should be noted that the bus did not experience any instabilities.

3.6.2 HSWD – High Surface Friction – GPOW Load Condition

HSWD test series results for the GPOW load condition on the dry high friction asphalt are presented in Table 3.33 and Table 3.34. The tables present the lowest steering scalar for each series of HSWD maneuvers that resulted in the loss of stability⁷. If there was no loss of stability then the series was considered test complete and were denoted as “TC” (130 percent steering scalar). Test series denoted as partially complete (PC) in the table were terminated early due to ESC system malfunction. Series marked “NT” were not tested because the test condition was not included in the test matrix at that point in time. Series marked “NTO” were not tested due to outrigger frame contact.

Table 3.33. GPOW condition HSWD stability results with ESC disabled.

Motorcoach	Lowest Steering Scalar that Resulted in Instability [ESC Disabled]								
	Freq. (Hz)	0.3		0.4		0.5		0.6	
	Dwell (sec)	0.5	1.0	0.5	1.0	0.5	1.0	0.5	1.0
MCI #1		100%	80%	NTO	NTO	NTO	NTO	NT	NT
MCI #2		80%	70%	TC	70%	TC	70%	TC	80%
Prevost		60%	60%	70%	60%	70%	60%	80%	60%

A - Steering Scalar is 110%, B - Steering Scalar is 100%, C - Steering Scalar is 80%

Table 3.34. GPOW condition HSWD stability results with ESC enabled.

Motorcoach	Lowest Steering Scalar that Resulted in Instability [ESC Enabled]								
	Freq. (Hz)	0.3		0.4		0.5		0.6	
	Dwell (sec)	0.5	1.0	0.5	1.0	0.5	1.0	0.5	1.0
MCI #1		PC ^{A#}	PC ^{A#}	NTO	NTO	NTO	NTO	NT	NT
MCI #2		TC	TC	PC ^{A#}	PC ^{A#}	PC ^{B#}	PC ^{B#}	PC ^{C#}	PC ^{C#}
Prevost		60%	60%	70%	60%	70%	60%	80%	60%

A - Steering Scalar is 110%, B - Steering Scalar is 100%, C - Steering Scalar is 80%

#- Maximum scalar tested due to ESC system malfunction

MCI #1 was not tested at the 0.6 Hz frequency. Furthermore, MCI #1 was only tested at two HSWD conditions, the two dwell times for 0.3 Hz, due to outrigger frame contact with the test surface.

⁷ SWD, HSWD, and RWD maneuver test series with the Prevost in the GPOW load condition were conducted with an unknown broken roll stabilizer bar link that likely increased roll propensity for this motorcoach. For more information see Section 3.7.4.

In the disabled condition, all three motorcoaches experienced roll instability, with instabilities occurring in 14 out of 18 combinations of maneuver frequencies and dwell times. Wheel lift was observed at steering scalars ranging from 60 to 100 percent, with all but the MCI #2 having wheel lift at all tested HSWD frequencies and dwell times with ESC disabled. With ESC enabled, the two MCI buses displayed no roll instability. With ESC enabled, the Prevost generated wheel lift in every condition at steering scalars between 60 and 80 percent.

Maximum yaw angle and roll angle were used to show the changes ESC was making to the lateral performance of the motorcoaches. Table 3.35 and Table 3.36 summarize the maximum yaw and roll angle results with ESC enabled and disabled with each motorcoach, frequency and dwell time evaluated. Angles from the maximum tested steering scalar are presented to show potential ESC effectiveness under the same HSWD test conditions.

Table 3.35. Yaw angle maxima from GPOW HSWD test series conducted on the dry asphalt.

Motorcoach	Maximum Yaw Angle (degrees)								
	Freq. (Hz)	0.3		0.4		0.5		0.6	
	Dwell (sec)	0.5	1.0	0.5	1.0	0.5	1.0	0.5	1.0
MCI #1	Enabled	31 ^B	33 ^D	NTO	NTO	NTO	NTO	NT	NT
	Disabled	48 ^B _{WL}	52 ^D _{WL}	NTO	NTO	NTO	NTO	NT	NT
MCI #2	Enabled	31 ^D	36 ^E	30 ^{A#}	33 ^D	23 ^{B#}	33 ^{B#}	18 ^{D#}	28 ^{D#}
	Disabled	43 ^D _{WL}	48 ^E _{WL}	35 ^A	44 ^D _{WL}	27 ^B	49 ^B _{WL}	21 ^D	34 ^D _{WL}
Prevost	Enabled	25 ^F _{WL}	32 ^F _{WL}	24 ^E _{WL}	29 ^F _{WL}	21 ^E _{WL}	27 ^F _{WL}	20 ^D _{WL}	27 ^F _{WL}
	Disabled	28 ^F _{WL}	36 ^F _{WL}	27 ^E _{WL}	31 ^F _{WL}	23 ^E _{WL}	28 ^F _{WL}	23 ^D _{WL}	29 ^F _{WL}

A - Steering Scalar is 110%, B - Steering Scalar is 100%, C - Steering Scalar is 90%, D - Steering Scalar is 80%, E - Steering Scalar is 70%, F - Steering Scalar is 60%

#- Maximum scalar tested due to ESC system malfunction

WL- Vehicle experienced wheel lift

Table 3.36. Roll angle maxima from GPOW HSWD test series conducted on the dry asphalt.

Motorcoach	Maximum Roll Angle (degrees)								
	Freq. (Hz)	0.3		0.4		0.5		0.6	
	Dwell (sec)	0.5	1.0	0.5	1.0	0.5	1.0	0.5	1.0
MCI #1	Enabled	7.9 ^B	8.1 ^D	NTO	NTO	NTO	NTO	NT	NT
	Disabled	10.9 ^B _{WL}	11.4 ^D _{WL}	NTO	NTO	NTO	NTO	NT	NT
MCI #2	Enabled	8.6 ^D	8.3 ^E	8.7 ^{A#}	8.8 ^D	8.3 ^{B#}	9.0 ^{B#}	8.6 ^{D#}	9.0 ^{D#}
	Disabled	11.0 ^D _{WL}	13.6 ^E _{WL}	10.2 ^A	14.6 ^D _{WL}	9.2 ^B	9.1 ^B _{WL}	9.2 ^D	11.9 ^D _{WL}
Prevost	Enabled	11.0 ^F _{WL}	11.5 ^F _{WL}	11.9 ^E _{WL}	11.6 ^F _{WL}	11.5 ^E _{WL}	11.8 ^F _{WL}	11.3 ^D _{WL}	11.9 ^F _{WL}
	Disabled	10.9 ^F _{WL}	11.6 ^F _{WL}	11.5 ^E _{WL}	11.0 ^F _{WL}	11.4 ^E _{WL}	11.8 ^F _{WL}	11.4 ^D _{WL}	11.7 ^F _{WL}

A - Steering Scalar is 110%, B - Steering Scalar is 100%, C - Steering Scalar is 90%, D - Steering Scalar is 80%, E - Steering Scalar is 70%, F - Steering Scalar is 60%

#- Maximum scalar tested due to ESC system malfunction

WL- Vehicle experienced wheel lift

When ESC was enabled, ESC reduced both yaw and roll angles sufficiently to prevent wheel lift events from occurring for the range of speed and steering inputs evaluated. MCI #1's ESC system reduced yaw angles an average of 26 percent, and roll angles by an average of 31 percent. MCI #2's ESC system was observed to reduced yaw angles by 19 percent, and roll angles by 8 percent. The ESC system in the Prevost was not observed to reduce peak roll or yaw angles generated in HSWD maneuvers from those observed when the system was disabled.

3.7 Maneuver Discussion and Summary

The test results in this chapter presented the test track performance data from motorcoaches equipped with and without ESC under two load conditions, two test surfaces, and a variety of maneuvers. Instabilities were limited to wheel lift; there were no spinouts. Wheel lift was observed in 31 of 105 ESC disabled test series and was reduced to 15 out of 107 when the systems were enabled. Results regarding the test surfaces, loading conditions, maneuvers and details regarding testing complications are further discussed in the following subsections.

3.7.1 Testing Surface

Test results from the maneuvers conducted on dry high friction and wet reduced friction surfaces show that ESC was active and reducing or increasing the dynamic motions of the motorcoaches to address vehicle roll and yaw stability as appropriate. Comparing differences between the enabled and disabled states on both surfaces show that the ESC systems were able to produce larger changes to the vehicles performance data on the dry surface. This was due to the larger amounts of friction available on the dry surface with which ESC used to generate wheel brake torques that provided the yaw and roll correcting moments to the vehicle. Since more friction was available on the dry

surface, more roll instabilities were observed with the system disabled. Overall, 52 out of 186 (28 percent) test series had roll instability on the high friction surface versus 0 (roll or yaw instabilities) out of the 38 test series performed on the reduced friction surface wet Jennite test surface. The motorcoaches experienced an understeering condition on the wet Jennite, but this condition was not considered an unstable yaw condition (such as a vehicle spinout due to severe oversteer).

Results from the reduced friction surface show that ESC can improve the dynamic performance on slippery surfaces. The test track data show that the RWD has the potential to validate ESC's engine torque reduction capabilities. Data collected from the RSM on this surface showed ESC was improving each motorcoach's position by reducing plow. An example from RSM test series conducted on the reduced friction surface is shown below in Figure 3.53, Figure 3.54, and Figure 3.55. This position plot shows that the performance of the three motorcoaches did not overlap and that the Prevost with and without ESC had a smaller turning radius for the given inputs. These types of observations show that improvements in performance are limited to comparing an individual vehicle's performance with and without ESC for maneuvers. These observations and the variability of the surface as shown in Figure 2.1 are similar to observations in past research [3]. The remaining discussion for this report will be focused on the maneuvers conducted on dry asphalt (high friction surface).

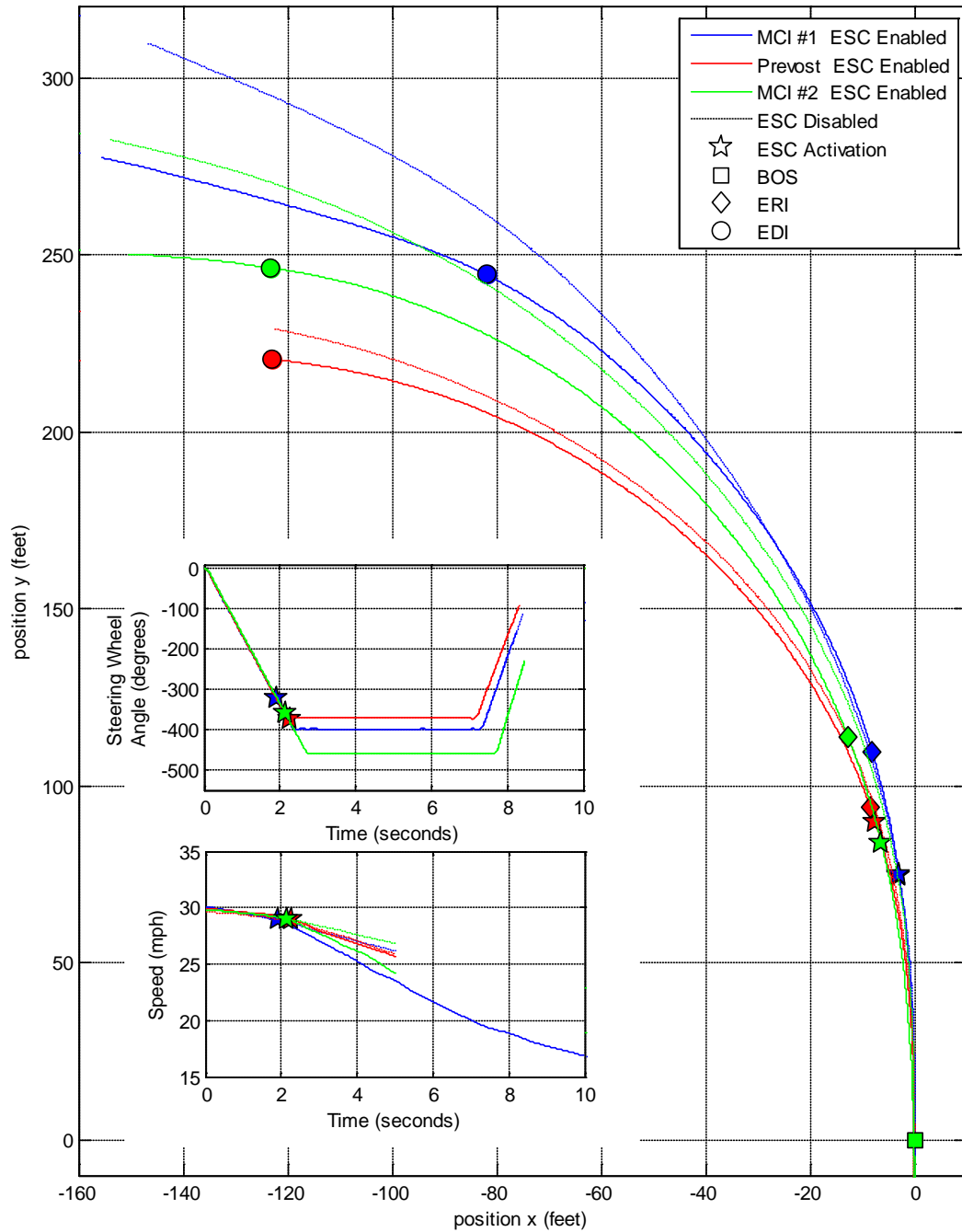


Figure 3.53. Position data of the motorcoaches performing the RSM on the reduced friction surface. Lines approximate the path of the center of the front axle.

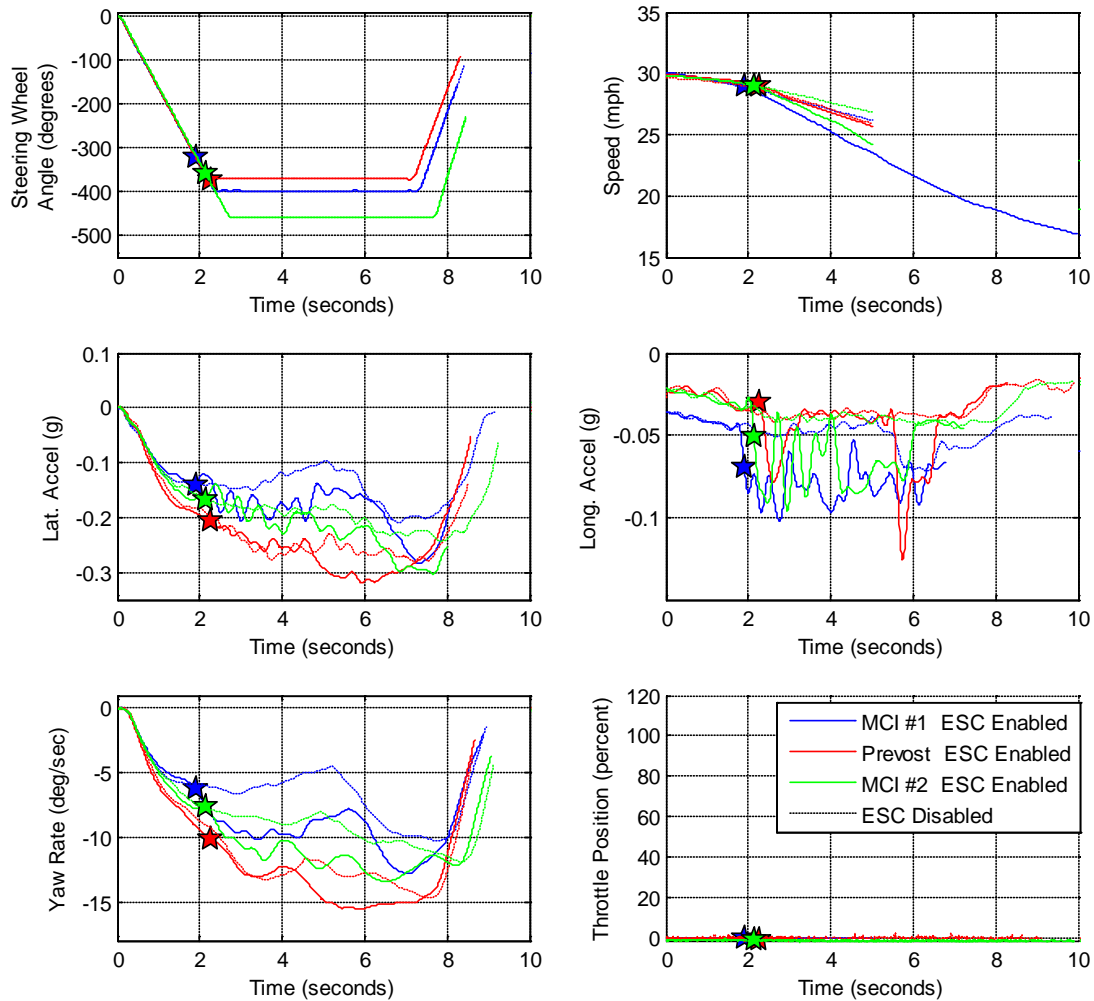


Figure 3.54. Time history data from the RSM test shown above in Figure 3.53.

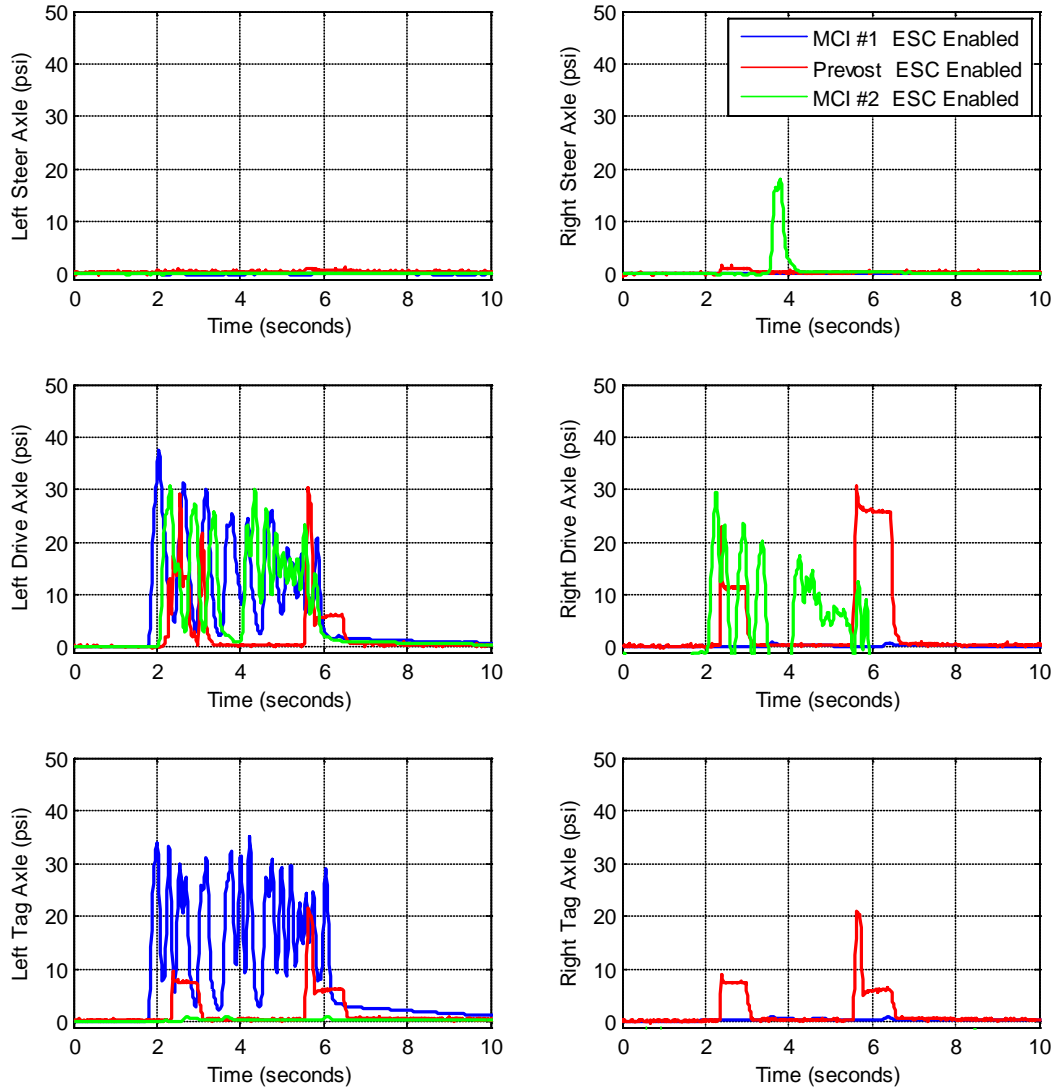


Figure 3.55. Time history data of brake pressures from test shown in Figure 3.53.

3.7.2 Loading Conditions

When comparing the performance of the vehicles in the LLVW to the GPOW load condition, the data from the dry asphalt shows that the LLVW loaded motorcoaches were more stable with only nine out of 98 (nine percent) test series resulting in instances of wheel lift as compared to 43 out of 88 (49 percent) test series with the GPOW load. Based on these results and the fact that the performance of motorcoaches when loaded with the simulated passengers is of greater interest, the focus of the rest of this section and the next chapter will be on test results obtained with the GPOW load condition.

3.7.3 Maneuvers

Test data from the SIS and CR maneuvers show that, whether speed is held constant and steering is slowly increased or speed is slowly increased and steering held

approximately constant, ESC intervenes before the vehicle reaches its dynamic limit. In these maneuvers, the system initially commanded an engine torque reduction and then applied light braking to reduce the longitudinal and lateral dynamics of the motorcoach. Both of these maneuvers show the ability of the system to reduce engine torque to increase stability as the vehicle approaches its lateral threshold in a gradual manner.

RSM test results demonstrate that ESC reduced the dynamic roll propensity of the motorcoaches. The test data illustrated ESC's ability to use the foundation brakes to reduce speed and lateral accelerations that caused wheel lift when the systems were disabled. These large reductions in lateral acceleration allowed the vehicles to enter the maneuver at 11 mph faster for the Prevost and over 15 mph faster for the two MCI motorcoaches.

Test track results from both the SWD and HSWD maneuvers with the motorcoaches show that the maneuvers were capable of exciting dynamic responses from vehicles of this size and mass. There were clear differences in lateral acceleration and yaw rate test data between ESC enabled and disabled test series that show ESC was reducing both rollover and spinout propensity. Both maneuvers were determined to be viable objective performance test candidates. However, the SWD was favored over the HSWD due to several tangible reasons. The SWD maneuver can be conducted in a smaller test area, was representative of crash avoidance or lane change type maneuvers, and its previous use in FMVSS No. 571.126 accelerated the measure of performance research.

Like the results obtained in SWD and HSWD maneuver development research with tractors [3], a longer dwell time produced larger dynamic responses with less steering amplitude. Maximum roll and yaw angle results show that larger angles were produced with the 0.4 and 0.5 Hz maneuvers for a majority of the GPOW SWD series conducted. Between those two frequencies, larger maximum roll angle responses were observed in three test series with the 0.5 Hz frequency, one series in which both frequencies produced equal maxima, and one series in which the maxima were observed at 0.4 Hz. Comparing maximum yaw angle responses with the GPOW condition, four series of SWD tests were observed to have larger maximum yaw angle responses with the 0.5 Hz frequency versus one series at 0.4 Hz and 0.6 Hz each. Based on these observations, the 0.5 Hz SWD (1.0 second dwell) was selected as the candidate SWD maneuver to use to evaluate ESC transient performance in motorcoaches.

The SIS, RSM, and 0.5 Hz SWD test track data from the motorcoaches in the GPOW load condition were used to assess potential measures of performance. Since these maneuvers and test results are similar to those determined for tractors, the same measures of performance were assessed against motorcoach data. These measures indicated that ESC systems were capable of exerting control over the engine/power unit (SIS test data) and of foundation braking control (RSM, and SWD test data), while maintaining maneuverability and steering responsiveness.

3.7.4 Broken Roll Stabilizer Link

Initial RSM tests conducted with the Prevost on 7/24/2009 showed that the vehicle experienced two inches of wheel lift at 48 mph configured in the GPOW load condition. RSM tests under the same conditions were repeated on 7/28/2009 and 7/30/2009. During these tests, wheel lift of 2 inches or greater was observed at 42 – 44 mph with ESC enabled. Upon further investigation when preparing to de-instrument the motorcoach, a broken roll stabilizer bar link was discovered. Researchers attributed the increase in roll propensity observed to the broken stabilizer link. Figure 3.56 compares initial test data for MES of 42 mph collected on the 24th (data traces shown in blue) and repeated maneuvers on the 28th (data traces shown in black). In the figure, for the test conducted on the 24th no wheel lift was observed, but on the 28th wheel lift of just over two inches was observed. The other observed difference between the two tests is the vehicle's roll angle. For testing on the 28th, the vehicle produced a larger roll angle response as compared to the test conducted on the 24th.

SWD, HSWD and RWD maneuvers conducted with the Prevost in the GPOW load condition were all conducted after the 24th with the unknown broken roll stabilizer bar link. As such the vehicles roll responses were negatively influenced and some of the instabilities observed in these maneuver test series were likely occurring at lower speeds than if the roll stabilizer bar link was intact.

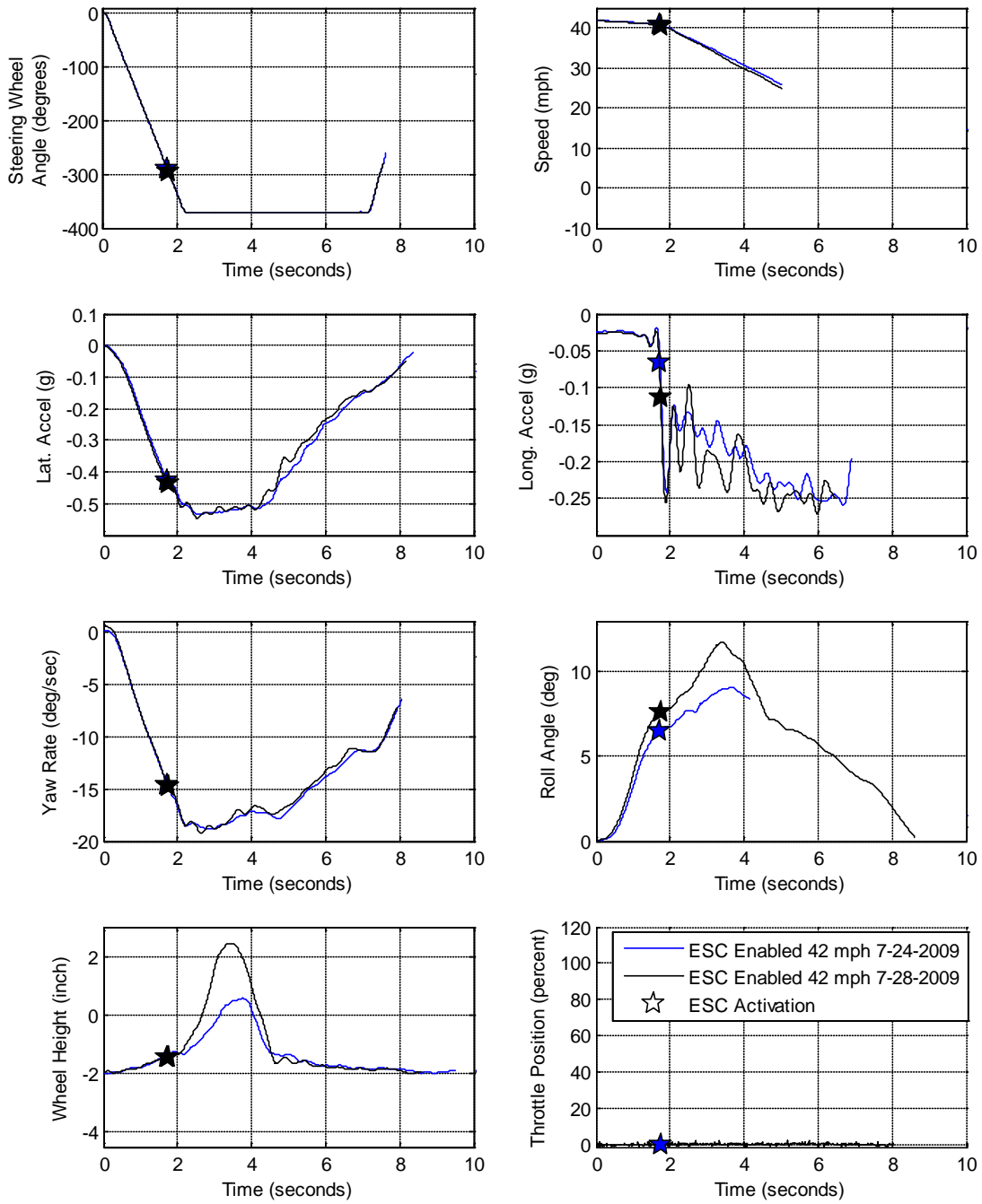


Figure 3.56. Graph shows test data from the Prevost RSM in the GPOW load condition with ESC enabled for two tests with a MES of 42 mph but conducted on different days.

4 MEASURES OF PERFORMANCE

The GPOW data from the SIS, RSM, and the 0.5 Hz, 1.0 second SWD maneuvers were examined to see if previously developed measures of performance for tractor-trailer systems would also work for motorcoaches. Those lateral performance measures were found to be capable of discerning vehicles equipped with electronic stability control systems from those not so equipped, and were correlated to effective increases in stability. Depending on the maneuver and the vehicle's response to the speed and steering inputs, ESC used different combinations of power unit and/or foundation braking control to improve lateral stability. The measures were aimed at assessing the system's sublimit ability to activate these controls and then its capability to mitigate a dynamic (limit) roll or yaw event.

Those measures were engine torque reduction, Lateral Acceleration Ratio (LAR) and Yaw Rate Ratio (YRR). Engine torque reduction is an indicator of how well an ESC system is able to improve the stability of the vehicle in which it is installed by exerting control over the power unit (engine). The other two measures indicate how well the ESC system is able to improve roll and yaw stability through use of the foundation brakes. The LAR measure was developed for both the RSM and SWD test track maneuvers. It was originally developed as a roll stability measure assessed from RSM test data. Subsequent research indicated it was also applicable and complementary to the YRR measure used with the SWD. Performance results for these stability measures are presented and discussed in the following subsections.

In the following discussion on measures of performance for motorcoaches, subsection 4.1 presents engine torque reduction observations from the SIS test data. Subsection 4.2 LAR presents measurement observations from RSM test data. Subsections 4.3 and 4.4 presents LAR and YRR measurements and responsiveness analyses from SWD test data.

4.1 Engine Torque Reduction in SIS maneuvers

Using GPOW load condition test data from the SIS maneuver, engine torque data collected from the vehicles' communication data bus were analyzed. Driver requested torque and engine torque output measures were concluded to be potential measures to indicate that engine torque was reduced, while the vehicles' forward speed could potentially be used as the performance measure. During normal operation, the "driver requested torque" and "engine torque" measures were observed to be equal to each other. During the SIS maneuvers, once ESC activated and invoked engine control the two measures were observed to separate. In all cases, the "engine requested torque" was much less than the "driver requested torque".

In Figure 4.1 each trace represents the average of the percent difference in the engine torque over one-half second intervals from the torque reduction event for each motorcoach tested. Included in the figure is the average of the difference (percent change) as described in tractor semitrailer testing [3]. The figure shows that a good region for assessing performance lies between 0.5 and 2 seconds. While this data

shows that the respective changes in engine torque were quite large, it was observed that a small (5-20 percent) change would be sufficient to be able to identify the torque reduction event.

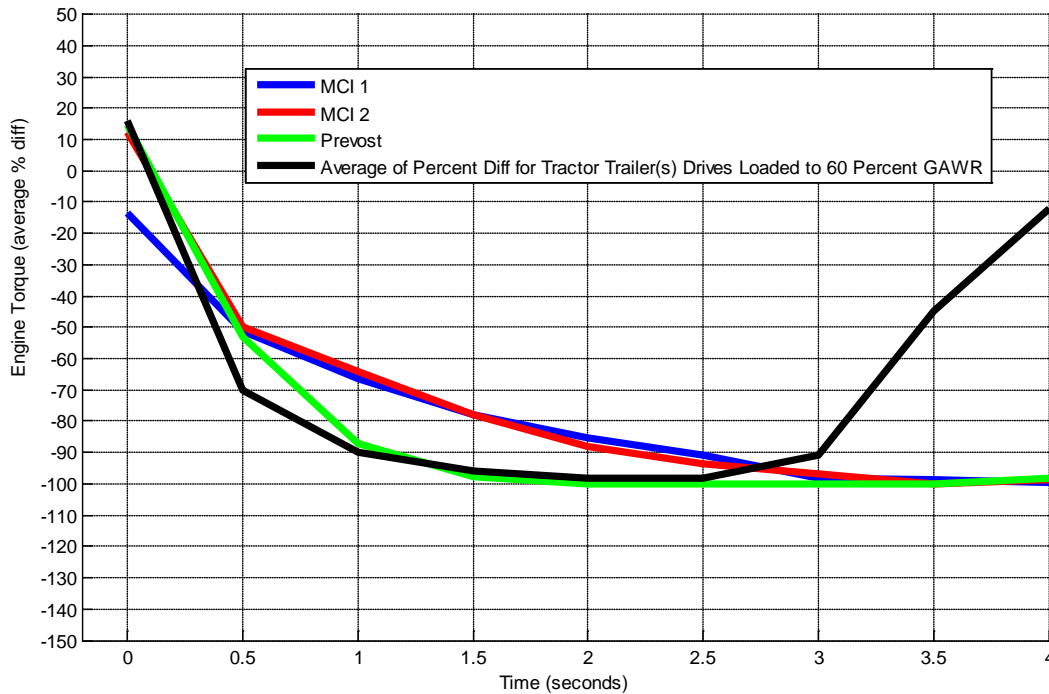


Figure 4.1. Average engine torque reduction for each motorcoach tested in the GPOW load condition. Also included was the average difference (percent change) for all tractors equipped with stability control tested in combination with four different trailers.

4.2 LAR from RSMs

Based on data that was presented in previous sections of this report, it can be observed that lateral acceleration was significantly reduced for RSM tests conducted with ESC enabled as compared to tests with the system disabled. ESC will reduce the lateral acceleration of the vehicle once it has exceeded a threshold in the RSM which simulates negotiating a curve. This would be apparent in test data for a given entrance speed and loading condition that produces a dynamic response from the vehicle requiring the ESC system to selectively apply the foundation brakes to improve stability. This intervention increases the roll stability of the vehicle(s) by reducing the tipping forces produced from lateral acceleration acting on the mass of the vehicle. Figure 4.2 shows an example of the ESC system's ability to reduce a motorcoach's lateral acceleration.

LAR as it was used with the RSM test data was calculated by dividing the lateral acceleration at the vehicle CG for given time increments by the lateral acceleration at the End of the Ramp Input (ERI). This measure reduces the effect of MES on vehicle performance and gives a point of reference from which to assess how the vehicle's lateral acceleration changes over time.

$$\text{RSM LAR} = \frac{A_y(\text{ERI} + 1.0, +2.0 \dots + 5.0 \text{ sec})}{A_y(\text{ERI})} \times 100$$

Figure 4.2 shows graphically the RSM timing events and data used to calculate LAR for an ESC enabled and disabled RSM tests at 30 mph. From top to bottom in the plots are steering wheel angle, lateral acceleration, and LAR versus time. LAR shows the change in lateral acceleration as a percentage of that produced at ERI with a substantial decrease in LAR dependent on whether the system was enabled or disabled.

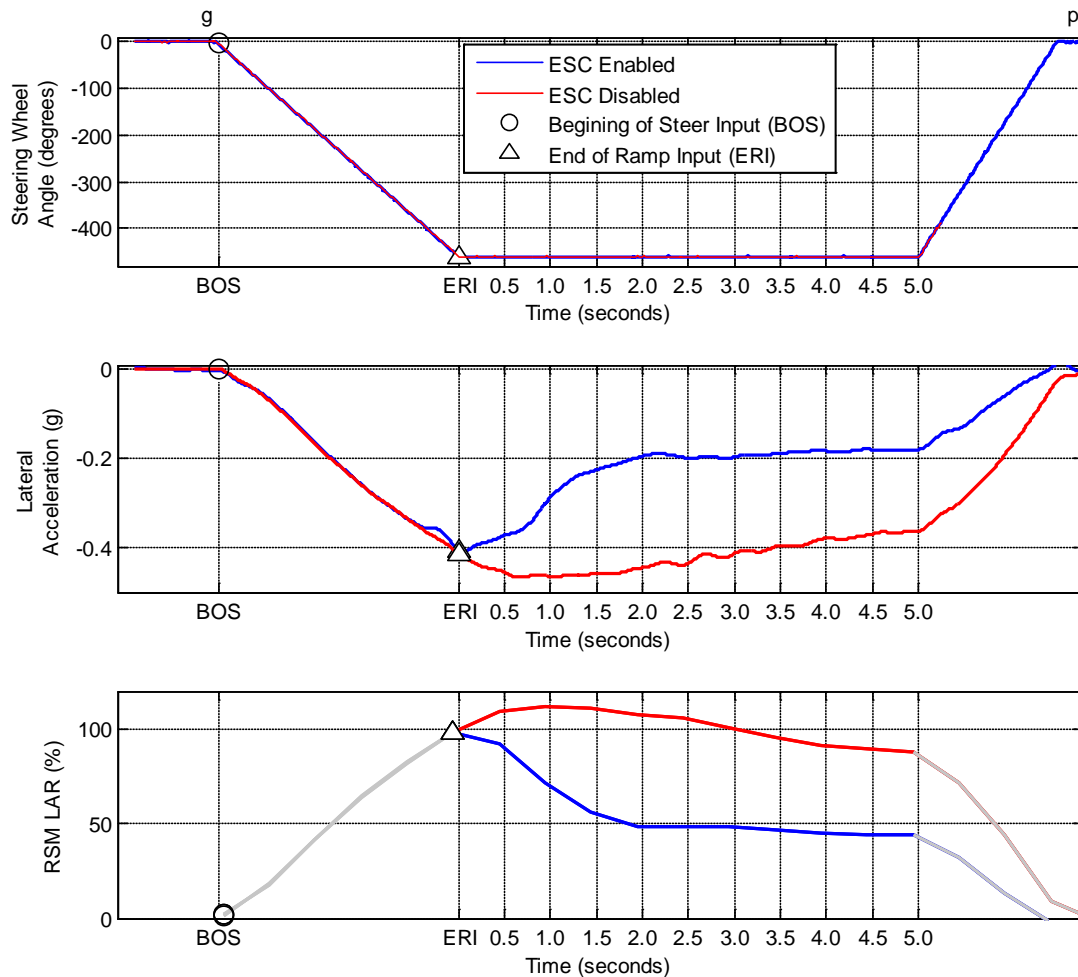


Figure 4.2. Time history data of steering wheel angle, lateral acceleration and the calculated LAR measure. This figure, key points of interest: BOS and ERI.

RSM LAR Applied to the Motorcoach GPOW Load Condition

LAR was calculated for 0.5 second intervals after ERI for all RSM's performed with the GPOW load conditions. Data were then plotted versus the 10 different time increments after ERI for a range of speeds. Figure 4.3 through Figure 4.5 show LAR versus time after ERI for the MCI #1, the Prevost, and the MCI #2 for MESs that ranged between 30–50 mph. The tests in which wheel lift were observed to be greater than two inches are shown with circles around the MES displayed for each test. This speed range was

selected because it encompassed all of the speeds at which instances of wheel lift were observed when ESC was either enabled or disabled.

Figure 4.3 shows RSM tests conducted with a MES speed range of 30–37 mph with ESC disabled, and 30–50 mph with ESC enabled for the MCI #1. The first observation of ESC activation for the MCI #1 was at a MES of 28 mph. As the figure shows (circles around MES), there was one case of wheel lift for the ESC disabled series at a MES of 37 mph. Clearly, the data shows that the largest LAR values were produced when the ESC was disabled, while the lowest values of LAR were observed with the ESC enabled. As speed was increased, the separation between the different stability control test states became more evident.

Figure 4.4 shows RSM tests conducted with a MES speed range of 30–39 mph ESC with disabled, and 30–48 mph with ESC enabled for the Prevost. The first observation of ESC activation for the Prevost was at a MES of 26 mph. As the figure shows (circles around MES), there were two cases of wheel lift for the ESC disabled series at MESs of 38 and 39 mph. At a MES of 38 mph, two inches of wheel lift was observed and at a MES of 39 mph the wheel lift was greater than two inches. For the ESC enabled tests, there was one case of wheel lift at a MES of 48 mph.

Figure 4.5 shows RSM tests conducted with a MES speed range of 30–35 mph with ESC disabled, and 30–50 mph with ESC enabled for the MCI #2. The first observation of ESC activation for the MCI #2 was at a MES of 26 mph. As the figure shows (circles around MES), there was one case of wheel lift for the ESC disabled series at a MES of 35 mph. Clearly, the data shows that the largest LAR values were produced when ESC was disabled, while the lowest values of LAR were observed with the ESC was enabled. As MES was increased, the separation between the different stability control test states became more evident.

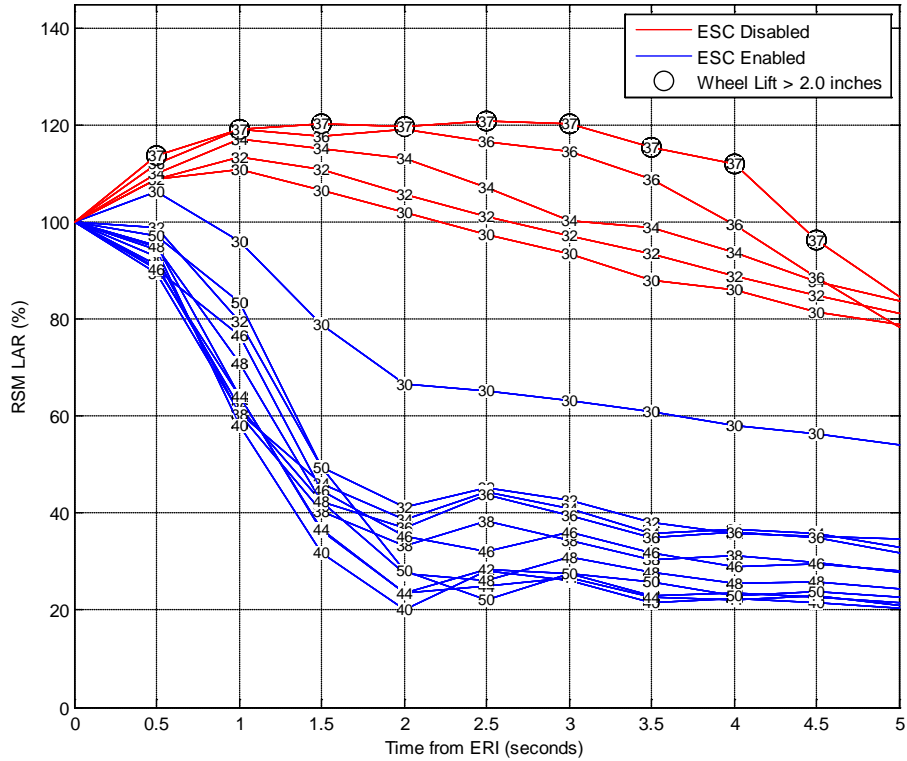


Figure 4.3. LAR versus time after ERI for MCI #1 RSM tests (GPOW load condition) conducted with a MES of 30–37 mph with ESC disabled and 30–50 mph with ESC enabled.

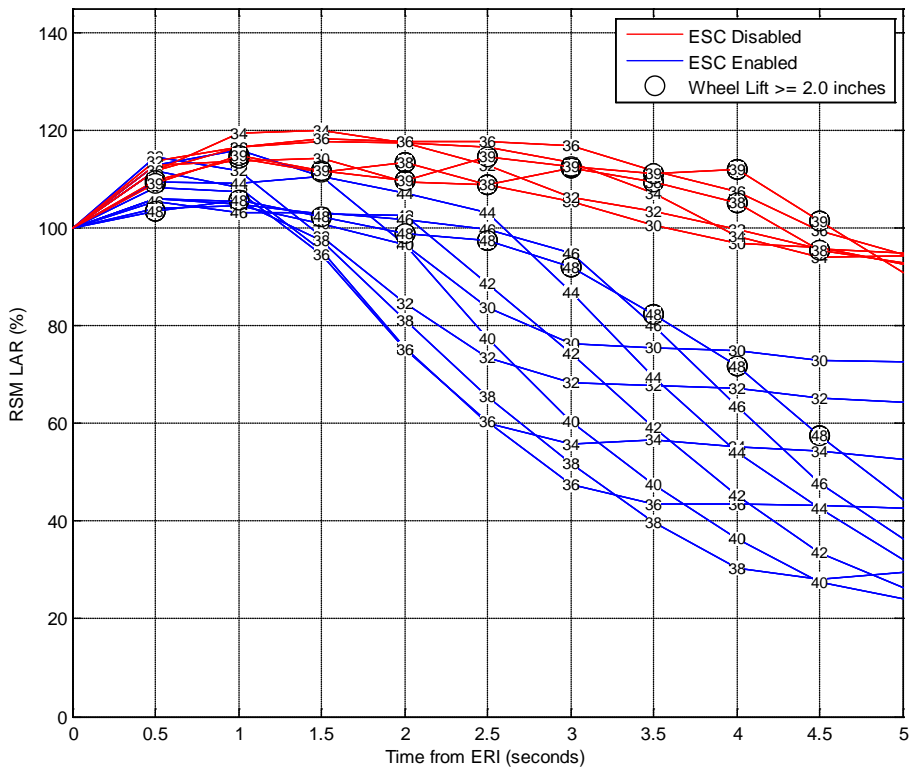


Figure 4.4. LAR versus time after ERI for Prevost RSM tests (GPOW load condition) conducted with a MES of 30–39 mph with ESC disabled and 30–48 mph with ESC enabled.

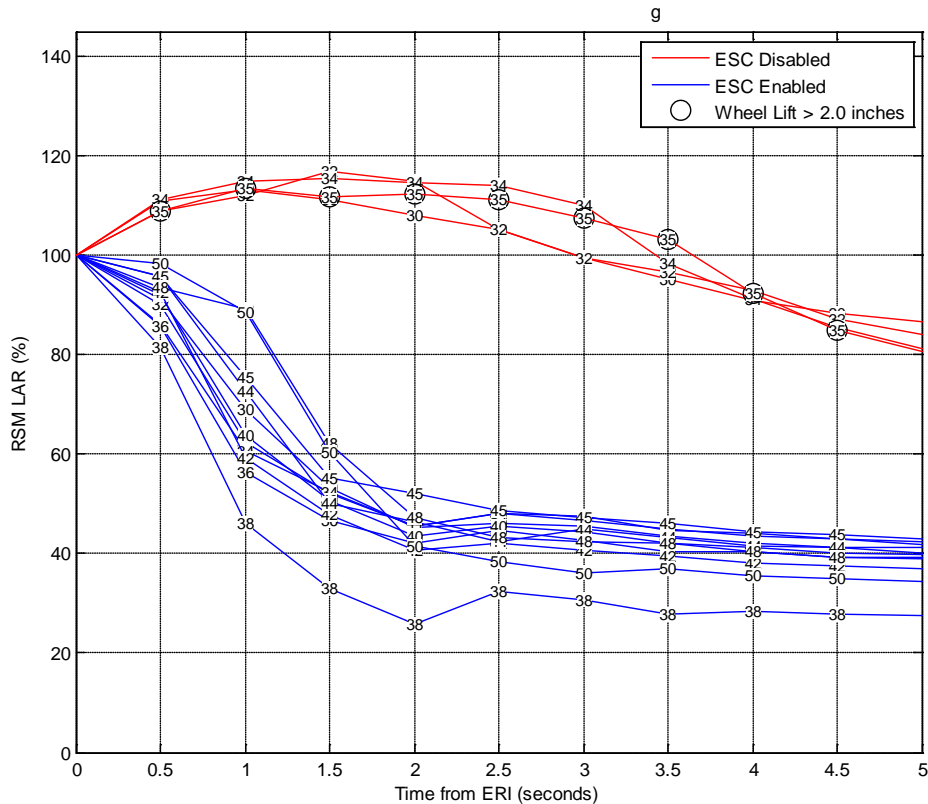


Figure 4.5. LAR versus time after ERI for MCI #2 RSM tests (GPOW load condition) conducted with a MES of 30–35 mph with ESC disabled and 30–50 mph with ESC enabled.

4.3 LAR and YRR from SWD maneuvers

Both LAR and YRR were developed and used in prior agency lateral stability research covering both light passenger cars and truck tractor and trailer combinations. For more information regarding the development of LAR see [3] and for more information regarding development of YRR see [22], [26] and [3].

Motorcoach ESC systems, when enabled, commanded foundation braking in every 0.5 Hz SWD (1.0 second dwell) test track series. When compared to the ESC disabled test series it was found that the foundation braking improved the roll and yaw stability in each of those comparisons. The SWD test data were investigated to see if these measures were also capable of assessing the lateral stability of motorcoaches equipped with ESC. LAR and YRR measures were studied first. These measures were preferred because they were easy to measure, filter, correct, and calculate compared to more involved measures such as yaw angle, articulation angle and wheel height. If they proved to be impracticable or unpredictable then other measures would be considered.

While LAR was not originally developed to assess stability in the SWD maneuver it was easily adapted and applied. LAR as it is used for SWD data was essentially the same equation as that used for YRR, where the yaw rate term is replaced with lateral acceleration. YRR by definition is the yaw rate at specified time intervals divided by the peak (max or maximum) yaw rate achieved between 1.0 and 3.0 seconds into the

maneuver. This time interval to assess peak yaw rate coincides with the 3rd quarter cycle, dwell, and 4th quarter cycles of the steering input (portion of steer with the opposite sign of the initial input).

Both LAR and YRR can be calculated over the entire time history of the maneuver. However, the time period of interest occurs after completion of steer (COS). This is due to the fact that the steering wheel has been returned to the zero position (straight forward travel is commanded). While the steering wheel angle is zero, LAR and YRR are calculated and observed to see how they behave. If these measures return to zero in a reasonable time frame (settling time) after COS then the system is stable. As the steering input (scalar) is incrementally increased in subsequent test runs and larger dynamic responses produced, the settling time tends to grow longer without ESC and can be indicative of a loss of stability. The equations for LAR and YRR are shown below, with both expressed as percentages.

SWD YRR Definition:
$$YRR = \frac{\Psi(COS + 1.0, +1.5... + 3.0 \text{ sec})}{MAX(\Psi)_{t=1.0}^{COS}} \times 100$$

Where:
 Ψ = Yaw rate of the motorcoach
 COS = Completion of Steer

SWD LAR Definition:
$$LAR = \frac{Ay(COS + 1.0, +1.5... + 3.0 \text{ sec})}{MAX(Ay)_{t=1.0}^{COS}} \times 100$$

Where:
 Ay = Lateral acceleration at C.G. of the motorcoach

Examples of these measures are shown in Figure 4.6. From top to bottom in the figure are SWD time history examples of steering wheel angle lateral acceleration and LAR, yaw rate, and YRR. The time domains used to determine peak lateral acceleration (Ay) and yaw rate are shown along with the COS event.

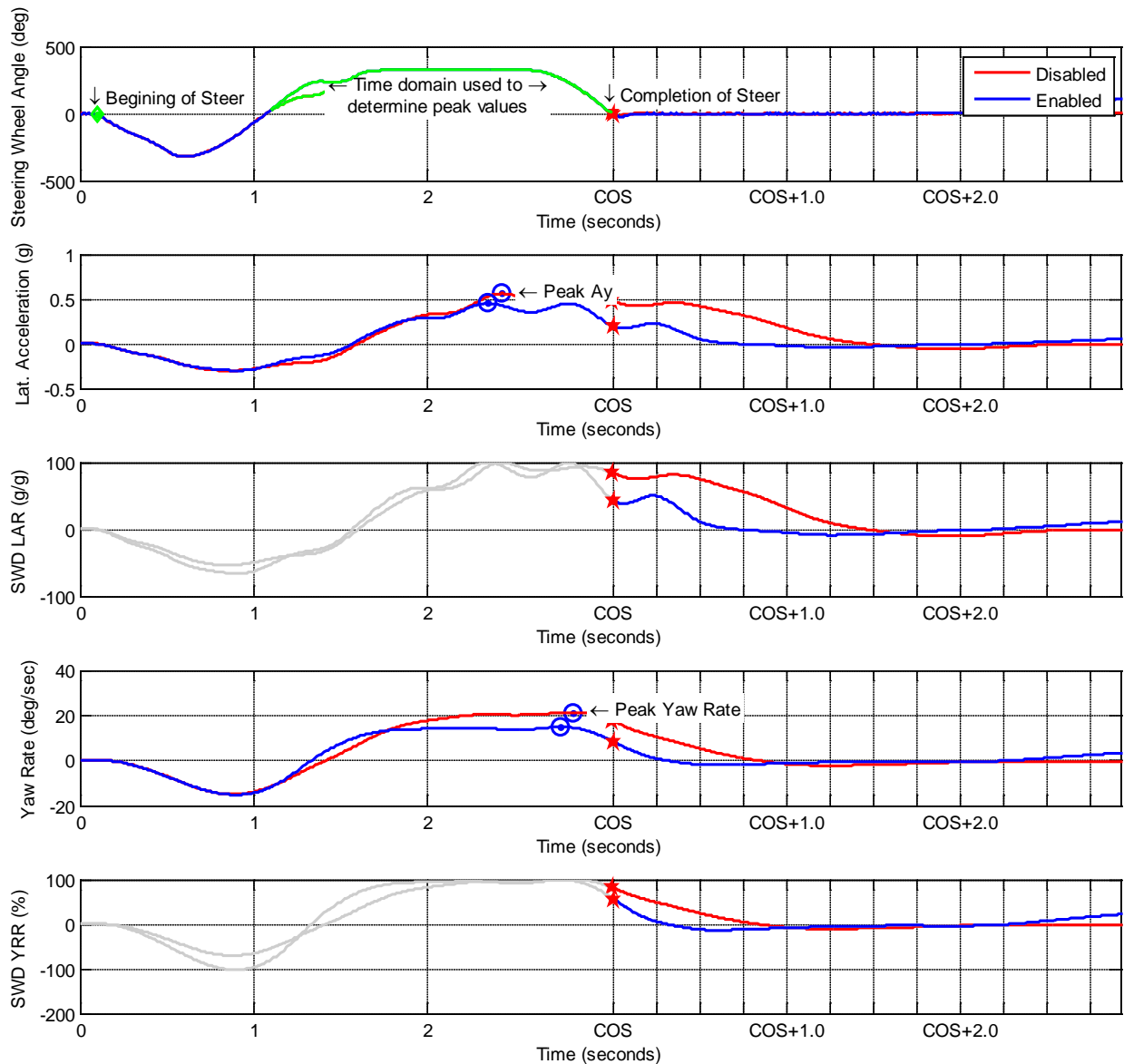


Figure 4.6. Key events in the SWD maneuver's steering input and measured lateral acceleration and yaw rate signals that were used calculate the LAR and YRR measures.

SWD LAR and YRR Applied to GPOW Test Condition

LAR and YRR were calculated at 0.25 second intervals after COS for all 0.5 Hz SWD (1.0 second dwell) tests performed with the GPOW load conditions. The data were then plotted for a range of steering scalars. Figure 4.7 through Figure 4.9 show LAR and YRR versus time after COS for the MCI #1, the Prevost, and the MCI #2. Steering scalars from 80–100 percent are shown for the two MCI motorcoaches and 70-100 percent for the Prevost. The tests in which wheel lift exceeded two inches are shown with circles around the steering scalar value displayed for each test. The scalar values shown in these figures were divided by 10 to reduce the length of the text in the plots.

These scalars were selected to encompass the SWD tests at which instances of wheel lift were observed when ESC was enabled and disabled.

Figure 4.7 shows SWD LAR and YRR results for tests conducted with steering scalars from 80–100 percent for the MCI #1. The figure shows the largest LAR and YRR values were produced when ESC was disabled, while the equivalent test results with ESC enabled were lower for all the time increments shown. For the MCI #1 the ESC system faulted and disabled itself for steering scalars from 100-130 percent, which corresponded to SWA's from 400–520 degrees. The ESC SWD test shown at 100 percent scalar also faulted but still shows that there was a reduction to the lateral dynamics experienced by the vehicle. SWD steering wheel inputs (greater than 400 degrees) were observed to overwhelm the motorcoach's power steering system and produced faults that disabled the motorcoaches ESC system. Interestingly, LAR for the scalars shown the with ESC disabled have a longer settling time than the YRR for the same SWD tests, indicating the vehicle drifted more as it settled out at 1.25 seconds after COS.

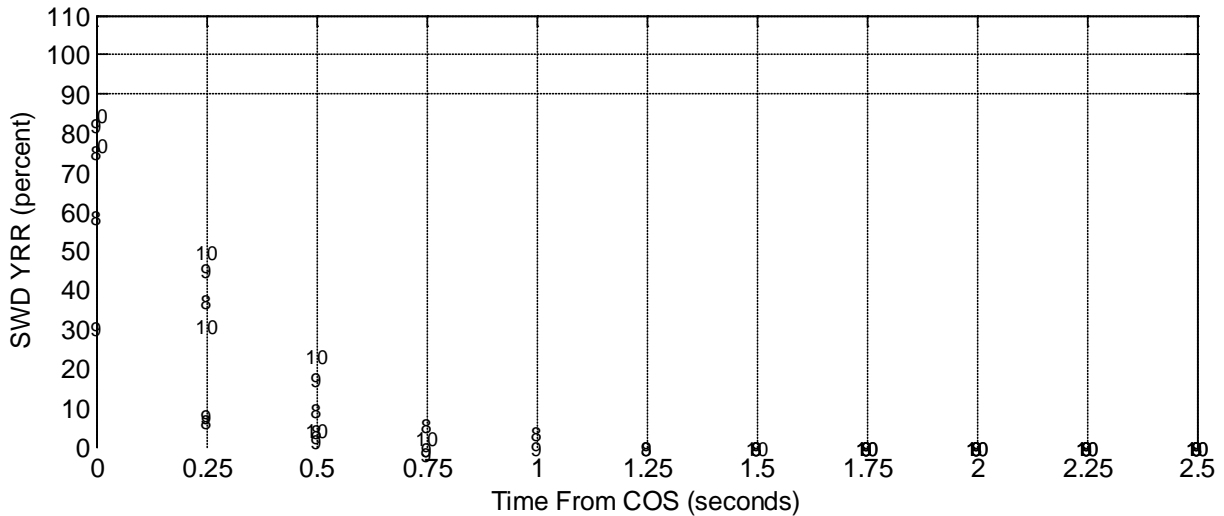
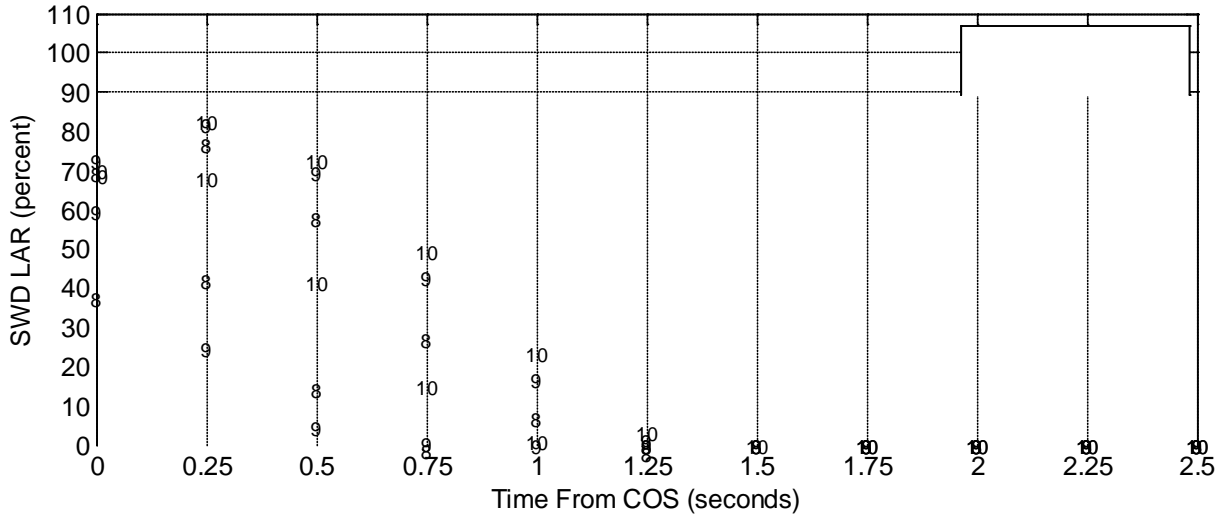


Figure 4.7. SWD LAR and YRR observations produced by the MCI #1 motorcoach with the GPOW load condition. Steering Scalars from 80–100 percent are shown for ESC enabled and disabled test series.

Figure 4.8 shows SWD LAR and YRR for tests conducted with at steering scalars from 70 – 100 percent for the Prevost. For this vehicle, the first observation of ESC activation and intervention was at a steering scalar of 30 percent. The figure shows the largest LAR and YRR values were produced when ESC was disabled while the equivalent test with ESC enabled was lower for all the time increments shown. With ESC disabled, wheel lift exceeded 2.0 inches at steering scalars of 75 and 80 percent (red lines marked with circle markers in the figure). When the system was enabled wheel lift was not observed until a steering scalar of 100 percent, denoted by a blue line with circle markers. ESC disabled tests not only had larger values but also required more time to settle out to zero.

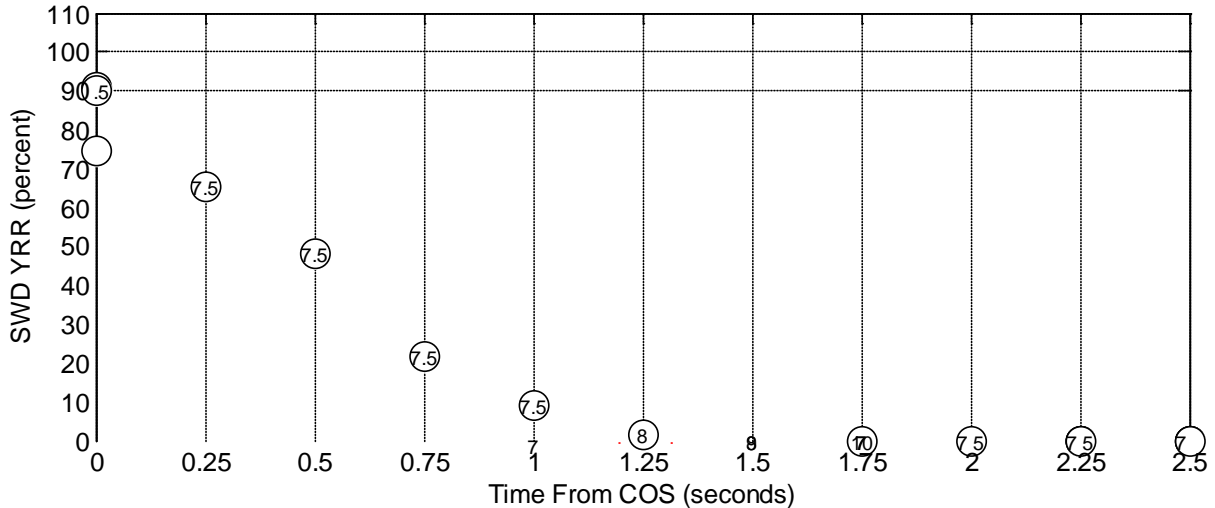
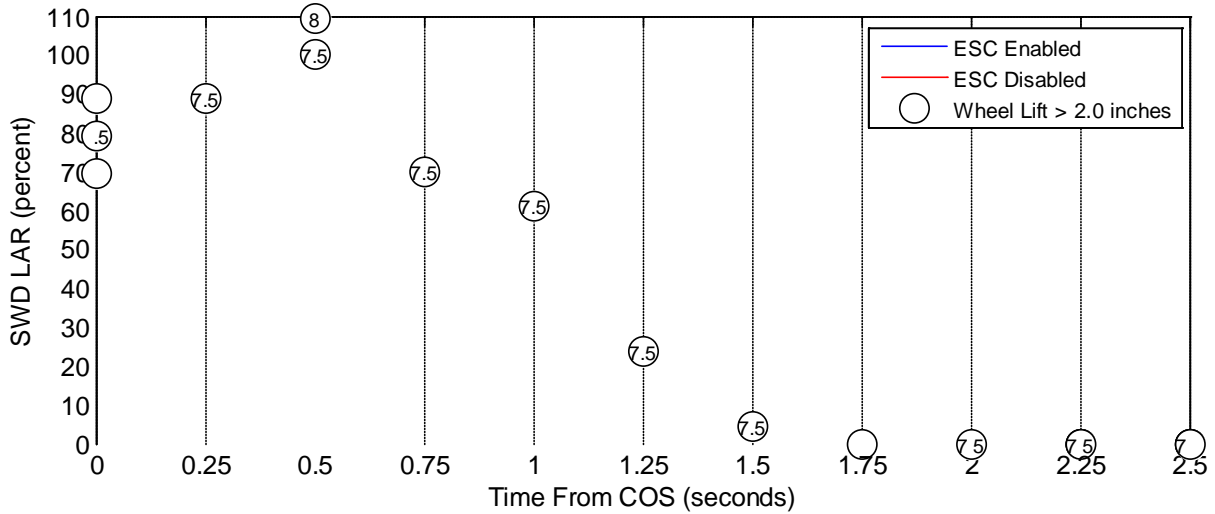


Figure 4.8. SWD LAR and YRR observations produced by the Prevost motorcoach with the GPOW load condition at steering scalars between 70 – 100 percent for ESC enabled and disabled.

Figure 4.9 shows SWD LAR and YRR for tests conducted with at steering scalars from 80–100 percent for the MCI #2. The figure shows the largest LAR and YRR values were produced when ESC was disabled while the equivalent test results with ESC enabled were lower for all the time increments shown. For the MCI #2 the ESC system faulted and disabled itself for steering scalars at 100 to 130 percent, which corresponded to SWA’s from 467–607 degrees. Unlike MCI #1, MCI #2 faulted early in the 100 percent steering scalar and was unable to reduce the lateral dynamics experienced by the motorcoach. SWD steering wheel inputs (greater than 400 degrees for the 0.5 Hz frequency) were observed to overwhelm the motorcoach’s power steering system and produce the faults that disabled the MCI’s ESC system. Like the MCI #1, MCI #2 LAR for the scalars with ESC disabled have a longer settling time than the YRR for the same SWD tests, indicating the vehicle drifted more.

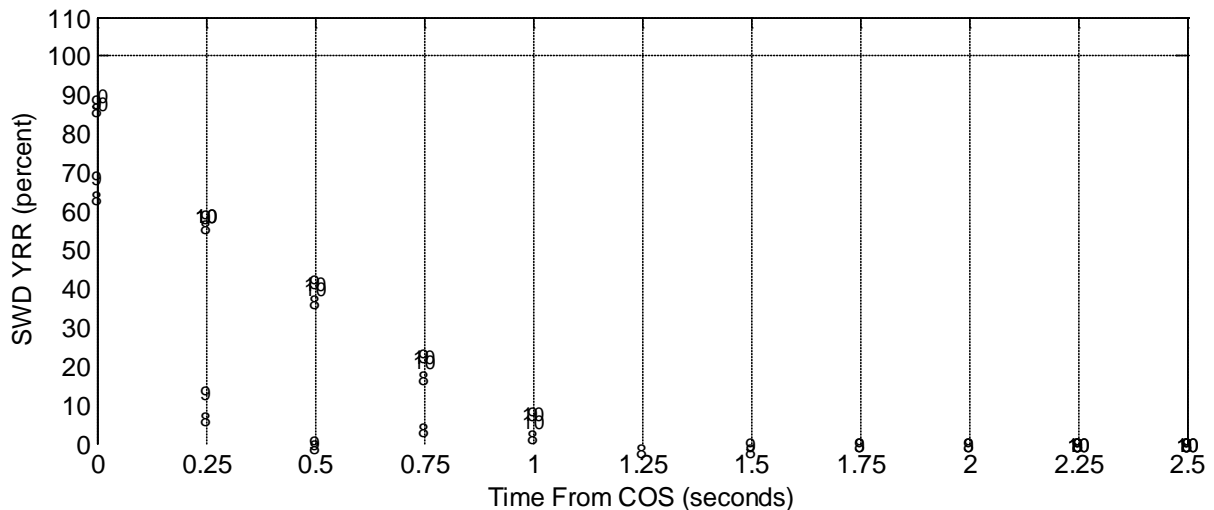
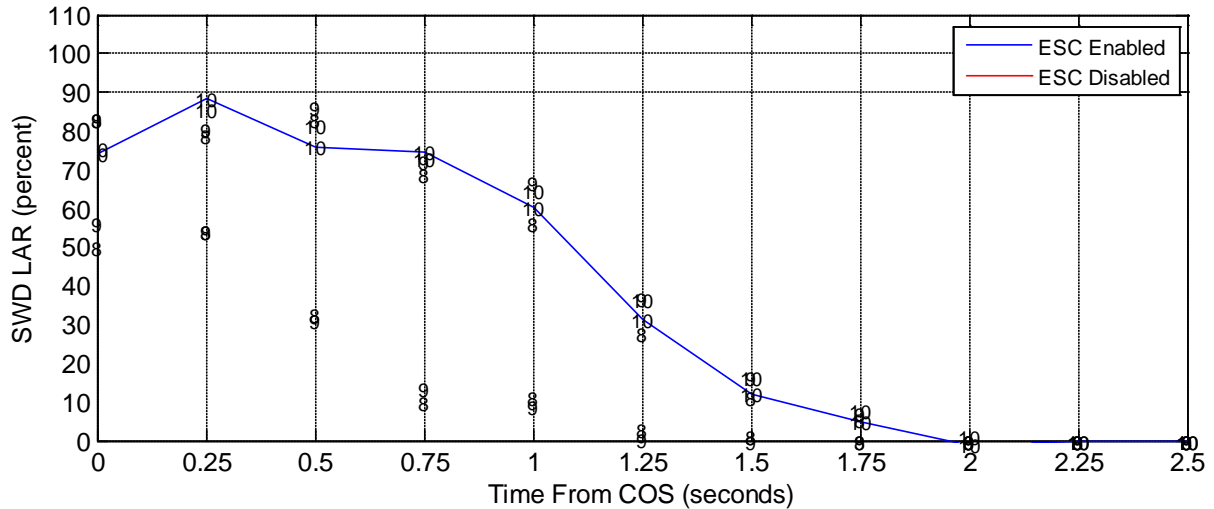


Figure 4.9. LAR and YRR observations produced by the MCI #2 motorcoach with the GPOW load condition. Steering Scalars between 80 – 100 percent are shown for ESC enabled and disabled tests.

4.4 Motorcoach Responsiveness

Stability control intervention has the potential to significantly increase the stability of the vehicle in which it is installed. A hypothetical way to improve stability control would be to either make the base vehicle or its stability control system intervention such that the vehicle is unresponsive to the speed and steering inputs. This would degrade the maneuverability required to avoid an obstacle. This hypothetical situation was addressed in DOT HS 809 974 [26]. That report details a “responsiveness” measure developed from SWD test data to assure that a balance between lateral stability and the ability of the vehicle to respond to the driver’s inputs was preserved. Though the SWD test results presented in that report do not show that any of the vehicles tested were out of balance with respect to stability or responsiveness, the rationale presented for a responsiveness assessment also was warranted for commercial vehicles. Therefore, a similar responsiveness measure based on the lateral displacement of the vehicle was

studied. It was found to be easy to measure and calculate, has good discriminatory capability for the vehicles tested and has a direct relation to obstacle avoidance. Based on those observations researchers decided to investigate lateral displacement measures to quantify the responsiveness of ESC equipped motorcoaches.

For this phase of research, the lateral displacement measure was determined as prescribed by FMVSS No. 571.126. Lateral displacement is calculated by double integrating and zeroing the corrected lateral acceleration measure. For motorcoaches the responsiveness would be measured at 1.5 seconds after the initialization of the maneuver. This time coincides with the end of the 3rd quarter cycle for a 0.5 Hz sine with 1.0 second dwell maneuver. This portion of the maneuver was considered the obstacle avoidance portion, while execution of the maneuver's dwell and 4th quarter cycles were considered the recovery portion of the maneuver. An example of this is provided in Figure 4.10.

From top to bottom, this figure presents examples of time history data for steering wheel angle, lateral acceleration, and calculated lateral displacement. Eight steering scalars are overlaid in plots to show how lateral displacement grows with each successive increase in steering input. Each plot has diamond, circle, and pentagram data markers denoting BOS, the 1.5 second responsiveness measure, and COS. The plot of steering wheel angle has the avoidance and recovery regions of the SWD maneuver highlighted. The figure shows that the responsiveness measure was taken at the end of the avoidance portion of the maneuver.

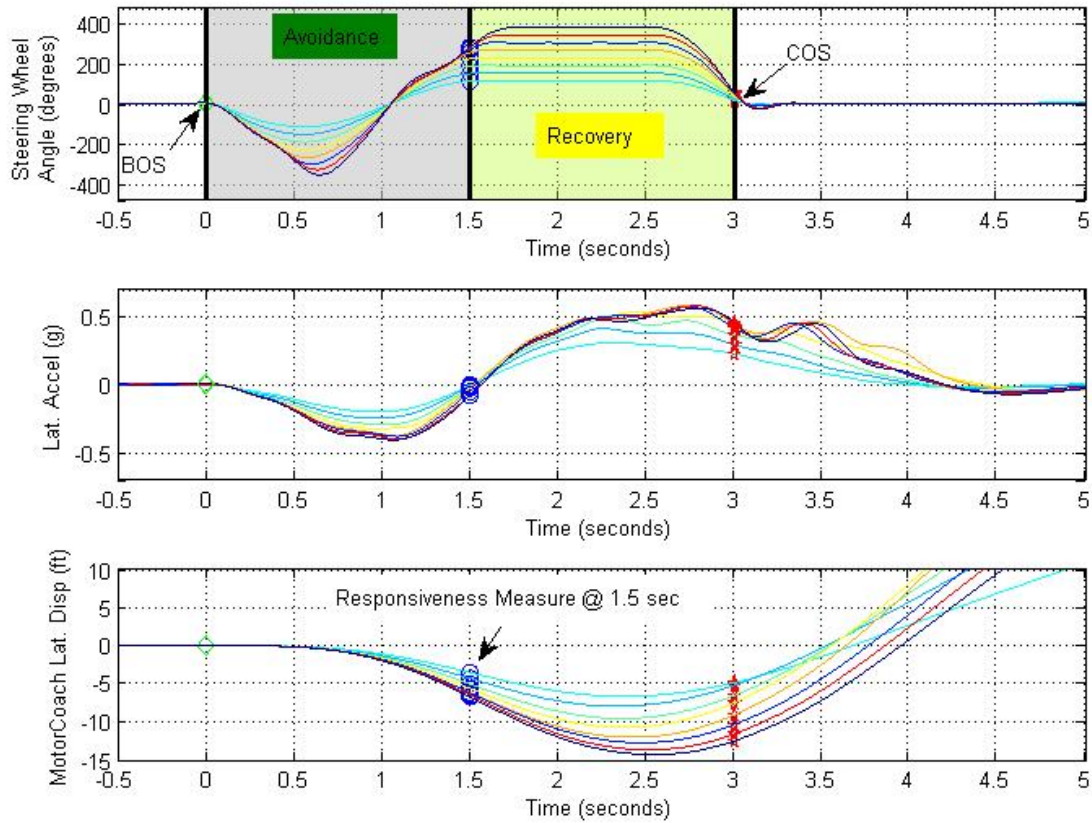


Figure 4.10. Time history data from the SWD denotes BOS, responsiveness measure, COS and the maneuver avoidance and recovery regions.

This lateral displacement measure was calculated and assessed for each 0.5 Hz Sine with 1.0 second Dwell maneuver. Figure 4.11 shows the displacement achieved 1.5 seconds into the SWD maneuver for each vehicle with ESC enabled and with ESC disabled, and the steering scalar value tested. Each data marker represents the lateral displacement measured for a single SWD maneuver. This figure shows that as the steering scalar was increased from 30 to 70 percent, the lateral displacement measure was also observed to increase. Note that the ESC enabled test series were not much different from the ESC disabled series. This indicates that the systems were not sacrificing maneuverability to increase stability.

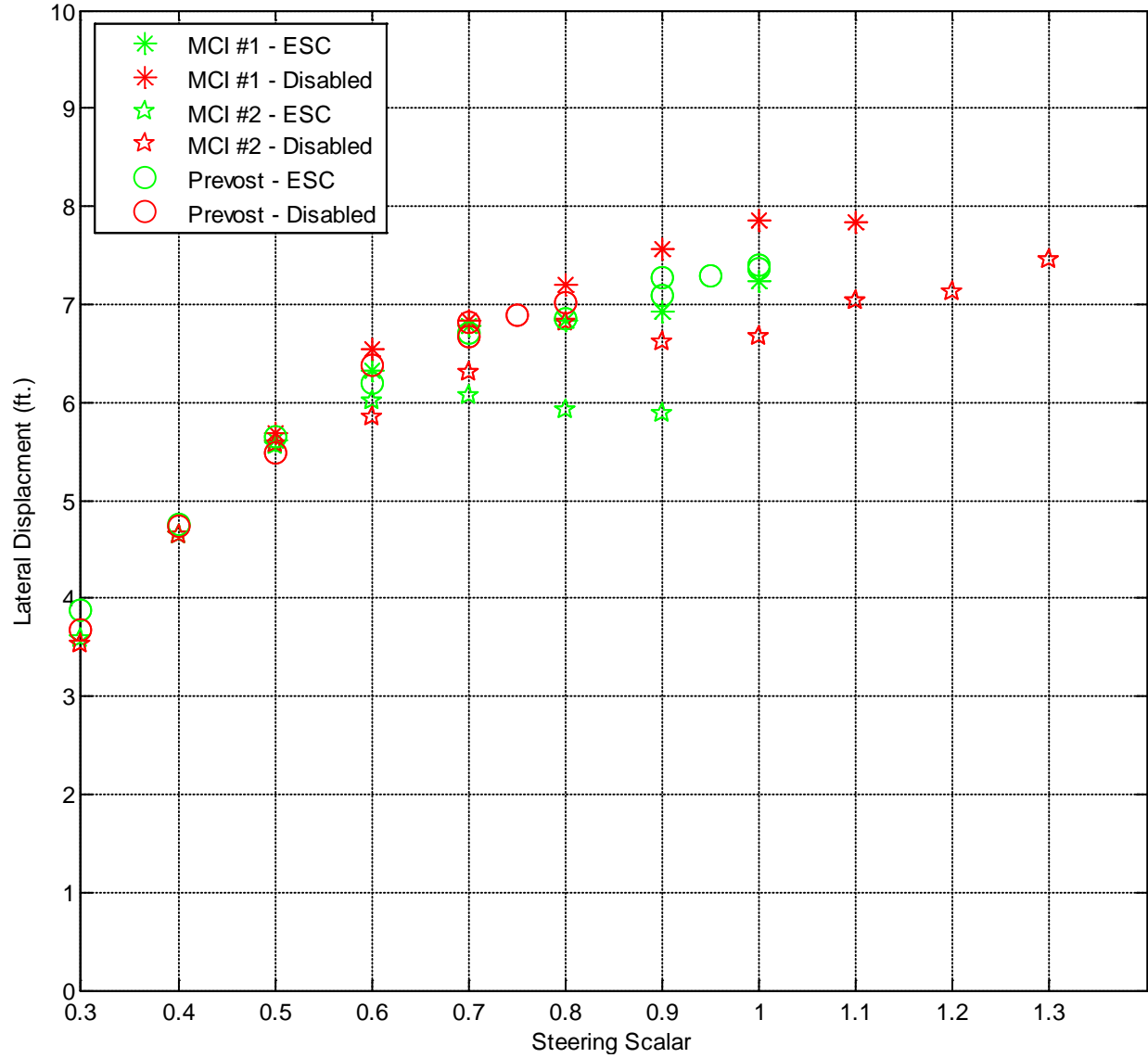


Figure 4.11. Lateral Displacement versus Steering Scalar 1.5 sec. after BOS for SWD test at 0.5 Hz with 1.0 sec. dwell.

5 CONCLUSIONS

5.1 Motorcoach Test Track Performance

Motorcoach ESC systems were observed to modify the handling characteristics as compared to the base vehicle without ESC. ESC changed performance by commanding engine torque reductions and selectively activating brakes to slow the vehicles down and generate moments to reduce both roll and yaw responses. While no yaw instabilities resulting in vehicle spinouts occurred during any of the test maneuvers, some roll instabilities events occurred with tests conducted in the GPOW load condition. In a few cases on reduced friction surfaces, ESC was observed to improve yaw responses by reducing plowout. These systems were observed to increase stability and responsiveness in a majority of the maneuvers evaluated and were not observed to degrade stability or test track performance in any of the maneuvers.

Comparing reduced and high friction test surfaces, test results from the dry high friction surface were found to produce larger responses and more consistent test results compared with the reduced friction surface. Additionally, there were more observations of instability and larger differences between ESC enabled and disabled test states on the high friction test surface. No instabilities were observed on the low friction surface, but the motorcoaches exhibited understeering characteristics on this surface. Tests were desired at higher entrance speeds on reduced friction surfaces but were limited by the physical area of both the approach route and the wet Jennite test surface.

Comparing the LLVW and GPOW loading conditions, testing observations indicated that these motorcoaches were not significantly adjusting pre-established activation thresholds based on changes to mass (adding passengers). This was observed by looking at the change in lateral acceleration at ESC activation between loading conditions for the SIS tests, shown in Table 5.1. For comparison, unloaded tractors were observed to have ESC activations between 0.40-0.53 g of lateral acceleration, while in the loaded condition the systems activated between 0.27-0.38 g.

Table 5.1. Lateral Acceleration at ESC activation in the SIS test maneuver.

Vehicle	Condition	Lateral Acceleration (g)	
		LLVW	GPOW
MCI #1	ESC Enabled	0.339	0.328
Prevost	ESC Enabled	0.299	0.279
MCI #2	ESC Enabled	0.326	0.313

These ESC systems were observed to use engine torque reductions combined with minor amounts of foundation braking to reduce the lateral dynamics in the SIS and CR maneuvers conducted on dry high friction asphalt for both load conditions.

For the RSM, SWD and HSWD maneuvers, ESC used moderate and heavy foundation braking to increase stability. From these maneuvers, data from the RSM and 0.5Hz SWD (1.0 second dwell) were used to investigate measures of performance that

indicated the roll and yaw responses were reduced such that the stability of the motorcoaches was increased.

5.2 Measures of Performance

The motorcoach ESC systems reduced engine torque in the SIS maneuvers. The engine torque and driver requested torque signals were shown to separate at the point ESC commanded an engine torque reduction. Data analysis indicated that for the vehicle to continue to respond in a stable manner to the increasing steer input, the speed input would have to be reduced and was correlated to the engine torque reduction event. These measures were capable of showing the systems' ability to manage stability of the vehicles as they approached the lateral limits in a curve in a gradual manner.

The reductions observed in LAR from the RSM test data show that the ESC systems were also able to mitigate roll instabilities in a curve where the limits were approached in a more dynamic manner as compared to the SIS. Figure 5.1 shows that RSM LAR was able to discriminate ESC enabled from disabled testing conditions and states of stability. Without ESC, LAR remained near or above 100 percent for MCI #1, Prevost, and MCI #2 and wheel lift is observed at 37, 39, and 35 mph. With ESC enabled at 40 mph, LAR was reduced and wheel lift was no longer observed at RSM speeds less than 48 mph.

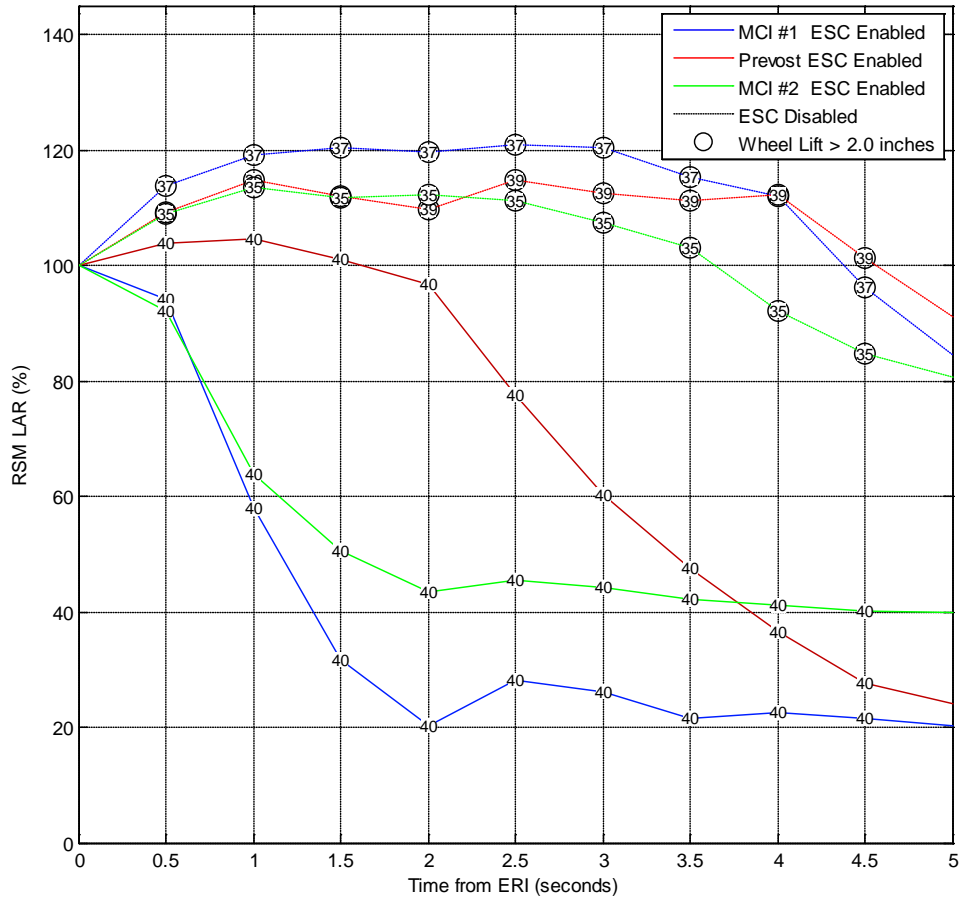


Figure 5.1. RSM LAR after ERI event for all three motorcoaches with ESC enabled at 40 mph (solid lines) and disabled (dotted lines) at 35 – 39 mph with the GPOW load condition

LAR and YRR measures of performance that were developed from SWD data were observed to discriminate tests with and without ESC technology for the evaluated motorcoaches. The measures show ESC system's ability to mitigate loss of roll and yaw control situations by reductions to the roll and yaw responses of the motorcoaches.

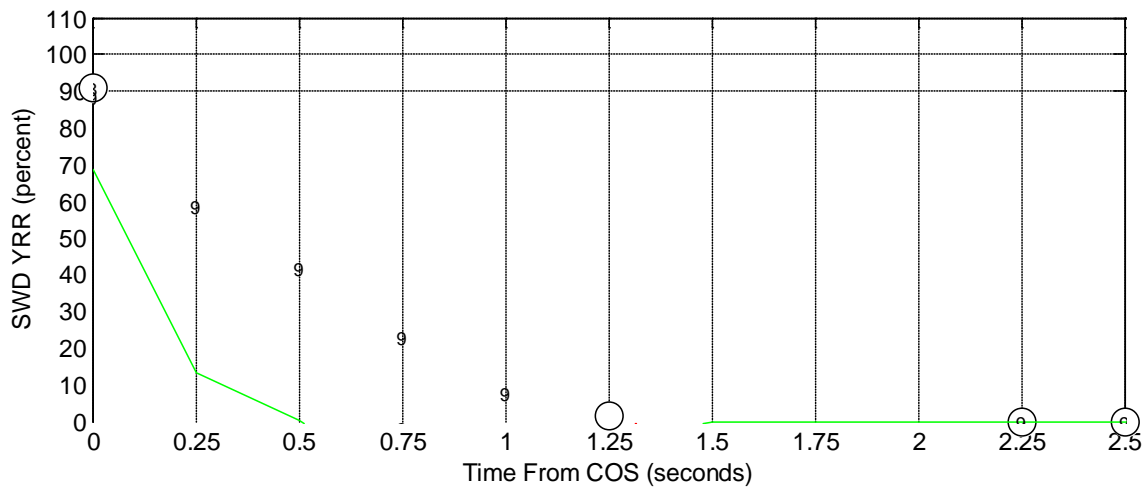
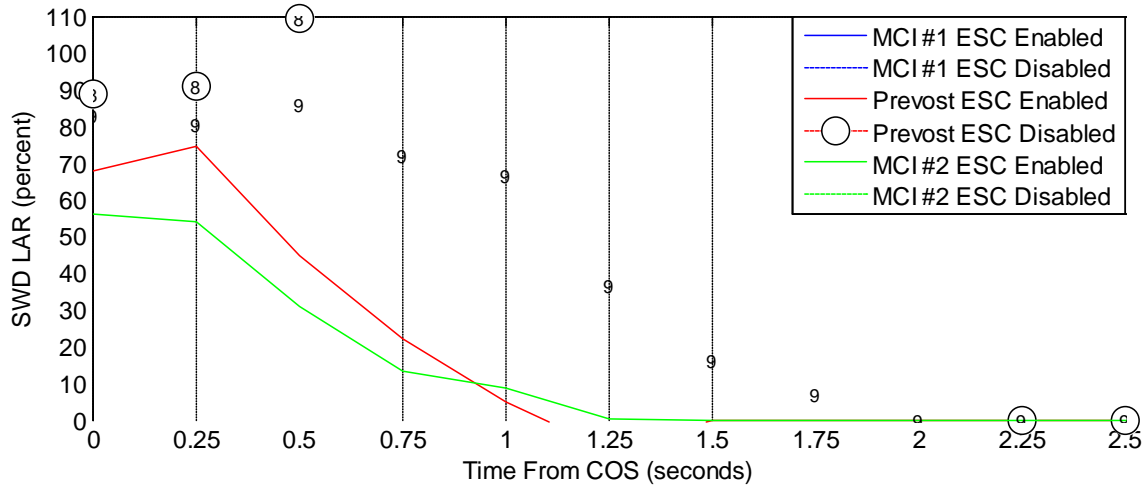


Figure 5.2. SWD LAR and YRR after COS event for all three motorcoaches with ESC enabled with the 90 percent steering scalar (solid lines denoted with “9”) and disabled tests with 80 – 90 percent steering scalars (dotted lines denoted with “8” or “9”) with the GPOW load condition.

Though these SWD LAR measures showed similar results to the tractors, the YRR data for motorcoaches did not have the same separation for ESC disabled tests as found with the tractor tests (this was expected since the motorcoaches were observed to be yaw stable in SWD tests). Also, the lateral responsiveness measure showed that the motorcoaches produced less lateral displacement for the same inputs. This was observed with the system enabled and disabled, indicating that the motorcoaches are naturally less responsive due to their physical characteristics and not from ESC intervention, shown in Figure 5.3.

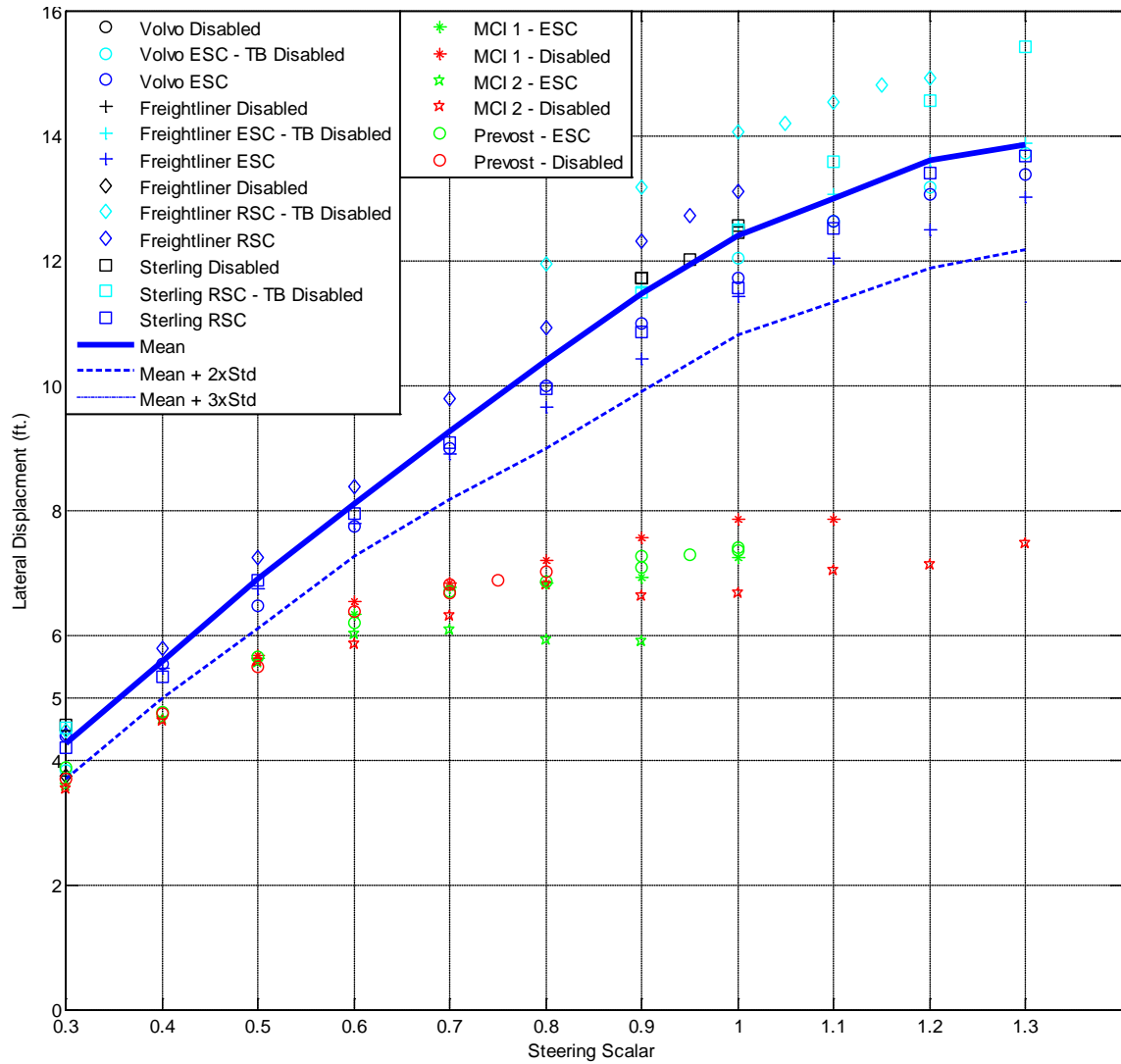


Figure 5.3. 0.5Hz SWD (1.0 second dwell) lateral displacement of truck-tractors and motorcoaches with and without stability control.

REFERENCES

- [1] Barickman, Frank S., Elsasser, Devin, Albrecht, Heath, Church, Jason, Xu, Guogang, "Tractor Semitrailer Stability Objective Performance Test Research – Roll Stability." NHTSA Technical Report, DOT HS 811 467, May 2011
- [2] Barickman, Frank S., Elsasser, Devin H., Albrecht, Heath, Church, Jason, Xu, Guogang, "NHTSA's Class 8 Truck-Tractor Stability Control Test Track Effectiveness." Proceedings of the 21st International Technical Conference on the Enhanced Safety of Vehicles, Paper No. 09-0552, June 2009
- [3] Barickman, Frank S., Elsasser, Devin, Albrecht, Heath, Church, Jason, Xu, Guogang, "Tractor Semitrailer Stability Objective Performance Test Research – Yaw Stability." NHTSA Technical Report, 2012
- [4] U.S. Department of Transportation, "U.S. Department of Transportation Motorcoach Safety Action Plan", DOT HS 811 177, November 2009
- [5] Analysis Division, Federal Motor Carrier Safety Administration, "Large Truck and Bus Crash Facts 2007." FMCSA-RTA-09-029, January 2009
- [6] Ervin, R., Winkler, C., Fancher, P., Hagan, M., Krishnaswami, V., Zhang, H., Bogard, S. "Two Active Systems For Enhancing Dynamic Stability In Heavy Truck Operations.", University of Michigan Highway Research Institute, Report No. UMTRI-98-39, July 1998
- [7] MacAdam, C., Hagan, M., Fancher, P., Winkler, C., Ervin, R., Zhou, J., Bogard, S., "Rearward Amplification Suppression (RAMS)", University of Michigan Highway Research Institute, Report No. UMTRI-2000-47, December 2000
- [8] Winkler, C., Sullivan, J., Bogard, S., Goodsell, R. Hagan, M., "Field Operational Test of the Freightliner/Meritor WABCO Roll Stability Advisor and Control at Praxair.", University of Michigan Highway Research Institute, Report No. UMTRI-2002-24, September 2002
- [9] "Final Report: Evaluation of the Freightliner Intelligent Vehicle Initiative Field Operational Test.", Batelle, September 2003
- [10] Ervin, R., Nisonger, R., Mallikarjunarao, Gillespie, T. "The Yaw Stability of Tractor Semitrailers During Cornering – Technical Summary Report.", University of Michigan Highway Research Institute, Report No. UM-HSRI-79-21-1, June 1979.
- [11] Woodrooffe, John, Blower, Daniel, Gordon, Timothy, Green, Paul E., Liu, Brad, Sweatman, Peter, "Safety Benefits of Stability Control Systems for Tractor Semitrailers" NHTSA Technical Report, DOT HS 811 205, October 2009.
- [12] U.S. Department of Transportation, "Laboratory Test Procedure for FMVSS 126, Electronic Stability Control Systems." TP-126-00, April 2007
- [13] Society of Automotive Engineers J1939, Surface Vehicle Standard, "Recommended Practice for Control and Communications Network for On-Highway Equipment." September 2000

- [14] Society of Automotive Engineers J1708 OCT2008, Surface Vehicle Recommended Practice, "Serial Data Communications Between Microcomputer Systems in Heavy-Duty Vehicle Applications." October 2008
- [15] Heitzman, E.J., and Heitzman, E.F., "A Programmable Steering Machine for Vehicle Handling Tests." SAE Paper 971057, SAE SP-1228, February 1997
- [16] Heitzman, E.J., and Heitzman, E.F., "The ATI Programmable Steering Machine." Automotive Testing, Inc. Technical Report, March 1997
- [17] National Highway Traffic Safety Administration, "Code of Federal Regulations, Title 49, Part 571, 571.121 Standard No. 121; Air Brake Systems." August 2009
- [18] "ASTM E1337 - 90(2008) Standard Test Method for Determining Longitudinal Peak Braking Coefficient of Paved Surfaces Using Standard Reference Test Tire." ASTM Volume 04.03 Road and Paving Materials; Vehicle-Pavement Systems, 2008
- [19] "ASTM E1136 - 93(2003) Standard Specification for A Radial Standard Reference Test Tire." ASTM Volume 09.02 Rubber Products, Industrial -- Specifications and Related Test Methods; Gaskets; Tires, 2003
- [20] "ASTM E274 - 06 Standard Test Method for Skid Resistance of Paved Surfaces Using a Full-Scale Tire." ASTM Volume 04.03 Road and Paving Materials; Vehicle-Pavement Systems, 2006
- [21] "ASTM E501 - 08 Standard Specification for Standard Rib Tire for Pavement Skid-Resistance Tests." ASTM Volume 04.03 Road and Paving Materials; Vehicle-Pavement Systems, 2008
- [22] National Highway Traffic Safety Administration, "Code of Federal Regulations, Title 49, Part 571, 571.126 Standard No. 126; Electronic stability control systems." September 2008
- [23] Society of Automotive Engineers J266, Surface Vehicle Recommended Practice, "Steady-State Directional Control Test Procedures for Passenger Cars and Light Trucks." January 1996
- [24] Forkenbrock, Garrick J., Garrott, W. Riley, Heitz, Mark, O'Harra, Brian C., "A Comprehensive Experimental Examination of Test Maneuvers That May Induce On-Road, Untripped Light Vehicle Rollover – Phase IV of NHTSA's Light Vehicle Rollover Research Program." NHTSA Technical Report, DOT HS 809 513, October 2002.
- [25] "Consumer Information; New Car Assessment Program; Rollover Resistance", Federal Register, Vol. 68, No. 198, October 14, 2003, Docket No. NHTSA-2001-9663; Notice 3, Page 59250.
- [26] Forkenbrock, Garrick J., Elsasser, Devin, O'Harra, Bryan C., Jones, Robert E., "Development of Criteria for Electronic Stability Control Performance Evaluation." NHTSA Technical Report, DOT HS 809 974, January 2005.
- [27] "Federal Motor Vehicle Safety Standards; Air Brake Systems", Federal Register, Vol. 74, No. 142, July 27, 2009, Docket No. NHTSA-2009-0083, Page 37122.

APPENDIX A

A. Testing Procedures

Vehicle Pre-Test Conditioning

1. Mass Estimation Drive Cycle
 - a. Accelerate to 40 mph
 - b. Decelerate at 0.3-0.4g to a stop
2. Ignition cycle will require new mass estimation drive cycle
3. Tire warm-up
Two circles to the left and two circles to the right at a speed that result in 0.1 G lateral acceleration. (Approximate 150 ft radius at 20 MPH.)
4. Brake warm-up
 - a. Use 40-20 mph snubs (0.3g decel.) to bring motorcoach brake temperatures to a minimum of 150-200 degrees [FMVSS 121]

SIS Characterization Maneuver

1. Perform Vehicle Pre-Test Conditioning
2. Perform SIS
 - a. Test (3 tests in each direction – LLVW or GPOW)
 - b. Speed = 30 mph
 - c. Steering = steering increases from 0 to δ^{SIS} @ 13.5 deg/sec.
3. Test Ends IF
 - a. Steering magnitude = δ^{SIS} deg
 - b. Motorcoach wheel lift is observed
 - c. Yaw angle change exceeds 90 degrees
4. Calculate RSM δ^{Test}

NOTE; Steering magnitude, δ^{SIS} , is selected on a per test vehicle basis such that the steering continues to increase for at least 5 seconds after ESC activation has been detected. For Example, if ESC activation is detected at 260 degrees, then $\delta^{SIS} = 260$ degrees + 13.5 deg/sec x 5.0 sec = ~328 degrees.

RSM Performance Maneuver

1. Perform Vehicle Pre-Test Conditioning
2. Perform RSM
 - a. steering magnitude = δ^{Test}
 - b. steering rate = 175 deg/sec
 - c. speed start= 20 mph

- d. At maneuver start: Drop throttle and clutch in. (Vehicles with automatic transmissions were set to neutral prior to initiating the maneuver)
 - e. Maneuver is triggered automatically by speed passing through the start speed trigger of the controller (simple comparator).
 3. Continue testing incrementing speed for each test @ 2 MPH until one of the following conditions occur.
 - a. Speed = 50 MPH – Test Complete
 - b. Motorcoach wheel lift occurs
 - c. Yaw angle change exceeds 90 degrees
 - d. If wheel lift is observed – jump to step 4. - The result will be considered wheel lift if it is obvious that any of the motorcoach wheels have come off the ground and/or the outriggers hit the ground during any part of the test.
 - e. Test Driver feels its unsafe to continue
 4. If wheel lift occurred, test should be decremented by 2 MPH.
 - a. Repeat test at major wheel lift speed – 2 MPH.
 - b. Repeat test at major wheel lift speed – 1 MPH.
 - c. Repeat test at major wheel lift speed
 - d. If wheel lift has not occurred, continue to increment speed until wheel lift occurs or test speed reaches 50 MPH.
 - e. Test is complete when wheel lift occurs or test speed reaches 50 MPH (jump to step 6).
 5. Test is complete when wheel lift has occurred 2 times or test speed reaches 50 MPH.
 6. Test Complete

Note: All tests are conducted to the left. Test drivers should be sensitive to this issue and make right turns when returning to the test start point so as not to bias any learning algorithms that a system may have. The number of left turns and right turns should be balanced as much as possible.

SWD and HSWD Test Procedure

- 1) Perform Vehicle Pre-Test Conditioning
- 2) Test (per each load condition)
 - a) steering magnitude start = $X\% * \delta^{Test}$ [$X_{start} = 30\%$]
 - b) steering frequency = 0.3, 0.5, or 0.7 Hz
 - c) speed = xx mph [this may increase depending on initial test results]
 - d) At maneuver start: Drop throttle and clutch in. (Vehicles with automatic transmissions were set to neutral prior to initiating the maneuver)
 - e) Maneuver is triggered automatically by speed passing through the start speed trigger of the controller (simple comparator).
- 3) Continue testing incrementing amplitude up by increasing X by 10% increments until one of the following conditions occur.
 - a) Amplitude = $130\% * \delta^{Test}$ degrees – Test Complete

- b) Wheel lift or yaw angle change greater than 90 degrees occurs
 - i) If wheel lift was observed jump to step 4. - The result will be considered wheel lift if any of the motorcoach wheels are observed to have come off the ground and/or the outriggers hit the ground during any part of the test or yaw angle change exceeded 90 degrees.
 - c) Test Driver feels its unsafe to continue
- 4) If wheel lift or yaw angle change greater than 90 degrees occurred, steering magnitude should be decremented by $(X-10\%)*\delta^{Test}$ degrees.
 - a) Repeat test at $-(X-10\%)*\delta^{Test}$ degrees.
 - b) Repeat test at $-(X-5\%)*\delta^{Test}$ degrees.
 - c) Repeat test at $-(X)*\delta^{Test}$ degrees
 - d) If wheel lift or yaw angle change greater than 90 degrees has not occurred, continue to increment steering $(X)*\delta^{Test}$ up.
 - e) Test is complete when wheel lift or yaw angle change greater than 90 degrees occurs (jump step 6).
- 5) Test is complete when wheel lift or yaw angle change greater than 90 degrees has occurred 2 times or condition 3a. has been met.
- 6) Test Complete

Note: For series in which tests are conducted in a single direction, test drivers should be sensitive to this issue and make opposite turns when returning to the test start point so as not to bias any learning algorithms that a system may have. The number of left turns and right turns should be balanced as much as possible.

RWD Test Procedure

- 1) 500 ft. Steering Calibration/Characterization
 - a) Perform on wet Jennite at prescribed load condition
 - b) In order to determine a speed and steering profile that will result in the desired vehicle response on a given surface, it is necessary to characterize the test vehicle. Performance of the maneuver described below will provide the characteristic information that is used to normalize the test maneuver to the vehicle and surface conditions.
 - c) Enter the Jennite following the 500 ft. radius curve, at a speed of approximately 20 mph, and drive through the entire curve. Repeat the run, adjusting the speed until the vehicle is traveling at the maximum speed possible while remaining in the marked lane, not to exceed 35 mph.
 - d) The following are defined based on the test results:
 - i) V_{dt} = Drive through speed
 - ii) δ_{dt} = Drive through steering angle
- 2) Ramp with Dwell - Yaw Stability Maneuver
 - a) Perform on wet Jennite at prescribed load condition

- b) The steering input can be described as a ramp with dwell that has amplitude directly related to the steering input required for the vehicle to negotiate the Jennite curve at the drive-through speed.
- c) The steering profile is constructed from the following steering amplitudes:
 - i) δ_{dt} is the drive-through steering input determined during the normalization procedure.
 - ii) δ_0 is defined as the drive-through steering input, δ_{dt} , rounded to the nearest 90 degree increment (e.g., 110 degrees is decreased to 90 degrees). The sole exception is: For all cases when δ_{dt} is less than 90 degrees, δ_0 is defined as 90 degrees.
 - iii) δ_m is defined as the maximum amplitude of the steering input during the maneuver. δ_m is equal to δ_0 multiplied by a scaling factor, K . K is an integer value ranging from 2 to 6.
- d) The steering profile is defined as:
 - i) $t < 0$: $\delta = \delta_{dt}$
 - ii) $t = 0$ to $t = 1$: Ramp from $\delta = \delta_{dt}$ to $\delta = K\delta_0$
 - iii) $t = 1$ to $t = 4$: $\delta = K\delta_0$
 - iv) $t = 4$ to $t = 5$: Ramp from $\delta = \delta_0$ to $\delta = 0$
- e) Test Maneuver
 - i) The speed at which the maneuver is conducted is at least 0.9 times the drive through speed, or 35 mph, whichever is less.
 - ii) Maneuver speed = $V_m \geq (0.9)(V_{dt})$ Drive the vehicle on the Jennite curve at a speed of V_m , using either constant throttle or cruise control to maintain the vehicle speed.
 - iii) For the first test run, execute the steering profile using a steering amplitude scaling factor, K , of 2. Maintain constant throttle or use cruise control.
 - iv) Repeat the maneuver using increasing values of K .

APPENDIX B

B. Motorcoach Parameters

AP Table 1. General Information

	Model Year	Model	VIN	Date of Manufacture	ESC Supplier
MCI #1	2007	D4500	1M8PDMEA77P05830	Feb 2007	Meritor WABCO ESC
Prevost	2009	H3	2PCH334979C711317	MAY 2008	Bendix ESC
MCI #2	2007	D4500	1M8PDMHA97P057713	Dec 2006	Meritor WABCO ESC

AP Table 2. Tire Specifications

	Tire Size	Tire Brand	Tire Model (Front, Rear)	Tire Pressure (psi)
MCI #1	315/80R22.5 J	Michelin	XZA	front_125,rear_85,inter_100
Prevost	315/80R22.5 J			front_120,rear_90,inter_100
MCI #2	315/80R22.5 J	Michelin	XZA	front_125,rear_85,inter_100

AP Table 3. GAWRs and GVWRs

(All weights in pounds)	GAWR Steer Axle	GAWR Drive Axle	GAWR Rear Tag Axle	GVWR
MCI #1	16,000	22,500	10,000	48,000
Prevost	16,500	22,500	14,000	53,000
MCI #2	16,000	22,500	12,000	48,000

AP Table 4. Dimensions

(All dimensions in inches)	Total Length	Steer Axle to Front Drive Axle	Drive Axle to Tag Axle	Wheelbase	Front Track Width	Drive Track Width (Center of Duals)	Tag Axle Track
MCI #1	545	317	48	317	87	76	86
Prevost	547	317	48	317	--	--	--
MCI #2	545	318	47	318	86	76	86

AP Table 5. CG Positions (LLVW Load Condition)

(All dimensions in inches)	Longitudinal CG (from front axle, positive toward rear)	Lateral CG (from centerline, positive to the right)	Vertical CG (from ground plane)
MCI #1	237	0.5	49.5
Prevost	240	0.0	48.0
MCI #2	232	-0.3	50.0

APPENDIX C

C. Instrumentation and Safety Equipment

Data Acquisition: In-vehicle data acquisition systems comprised of ruggedized industrial computers, recorded outputs from the previously mentioned sensors during the conduct of test maneuvers.

The computers employed the DAS-64 data acquisition software developed by VRTC. Analog Devices Inc. 3B series signal conditioners were used to condition data signals from all transducers listed in Table 2.2. Measurement Computing Corporation PCI-DAS6402/16 boards digitized analog signals at a collective rate of 200 kHz. The test drivers armed the trigger for data collection prior to each test; however, actual data collection was automatically initiated the instant the steering machine began to execute its commanded inputs (i.e., at the desired test speed). To provide the initial conditions just prior to execution of each test maneuver, a short period of pre-trigger data were recorded.

A second data acquisition system ADERS (Analog Digital Event Recording System) recorded J1939 signals from the vehicle's bus. Table 2.3 lists the signals recorded.

Signal Conditioning: Signal conditioning consisted of amplification, anti-alias filtering, and digitizing. Amplifier gains were selected to maximize the signal-to-noise ratio of the digitized data. Signals are analog filtered using a 20 Hz, 2 pole Butterworth filter.

Steering Wheel Angle: Steering wheel angle was recorded from an optical encoder that is part of the programmable steering machine.

Brake Treadle Application: Brake treadle was measured with a normally open switch mounted underneath the dash making contact with the brake pedal. It was important to monitor the driver's braking activity during testing. If the driver applied the brake during the maneuver the test was invalid.

Throttle Position: Throttle position was measured directly from the vehicle's OE throttle position sensor. The signal is buffered with an instrumentation amplifier so as not to interfere with its normal operation. In some vehicles the throttle position had be recorded from the vehicle bus. It was important to monitor the driver's throttle position activity during testing. If the driver was requesting throttle during certian maneuvers the test was invalid.

Inertial Sensing System: A multi-axis inertial sensing system was used to measure accelerations and roll, pitch, and yaw angular rates. The system was placed near the vehicle's CG so as to minimize roll, pitch, and yaw effects. Since it was not possible to position the accelerometers precisely at the vehicle's CG for each loading condition, sensor outputs were corrected during post-processing of the data to translate the motion of the vehicle at the measured location to that which occurred at the actual CG.

The sensing system did not provide inertial stabilization of its accelerometers. Lateral acceleration was also corrected for vehicle roll angle during post processing using ride height data.

Frame Rail Height: An infrared distance measurement system was used to collect left and right side vehicle ride heights for the purpose of calculating vehicle roll angle. Vehicle roll angle was computed with data output from the two sensors, used in conjunction with roll rate data measured by the multi-axis inertial sensing system.

Rear Axle Height: An infrared distance measurement system was used to collect left and right side axle ride heights for the purpose of calculating vehicle wheel lift. Wheel lift for each motorcoach was defined in the lab by doing a static calibration.

Vehicle Speed: Vehicle speed (i.e., longitudinal velocity) was measured with a non-contact speed sensor mounted above the roof of each vehicle. Sensor outputs were transmitted to the data acquisition system, dashboard display unit, and to the steering machine. The steering machine can use vehicle speed to activate.

Brake Pressures: Brake pressures were measured at each brake chamber. The data could be evaluated to determine which brakes the motorcoach ESC systems were applying during ESC activation.

J1939 Communication Bus: See Table 2.3.

Programmable Steering Machine: A programmable steering machine was used to provide steering inputs for all ESC test maneuvers. Descriptions of the steering machine, including features and technical specifications, have been previously documented and are available in [15], [16].

Safety Equipment: Before the conduct of any test, safety equipment was installed on each motorcoach. These supporting safety devices may not be necessary to safely conduct these tests, however, given the exploratory nature and potential test severity it was decided to err on the side of caution.

Safety Outriggers: Low inertia outriggers were developed for this testing. The outrigger system adds approximately 1500 lbs to the vehicle but was designed to minimize roll and yaw inertias. When deployed, the outriggers span 315 inches across from wheel to wheel. Further information and detailed specifications of the outriggers can be obtained in, DOT HS 811 289 and in Appendix 0.



AP Figure 1. Outriggers.

Driver Restraint System: The driver restraint system consists of a racing seat and a 5 point restraint harness. The racing seat allowed the harness to be properly installed in the cab without the risk of compressing the driver in the event of a rollover. Additionally, the racing seat provided stability for the driver when conducting maneuvers that generated high lateral forces.



AP Figure 2. Driver restraint system.

APPENDIX D

D. Load Condition Information

Two load conditions were used for the work described in this report. The following sections provide descriptions of the load conditions and the rationale behind their selection.

LLVW (Lightly Loaded Vehicle Weight):

The LLVW load condition was comprised of the test vehicle, a driver, instrumentation (including a programmable steering machine), and safety equipment (aftermarket seat, five-point safety harness, and outriggers). Each vehicle’s fuel tank was at least three-quarters full.

AP Table 6. LLVW Load Condition Weights

(All weights in pounds)	Steer Axle Total	Drive Position Total	Tag Position Total	Total Weight
MCI #1	11828	19216	9920	40964
Prevost	10860	16840	10610	38310
MCI #2	11410	16950	11370	39730

GPOW Load Condition:

GPOW load condition includes all equipment and instrumentation from LLVW condition plus 175 lb water dummies to simulate passengers. Simulated passengers were added until the measured weight was at the placarded GVWR. AP Figure 3 shows a photograph of the water dummies placed in the passenger seats of a motorcoach.

AP Table 7. GPOW Load Condition Weights

(All weights in pounds)	Steer Axle Total	Drive Position Total	Tag Position Total	Total Combination Weight
MCI #1	13730	22560	11540	47830
Prevost	13830	20450	12900	47180
MCI #2	13700	20630	13720	48050



AP Figure 3. 175 lb. water Dummies were used to ballast the motorcoaches to the GPOW load condition.

APPENDIX E

E. Safety Outrigger Information and Drawings

To provide an effective safety margin during severe dynamic roll stability testing, outriggers for Class 8 motorcoaches were designed and fabricated as a safety device by the Vehicle Research and Test Center (VRTC). AP Table 8 contains NHTSA outrigger design specifications. From left to right, the table shows a design length of 315 inches. Next it shows the load capacity of the outrigger and the minimum safety factor associated with that load capacity. It then shows the design incorporated foldable outriggers and height adjustable mounts.

AP Table 8. NHTSA Outrigger Specifications

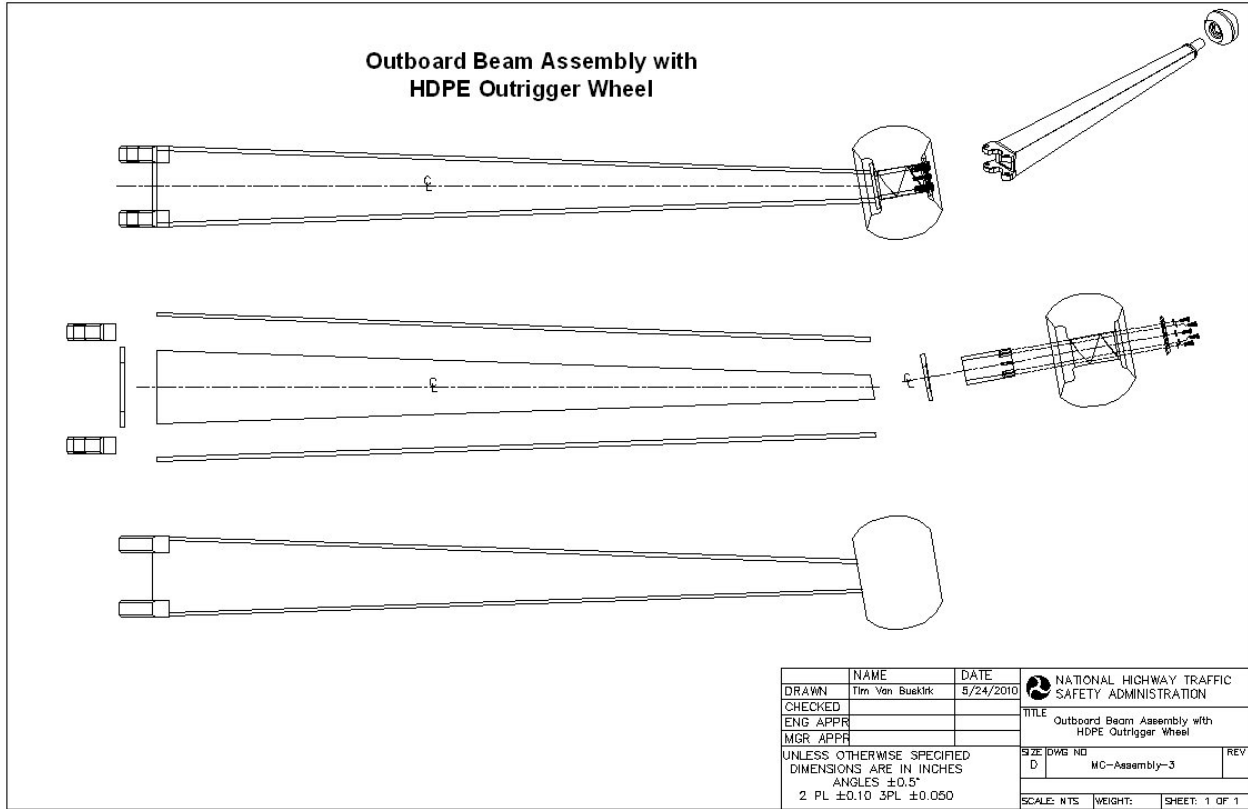
Length (in)	Load Rating (lbs)	Minimum Safety Factor	Foldable	Height Adjustable
315	9,000	3	Yes	Yes

Mounting frames and brackets were custom fabricated to fit a Prevost motorcoach and a Motor Coach Industries (MCI) motorcoach (i.e., MCI #2). While the mounting frames and brackets for the Prevost motorcoach were designed and built in-house, the mounting frames welded to the MCI motorcoach were supplied by MCI. High Density Polyethylene (HDPE) wheels located at the ends of the outboard beams provided support and a wear surface to help prevent trips and rollover during limit tests. Each outrigger outboard beam was fabricated from the parts listed in AP Table 9 which also includes the outrigger wheel and wheel retainer to make up the outboard outrigger assembly.

AP Table 9. Outrigger Outboard Beam Assembly Parts

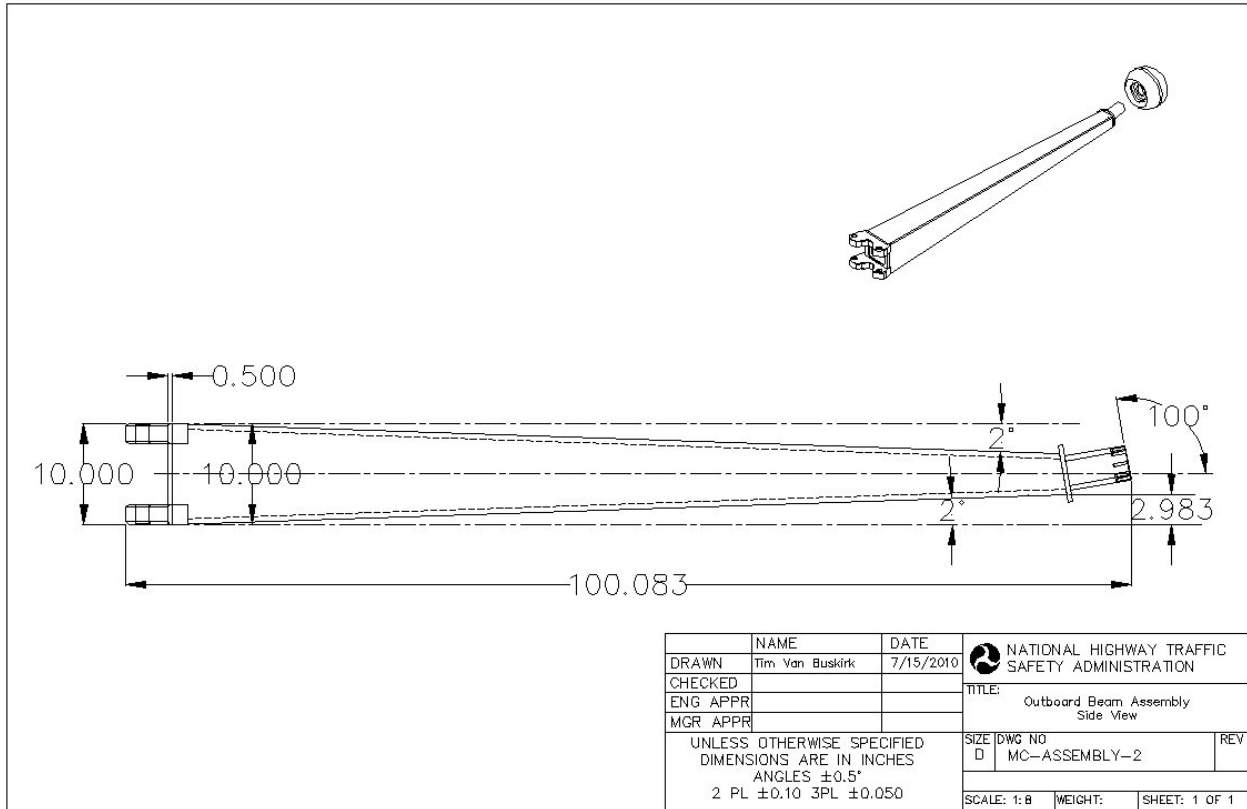
Part Name	Material	Quantity	Drawing Number
Top Plate	A514 Steel Plate, 0.50 inch thickness	1	OBC-1
Bottom Plate	A514 Steel Plate, 0.50 inch thickness	1	OBC-2
Side Plate	A514 Steel Plate, 0.25 inch thickness	2	OBC-3
Base Plate	A514 Steel Plate, 0.50 inch thickness	1	OBC-4
End Plate	A514 Steel Plate, 0.50 inch thickness	1	OBC-5
Axle	ASTM Sch. A53 pipe, 0.50 inch wall thickness	1	OBC-6
Outrigger Wheel	HDPE 14 inch round	1	OBC-7
Wheel Retainer	6061-T6 Aluminum, 0.50 inch thick	1	OBC-8

The exploded drawing of the outboard outrigger beam assembly is shown below in AP Figure 4. Two outboard outrigger beam assemblies are required for a vehicle set. All of the components of the outrigger outboard beam are shown in the assembly drawing in AP Figure 4. The middle figure in the drawing depicts the exploded assembly. The top figure is a view of the parts assembled, and the bottom figure is the assembled view with no hidden lines.



AP Figure 4. Outboard Outrigger Beam Assembly Drawing – Exploded View.

The outboard beam is made of A514 steel plates and A53 steel pipe (axle). It is a tapered hollow beam design that is welded together to get a decreasing weight/linear foot towards the axle end of the outrigger. Parts with thicknesses of 0.75 inch and smaller were laser cut. Parts with thicknesses greater than 0.75 inches were water cut and then machined to final dimensions. A side-view dimensional drawing for the outboard beam follows in AP Figure 5.



AP Figure 5. Dimensional Outrigger Assembly Drawing - Side-view.

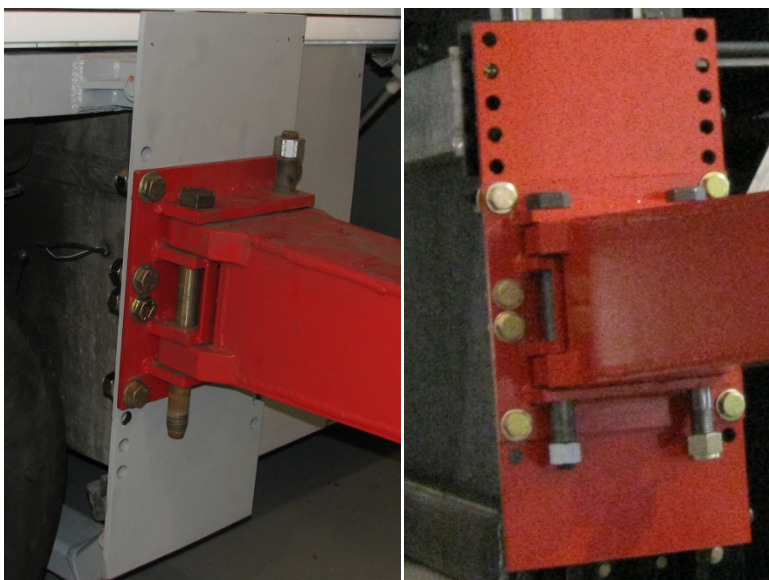
Engineering drawings and pictures from fabrication of the outboard beam can be found in DOT HS 811 289. AP Figure 6 shows the completed outboard outrigger beam assembly in a photograph viewed from the driver's side front towards the rear of the motorcoach. The outrigger was in the folded position installed on a motorcoach test vehicle.



AP Figure 6. Completed outrigger assembly installed on a motorcoach.

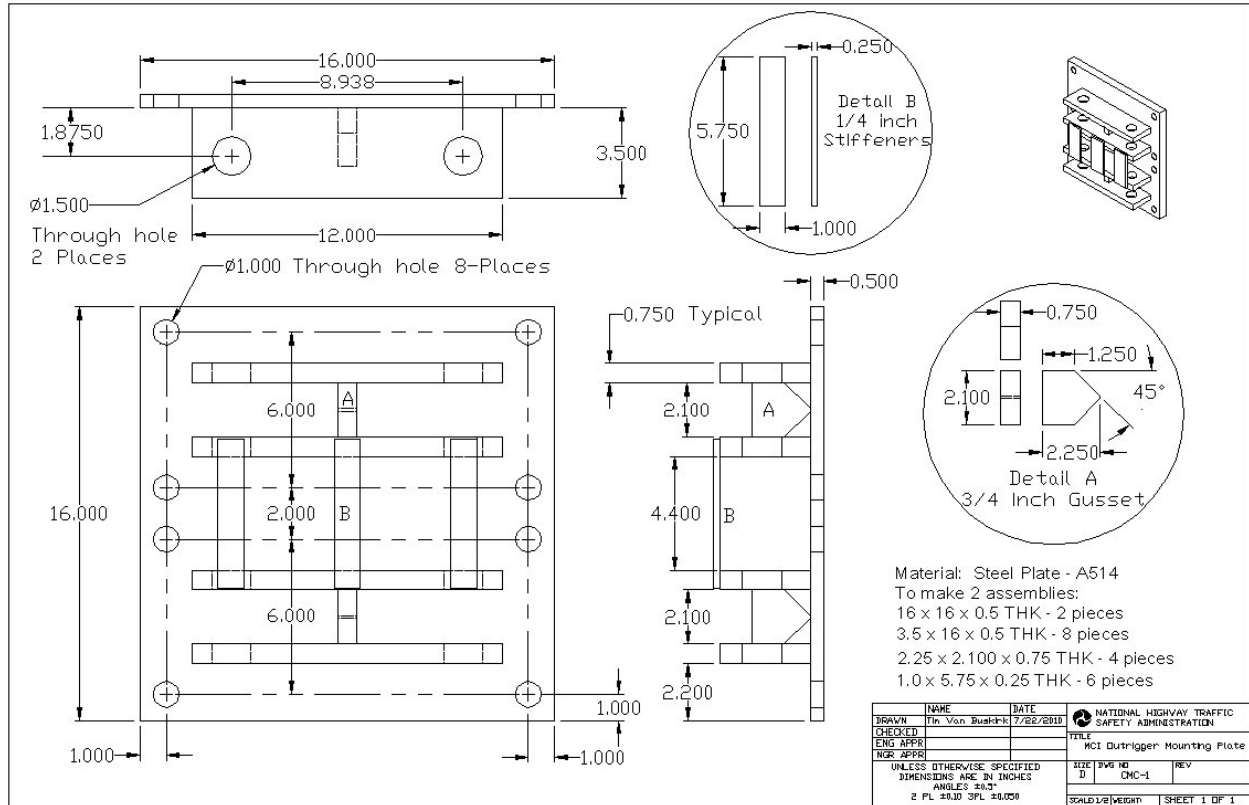
Mounting the Outriggers

The mounting framework for the Prevost motorcoach was designed and fabricated in-house. The mounting framework and outrigger adjustment plate for the MCI motorcoach were supplied by MCI to specifications for the outboard outrigger assembly. The outrigger beam mounting plate, onto which the outrigger beam was bolted, was a common component used in the outrigger installation on each motorcoach. The adjustment plate was similar in design for each vehicle, but in each case was adapted to fit the specific mounting framework. This allowed the outboard outrigger beam assembly to be installed on either motorcoach mounting framework. The adjustment plate was bolted to the motorcoach outrigger mounting framework with SAE grade 8 bolts at top and bottom. The two sets of one inch through holes on the adjustment plate allowed for vertical height adjustment of the outrigger beam when bolted to the outrigger mounting plate. AP Figure 7 contains photographs of the MCI installation (left) and of the Prevost installation (right) using these components.



AP Figure 7. Photographs of adjustment plate and mounting plate in the MCI installation (left photo) and in the Prevost installation (right photo).

The outrigger beam mounting plate was fabricated from A514 steel plate. Four 0.75 inch thick plates were welded to a 16 inch square plate, 0.50 inch in thickness to form the mounting plate half of the outrigger hinge-set. Two 1.50 inch holes were drilled in these plates to align with the 1.50 inch holes on the outrigger beam hinge brackets. Two 0.75 inch thick steel gussets and three 0.25 inch thick steel stiffeners were added to help keep the plates in alignment. Two outrigger beam mounting plates were needed for each vehicle set of outriggers. AP Figure 8 contains a dimensional drawing of this component. The photograph in AP Figure 9 shows the outrigger mounting plate during fabrication. A total of two outrigger mounting plates were required for each outrigger set.

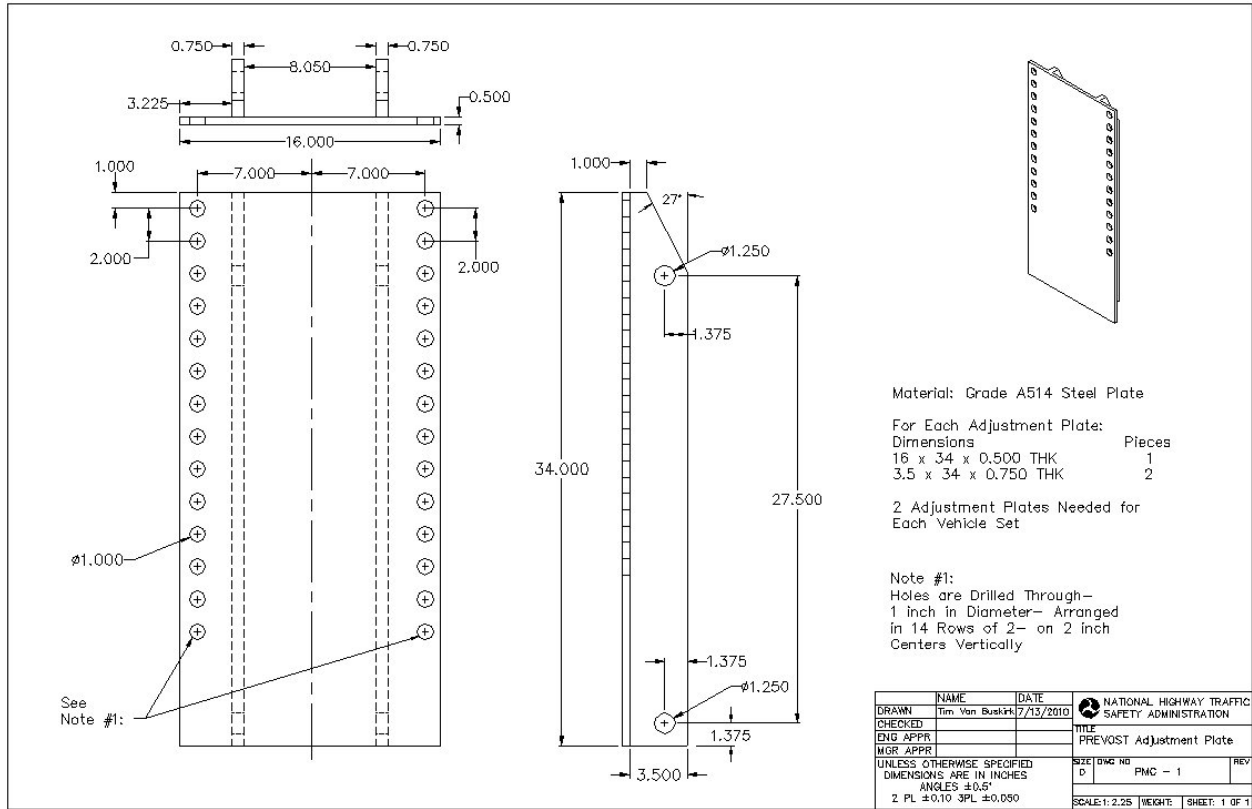


AP Figure 8. Dimensional drawing of the outrigger mounting plate.



AP Figure 9. Photograph of the outrigger mounting plate during fabrication.

The Prevost adjustment plate was fabricated from A514 steel plate. The 16 x 34 inch plate was 0.50 inch thick and the two vertical mounting flanges were 0.75 inch thick. A total of two adjustment plates were required for each vehicle outrigger set. The location of the holes and the relative position of the three parts that make up this component are shown in the dimensional drawing represented in AP Figure 10.



AP Figure 10. Dimensioned drawing for the Prevost adjustment plate.

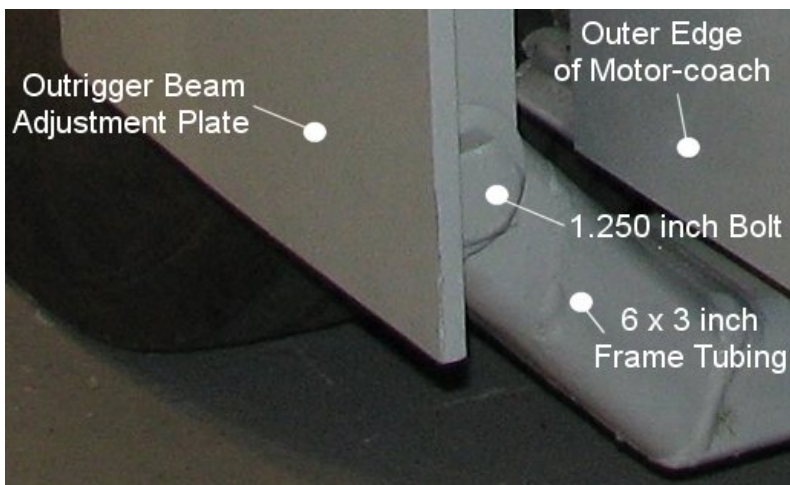
MCI Fabrication of Mounting Framework

To mount the NHTSA outriggers to the MCI motorcoach, MCI supplied a mounting framework that was integrated and welded into the main chassis of the leased motorcoach. The integrated framework consisted of three main components: a lower under-slung frame assembly, and an upper left side and an upper right side mounting framework. The under-slung frame assembly was fabricated and secured between clamping plates that were welded to the end of the motorcoach's jacking points on vertical suspension struts. Two bottom plates were attached with SAE grade 8 bolts, thus securing the tubing frame in position under the vehicle as shown in the photograph in AP Figure 11.



AP Figure 11. Photograph of the under-slung (lower) mounting frame installed on the MCI motorcoach.

The lower frame assembly consisted of two lower mounting frame tubes and a tube center joiner. The lower outer frame members were fabricated from 6 x 3 inch A500 steel tubing that had a 0.50 inch wall thickness. The outboard ends of the 6 inch x 3 inch frame angled up 60 degrees at the point where the steel tube cleared the outer edge of the motorcoach. 1.25 inch holes were drilled through the width of the 6 x 3 inch tube frame. The adjustment plate then could be mounted to the tube frame member with 1-1/4 – 7 UNC grade 8 bolts as shown in the photograph in AP Figure 12.



AP Figure 12. Photograph of the attachment of the adjustment plate to the lower frame.

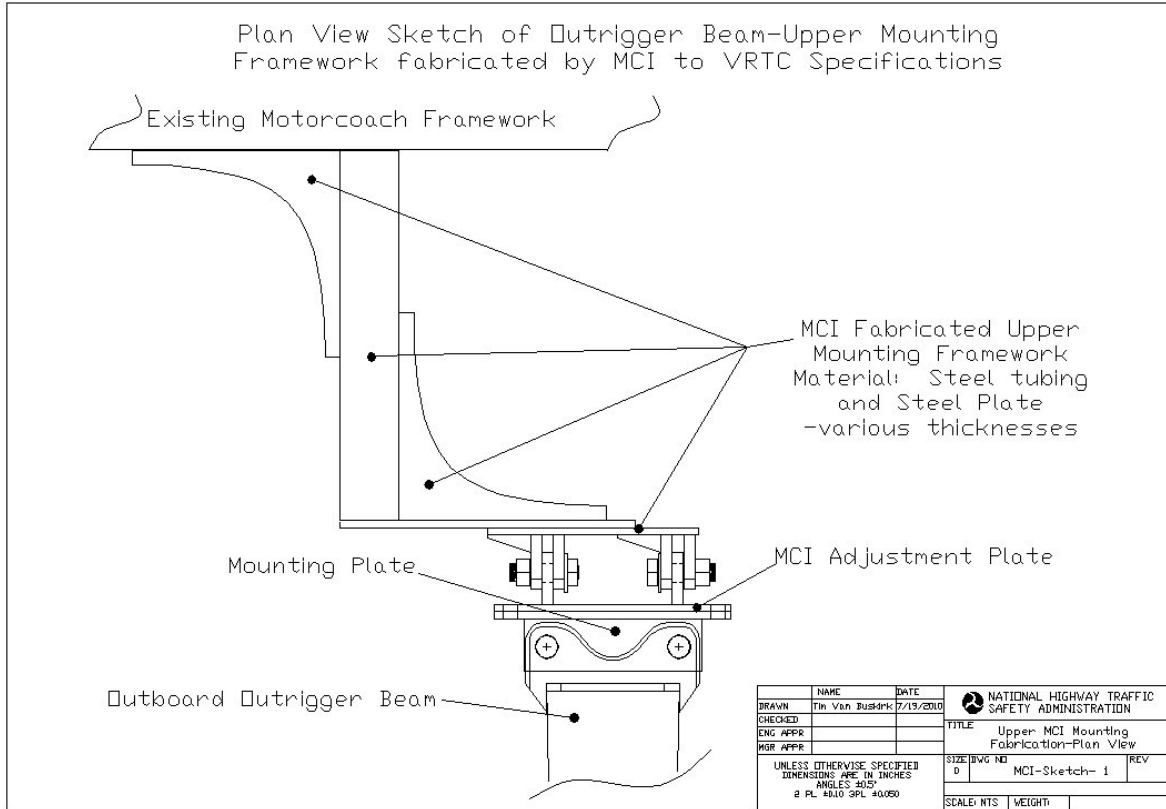
The tube center joiner was fabricated from A500 steel tube, 4 x 8 inch cross-section, and wall thickness of 0.50 inch. The lower mounting frame tubes were inserted into the tube center joiner and secured with 0.750 inch SAE grade 8 bolts. The photograph in AP Figure 13 shows how the two mounting frame tubes are joined with the tube center joiner in a view from the curbside of the motorcoach. The tube center joiner is located

in the right center of the photo flanked by the right and left side clamping plates. The right (curbside) adjustment plate can be seen in the upper left of the photograph.

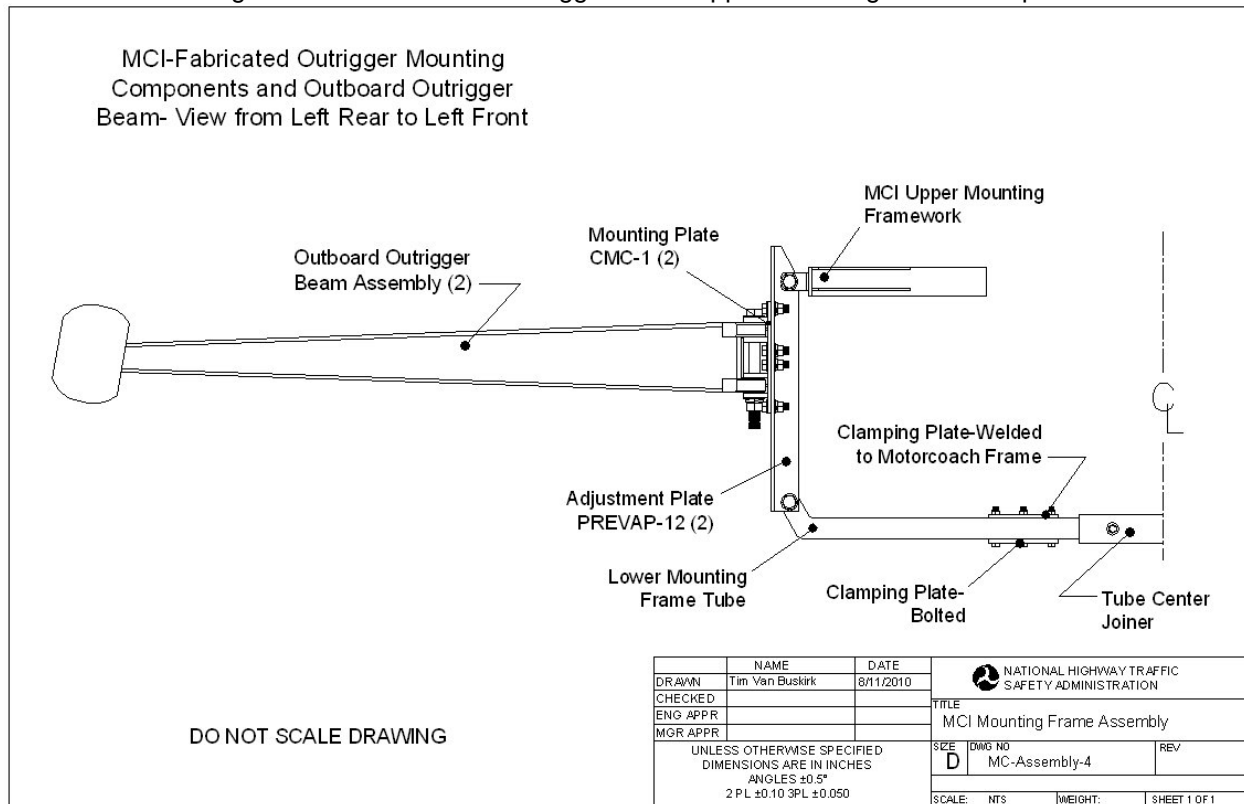


AP Figure 13. Photograph of the tube center joiner

A framework assembly welded to the motorcoach frame supported the top of the outrigger beam adjustment plate with 1-1/4 – 7 UNC SAE grade 8 bolts. This weldment consisted of a horizontal member fabricated from 4 inch square tubing welded perpendicular to a longitudinal vehicle frame member and extending out to the motorcoach's side. A steel plate bracket assembly was welded to the end of the 4 inch square tubing. The bracket assembly had two steel tabs welded to the steel plate on which to mount the upper end of the MCI adjustment plate. 0.25 inch thick steel gussets were welded both fore and aft of the 4 inch square steel tubing. These features are represented in AP Figure 14, a plan view sketch of the MCI upper mounting framework and in AP Figure 15, a side view drawing of the complete MCI mounting framework shown with the outboard outrigger beam assembly. AP Figure 16 contains a photograph of the right (curb-side) upper mounting assembly fabricated by MCI.



AP Figure 14. Sketch of the outrigger beam-upper mounting framework-plan.



AP Figure 15. Side view drawing of the complete MCI mounting framework shown with the outboard outrigger beam assembly.



AP Figure 16. Photograph of MCI upper mounting framework.

Prevost Fabrication of Mounting Framework

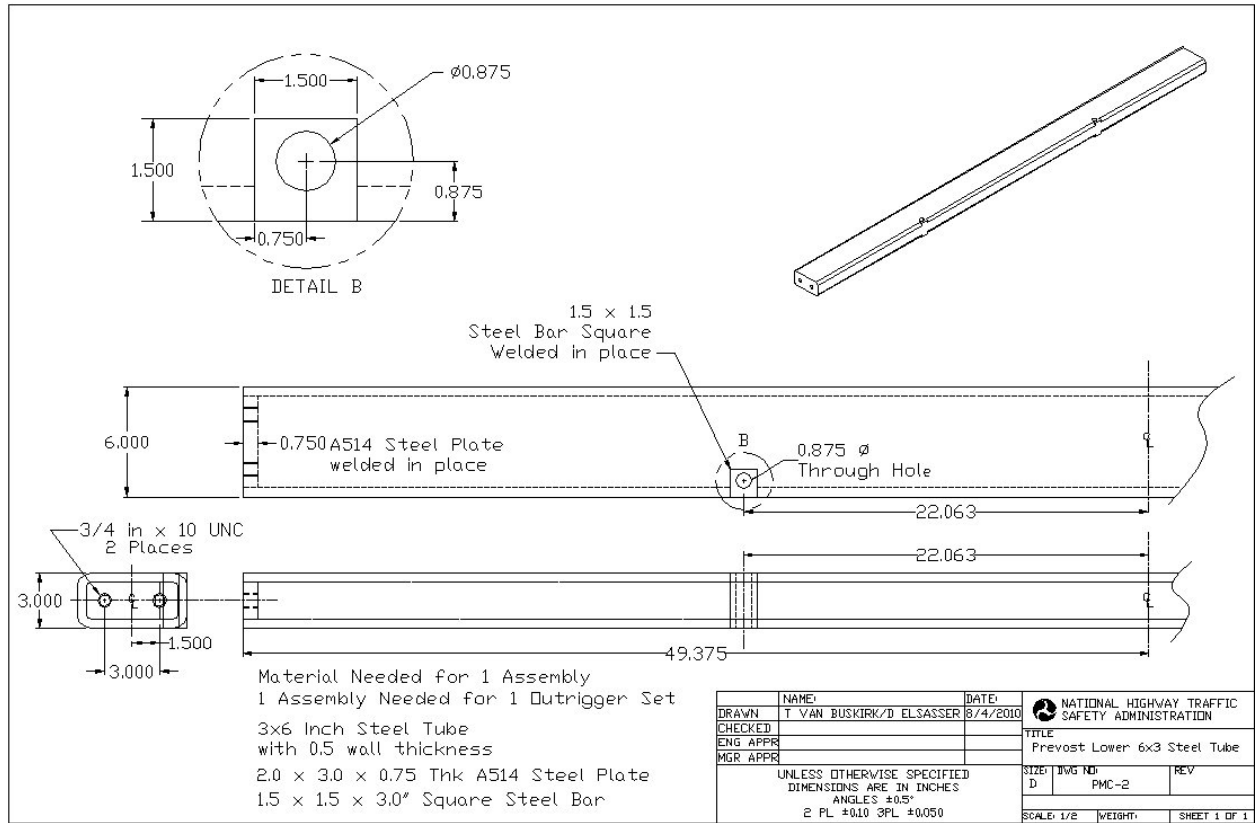
To mount the outrigger outboard beams to the Prevost motorcoach, a system of mounting attachments were developed and fabricated in-house. One advantage of the mounting scheme used for the Prevost was that the mounting frame members were attached by using various clamping plates so that no welds or permanent attachments were made to the motorcoach.

The components of this system were:

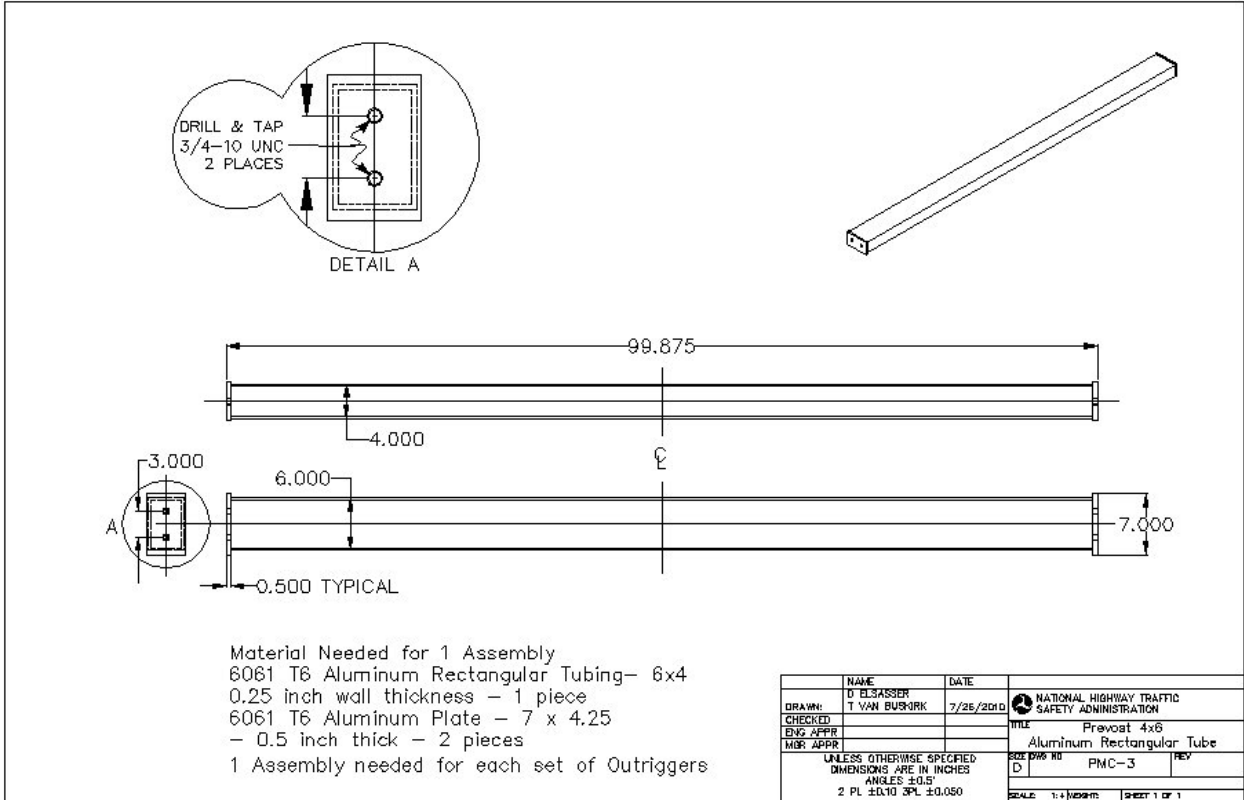
- Prevost Lower 6x3 inch Steel Tube
- Prevost 4 x 6 inch Aluminum Rectangular Tube
- Prevost Steel Lower Support
- Prevost Upper Support Tubes
- Prevost Connecting link
- Prevost Upper Mounting Plates
- Prevost Lower Mounting Plates
- Various clamping plates

Two mounting frame members that spanned the width of the motor coach were located in the luggage compartment just forward of the rear axles. The Prevost lower 6 x 3 inch steel tube was fabricated from 6 x 3 inch steel tubing with $\frac{3}{4}$ inch steel plate inserted and welded into the ends. The ends were threaded for two $\frac{3}{4}$ – 10 UNC SAE grade 8 bolts. AP Figure 17 is a dimensioned engineering drawing of this component. This frame member was located at floor level in the luggage compartment and bolted to the lower mounting plate on each side of the motorcoach; which in turn fastened to the bottom of the outrigger adjustment plate. The lower 6 x 3 inch steel tube also was bolted to the Prevost steel lower support with $\frac{3}{4}$ inch SAE grade 8 bolts through the rear luggage compartment wall. The Prevost 6 x 4 inch aluminum rectangular tube was fabricated from 4 x 6 inch aluminum rectangular tubing and aluminum plates welded to the ends. Two holes were drilled and tapped for $\frac{3}{4}$ – 10 UNC threads. See AP Figure

18 for an engineering drawing of this part. This upper frame member bolted to the upper mounting plates (brackets) in the same manner as the steel frame member described above. AP Figure 19 is a photograph of these components viewed from the right (curbside) of the motorcoach from just in front of the drive axle wheels to slightly rearward through the luggage compartment.



AP Figure 17. Dimensioned engineering drawing of the Prevost lower 6 x 3 inch steel tube.



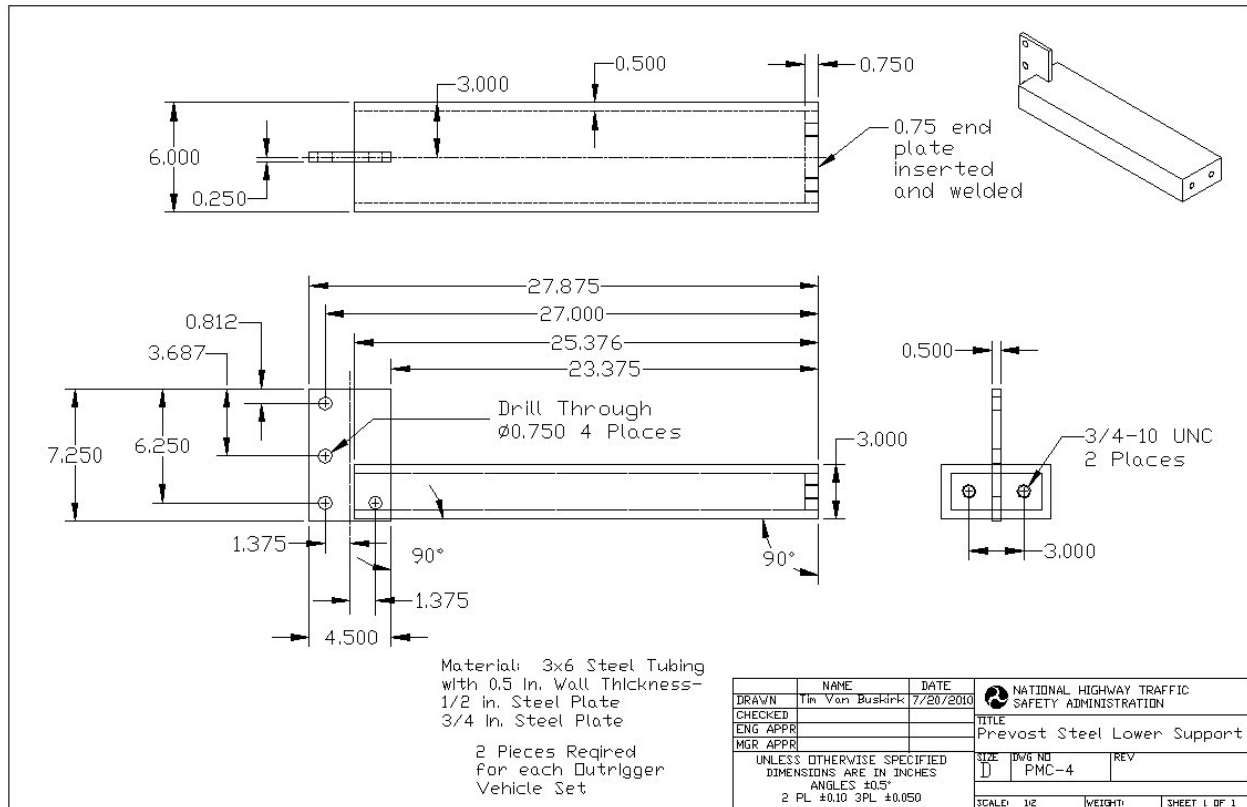
AP Figure 18. Engineering drawing of the PrevoSt 6 x 4 inch aluminum rectangular tube.



AP Figure 19. Photograph of PrevoSt lower 6 inch x 3 inch steel tube and the 6 inch x 4 inch aluminum rectangular tube.

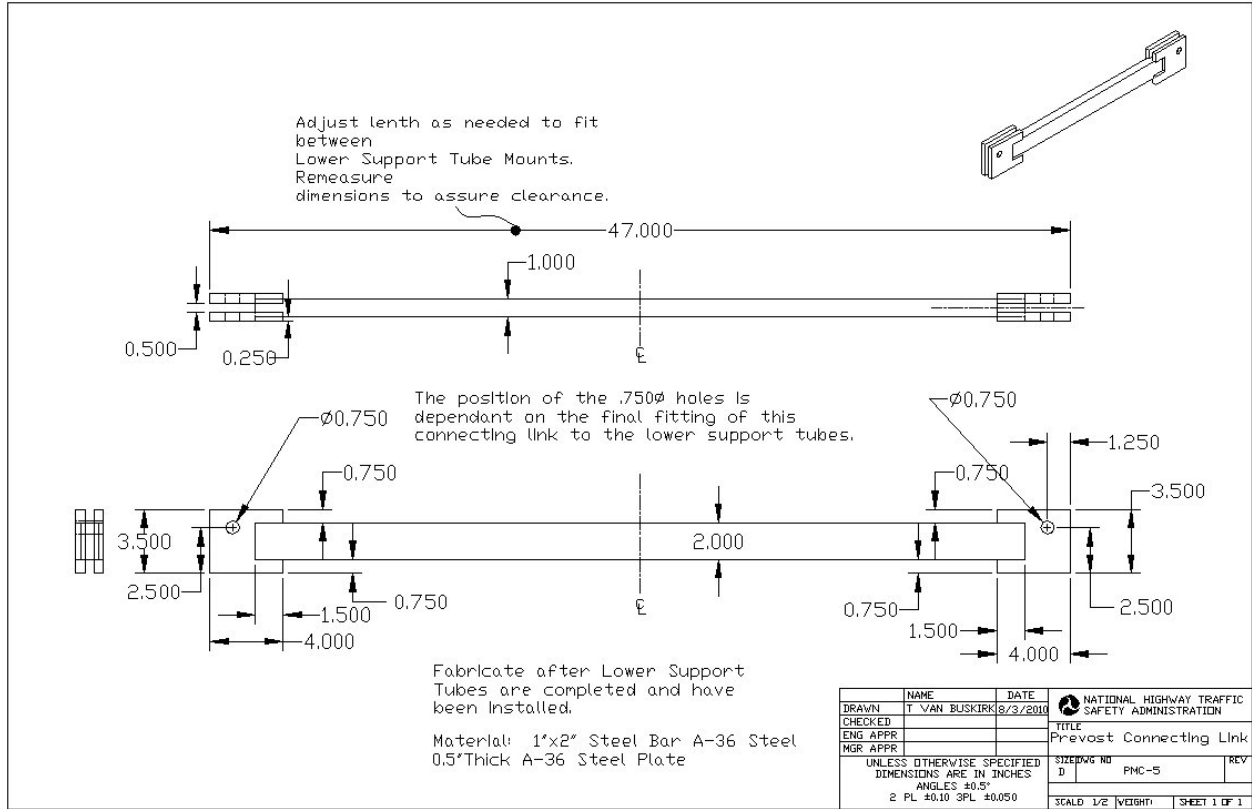
The lower mounting frame located below and to the rear of the luggage compartment wall consisted of two steel lower supports with a center connecting link. The PrevoSt steel lower supports were fabricated from 6 x 3 inch steel tubing with 0.5 inch wall thickness. The outboard ends had 3/4 inch steel plate welded into the end and drilled and tapped for 3/4-10 UNC threads. A vertical flange with 3/4 inch holes was welded to the inboard end. The PrevoSt lower mounting plates bolted to the outboard ends of the

Prevost steel lower support. The inboard ends were bolted to the Prevost lower 6 x 3 inch steel tube through the luggage compartment wall and the ends of the Prevost connecting link. AP Figure 20 is an engineering drawing of the Prevost lower steel support.



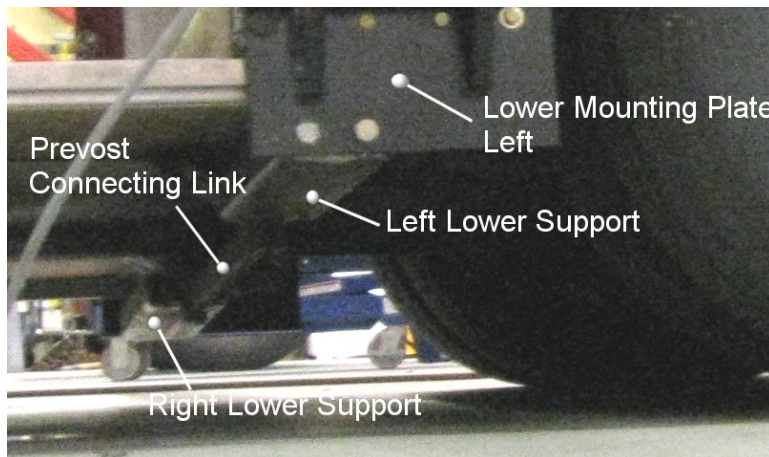
AP Figure 20. Engineering drawing of the Prevost lower steel support.

The Prevost connecting link was fabricated from 1 x 2 inch A-36 steel bar with two 0.5 inch thick A-36 steel plates welded to each end to form bolt flanges. Each of the flanges had 3/4 inch bolt holes drilled through for attachment to the Prevost steel lower supports. As noted in the drawing, the Prevost connecting link must be fabricated after the lower steel supports have been completed and installed, so that the length of the bar and the position of the 0.75 inch holes can be determined. AP Figure 21 is an engineering drawing of the Prevost connecting link. Two steel lower supports and one connecting link are required for installation of one set of outriggers. The Prevost lower steel supports (left and right) ends were bolted to the left and right Prevost lower mounting plates.



AP Figure 21. Engineering drawing of the Prevost connecting link.

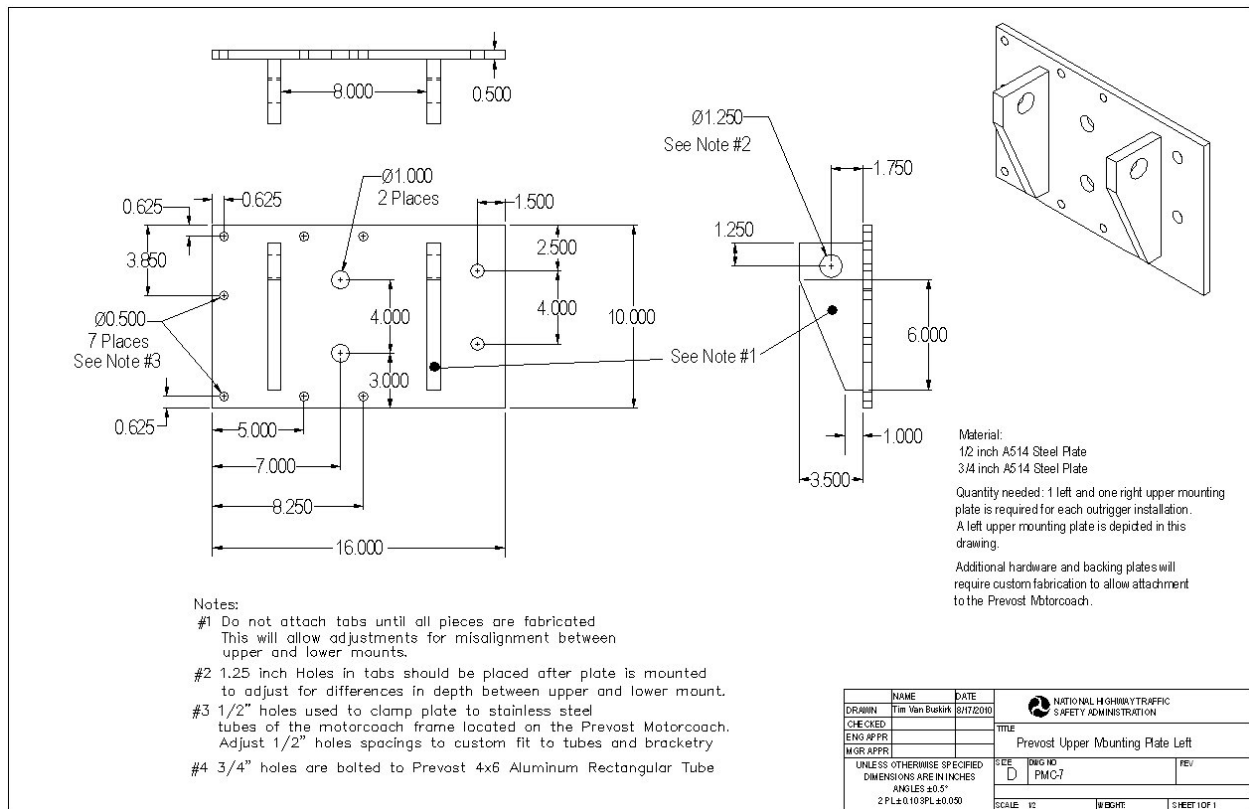
AP Figure 22 is a labeled photograph that shows the Prevost lower steel supports and the Prevost connecting link in place under the motorcoach during static load testing of the outriggers. The lower left mounting plate can also be seen in the top center of photo



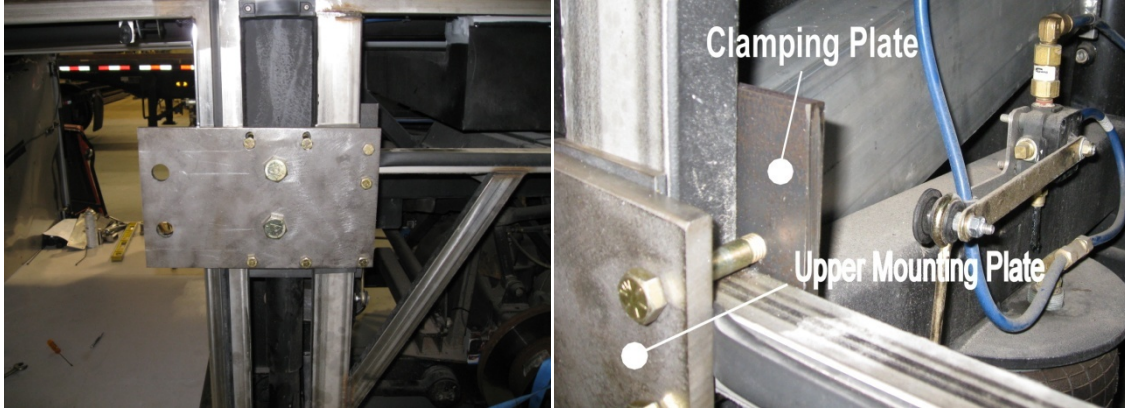
AP Figure 22. Labeled photograph of the steel lower supports and Prevost connecting link.

The Prevost upper mounting plates (left side and right side) were fabricated from 1/2 inch A514 steel plate and 3/4 inch A514 steel plate. The 16 x 11.25 inch support plates had 3/4 inch and 1.0 inch through holes to allow the 6 x 4 inch aluminum rectangular tube and the Prevost upper support tubes respectively, to be bolted to Prevost upper mounting

plates. Two 3/4 inch thick bracket tabs were welded to the mounting plates after the plates were installed. The mounting plates were secured to the stainless steel tubes of the motorcoach frame with various clamping plates and 1/2 inch SAE grade 8 bolts. The positions for the 1/2 inch bolts, the attachment of the tabs, and the placement of the 1.25 inch holes in the tabs were determined after the mounting plates were installed. This allowed for adjustments for misalignment between the upper and lower mounts and for differences in depth between upper and lower mounts. The 1.25 inch holes allowed the Prevost adjustment plates to be attached with 1.25 inch SAE grade 8 bolts. AP Figure 23 is a dimensional drawing of the Prevost upper mounting plate left and AP Figure 24 contains photographs of the development and fabrication of the Prevost upper mounting plates.

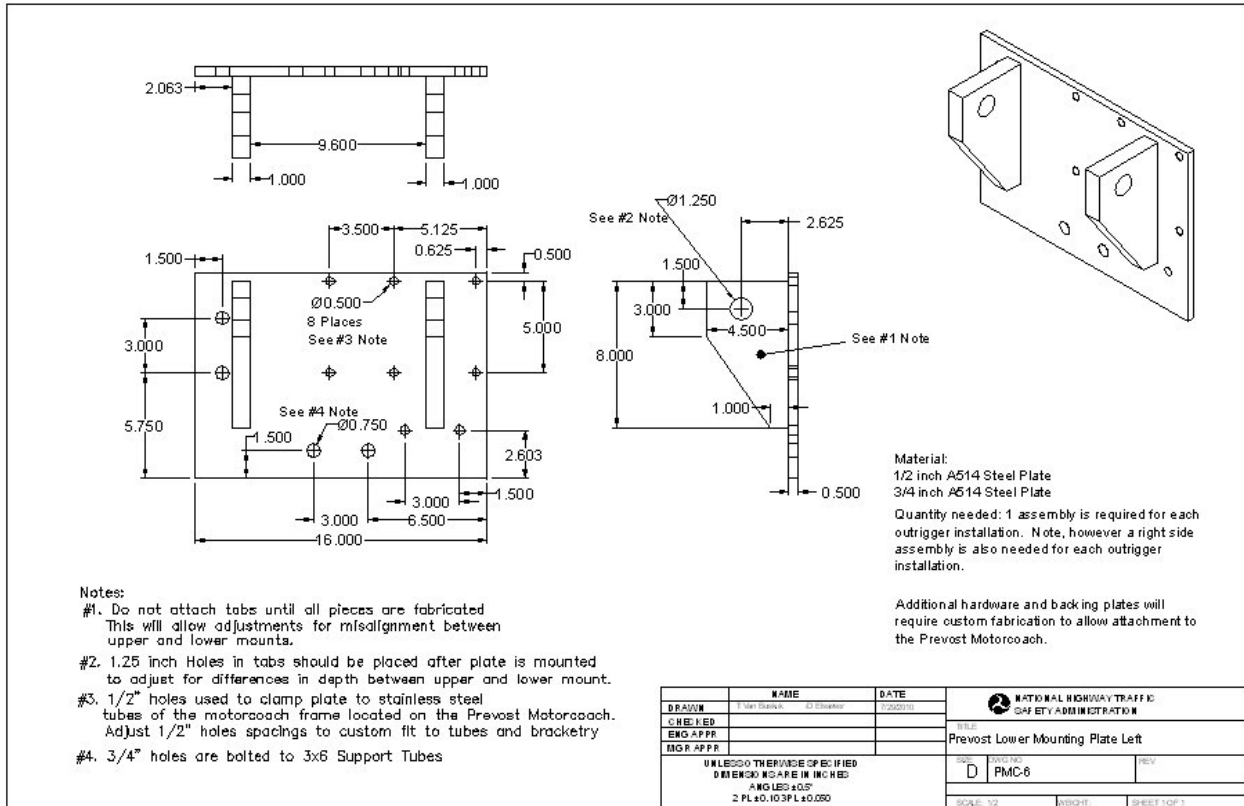


AP Figure 23. Dimensioned drawing of the Prevost upper mounting plate, left side.

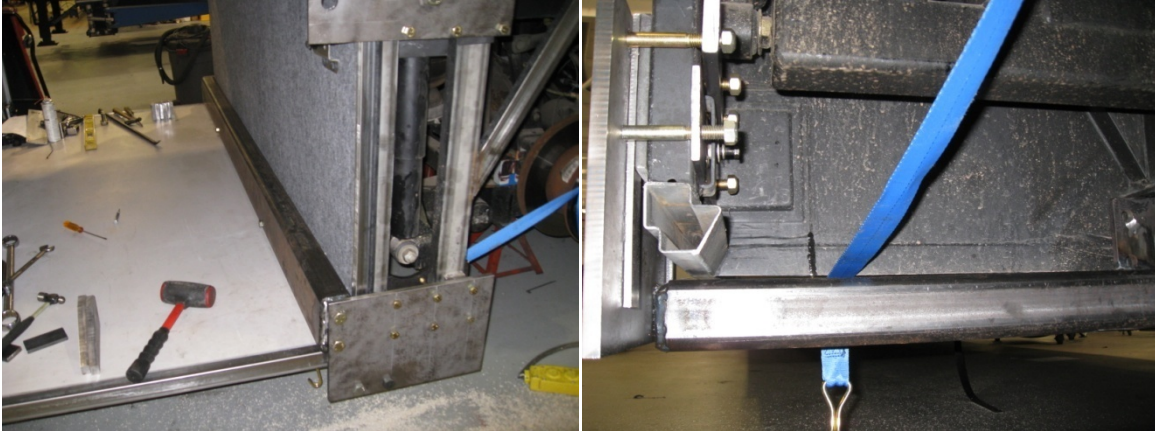


AP Figure 24. Photographs of the fabrication of the Prevost upper mounting plates. Left: Driver-side upper mounting plate bolted in place with clamping plates and the upper support Tube before the tabs were installed. Right: This photo is of the same mounting plate shows the clamping plate on the inside of the stainless steel tubing of the motorcoach and the aluminum upper support tube (center background).

The lower mounting plates (left side and right side) were bolted to the ends of the Prevost lower 6 x 3 inch steel tube and the Prevost steel lower supports. The lower mounting plates were also secured to the stainless steel tubes of the motorcoach frame with clamping plates. AP Figure 25 is a dimensional drawing of the Prevost lower mounting plate Left and AP Figure 26 contains photographs of the fabrication of the Prevost lower mounting plates.

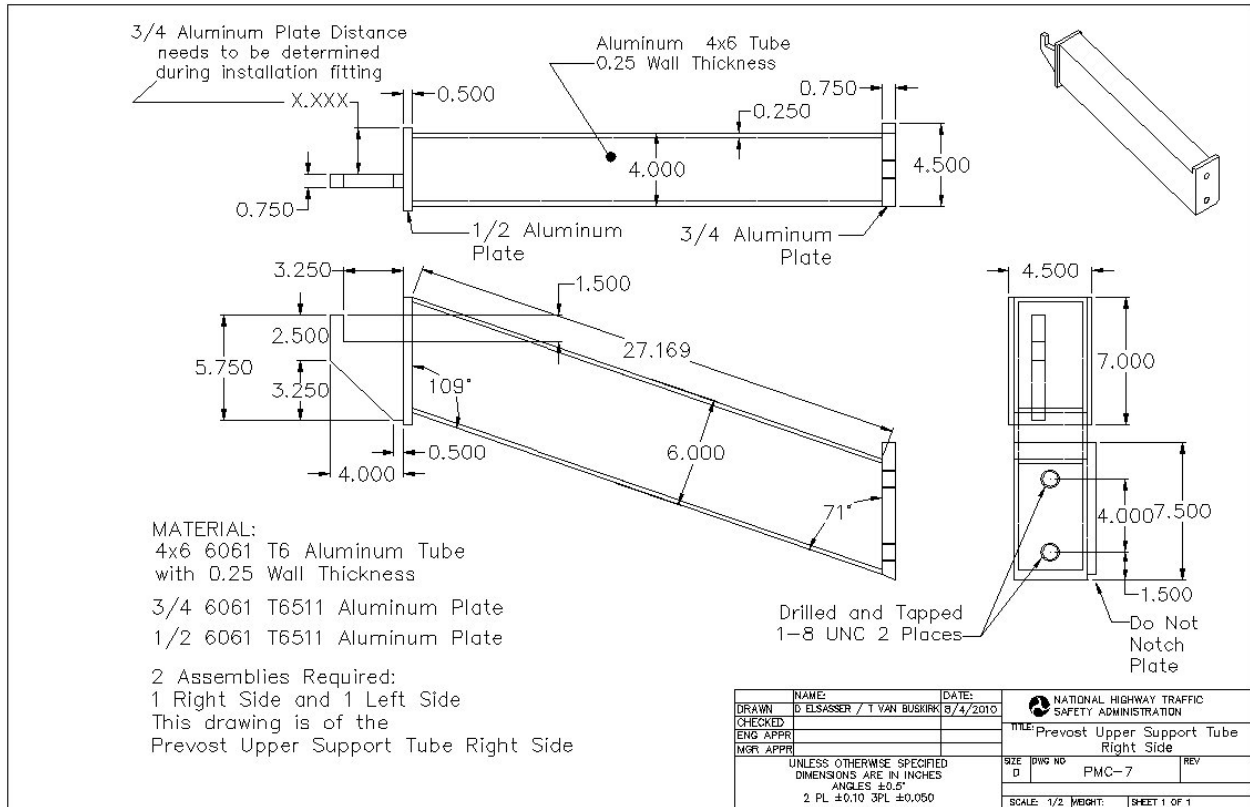


AP Figure 25. Dimensioned drawing of the Prevost lower mounting plate for the left side.

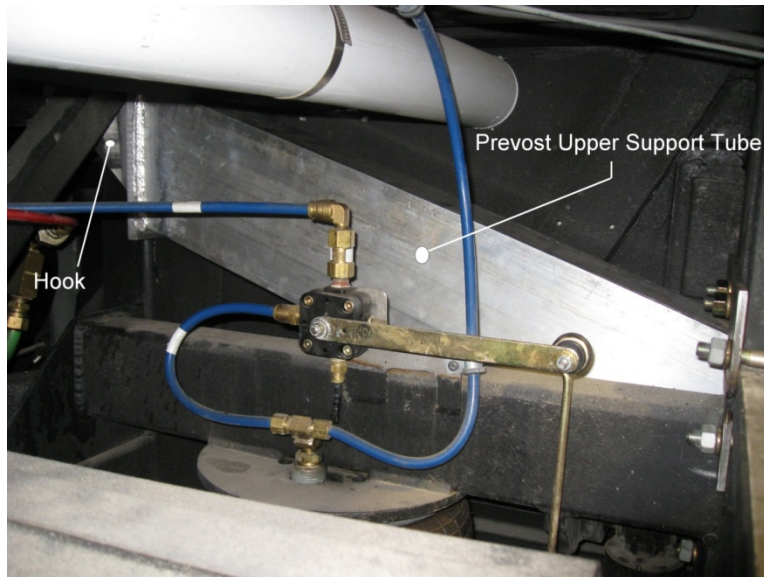


AP Figure 26. Photographs of the fabrication of the Prevost lower mounting plates. Left: Driver-side lower mounting plate is bolted to the Prevost lower 6 x 3 inch steel tube and with clamping plates. Right: This photo is of the same mounting plate showing the clamping plate on the inside of the stainless steel tubing of the motorcoach and the Prevost steel lower support tube.

To provide additional stability and rigidity to the outrigger assembly the Prevost upper support tubes (left and right) are bolted to the left and right upper mounting plates. The Prevost upper support tubes were bolted to the inboard sides of the upper mounting plates secured to the motorcoach frame with a hook on the inboard end. The Prevost upper support tubes were fabricated from 4 x 6 inch aluminum tubing and aluminum plate. See AP Figure 27 for a dimensioned engineering drawing of the Prevost upper support tube right side. The outboard end was drilled and tapped for 1-8 UNC threads so that it could be bolted to the upper mounting plate. The inboard end had a square-throated hook fabricated from $\frac{3}{4}$ inch aluminum plate welded to the end plate of the support tube that cradled an inner motorcoach frame member. Installed, the upper support tubes angled up 71 degrees from the outboard ends to the inboard ends. AP Figure 28 is a photograph of the right side Prevost upper support tube installed. In the upper left of the photo the partially obscured hook is labeled.

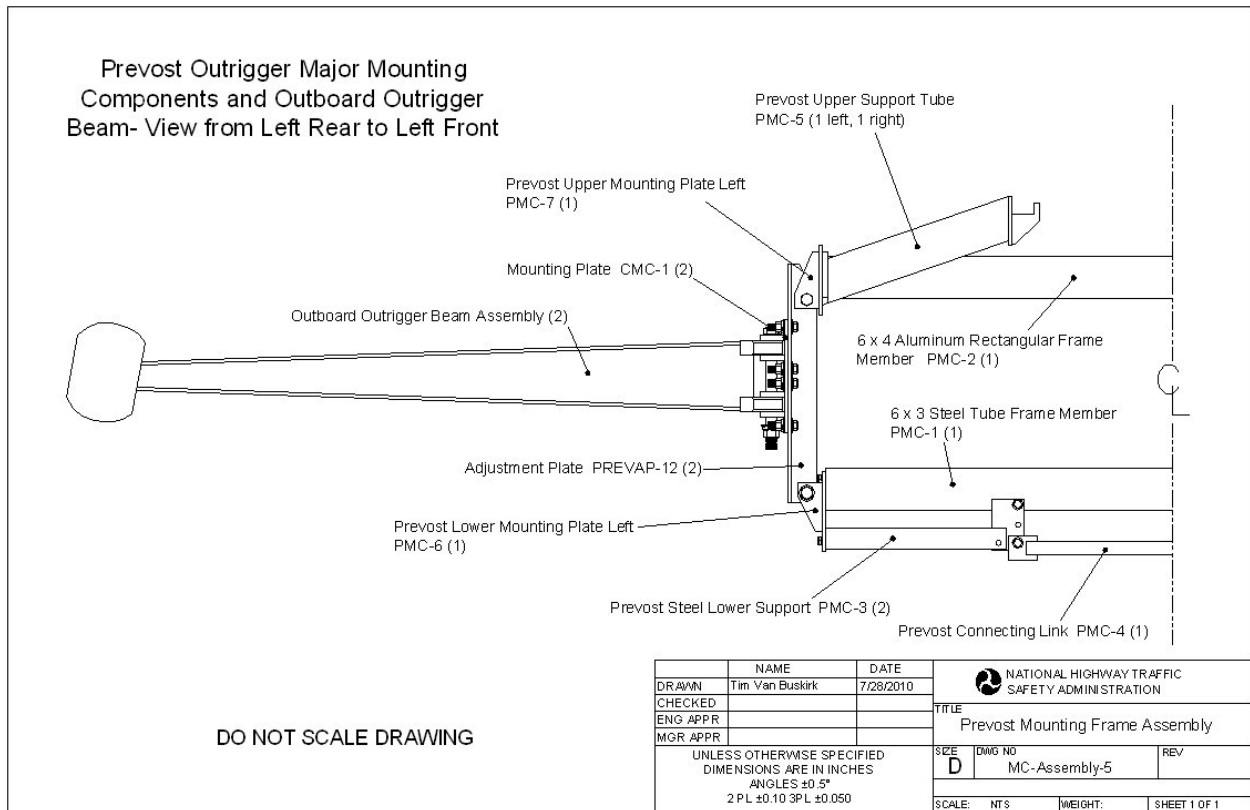


AP Figure 27. Engineering drawing of the Prevost upper support tube for the right side.



AP Figure 28. Photograph of the right side Prevost upper support tube installed.

The drawing presented in AP Figure 29; Prevost mounting frame assembly drawing contains the major components for attaching the outboard outrigger beam to the Prevost motorcoach. Each part is labeled and has the quantity needed in parenthesis of that part for a vehicle set of outriggers.



AP Figure 29. Prevost mounting frame assembly drawing view from the left rear of the motorcoach.

Outrigger Static Load Testing

Static loads were applied to the outriggers after they were installed on a test vehicle prior to performing any dynamic maneuvers. This allowed researchers to evaluate the mounts and newly fabricated outrigger in a controlled manner. The setup used for the static testing is shown in the photographs in AP Figure 30. From the figure, an overhead crane and tensile load cell are used to incrementally apply vertical loads to the axle shaft of one of the outriggers. The opposite outrigger is blocked to prevent the motorcoach from rolling and to allow the opposite outrigger to provide the reaction forces against those created by lifting with the crane. The crane was then used to apply force in 1,000 lb increments (up to 7,700 lbs at the HDPE plastic wheel in the case of the MCI motorcoach). All welds, bolts and joints were then inspected for any problems at the maximum load. This methodology was then used to evaluate the mounting brackets by removing the blocks under the outrigger on the opposite side. Loads applied to the outrigger to evaluate the mounts were varied with test vehicles.



AP Figure 30. Photographs of the motorcoach outrigger and mount static load testing. Left: MCI motorcoach. Right: Prevost motorcoach.

List of Numbered Drawings

Part Name	Drawing Number
Outboard Outrigger Beam Assembly Side View	MC-Assembly-2
Outboard Outrigger Assembly 3 Views	MC-Assembly-3
Mounting Plate	CMC-1
Prevost Adjustment Plate	PMC-1
MCI Mounting Fabrication Sketch– Upper – Plan View	MCI-Sketch-1
MCI Mounting Frame Assembly	MC-Assembly-4
Prevost Lower 6 x 3 Steel Tube	PMC-2
Prevost 6 x 4 Aluminum Rectangular Tube	PMC-3
Prevost Steel Lower Support	PMC-4
Prevost Connecting Link	PMC-5
Prevost Lower Mounting Plate Left	PMC-6
Prevost Upper Support Tube	PMC-7
Prevost Mounting Frame Assembly	MC-Assembly-5

DOT HS 811 633
April 2013



U.S. Department
of Transportation
**National Highway
Traffic Safety
Administration**



8627-041513-v5